

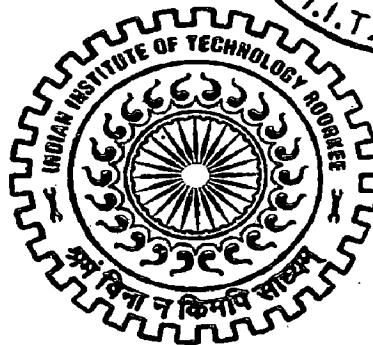
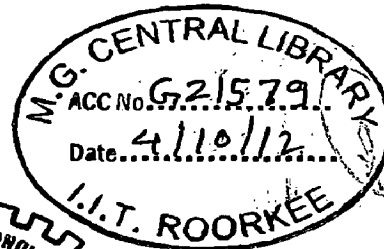
PERFORMANCE ANALYSIS AND EFFECT OF TERRAIN ATTENUATION ON OUTDOOR PROPAGATION MODELS

A THESIS

*Submitted in partial fulfilment of the
requirements for the award of the degree
of*
DOCTOR OF PHILOSOPHY

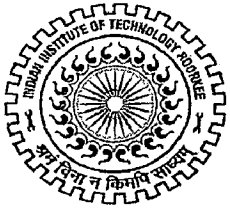
by

VISHAL GUPTA



**DEPARTMENT OF PAPER TECHNOLOGY
INDIAN INSTITUTE OF TECHNOLOGY ROORKEE
ROORKEE-247 667 (INDIA)**

APRIL, 2012



INDIAN INSTITUTE OF TECHNOLOGY ROORKEE

CANDIDATE'S DECLARATION

I hereby certify that the work which is being presented in the thesis entitled "**PERFORMANCE ANALYSIS AND EFFECT OF TERRAIN ATTENUATION ON OUTDOOR PROPAGATION MODELS**" in partial fulfilment of the requirements for the award of the degree of Doctor of Philosophy and submitted in the Department of Paper Technology, of the Indian Institute of Technology Roorkee is an authentic record of my own work carried out during a period from **Jan. 2008 to April 2012** under the supervision of Dr. S.C. Sharma, Associated Professor and Dr. M.C. Bansal, Professor, Department of Paper Technology, Indian Institute of Technology Roorkee , Roorkee.

The matter presented in the thesis has not been submitted by me for the award of any other degree of this or any other instituté.

(Vishal Gupta)

This is to certify that the above statement made by the candidate is correct to the best of our knowledge.

(M. C. Bansal)
Supervisor
(S. C. Sharma)
Supervisor

Date: 10-04-2012

The Ph.D. Viva-Voce Examination of **Mr. Vishal Gupta**, Research Scholar, has been held on03...07...2012

Signature of Supervisor(s)
Chairman SRC
Signature of External Examiner
Head of the Department/Chairman ODC

ABSTRACT

INTRODUCTION

Network planning is a complicated process consisting of several phases and involves through estimation by outdoor propagation models. The final target for the network planning process is to define the network design, which is then built as a cellular network. The network design can be an extension of the existing GSM network or a new network to be launched. The difficulty in network planning is to combine all of the requirements in an optimal way and to design a cost-effective network using outdoor propagation models. Outdoor propagation models helps in calculating propagation loss using collected data. The basic requirements for the cellular network are to meet coverage and quality targets. Terrain factors such as area, foliage, rain etc also greatly affect network planning.

BACKGROUND OF RESEARCH WORK

Careful network planning has become increasingly critical with the rising deployment, coverage and congestion of wireless area networks. Efforts have been made by researchers to analyze the performance of outdoor propagation models. Some researchers have even designed new waveguides and algorithm. Outdoor propagation models have been analyzed on the basis of collected data which allow estimating cell coverage area while minimizing path loss. Models analysis describes features, configuration requirements, parameters, statistics and scenarios for network planning. Propagation models have been estimated for performance analysis in terms RxLevel strength and Errors. In the present analysis an attempt has been made to achieve prediction accuracy of Okumura, COST 231 HATA, COST W-I, Egli and ECC 33 models for fringe area of Uttarakhand. Best model is selected and tuned to minimize path loss. Further the analysis is extended to analyze the effect of terrain on electromagnetic wave.

OBJECTIVE OF THE PRESENT RESEARCH WORK

Efficiency of present path loss models suffers when they are used in the environment other than for which they have been designed. If these models are used for network planning in any place other than where they are designed, than correction factor is to be introduced and tuning has to done according to new environmental conditions. The aim of the present research is to analyze

outdoor propagation models like eg. Okumura, COST 231 HATA, COST W-I, Egli and ECC 33 for efficient network planning and tuning of best fit model is estimated to minimize path loss in the fringe area of Uttarakhand. Further the effect of terrain on wave propagation has been analyzed and rain fade margin is introduced during link budget design.

The outline of present analysis is as follows:

- Outdoor propagation models available in open literature has been reviewed
- Field data of BSNL GSM network has been collected over the period of one year using TEMS 8.01 navigation tool in changing environmental conditions of Dehradun - Uttarakhand.
- Performance analysis of the Okumura, COST 231 HATA, COST W-I, Egli and ECC 33 outdoor propagation models has been carried out.
- Tuning of best fit outdoor propagation model for Dehradun- Uttarakhand region has been estimated.
- Effect of attenuation on electromagnetic waves due to rain has been analyzed using fuzzy approach.
- Proper link budget has been estimated by introducing rain fade margin in up link and down link.

Outdoor propagation models and methodology of field data collection:

For carried out the above analysis in fringe area of Dehradun Uttarakhand Coordinates, *LATITUDE: 30.3539 LONGITUDES: 78.0245* is chosen. Data (RxLev., SQI, Interference etc) has been collected in a measurement campaign accomplished in three areas of Dehradun.

- BSNL GSM (900-1800MHz) network has been selected for field data collection.
- Field measurement data is collected using Ericson's TEMS investigation 8.0 and 10.0 the leading air interface test tool for GSM network. TEMS drive test for route analysis has been carried out in changing environmental condition over the course of one year.
- Data is collected over the range of 100 m to 2 km and its analysis is used to tune an empirical path loss model for the fringe area of Uttarakhand. Region around the BTS is divided into 3 sectors α , β , γ each 120° oriented and drive for data collection is made around it starting from 100 m to 2 Km. The mean value of received signal levels for each

location is calculated by averaging the total number of samples within that particular measurement sector.

Performance Analysis and tuning of outdoor propagation models

The collected data (RxLev, SQI, Interference etc) has been analyzed using DESKCAT and Mapinfo simulation tools. The present analysis is carried out in a frequency range of 900 and 1800 MHz that is globally being allocated for broadband wireless GSM network. The dependency of the propagation models on excess path loss and terrain in different seasons has been investigated by researchers.

Our contribution

- Path loss for above propagation models is determined using the parameter of four BTS ID's selected at Dehradun Uttarakhand.
- The results have been used to evaluate the performance analysis of Okumura, COST 231 HATA, COST W-I, Egli and ECC 33 outdoor prediction models.
- Model has been selected to estimate the path loss.
- Correction factor has been introduced for tuning of best fit model in order to improve its performance.
- Finally path loss is plotted as a function of path distance by using linear regression analysis, obtain best fit model at minimum of path loss curve.

The assessment of effect of rain fall attenuation on outdoor propagation model using fuzzy approach:

Fuzzy logic is a branch of science which rationalizes uncertain events. It is more of a mathematical tool dealing with uncertainties. Fuzziness in real terms is defined as the degree of impreciseness associated with a certain problem of significance. Fuzzy logic has been extensively implemented in many fields like Communication, Process, and Power etc. for solving problems. Propagation prediction is a combination of Science, Engineering and Art. An experience RF engineer, willing to compromise between theory and practice, would accomplish the most. In the present analysis fuzzy logic approach has been used to predict the signal

attenuation related to terrain like rain, foliage, building etc. At the core of the functionality of Fuzzy prediction technique, ITU-R model fundamentals have been deployed. The annual rainfall data for district Dehradun –Uttarakhand, has been obtained as per the courtesy of Indian Meteorological Department, Hydrometeor division for the time period of 2006-2010. Fuzzy system involves analysis of rainfall data & prediction of attenuation for each month specifically for year from 2009 to 2010. The more emphasis has been laid on the months of monsoon season i.e. May, June, July, August & September.

Our contribution

- Field data is collected in different rain fall rates and terrain. Based on this data fuzzy inference system estimates specific attenuation as an output.
- Different fuzzy rule based has been estimated using MATLAB.
- The range of membership functions have been classified as: Low, Very-low, Medium, High, and Very-high in ANFIS to depict the attenuation prediction logically.
- Mamdani FIS based scheduling has been used to predict rainfall attenuation to different terrain.
- Based on the fuzzy results efficient network planning for other regions of Uttarakhand having same rain rate and terrain can be predicted.
- From the result it has been examined analyzed that fuzzy logic approximation is effective to determine an unknown terrain from the set of known terrain anywhere in Uttarakhand.

The assessment of effect on link budget due to rain fade margin:

Insufficient link budget planning can result in overdesign, under design, wastage of resources health hazards and poor system performance. Prior to planning a network, the parameters controlling the performance of each individual link must be understood. For link planning, a link budget is prepared that accounts for the transmitter effective isotropically radiated power (EIRP) and all of the losses in the link prior to the receiver. Link budget parameters has been analysed by several researchers for solving constrain of path loss during up link and down link. The link budget is computed in decibels (dB), so that all of the factors become terms to be added or subtracted. Radio equipment is designed in such a way that when the link budget for the uplink

and downlink are put together, they should have the same maximum allowable path loss in both directions. Rain fades is a significant factor depending upon the link distance and the geographic location. There is always the temptation to argue that the rain margin is not being used most of the time, so it can be used to compensate for link budget shortfalls. The measurement is conducted in Fringe area of Uttarakhand in order to determine the amount of attenuation caused by the rain. Four base stations is selected for measurement. Measurements is performed at the edge of each selected site, during rain which gives the maximum rain attenuation experienced by Mobile Station in a cell.

Our Contribution

Based on the collected data it is observed that difference in the path loss without rain and path loss during rain indicates that there is a need of rain fade margin to be introduced in link budget.

- The amount of rain attenuation estimated is used as rain fade margin and it is incorporated in the link budget.
- From the result it has been analyzed that there is significant path loss with respect to the power budget considering the rain attenuation. The maximum allowable path loss with and without rain fade is analyzed for proper link budget design.
- We analyzed that due to increase in path loss the maximum allowable coverage result in decreases of cell radius by 10 m.
- In order to compensate this loss caused by the rain, there is a need to increase the link budget.

Future scope and feasibility of implementation of current research results

Based on the results of current research GSM network planners can adopt outdoor propagation model after analysis of their performance. Tuning and correction factor implementation provide more precise network planning. A fuzzy logic result of current research is effective to determine an unknown environment from the set of known environment anywhere in Uttarakhand. Further embedded system may be designed which can accommodate variable gain depending on tuning.

ACKNOWLEDGEMENT

I feel expedient to express my profound indebtedness & deep sense of gratitude and sincere thanks to Dr. S.C. Sharma, Associate Professor, Electronics & Computer Discipline, DPT, Indian Institute of Technology, Roorkee, for their valuable guidance, inspiration, encouragement and whole hearted co-operation in understanding the relevant field and help in presenting this work. Their keen interest and efforts in planning the work in this form can not be expressed in words, as they devote their valuable time in discussions and in critical analysis of the work. I am highly obliged to them. It is a great opportunity to express my respect and gratitude to Dr. M. C. Bansal, Retd. Professor, IIT Roorkee for all his valuable guidance, inspiring discussions and overall motivation during my Ph.D. I would also like to thank Dr. Mohan Lal, Assistant Professor, ICC, for providing me with valuable suggestions and guidance during my study. I am extremely grateful to Dr. Satish Kumar, Professor and Head, DPT, IIT Roorkee, for providing necessary administrative help for carrying the work. The author is also thankful to Prof. A.K. Singh, Chairman, DRC, DPT, IIT Roorkee and members of SRC, whose co-operation and encouragement helped a great deal in this endeavor. I am also thankful to research colleague Ms. Leena Arya, Dr. A. K. Jain, Dr. Kumar Manoj, Dr. Shamimul Qamar, Parmanand, Santosh Kumar, and Dr. Amit Dixit for providing me necessary help to complete this work. I am also special thankful to my colleagues Dr. Sandip Vijay for inspiring me and providing necessary support to complete this work.

I would like to express my sincere thanks and regards to Dr. Chhaya Sharma, Asstt. Prof, DPT, IIT Roorkee, and her family for giving me morale support and inspiration from time to time and Mr. Balraj (G.M.), BSNL for providing me software and support for data collection.

It is my pleasant duty to acknowledge my thanks to all my well wishers, employees of D.P.T, (Since it is not possible to mention all the names), who support, and inspired me through their love and regards directly or indirectly. No words, no language is ever adequate to express my heartfelt veneration for my respected parents Shri Kailash Chand Gupta, Mrs. Meera Devi, my inlaws ,my brothers and specially my wife Mrs. Akanksha Gupta and my loving daughter “Avishi” and all my family members for their cheerful, enthusiastic, dedicated and unconditional efforts to engage myself in high pursuits.

Above all, I praise the almighty ‘God’ for his blessings.

Dated: April, 2012



(Vishal Gupta)

CONTENTS

CANDIDATE'S DECLARATION	i
ABSTRACT	ii
ACKNOWLEDGEMENTS	vii
CONTENTS	ix
LIST OF ACRONYMS	xv
LIST OF FIGURES	xviii
LIST OF TABLES	xxiv
GLOSARRY	xxvi
LIST OF PUBLICATIONS BASED ON WORK	xxvii
CHAPTER 1 : INTRODUCTION	
1.1 Background	1
1.2 Spectral Radio Differentiation	3
1.3 Wireless Radio Standard	5
1.3.1 First Generation Systems [1G]	5
1.3.2 Second Generation Systems [2G]	6
1.4 3 G Cellular System (WCDMA)	13
1.4.1 Specification of 3G (WCDMA)	15
1.5 Effect of Terrain on Signal Propagation	17

CHAPTER 2: OUTDOOR PROPAGATION MODELS AND METHODOLOGY OF FIELD DATA COLLECTION

2.1	Background	23
2.2	Pathloss Prediction Model	24
	2.2.1 Indoor Model	25
	2.2.2 Outdoor Model	25
2.3	Empirical Outdoor Propagation Models	27
	2.3.1 Free Space Path Loss Model	27
	2.3.2 Egli Model	27
	2.3.3 Okumura Model	27
	2.3.4 Hata Model	28
	2.3.5 COST 231 Hata Model	29
	2.3.6 ECC 33 Model	29
	2.3.7 Lee Model	29
2.4	Methodology of Field Data Collection	31
2.5	Drive Test Tool for Measurement	31
	2.5.1 NEMO	31
	2.5.2 Agilent	32
	2.5.3 TEMS	33
2.6	Terminology Associated With Drive Test	37
2.7	Check List for Field measurement	40

2.8	Hardware Requirement	40
2.9	Software Requirement	40
	2.9.1 Specification of Hardware and Software	41
2.10	Assembling/Installation /Setup Procedure	44
	2.10.1 Plugging in Phones and Data Cards	44
	2.10.2 Plugging in GPS Units	44
	2.10.3 Configuring TEMS Investigation software for Data Collection	45
	2.10.4 Recording Log Files	46
2.11	Loading Site Data , Vector, Map , Path	46
2.12	Test Procedure for Drive Test	48
2.13	Various issues during Measurement	49
2.14	Data Analysis Tool	52
 CHAPTER 3 : PERFORMANCE ANALYSIS AND TUNING OF OUTDOOR PROPAGATION MODELS		53
3.1	Background	55
3.2	Related Work	55
3.3	Estimation of path loss from field collected data during Drive Test at Dehradun	56
	3.3.1 BTS identification using Google Earth Presentation and GPS	57
	3.3.2 Channel Window Parameters	58
	3.3.3 Line chart for log file	58
	3.3.4 Samples Averaging	59
	3.3.5 Adaptation of sample rate to Vehicle Speed	60
3.4	Received signal strength from selected	62

	sites	
3.5	Path loss calculation	62
	3.5.1 Simulation Parameters	64
3.6	Performance Analysis and Comparison of Free Space Path Loss (FSPL) Model with Measured Path Loss using MATLAB and Linear Regression	65
	3.6.1 Why Least Square Approximation using Linear Regression?	67
3.7	Performance analysis and comparison of Okumura Model with Measured Path Loss using MATLAB and Linear Regression	68
3.8	Performance analysis and comparison of Egli Model with Measured Path Loss using MATLAB and Linear Regression	70
3.9	Performance analysis and comparison of COST 231 Model with Measured Path Loss using MATLAB and Linear Regression	73
3.10	Performance analysis and comparison of COST WI Model with Measured Path Loss using MATLAB and Linear Regression	76
3.11	Performance analysis and comparison of ECC-33 MODEL with MEASURED PATH LOSS using MATLAB and LINEAR REGRESSION	80
3.12	COMBINED GRAPH OF PERFORMANCE ANALYSIS AND COMPARISON OF FSPL, OKUMURA, EGLI, COST 231, COST WI AND ECC 33 MODEL WITH MEASURED FIELD PATH LOSS USING MATLAB	82
3.13	Performance analysis of Outdoor Path Loss Models with Measured Path Loss using Linear Regression	83
3.14	Selection of best fit model	84
3.15	Model tuning	85
	3.15.1 Tuned COST WI model	86
3.16	CONCLUSION	87
	CHAPTER 4 : THE ASSESSMENT OF EFFECT OF RAIN FALL ATTENUATION ON OUT DOOR PROPAGATION MODEL USING FUZZY APPROACH	89
4.1	Background and Motivation	89

4.2	Why Fuzzy Logic for attenuation prediction due to rainfall?	90
4.3	Rain fall attenuation analysis	91
4.4	Rain fall attenuation effect	93
4.5	Rainfall –attenuation prediction models	95
	4.5.1 Rain model selection	98
4.6	Fuzzy approach	98
	4.6.1 Data specifications and site-selection	98
	4.6.2 Analysis of data with ITU-R	100
	4.6.3 Fuzzy input and output variables	107
	4.6.4 Mamdani Fuzzy Approach	111
	4.6.5 Fuzzy membership function	112
	4.6.6 Analysis of Result	113
4.7	Conclusion	122
 CHAPTER 5: THE ASSESSMENT OF EFFECT ON LINK BUDGET DUE TO RAIN FADE MARGIN		123
5.1	Background and Objective	124
5.2	Generic Link Diagram	126
5.3	Link Budget Calculation	129
	5.3.1 Receiver Sensitivity	132
	5.3.2 MS Sensitivity	133
	5.3.3 BTS sensitivity	134

5.3.4 MS and BTS powers	134
5.3.5 Antenna gains	136
5.3.6 Diversity gain	137
5.3.7 Feeder and connector loss	137
5.3.8 Tuning Units, Amplifiers and Combiners	137
5.3.9 Mast Head Amplifier (MHA) and Booster	138
5.3.10 Interference degradation margin	140
5.3.11 Polarization Loss	140
5.4 Link Budget Balancing	142
5.5 Effect of rain on Link Budget	143
5.6 Conclusion	146
CHAPTER 6: CONCLUSION AND FUTURE WORK	149
<i>APPENDIX</i>	

LIST OF ACRONYMS

FM	Frequency Modulation
QoS	Quality of Service
WLAN	Wireless Local Area Network
VLF	Very Low Frequency
MF	Medium Frequency
ATM	Asynchronous Transfer Mode
VHF	Very High Frequency
BER	Bit error rate
BS	Base station
BSS	Basic Service Set
BWA	Broadband wireless access
SHF	Super High Frequency
WARC	World Allocation Radio Conference
NTT	Nippon Telephone and Telegraph
NMT	Nordic Mobile Telephone
CDMA	Code division multiple access
AMPS	Advanced Mobile Phone Service

GSM	Global System for Mobile Communications
CEPT	Conference of European Postal and Telecommunications Administrations
DCS	Digital Cellular System
PCNs	Personal Communication Networks
BSNL	Bharat Sanchar Nigam Limited
PDC	Personal Digital Cellular
PABX	Private Access Business Exchange
ITU	International Telecommunication Union
IMT	International Mobile Telecommunications
WCDMA	Wideband Code Division Multiple Access
TDD	Time Division Duplex
EIRP	Effective Isotropic Radiated Power
PCS	Personal Communication System
LOS	Line of Sight
GBSBM	Geometrically Based Single Bounce Macro cell
FER	Frame Error Rate
HSDPA	High Speed Downlink Packet Access
HSUPA	High Speed Uplink Packet Access
iDEN	Integrated Digital Enhanced Network
WiMAX	Worldwide Interoperability for Microwave Access

SQI	Speech Quality Index
EFR	Enhanced Full Rate
FSPL	Free Space Path Loss
SACCH	Stand Alone Common Channel
DSD	'Drop-Size Distribution'
MIMO	Multiple-In Multiple-Out

LIST OF FIGURES

Figure No.	Caption	Page No.
1.1	A Fundamental Wireless communication system	2
1.2	The electromagnetic spectrum	3
1.3	Time slot format for GSM	10
1.4	Burst format for IS 54 /136 traffic channel	11
1.5	Time slot format of Japanese PDC	12
1.6	Diffraction Loss	17
1.7	Reflection Loss	18
1.8	Cell Structure	20
2.1	Elements of a wireless communication system	23
2.2	Median attenuation relative to free space $A_{mu}(f,d)$, over a quasi-smooth terrain	28
2.3	Features of Nemo drive test tool	32
2.4	E7478A Drive Test System with E6455C IMT2000 Digital Receiver	33
2.5	HSPA Classification	37
2.6	Drive Test principle illustration	41
2.7	TEMS test kit	41
2.8	TEMS window	45
2.9	Equipment Configuration window	46
2.10	Cell data configuring window	47
2.11	Example of Overshooting	49
2.12	Example of Bad quality	50
2.13	Example of Bad coverage	50

2.14	Example of Call block	51
3.1	FLOW CHART OF STEP BY STEP EXECUTION OF WORK	54
3.2	Channel window showing Coordinates and Parameters	58
3.3	Line Chart of Log file for current cell	59
3.4	Samples-RxLev of field collected data.	60
3.5	Code of color for received signal strength "X" in (dBm)	61
3.6	Measured received signal power in dBm from four selected BTS ID's	62
3.7	Measured path loss from received signal power at selected sites	63
3.8	Measured path loss from received signal power at selected sites using MATLAB	63
3.9	Measured path loss and least squares approximation for field collected sample data	64
3.10	Comparision of Free Space Path Loss (FSPL) empirical model with measurements from selected sites	66
3.11	Comparision of Free Space Path Loss (FSPL) empirical model with measurements from selected sites using MATLAB	66
3.12	FSPL and least squares approximation using linear regression for field collected sample data set	67
3.13	Comparision of Okumura empirical model with measurements from selected sites	68
3.14	Comparision of Okumura empirical model with measurements from selected sites using MATLAB	69
3.15	Okumura and least squares approximation using Linear Regression for field collected sample data set	69
3.16	Comparision of Egli empirical model with measurements at	71

	selected sites	
3.17	Comparison of Egli empirical model with measurements at selected sites using MATLAB	71
3.18	Egli and least squares approximation using linear regression for field collected sample data set	72
3.19	Comparison of COST 231 empirical model with measurements at selected sites	74
3.20	Comparison of COST231 empirical model with measurements at selected sites using MATLAB	74
3.21	COST 231 and least squares approximation using linear regression for field collected sample data set	75
3.22	Comparison of COST- WI empirical model with measurements at selected sites	78
3.23	Comparison of COST-WI empirical model with measurements at selected sites using MATLAB	79
3.24	COST -WI and least squares approximation using linear regression for field collected sample data set	79
3.25	Comparison of ECC -33 empirical model with measurements at selected sites	80
3.26	Comparison of ECC-33 empirical model with measurements at selected sites using MATLAB	81
3.27	ECC-33 and least squares approximation using linear regression for field collected sample data set	81
3.28	Combined graph of performance analysis of Free Space Path Loss, Okumura's, Egli, COST 231, COST WI, ECC 33 models with field measurement data using MATLAB	82
3.29	Combined performance analysis of (a)FSPL model (b) ECC 33 model (c) Egli model (d) Cost 231 model (e) COST WI model (f)Okumura model (g)Combined Plot of all models with measured path loss using LINEAR REGRESSION	83
3.30	Relative Errors of the measured path loss to the existing path	85

	loss of the models	
3.31	Mean error of path loss model	85
3.32	Tuned COSTWI model with minimum mean error	87
4.1	General Fuzzy Inference System	91
4.2	Depolarization of rain drops	95
4.3	Division of geographical region in to different climatic zones [Courtesy: ITU-R]	101
4.4	Indian physiographic subdivisions depicting location of Uttarakhand	102
4.5	View of regional subdivisions of Uttarakhand (Dehradun)	102
4.6	Rainfall rate exceedance curve as per ITU-R tables for some of the world physiographic divisions	103
4.7	Rainfall-rate variation for months from Jan to Dec from 2006- 2010 for Dehradun	104
4.8	Rainfall rate monthly variations for different years from 2006-2010 for Dehradun	106
4.9	Membership function defined for attenuation with horizontal polarization	109
4.10	Membership function defined for attenuation with vertical polarization	110
4.11	Membership function defined for circular polarization	110
4.12	Membership function defined for rainfall-rate	110
4.13	Fuzzy rainfall attenuation prediction module using Mamdani ANFIS	111
4.14	Fuzzy membership function	113
4.15	Total predicted specific attenuation w.r.t horizontal polarization and vertical polarization	113
4.16	Total predicted specific attenuation w.r.t horizontal polarization and circular polarization	114

4.17	Total predicted specific attenuation w.r.t horizontal polarization and rain fall rate	115
4.18	Total predicted specific attenuation w.r.t vertical polarization and rainfall-rate	115
4.19	Total predicted specific attenuation w.r.t circular polarization and rainfall-rate	116
4.20	Total predicted specific attenuation with rainfall-rate	117
4.21	Total predicted specific attenuation with horizontal polarization	117
4.22	Total predicted specific attenuation with vertical polarization	118
4.23	Total predicted specific attenuation with circular polarization	118
4.24	Graph showing results between path loss exponent, rainfall rate and transmitted power	119
4.25	Variation of path loss factor with rainfall rates	120
4.26	Variation of transmitted power and received power with path loss exponent	120
4.27	2 D view of received power versus path loss factor	121
4.28	Dual-level comparison of rainfall rate and received power with path loss factor	121
5.1	FLOW CHART OF STEP BY STEP IMPLIMENTATION OF WORK	124
5.2	Elements of Link Budget	125
5.3	Generic Link Budget	127
5.4	Generic link, showing typical elements that may be present in a Radio system	128
5.5	Link budget parameters	129
5.6	Gain and loss components in a typical uplink budget	130
5.7	Gain and loss components in a typical downlink budget	131

LIST OF TABLES

Table No.	Caption	Page No.
1.1	First Generation cellular standard	6
1.2	Second generation Digital Cellular Standards	7
1.3	Second generation digital cellular standards PDC and IS-95	8
1.4	Cordless telephone standard	13
1.5	Comparison table between 3G and 2G	14
1.6	Comparison table between WCDMA and IS-95 air interfaces	16
1.7	WCDMA parameters	17
2.1	Comparison of Air Navigation Tool	34
2.2	Features of TEMS 10.0, TEMS 9.1, TEMS 9.0, TEMS 8.0	36
2.3	TEMS supported Mobile phone's feature	42
3.1	Simulation Parameters	65
4.1	Comparison of different DSD functions	92
4.2	Typical rain drop classification based on sizes	93
4.3	Comparison table of different rain models	97
4.4	Annual rainfall distribution with % departures from mean values for the year 2006-2010	99
4.5	Elevation variability	107
4.6	Polarization variability	108
4.7	Rainfall variability	108
4.8	Rainfall-Attenuation classification	109

5.1	Mobile Power Class and Their Tolerance	134
5.2	Power Steps and Their Tolerance	135
5.3	BTS Power Class and Their Tolerance	135
5.4	Link Budget for GSM 1800	139
5.5	Power budget calculation including rain fade margin	146

GLOSARRY

PCMCIA Card: It is used to connect the trace phone and GPS to a notebook computer. The test data will be transferred from the trace phone and GPS to the notebook computer through this card.

Average end-to-end delay: This indicates the end-to-end delay experienced by packets from source to destination. This includes the route discovery time, the queuing delay at node, the retransmission delay at the MAC layer and the propagation and transfer time in the wireless channel.

Speech Quality Index (SQI)

SQI is an estimate of the perceived speech quality as experienced by the mobile user, is based on handover events and on the bit error and frame erasure distributions [53]. The SQI scale goes from -15 to 21 for Full Rate (FR) speech coders and from -15 to 30 for Enhanced Full Rate (EFR) speech coders.

Integrated Digital Enhanced Network (iDEN)

This mobile telecommunications technology is developed by Motorola. iDEN Network seats more users in a specified spectral space, compared to analog cellular and two-way radio systems, by using speech compression and Time Division Multiple Access (TDMA).

Network Intrusion Detection System (NIDS)

It is an invasion detection system which detects malevolent activities such as defense of service attacks, port scans or even attempts to crack into computers by monitoring network traffic.

High Speed Uplink Packet Access (HSUPA)

It is a 3G mobile telephony protocol in the HSPA family with uplink speeds up to 5.76 Mbit/s. The official 3GPP name for 'HSUPA' is Enhanced Uplink (EUL).

PUBLICATIONS BASED ON THE RESEARCH WORK

Presented a paper on network planning concept in MWON-2008 , 17-19 Dec at **Bangkok, Thailand** sponsored by **Department of Science and Technology (DST)**.

Gupta Vishal, Sharma S.C., “Efficient Path Loss Prediction in Mobile Wireless Communication Network” MWON 2008 - International Conference on Mobile, Wireless and Optical Communications Networks, Bangkok, Thailand, December 17-19, 2008.

Based on the research work project has been accepted in Uttarakhand Council of Science and Technology (UCOST).

Papers uploaded in IEEE digital library

Gupta Vishal , Sharma, S.C., “ Secure Path Loss Prediction in Fringe Areas Using Fuzzy Logic Approach” International conference on Advances in Computing, Control, & Telecommunication Technologies, Trivandrum, Kerala, **Print ISBN: 978-1-4244-5321-4**,pp. 372 - 375 ,28-29 Dec. 2009.

Paper in international journal and conferences

Sharma S.C., **Gupta Vishal** “Efficient Path Loss Prediction In Mobile Wireless Communication Network” *world academy of science, engineering and technology*, vol.36, 2008 ISSN 2070-3740. [Communicated: June 12, 2008; Accepted: October 15, 2008; Published: December 16, 2008]

Gupta Vishal, M C Bansal, Sharma S.C. “Fringe Area Path Loss Correction Factor for Wireless Communication” *International Journal of Recent Trends in Engineering* [ISBN 978-952-5726-04-6 (Print); ISBN 978-952-5726-05-3 (CD-ROM)], Finland.

Gupta Vishal , Sharma S. C. “Efficient Path Loss Prediction in Mobile Wireless communication Networks” *International Conference on Intelligent Systems & Networks (ISN-2008)*, Kalawad, Y. Nagar, Pp: 271-273, Feb. 22-24, 2008.

Gupta Vishal, Sharma S.C. “Efficient Path Loss Prediction in Wireless Sensor Network Using Fuzzy Logic Approach” *Advanced Computing and Communication Technologies (ICACCT-2008)*, Panipat, ISBN- 81-87433-68-X, Pp: 596-600, Nov. 08-09, 2008.

Gupta Vishal, Sharma S.C., M C Bansal, “Fuzzy Logic: An Efficient Approach for Predicting Path Loss in Fringe Areas” *ICE-FST’09, L.I.E.T , Alwar , Rajasthan* on 9-11 April 2009, Pp:517-522.

Sharma S.C., **Gupta Vishal** “Fuzzy Model Approach for reduction of Path Loss” *Proceeding of Fourth IEEE Conference on Wireless Communication and Sensor Networks (WCSN-2008)*, IITA & DAVV, Indore, IEEE Catalog Number. CFP0875D, ISBN: 978-1-4244-3328-5, Library of Congress: 2008909475, Dec. 27-29, 2008, Pp: 236-239

CHAPTER 1

INTRODUCTION

In the present scenario wireless communication is spreading throughout the world, it has covered each and every area and can reach anywhere in any form [17], [6]. In the recent years, for increasing the intensity of the wireless communication technology is changing exponentially with the telecommunication landscape continuously. Next generation will be benefitted by the introduction of the high speed data communication in addition to voice calls[103],[96]. For getting efficient utilization of the mobile networks, factors like cost effective, high quality services and effect of terrain should be taken into account. Propagation models are used to calculate the propagation characteristics. The propagation channel [3] is used to characterize the mobile radio system in terms of transmission power and frequency re-use. The accuracy of propagation model should be high due to the increased expectation of the customers as compare to the past users whose requirements are limited and vendors does not identify the uncovered bins[97],[29],[49].

1.1 Background

Radio systems and technologies have undergone a wide change, since the first cellular and cordless telecommunication devices were introduced in 80's. The 1G cellular and cordless telecommunication devices were based fundamentally on the foundation of analog Frequency Modulation (FM) and were deployed only for carrying narrow-band voice data. Whereas 2G cellular and telecommunication systems introduced in the early 90's were focused more on digital modulation techniques and provided better spectral efficacy and quality. Still, these systems were deployed for voice and data transmission only. 3G wireless systems, presently under development can offer easefully higher data rates ranging from 9.6 kb/s for satellite propagation, 144 kb/s for mobility prone transmission, 384 kb/s for steeply mobile propagations to 2.048 Mb/s for indoor profile propagations

[93]. These are deployed to provide audio, data, and the bandwidth hungry multimedia services, while following constraints of tight availability and Quality of Service (QoS) requirements in all varieties of available niches. Fourth generation devices in near future are expected to further strengthen the broadband wireless services with a variety of available bit rate packages that too in increased size. The present analysis is based on 2G and 3G network. To design an efficient wireless network system in a given region, proper understanding and awareness regarding the radio wave propagation models is required. Wireless propagations are fundamentally described on the basis of region of influence and available bandwidth (as depicted in Figure 1.1) Mobility prone satellite communications offer wide influence to mobile subscribers but at a reduced data rate. Terrestrial mobile radio vendors deploy cell-site and microcell-site configuration approach to achieve wider influence zone as compared to other kinds of mobile services. Pivoted radio deployment can establish connection-links throughout the street or any institutional zone to accessing subscribers. Moreover, WLAN can provide indoor subscriber's high data rate derived performance.

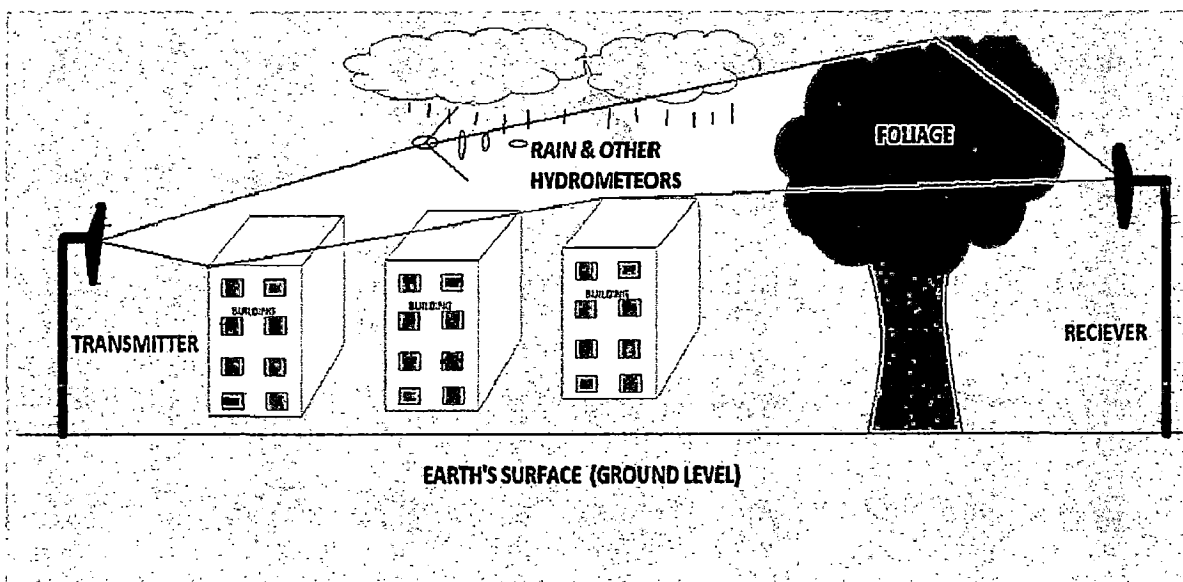


Figure 1.1: A Fundamental Wireless communication system

1.2 Spectral Radio Differentiation [35]

Radio spectrum is generally differentiated into various frequency based sub-bands for a particular class of implementation. Deployment stability is directly proportional to the atmospheric propagation characteristics for a specified frequency and other parameters such as transmitter height and channel vulnerabilities [70]. Laid on such fundamental aspects, the radio spectrum is primarily resolved into the following sub-spectra's:

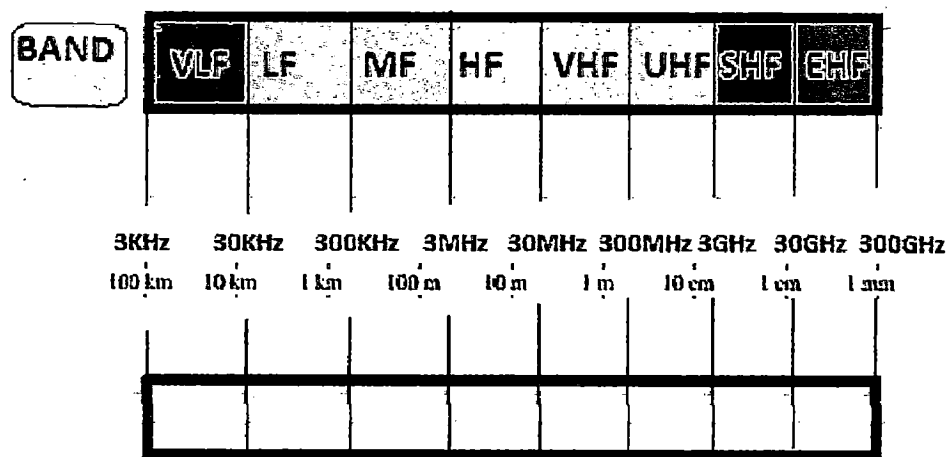


Figure 1.2: The Electromagnetic Spectrum

Extremely Low Frequency (ELF) [300 – 3000 Hz]

Very Low Frequency (VLF) [3 – 30 kHz]

Propagation Features: The wave propagates between the surface of the Earth and the ionosphere. It can penetrate deep underground and underwater. As the required antenna size is proportional to the wavelength, the large wavelength in this case mandates the use of large antennas.

Use: mining, underwater communication (submarines), SONAR.

Low Frequency (LF) [30 – 300 kHz]

Propagation Features: Here ground wave is the dominant mode and the radiation characteristics are strongly influenced by the presence of the Earth. The antennas which are used for these ranges are still quite large and high power transmitters are used.

Use: broadcasting, radio navigation.

Medium Frequency (MF) [300 – 3000 kHz]

Propagation Features: The propagation characteristics are similar to the LF but the increased in bandwidth allow MF band application for commercial purpose. Ground wave gives usable signal strength up to 100 km from transmitter.

Use: AM radio broadcasting (550 – 1600 kHz).

High Frequency (HF) [3 – 30 MHz]

Propagation Features: Ground wave propagation also exists in HF band but the sky wave is the main propagation mode. The ground wave is used for communication over shorter distances than the sky wave. As propagation loss increases with increase in frequency, the use of repeaters is required.

Use: Broadcasting over large areas, amateur radio and citizens band (CB) radio.

Very High Frequency (VHF) [30 – 300 MHz] [107]

Propagation Features: Diffraction (bending of waves due to obstruction) and reflection give rise to communication beyond the horizon. Propagation distances are thousands of kilometers. The diffraction and reflection enables reception within buildings.

Use: TV broadcast, FM radio (88 – 108 MHz), radio beacons for air traffic control.

Ultra High Frequency (UHF) [300 – 3000 MHz] [107]

Propagation Features: Reflection via atmospheric layers is possible. Impact of rain and moisture are negligible.

Use: satellite broadcasting, all generation land mobile phones, cordless, air traffic control.

Super High Frequency (SHF) [3 – 30 GHz]

Propagation Features: Range becomes limited and the attenuation of radio waves becomes more prominent as the frequency increases. Propagation is limited by absorption, rain and clouds.

Use: Satellite services for telecommunications, mobility prone services of future

Extremely High Frequency (EHF) [30 – 300 GHz]

Propagation Features: Considerable attenuation via. Hydrometeors like water, oxygen and vapors.

Use: Short distance communications (within line of sight), satellite broadcasting in HDTV (for information exchange between satellites in space)

BSNL Wireless system used in current analysis falls in the radio spectrum between Ultra High Frequency (UHF) [300 – 3000 MHz].

Now after a brief study of the radio spectrum and its differential classification we need to consider different available wireless radio systems and standards which form the core of modern day technology lead communications. Moreover, this will also facilitate better perception of the radio propagation deployment in use today.

1.3 Wireless Radio Standards [7], [51]

The development in the field of radio communication technology has been going on since the late 50's, although the first business technology was brought into existence in the late 70's and early 80's. Here a short block on the radio wireless technologies and the related networks is presented which created a considerable impact on the fast evolution of the wireless communications[38],[47],[45].

1.3.1 First Generation Systems [1G]

In 1976, the World Allocation Radio Conference (WARC) passed the bandwidth approval for cellular communications for implementation of mobile systems. In the early 1980s, most of the nations across the world began implementation of 1G cellular systems based

on frequency division multiple accesses (FDMA) and analog FM technology. During 1979, the first analog cellular system, the Nippon Telephone and Telegraph (NTT) system, came in to functionality. In 1981, Ericsson Radio Systems AB fielded the Nordic Mobile Telephone (NMT) 900 system, and in 1983 AT&T deployed the Advanced Mobile Phone Service (AMPS) as a trial in USA. Several other first generation analog systems were also deployed in the early 1980s including TACS, ETACS, NMT 450, C-450, RTMS, and RADIOCOM 2000 in Europe, and JTACS/NTACS in Japan. The basic parameters of NTT, ETACS, and AMPS are shown in Table 1.1.

Table 1.1: First Generation cellular standard

CHARACTERSTICS	NTT	ETACS	AMPS
Frequency Band [Forward and Reverse]	925-940 and 870-885	935-960 and 890-915	824-849 and 869-894
Channel spacing	25KHz	25KHz	30KHz
Spectral Efficiency	0.012 bps/Hz	0.33 bps/Hz	0.33 bps/Hz

1.3.2 Second Generation Systems [2G]

Second generation digital cellular systems include the GSM/DCS1800/PCS1900 standard in Europe, the PDC standard in Japan and the IS-54/136 as well as IS-95 standards in the United States. Parameters of the air interfaces of these standards are summarized in Table 1.2 and 1.3.

Table1.2: Second generation Digital Cellular Standards

Feature	GSM/DCS1800/PCS1900	IS-54/136
Frequency Band	GSM:890-915	824\829
RL/FL (MHz)	935-960	869/894
Multiple Access	TDMA	TDMA
Carrier Spacing (KHz)	200	30
Modulation	GMSK	$\pi/4$ -DQPSK
Baud Rate (Kb/s)	270.833	48.6
Frame Size (ms)	4.615	40
Slots/Frame	8/16	3/6
Voice Coding (Kb/s)	VSELP(HR 6.5) RPE-LTP (FR 13) ACELP (EFR 12.2)	VSELP(FR 7.95) ACELP (EFR 7.4) ACELP (12.2)
Channel Coding	Rate-1/2 CC	Rate-1/2 CC
Frequency Hopping	yes	no
Handoff	hard	hard

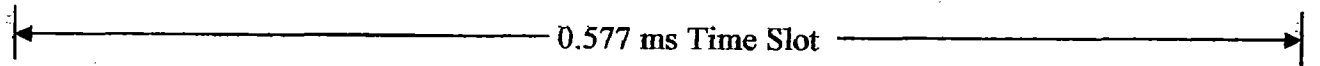
Table 1.3: Second generation digital cellular standards PDC and IS-95

Feature	PDC	IS-95
Frequency Band	810-826	824-829
RL/FL (MHz)	940-956 1429-1453 1477-1501	869-894 1930-1990 1850-1910
Multiple Access	TDMA	CDMA
Carrier Spacing (KHz)	25	1250
Modulation	$\pi/4$ -DQPSK	QPSK
Baud Rate (Kb/s)	42	1228.8 M chips/s
Frame Size (ms)	20	20
Slots/Frame	3/6	1
Voice Coding (Kb/s)	PSI-CELP(HR 3.45) VSELP (FR 6.7)	QCELP(8,4,2,1) RCELP
Channel Coding	Rate-1/2 BCH	FL: Rate-1/2 CC
Frequency Hopping	no	N/A
Handoff	hard	soft

Global System for Mobile Communications (GSM) [108]

European countries witnessed the deployment of incompatible first generation cellular systems which prevents roaming throughout the Europe. As a result, a Conference of European Postal and Telecommunications Administrations (CEPT) took place and as an outcome of this Groupe Speciale Mobile (GSM) in 1982 with the mandate of defining standards for future Pan-European cellular radio systems were formed. The GSM system (now "Global System for Mobile Communications") was nourished to operate in a new frequency band and to be more quality based, Pan-European roaming and the support of data services was its prime aim[34]. GSM came in to deployable phase in late 1992 as the world's first digital mobile system. In its present form, GSM facilitate full and half rate

functionality provides different aligned and non-aligned communication services at 2.4, 4.8, and 9.6 kb/s that operate in interfacial mode with voice band modems. GSM deploys TDMA with 200 kHz carrier separation, eight channels per carrier with a time slot (or burst) duration of 0.577 milli-seconds, and Gaussian minimum shift keying (GMSK) modulation technique with a rough data rate of 270.8 kb/s. The time slot outlook of the GSM traffic channels is shown in Figure 1.3. Varieties of GSM are available now days to operate in higher frequency bands. In Europe, the Digital Cellular System 1800 (DCS 1800) was developed by ETSI as a standard for Personal Communication Networks (PCNs). DCS 1800 was derived from the GSM system, but differs in a number of ways. Firstly, DCS1800 operates in the 1710-1785 MHz (MS transmit) and 1805-1880 MHz (BS transmit) bands, whereas GSM operates in the 900-1800 MHz band. Secondly, DCS 1800 is optimized for two classes of hand held portable units (rather than mobile units) with a peak power of 1 W and 250 mW, respectively. There are also some changes in the DCS 1800 standard to support overlays of macro cells and micro cells. GSM is deployed in North America as PCS 1900 and operates in the 1880-1990MHz PCS bands. PCS 1900 is similar to DCS 1800, but with a few differences. One is the use of the ACELP EFR (Enhance Full Rate) vocoder that was developed for the North American market. GSM has been a phenomenal success. In late 1997, 66 million GSM subscribers were serviced by 256 network operators in 110 countries. Moreover nearly 80% of world's communication systems are GSM driven. Four BTSID of BSNL GSM network has been chosen for data collection in current analysis.



R	TCH	C	SW	C	TCH	R	G
3	57	1	26	1	57	3	8.25

R Guard time for burst transient response (Ramp time)

TCH Traffic Channel

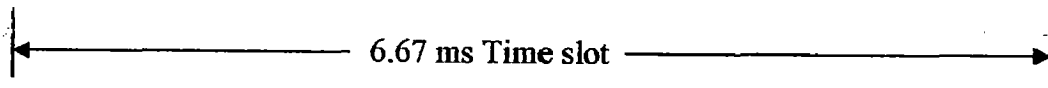
C Control Bit

SW Synchronization word

G Guard bits

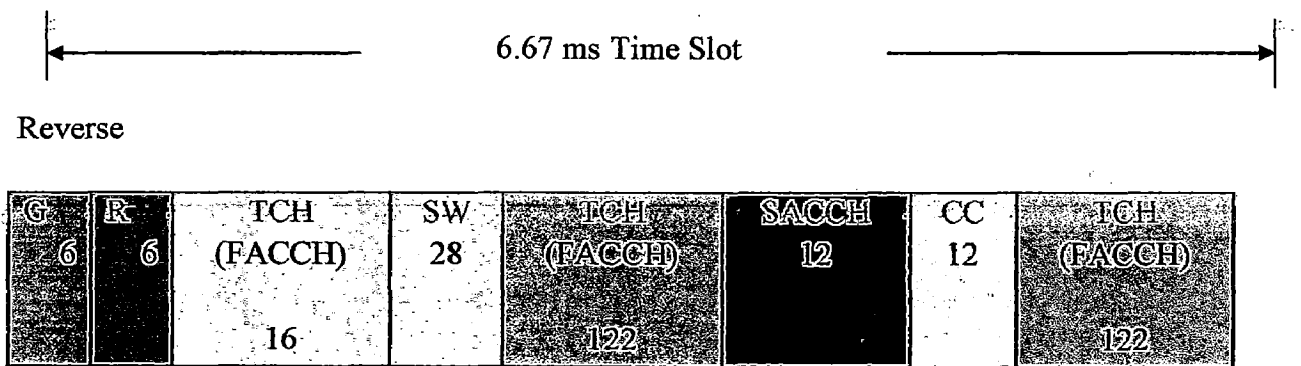
Figure 1.3: Time slot format for GSM

IS-54/136 and IS-95



Forward

SW 28	SACCH 12	TCH (FACCH) 130	CC 12	TCH (FACCH) 130	RVSD 12
----------	-------------	-----------------------	----------	-----------------------	------------

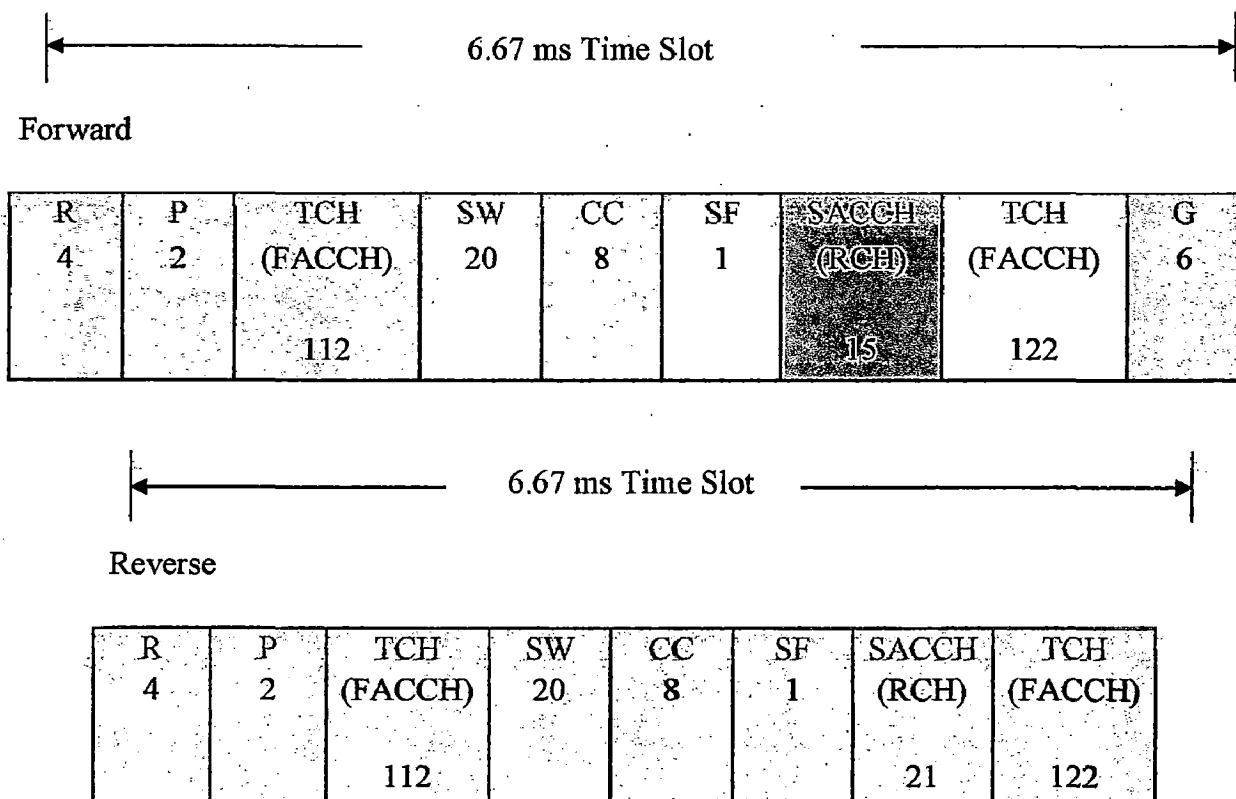


- G Guard Bits
- R Guard Time for burst transient response (Ramp Time)
- SACCH Slow Associated Control Channel
- FACCH Fast Associated Control Channel
- SW Synchronization Word
- CC Color Code
- TCH Traffic Channel
- RSVD Reversed

Figure 1.4: Burst format for IS-54/136 traffic channel

Personal Digital Cellular

Around 1991, the Ministry of Posts and Telecommunications in Japan authorized Personal Digital Cellular (PDC). The free to air interface of PDC is alike in some of the aspects as to IS-54/136. It deploys TDMA with 6 half speed channels per carrier, 25 KHz carrier separation and 45° DQPSK modulation techniques with a rough information rate of 42 Kb/s.



- G Guard bits
- R Guard time for burst transient response (Ramp Time)
- SACCH Slow Associated Control Channel
- FACCH Fast Associated Control Channel
- SW Synchronization Word
- CC Color Code
- TCH Traffic Channel, RSVD Reversed
- P Preamble
- SF Steal Flag

Figure 1.5: Time slot format of Japanese PDC

Cordless Telephone Systems

Cordless equipment has several applications including local telephones, telepoint (cordless phone booth), wireless PABX (Private Access Business Exchange), and wireless local loops or radio drops. Similar to cellular telephones, first generation cordless telephones were used to work on analog FM technology.

Table 1.4: Cordless Telephone Standard

Feature	CT2	CT2+	DECT	PHS
Frequency Band (MHz)	864-868	914-918	1880-1900	1895-1913
Multiple Access	FDMA	TDMA	TDMA	TDMA
Duplexing	TDD	TDD	TDD	TDD
Carrier Spacing	100	100	1728	300
Bit rate (kb/s)	72	72	1152	384
Speech Coding	ADPCM	ADPCM	ADPCM	ADPCM
	32 kb/s	32 kb/s	32 kb/s	32 kb/s
Frame Size (ms)	2	2	10	5
Mean TX Power (mW)	5	5	10	10
Peak TX Power (mW)	10	10	250	80

1.3 3G Cellular System (WCDMA) [32]

The third generation cellular networks were developed with a target of offering high speed information [2] and multimedia services to the subscribers. The International Telecommunication Union (ITU) [41] under the initiative IMT-2000 has defined 3G systems as being capable of supporting high speed data ranges of 144 kbps to greater than 2 Mbps. A few technologies are able to fulfill the International Mobile Telecommunications (IMT) standards, such as CDMA [4], [43], UMTS and some variation of GSM such as EDGE. WCDMA (Wideband Code Division Multiple Access) is the main third generation air interface in the world and deployment of third generation cellular

networks has been started in Europe, Asia, Japan and Korea, in the frequency band around 2 GHz [112],[111].

Table 1.5: Comparison between 3G and 2G

PARAMETERS	WCDMA(3G)	GSM(2G)
Carrier spacing	5 MHz	200 kHz
Frequency reuse factor	1	1-18
Power control frequency	1500 Hz	2 Hz or lower
Quality control	Radio resource management algorithms	Network planning (frequency planning)
Frequency diversity	5 MHz bandwidth gives multipath diversity with receiver	Frequency hopping
Packet data	Load-based packet scheduling	Time slot based scheduling with GPRS
Downlink transmit diversity	Supported for improving downlink capacity	Not supported by the standard, but can be applied

The main differences between the third and second generation air interfaces are described in Table 1.5. BSNL 900-1800 MHz GSM and IS-95 (the standard for CDMA systems) are the second generation air interfaces considered in thesis. Table 1.6 gives difference between WCDMA and IS-95. In this comparison only the air interface is considered. GSM also covers services and core network aspects, and this GSM platform will be used together with the WCDMA air interface.

Table 1.6: Comparison table between WCDMA and IS-95 air interfaces

PARAMETERS	WCDMA	IS-95
Carrier spacing	5 MHz	1.25 MHz
Chip rate	3.84 Mcps	1.2288 Mcps
Power control frequency	1500 Hz, both uplink and Downlink	Uplink: 800 Hz, downlink: slow power control
Base station synchronization	Not needed	Yes, typically obtained via GPS
Inter-frequency handovers	Yes, measurements with slotted mode	Possible, but measurement method not specified
Efficient radio resource management algorithms	Yes, provides required quality of service	Not needed for speech only Networks
Packet data	Load-based packet scheduling	Packet data transmitted as short circuit switched calls
Downlink transmit diversity	Supported for improving downlink capacity	Not supported by the standard

1.4.1 Specification of 3G (WCDMA) [75]

WCDMA has two modes characterized by the duplex method i.e. FDD (Frequency Division Duplex) and TDD (Time Division Duplex), for operating with paired and unpaired bands. The chip rate of the system is 3.84 Mcps. The frame length is 10 ms and each frame is divided into 15 slots (2560 chip/slot at the chip rate 3.84 Mcps). Spreading factors range from 256 to 4 in the uplink and from 512 to 4 in the downlink. Table 1.7 lists the parameters of WCDMA.

Table 1.7: WCDMA parameters

Multiple access method	DS-CDMA
Duplexing method	Frequency Division Duplex/Time Division Duplex
Base station synchronization	Asynchronous operation
Chip rate	3.84 Mcps
Frame length	10 ms
Service multiplexing	Multiple services with different quality of service requirements multiplexed on one connection
Multirate concept	Variable spreading factor and multicode
Detection	Coherent using pilot symbols or common pilot
Multiuser detection, smart antennas	Supported by the standard, optional in the implementation

Table 1.7 summaries the main parameters related to the WCDMA air interface. Signal transmitted from transmitter to receiver in 1G, 2G and 3G has to face different channel noises and propagation loss which is unpredictable to the receiver, so for the wireless network design the propagation effect, channel noises and fading must be consider to deliver the baseband signals to its final destination with as few error as possible.

1.5 Effect of terrain on signal propagation [17]

Path loss [7]

Path loss normally includes propagation losses caused by spreading of radio waves (Diffraction, Absorption, Reflection, Refraction, and Shadowing) in free space from transmitting antenna which result in overall decrease in signal/field strength and it depends on the distance between the transmitter and receiver. Outdoor propagation models are used to determine the path loss due to terrain i.e. foliage, rain, buildings etc.

Diffraction loss

When a part of radio wave front is obstructed by an obstacle then losses occur in signal is known as diffraction loss (Figure 1.6). In outdoor propagation this loss occurs due to building, mountains etc.

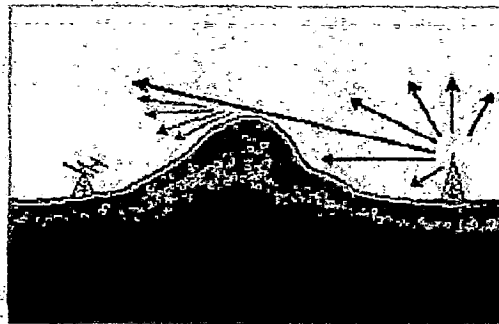


Figure 1.6: Diffraction Loss

Absorption loss

When the signal passes through media not transparent to electromagnetic waves then penetration losses occur in signal which is also known as absorption losses. In fringe area of Dehradun , Uttarakhand this loss occurs due to rain , fog etc.

Reflection losses [61]

Reflection occurs in signal from the smooth surfaces of walls and hills produce losses in signal which is known as reflection losses (Figure 1.7).

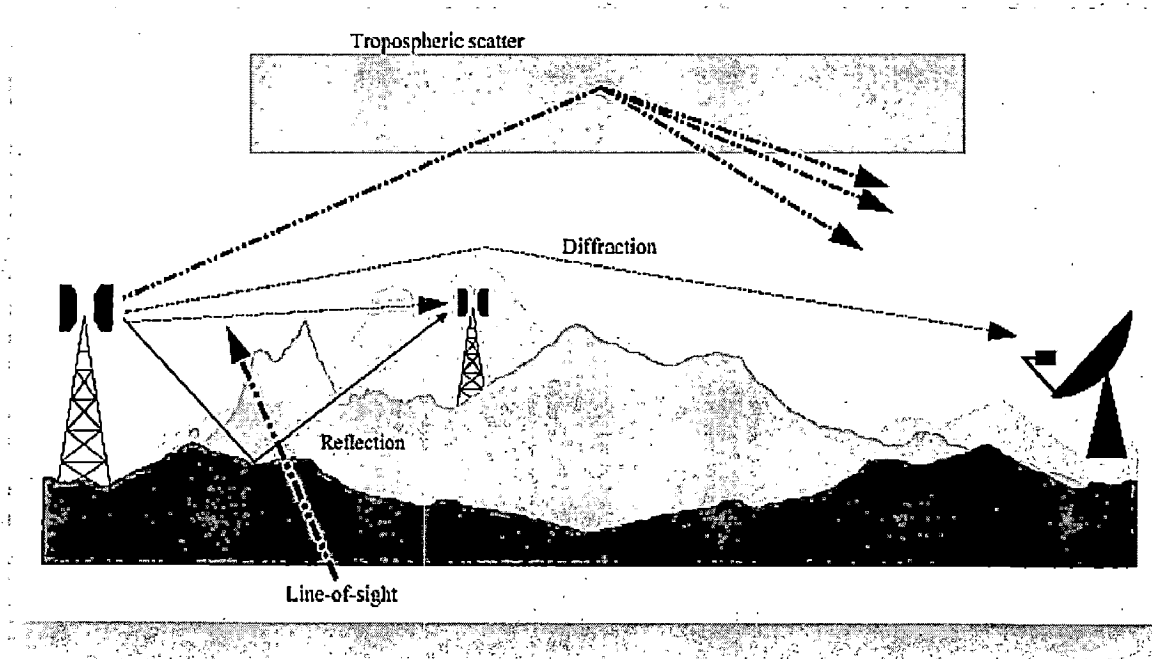


Figure 1.7: Reflection Loss

Refraction losses

Due to different layers of atmosphere refraction takes place which result in refraction losses in signal. Losses due to scattering of signal from the surfaces which are not smooth such as sea, rough ground, branches and leaves of trees.

Shadowing

Shadowing is caused by the superimposing of signal via refraction, reflection etc. shadowing is also known as slow fading. When the amplitude of radio signal changes

FRINGE AREAS OF DEHRADUN, UTTARAKHAND-INDIA



quickly in a short time period or in a short travel distance then it cause slow fading in signal.

Fast fading

The signal radiated by transmitter to a receiver may also travel along simultaneously different paths and at receiving antenna these multipath waves combined to produce resultant receiving signal that may vary widely, depending on relative time of propagation of signal, transmitted signal bandwidth and on the distribution of the intensity. These occurs fading in signal which is known as multipath fading and also called as fast fading. Concentrating the size of antenna and traffic densities in the process of wireless communication there are two main outdoor systems which are microcells and microcells.

Macro cells

To provide mobile services with in medium traffic densities areas macro cells are used [16]. These macro cells are designed basically in rural and suburban areas [99] and other areas having medium traffic densities with base station antenna having greater heights than the surrounding buildings. As in these cells traffic density is low so it can cover large region and hence providing a cell radius from around 1 km to many 5 Km. It is mostly operated at VHF and UHF. According to the definition of a macro cells: $h_b > h_{obst}$

Microcells

To provide mobile services in high traffic densities areas microcells are used. Microcells are defined in urban and suburban areas and other areas having high traffic densities with base station antennas having lower heights than nearby building rooftops. As it is used for high traffic densities so it can cover small region and hence having cell length up to around 500m. It also mostly operated at VHF and UHF. According to the definition of microcells:

$h_b < h_{obst}$

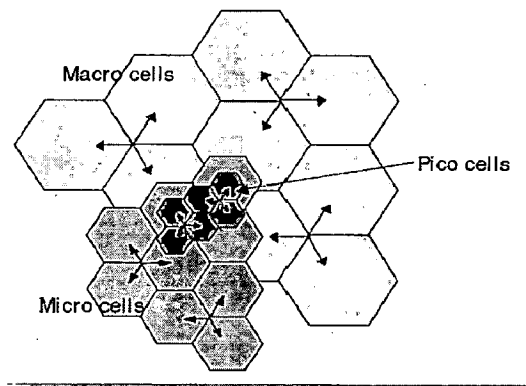


Figure 1.8: Cell Structure

Pico cells

Pico cells are defined as the same layer as micro cells and are usually used for indoor coverage.

1.6 Area Types [16]

The clutter areas generally classified as four types those are mentioned below:

Dense Urban

The dense urban area contains large population and high buildings. In this type of areas there exist few or no trees due to the density of buildings. In India Southern part of Mumbai can be taken as an example for dense urban areas. In these types of environments, even 100-foot cells have micro cell preparation, which is dominated by building location.

Urban

The urban of areas contains metropolitan regions (cities), industrial areas and closely spaced residential building and multistoried apartments. Building density is high along with trees and some other vegetation.

Suburban

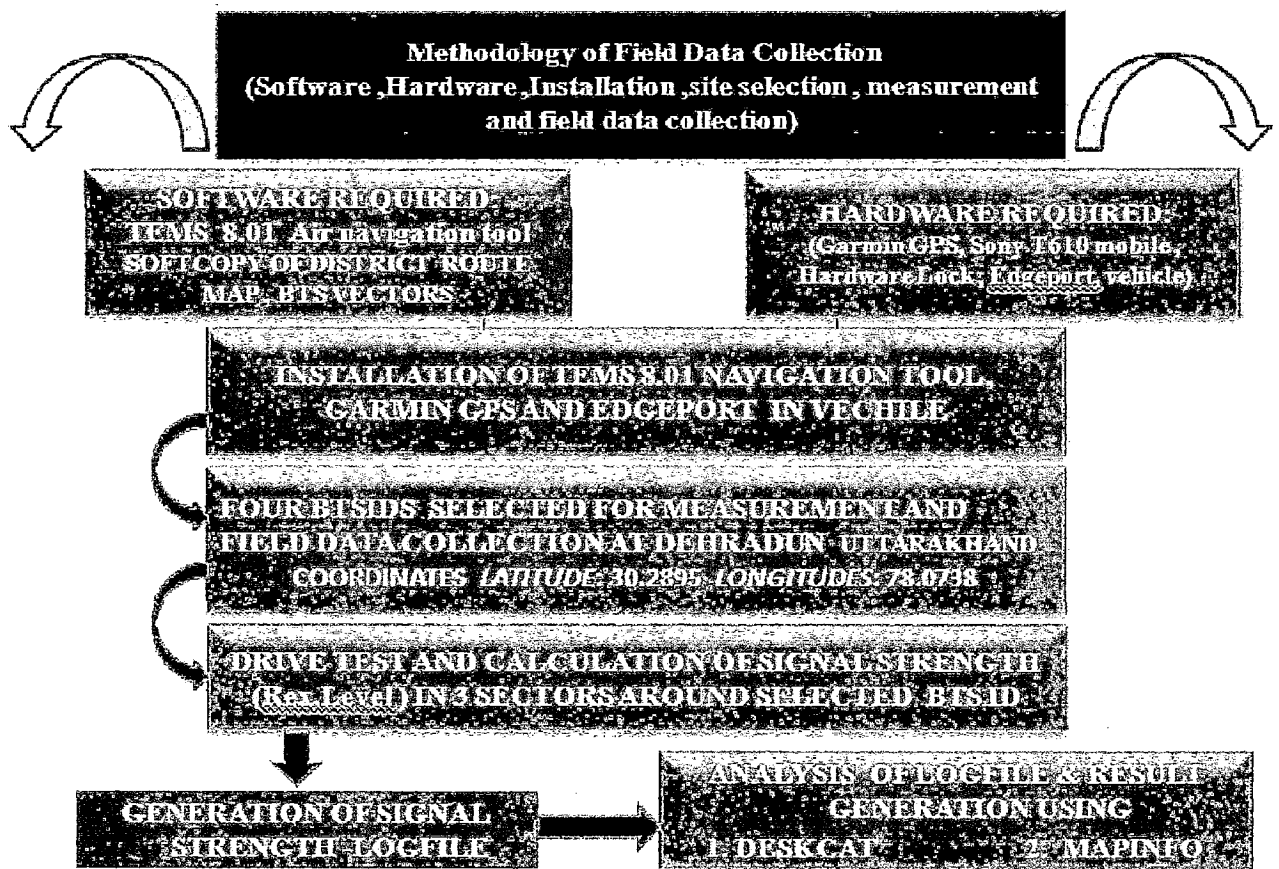
The sub urban areas consist mainly of single family homes, shopping malls and office parks along with noticeable vegetation and tree. In this area most Buildings are 1 to 3 stories but significant exceptions do occur. Towns near to urban areas are main examples of this type of environment.

Rural

The Rural areas consists lots of open space with few residential areas and less population. The significant variations in cell coverage area are found in rural areas due to differences in vegetation and terrain.

This Chapter deals with the basic background of wireless communication followed by brief description of the parameter i.e. Spectrum allocation, wireless radio standards, 1G, 2G, GSM, cordless telephone systems and 3G, selected for present analysis. Most of the description like comparison of 2G, 3G are shown in the tabular (Table 1.1 – 1.7) form.

Different outdoor path loss models are introduced in wireless communication system to predict the path loss encountered in macro cells between the base station and every possible mobile location. The brief description of different outdoor path loss models are described in Chapter 2.



FLOW CHART OF METHODOLOGY OF DATA COLLECTION

CHAPTER 2

OUTDOOR PROPAGATION MODELS AND METHODOLOGY OF FIELD DATA COLLECTION

2.1 Background

Path loss is the phenomenon which occurs when the received signal becomes weaker and weaker due to increase in the distance between mobile and base station. The path loss between a pair of antennas can also be expressed as the ratio of the transmitted power to the received power. It includes all of the possible elements of loss associated with interactions between the propagating wave and any objects between transmit and the receive antennas. The elements of a simple wireless link are shown in Figure 2.1. The power appearing at the receiver input terminals P_R , is expressed in equation 2.1

$$P_R = (P_T G_T G_R) / L_T L L_R \quad (2.1)$$

where G_T is Transmitting antenna gain, G_R Receiving antenna gain L_T Transmitting Feeder Loss, L Path Loss expressed as power ratios and powers expressed in watts.

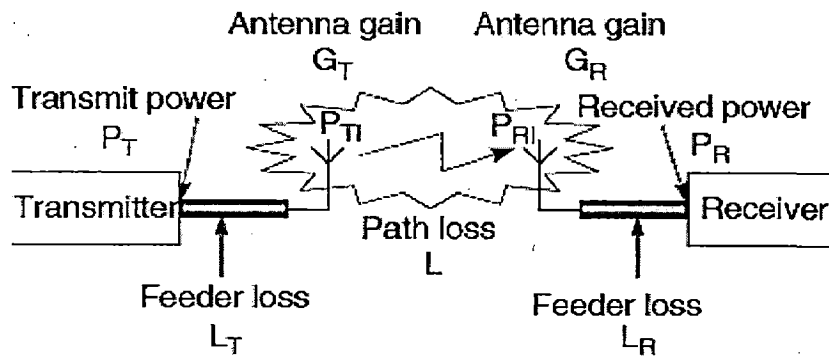


Figure 2.1: Elements of a wireless communication system

The antenna gains are expressed with reference to an isotropic antenna, which radiates the power delivered to it equally in all directions. The Effective Isotropic Radiated Power (EIRP) is given by equation 2.2.

$$EIRP = (P_T G_T) / L_T = P_{TI} \quad (2.2)$$

where, P_{TI} is the effective isotropic transmit power. Similarly, the effective isotropic received power P_{RI} , is given in equation 2.3.

$$P_{RI} = (P_R L_R) / G_R \quad (2.3)$$

The advantage of expressing the powers in terms of EIRP is that the path loss L , can then be expressed independently of system parameters by defining it as the ratio between the transmitted and the received EIRP,

Path loss,

$$L = P_{TI} / P_{RI} = (P_T G_T G_R) / (P_R L_T L_R) \quad (2.4)$$

The main goal of propagation modeling is to predict L as accurately as possible, allowing the range of a radio system to be determined before installation. The maximum range of the system occurs when the received power drops below a level which provides just acceptable communication quality. This level is often known as the receiver sensitivity. The value of L for which this power level is received is the maximum acceptable path loss. The path loss in decibels can be expressed as equation 2.5

$$L (dB) = 10 \log (P_{TI} / P_{RI}) \quad (2.5)$$

2.2 Path Loss Prediction Model

The prediction of path loss is a very important step in planning a mobile radio system, and accurate prediction methods [71] are needed to determine the parameters of a radio system, which will provide efficient and reliable coverage of a specified service area. A path loss prediction or propagation model is the fundamental tool for designing any wireless communication system. Since it become very costly if site measurements is used to design a system, so as an alternative propagation model has been developed which are more suitable, convenient and low cost. These models typically focus on path loss realization and predict what will happen to the transmitted signal as it travel from transmitter to the receiver. The propagation model can be broadly categorized into outdoor and indoor

propagation models. The outdoor propagation models are used to understand the link performance of macro cellular systems while indoor model are used for micro cellular environment.

2.2.1 Indoor Models

With the advent of Personal Communication System (PCS), there is a great deal of interest in characterizing radio propagation inside buildings. Indoor channels may be classified either as Line of Sight (LOS) or obstructed, with varying degrees of clutter. Some of the key models which have recently emerged for Indoor are:

- a) Log distance Path Loss Model
- b) Ericsson Multiple Breakpoint Model
- c) Attenuation factor model

2.2.2 Outdoor Models

Radio transmission in a mobile communication system [105],[106] often takes place over irregular terrain. The terrain profile of a particular area needs to be taken into account for estimating the path loss. The terrain profile varies from a simple curved earth profile to a highly mountainous profile. The presence of trees, building and other obstacles also must be taken into account. A number of outdoor propagation models are available to predict path loss over irregular terrain. While all these models aim to predict signal strength at a particular receiving point or in a specific local area (called a sector), the methods vary widely in their approach, complexity and accuracy. Most of these models are based on a systematic interpretation of measured data obtained in the service area. The outdoor propagation models can further be classified as **Theoretical, Physical and Empirical.**

Theoretical Model

Theoretical models are based on some theoretical assumptions about the propagation environment. These models are also called statistical model. These models are useful for analytical studies of the behavior of communication systems under a wide variety of channel response circumstances. These models do not deal with any specific propagation

information, so they are not suitable for planning communication systems to serve a particular area. These types of models usually rely on assumptions that lead to mathematical formulations. The Geometrically Based Single Bounce Macro cell (GBSBM) channel model and Quasai – Wide Sense Stationary Uncorrelated Scattering (Quasi-WSSUS) channel model are examples of theoretical models.

Physical Model

Physical models depend on the basic principles of physics and take into account the propagation environment. These models can be either site specific or not site specific. An example of these types of models is Walfisch-Bertoni model given by W. Ikegami and H.L. Bertoni for mobile radio systems in urban areas, where roof edges are considered as a series of diffracting screens with final diffraction from building roof to the street level being included. A physical and site specific channel model not only uses the physical law of electromagnetic wave propagation but also have a systematic technique for mapping the real propagation environment into a model of propagation environment. Epstein-Peterson method, Deygout method, Longley Rice model, Anderson two dimensional (2D) model which only predict signal attenuation over terrain and ray tracing model, which provides time dispersion information and angle of arrival information are the examples of physical and site specific channel model. These models make use of the laws governing electromagnetic wave propagation in order to determine the received signal power in a particular location.

Empirical Model

Empirical models fundamentally use experimental measurement data to produce a relationship between the propagation circumstances and expected field strength or time dispersion results. It can also be developed from measurements made in laboratory or with scale models of propagation environments. This approach is based on fitting curves or analytical expressions that recreate set of measured data. This has advantage of taking account all propagation factors, both known and unknown through actual field measurements. However, the validity of an empirical model at transmission frequencies or

environments other than those used to derive the model can only be established by additional measured data in new environment at the required transmission frequency. By definition, an empirical model is based on data used to predict, not explain a system and are based on observations and measurements alone. It can be split into two subcategories, time dispersive and non-time dispersive.

2.3 Empirical Outdoor Propagation Models [99],[101]

2.3.1 Free Space Path Loss Model

Free space path loss is a loss in an electromagnetic wave's signal strength that would result from an unobstructed line of sight path through free space.

2.3.2 Egli Model

Ease of implementation and agreement with the empirical data makes Egli model a popular choice for a first analysis. Egli model provides the entire path loss, whereas the Okumura model discussed below provides the path loss in addition to free space loss [72],[109]. This model is empirical in nature and applicable to scenarios where the transmission has to pass an irregular terrain. Egli model is not applicable to scenarios where some vegetative obstruction is in the middle of the link.

2.3.3 Okumura Model

Okumura model is the most widely used model for signal prediction in the urban areas. This model is applicable for frequencies in the range 150 MHz to 1920 MHz (although it is typically extrapolated up to 3000 MHz) and distances to 1 km to 100 km. It is used for base station antenna heights ranging from 30 m to 1000 m.

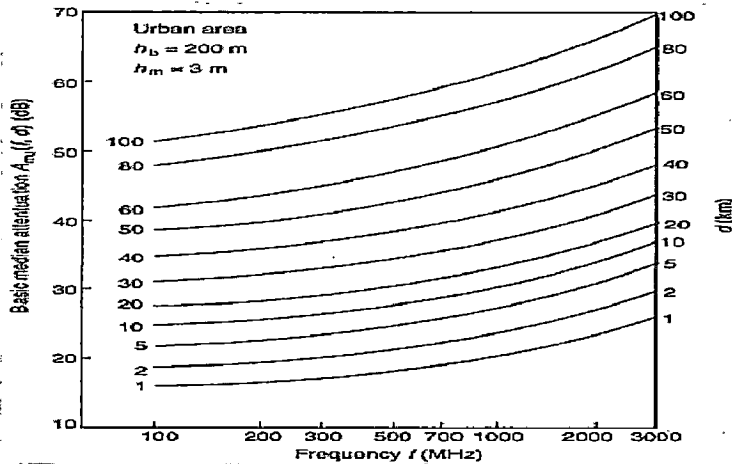


Figure 2.2: Median attenuation relative to free space $A_{\mu}(f,d)$, over a quasi-smooth terrain

A set of median attenuation curves relative to free space (A_{μ}) were developed by Okumura (Figure 2.2), in an urban area over quasi smooth terrain with a base station effective antenna height (h_{te}) of 200 m and a mobile antenna height (h_{re}) of 3 m. These curves were developed from extensive measurement using vertical omni directional antennas at both the base and mobile. Curves are plotted as a function of frequency in the range 100 MHz to 1920 MHz and also as a function distance from base station in the range 1 km to 100 km. To determine path loss using Okumura model, the free space path loss between the points of interest is first determined and then the value of A_{μ} (from curve) is added to it along with the correction factors to account for the terrain type [76].

2.3.4 Hata Model

Hata developed a mathematical formulation from Okumura prediction curves in order to obtain simple computational applications. Therefore, this model is then called Okumura-Hata model or Hata model. Hata prediction model is based on propagation measurement conducted in Kanto (near Tokyo), Japan by Okumura. This model presents signal strength prediction curves over distance in a quasi-smooth urban area (terrain undulation is less than 20 m). In order to predict other types of area classifications, correction factors for suburban and open areas is considered [73], [74].

2.3.5 COST 231 Hata Model

A model that is widely used for predicting path loss in mobile wireless system is the COST 231 Hata model . It was an extension of Hata model. The COST 231 Hata model is designed to be used in the frequency band from 1500 MHz to 2000 MHz. It also contains corrections for urban, suburban and rural (flat) environments.

2.3.6 ECC-33 Model [22]

The medium city model is more appropriate for European cities whereas the large city environment should only be used for cities having tall buildings. It is interesting to note that the predictions produced by the ECC-33 model do not lie on straight lines when plotted against distance having a log scale.

2.3.7 Lee Model

The Lee model is a modified power law model, with parameters taken from measurements in a number of locations, together with a procedure for calculating an effective base station antenna height which takes account of the variations in the terrain.

MODELS	FREQUENCY RANGE	APPLICABLE	DRAWBACKS/ DIFFERENT TERRAIN SUPPORT
ITU Terrain Model	Any	LOS	Support all terrains based on diffraction theory
Egli model	Not specified	LOS	Not applicable in the foliage area, rugged terrain and significant obstruction.
Weissberger's model	230 MHz-95 GHz	LOS	Only applicable when foliage obstruction in the microwave link
Lee model	900 MHz	LOS/NLOS	Use more correction factors to make it flexible in all conditions
Longley –Rice model	20 MHz-20 GHz	LOS/NLOS	Suitable in VHF and UHF use. Cannot consider the correction factor due to building and foliage.
Okumura Model	150 MHz-1920MHz	LOS	Multipath is not considered. Slow response to rapid changes in terrain. It is not good for rural area.

Hata Model	150 MHz-1500MHz	LOS	It does not provide for any path specific correction factor , as is available in Okumura Model. For distance $d > 1\text{km}$, The Hata model well approximate the Okumara model. Not good for personal communication
Cost- Hata Model	1500MHZ-2GHz	LOS	It has the correction factor for urban, suburban and, rural area. This model does not consider the impact of diffraction from rooftops, building and scatter loss.
Cost 231-walfish-Ikegami Model	2.5 GHz – 2.7GHz	LOS	It is improved version of Cost-Hata model.
Stanford University Interim (SUI)	Up to 2 GHz	LOS	It is used to predict the path loss in all three environments.
ECC-33		LOS	This is modified version of Okumura model. It gives better response in medium city. It does not give good result in rural environment.
Bullington Model		LOS	This is used to compute the diffraction loss over multiple knife edge. Not applicable for suburban areas.

2.4 Methodology of Field Data Collection

The collection of data is necessary requirement to ensure the acceptance of existed design. The collection of data or measurement procedure is generally based on the drive test system. The meaning of drive test is simply collecting or testing the data while, the mobile station is moving. RF coverage details or the performance of a network details can be collected by using drive test. The RF coverage includes the performance such as power strength (E_b/I_0), the transmitting power (Tx), the downlink receive power (Rx) and the Frame Error Rate (FER) while roaming in the wireless network. Prior to the evaluation of drive test it is important to identify the base stations in the route in which drive test to be carried out.

2.5 Drive Test Tool for Measurement

The tools contain both software and hardware devices. In the present day scenario various test tools are available to calculate the Field data, some of the tools are as follows:

2.5.1 NEMO

NEMO is a drive test tool for measuring and monitoring the air interface of wireless networks with outdoor and indoor measurement with various options like voice , video quality, data and application.

Characteristics of NEMO

- Concurrent testing of different network standards
- Multiple voice and data measurements
- Single, multi voice and data measurements
- Frequency scanning can be done with external scanner
- Compatible for MapInfo digital maps
- In single software platform it supports more than 40 test terminals like Nokia, Sagem, Motorola, LG, Samsung, and Qualcomm etc.

- It also supports all major wireless technologies like GSM, HSCSD, GPRS, EDGE, WCDMA, HSDPA, AMPS, TDMA, CDMAOne, CDMA2000 and TETRA as shown in Figure 2.3.

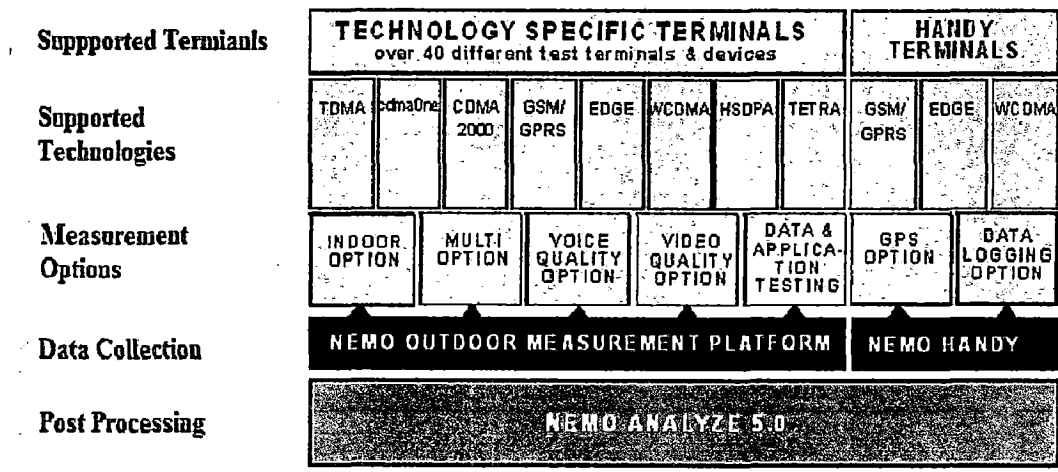


Figure 2.3: Features of NEMO drive test tool

2.5.2 Agilent

Agilent's data test platform or GPRS presents a true drive test solution.

Features of Agilent :

- It provides End to End data testing combined with air interface testing.
- It allows the addition of up to four phones or a combination of phones and digital receivers as shown in Figure 2.4.
- It can evaluate 2G, 2.5G and 3G networks simultaneously from the same laptop.

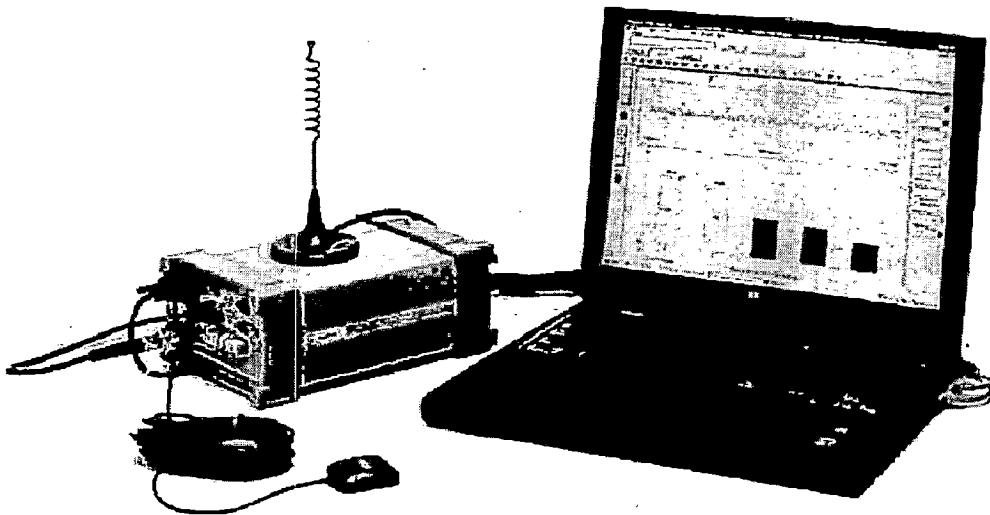


Figure 2.4: E7478A Drive Test System with E6455C IMT2000 Digital Receiver.

- It allows complete scalability on current formats (GSM, GSM-GPRS 900/1800/1900, TDMA, CDMA, W-CDMA/UMTS).
- The E7478A has features for site selection, optimization, troubleshooting, end to end data measurement, data application simulation, indoor analysis, and benchmarking

2.5.3 TEMS

It offers one equipment with many functions like collection of data, analyzing and post processing the network data used on a daily basis for network monitoring, troubleshooting and optimization. This reduces the complexity of multiple tools, costs and time. TEMS protects network integrity and provides benefits of the network at the same time. It collects data beyond the abilities of other tools in the market. It employs specially developed algorithms [33] to collect unique information not available in other vendor's tools.

Table 2.1: Comparison of Air Navigation Tool

	Aircomm TEMS 10.1	Qualcomm RandS (RohdeandSchwarz) ROMES4	Anite NEMO Outdoor 5.40
Supported Technology	GSM/EDGE, WCDMA/HSPA+, CDMA2000@ 1xEV-DO Rev.A, WLAN (IEEE 802.11b, g), WiMAX™(IEEE 802.16e),LTE ,iDEN, TS-CDMA Support both circuit-switched and packet switched measurement	GSM/EDGE, WCDMA/HSPA+, CDMA200, 1xEV-DO Rev.A, WLAN (IEEE 802.11b, g), WiMAX™(IEEE 802.16e),LTE,DAB, DVB-T,DVB-H and TETRA Support both circuit-switched and packet switched measurement	TETRA, GSM/EDGE/GPRS, WCDMA2100/1900, CDMA2000, 1xEV-DO, DVB-H, HSDPA/HSUPA/HSPA+, WiMAX, LTE Support both circuit-switched and packet switched measurement.
QoS measurements	Voice quality, video quality, voice call quality, video streaming quality, C/I Measurement (GSM), Video Streaming Quality Index – VSQI, Video Streaming and the Video Monitor (UMTS) measurement are supported.	GSM Interference, Position Estimation, Data Quality Analyzer for Quality of Service Measurements (DQA), Handover/Neighborhood Analysis for 3GPP (HOA/NBA 3GPP), Speech Quality, Speech Quality Server Software	Voice quality, video quality, voice call quality and psytechnics PVI video streaming quality measurement are supported.
Application Testing	FTP, SMS, MMS, E-mail, HTTP, Ping, Video Streaming and WAP measurement	SMS, MMS, email (POP3 and IMAP), ping, UDP, FTP, HTTP, video streaming	End to End SMS and MMS application Testing, FTP, PoC, Video Streaming, E-mail, ICMP Ping, Video call ,WAP, TCP/UDP testing / measurements
Supported Format	Support of numerous map data formats such as MapInfo, ArcView, Macroni Planet, Ethereal and MDM. Maps can be exported to Google Earth maps.	Support of numerous map data formats such as MapInfo, ESRI, Map and Guide, LS telcom and CMRG Measurement data can also be converted to Google Earth format in addition to an ASCII export allowing users to easily visualize a test drive on maps without any additional expense.	Data formats such as MapInfo is supported. NEMO Outdoor maps can be exported to Google Earth maps.

The present analysis has been carried out using TEMS navigation 8 and 10 versions.

It also supports multimode functionality for system verification, troubleshooting and optimization of WCDMA/HSPA, CDMA and GSM/GPRS/EDGE networks.

This unique multi-mode functionality makes the following possible to:

- Verify , optimize intersystem handover and cell reselection
- Verify compressed mode behavior
- Verify , compare coverage and performance
- Verify WCDMA/HSPA and GSM system accessibility

Introduction to TEMS Investigation

TEMS Investigation 10.0 is an air interface test tool for cellular for networks which is used for measurement, it supports more technologies like GSM/GPRS/EGPRS (including interaction with GAN), WCDMA/HSDPA/HSUPA/HSPA+, TD-SCDMA (including interaction with GSM), CDMA One/CDMA2000/1xEV-DO, plus basic iDEN support. Table 4.1 shows the ability of scanning LTE and WiMAX carriers [102]. It has the ability to check the voice and video telephony as well as a variety of data services over packet switched and circuit switched connections. TEMS offers all in one product because it investigation combines data collection, real time analysis and post processing. The Data Collection and Route Analysis are two modules. Data Collection is the part of TEMS Investigation that interfaces with phones and other measurement devices, collects data and records it in log files. It also allows presentation and analysis of a single log file at a time. It also includes major functionality found in TEMS Investigation CDMA 4.0. Route Analysis is a module that allows rapid analysis of multiple log files, originating from TEMS Investigation itself or from TEMS Automatic, TEMS Drive Tester, or TEMS Pocket. Statistical binning of log file data by area, time, or distance is supported. The means of presentation – maps, line charts and so on are fundamentally the same in both modules.

	TEMS 10.0	TEMS 9.1	TEMS 9.0	TEMS 8.0
CDMA support	Yes	Yes	Yes	Yes
Audio quality measurement with PESQ	Yes	Yes	Yes	Yes
HSUPA support	Yes	Yes	Yes	Yes
Video Telephony Quality Index (VTQI)	Yes	Yes	Yes	Yes
Video Streaming Enhancements	Yes	Yes	Yes	Yes
WiMAX Support	Yes	Yes	Yes	No
WCDMA / GSM Scanning	Yes	Yes	Yes	No
LTE Support	Yes	Yes	No	No
NIDS Support	Yes	Yes	No	No
Mobile to mobile Audio Quality Measurement (AQM)	Yes	Yes	No	No
TD-SCDMA Support	Yes	No	No	No
iDEN Support	Yes	No	No	No
HSPA Support	Yes	No	No	No

Table 2.2: Features of TEMS 10.0, TEMS 9.1, TEMS 9.0, TEMS 8.0

2.6 Terminology associated with Drive Test [12]

High Speed Packet Access (HSPA)

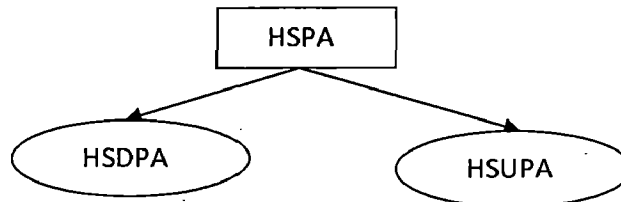


Figure 2.5: HSPA Classification

HSPA is an union of two mobile telephony protocols, one is High Speed Downlink Packet Access (HSDPA) and second is High Speed Uplink Packet Access (HSUPA), that extends and improves the performance of existing WCDMA protocols.

Integrated Digital Enhanced Network (iDEN)

This mobile telecommunications technology is developed by Motorola. iDEN Network seats more users in a specified spectral space, compared to analog cellular and two-way radio systems, by using speech compression and Time Division Multiple Access (TDMA).

Network Intrusion Detection System (NIDS)

It is an invasion detection system which detects malevolent activities such as defense of service attacks, port scans or even attempts to crack into computers by monitoring network traffic.

High Speed Uplink Packet Access (HSUPA)

It is a 3G mobile telephony protocol in the HSPA family with uplink speeds up to 5.76 Mbit/s. The official 3GPP name for 'HSUPA' is Enhanced Uplink (EUL).

3GPP Long Term Evolution (LTE)

LTE is the latest standard in the mobile network technology tree that produced the GSM/EDGE and UMTS/HSPA network technologies. It is a project of the 3rd Generation Partnership Project (3GPP), operating under a name trademarked by one of the associations within the partnership, the European Telecommunications Standards Institute. The current generation of mobile telecommunication networks is collectively known as 3G (for "third generation"). Although LTE is often marketed as 4G, first release LTE does not fully comply with the ITU Advanced 4G requirements. The pre-4G standard is a step toward LTE Advanced, a 4th generation standard (4G) of radio technologies designed to increase the capacity and speed of mobile telephone networks. LTE Advanced is backwards compatible with LTE and uses the same frequency bands, while LTE is not backwards compatible with 3G systems.

WiMAX [11], [15]

Worldwide Interoperability for Microwave Access (WiMAX) is telecommunications protocol that provides fixed and mobile internet access.

Handoff [30], [95]

The coverage area in cellular mobile communication [104] is divided into number of cells. Each cell is covered by an individual base station. When a mobile unit is moving from one cell area to another adjacent cell area Handoff takes place [55]. In cellular telecommunications, the term handoff refers to the process of transferring an ongoing call or data session from one channel connected to the core network to another [9]. It is a flawless service to active mobile phone users while data transfer is in progress.

Purpose

- When the mobile user is moving away from the range of one cell to another cell then the call is transferred to the second cell by avoiding call termination when the mobile user went outside the range of the first cell.
- The capacity of connecting new calls of one cell can be shared with another.

- When mobile user is moving faster than a certain threshold, the call can be transferred to a larger umbrella-type of cell to minimize the frequency of the handoffs due to this movement.
- In CDMA networks a soft handoff may be induced to reduce the interference to a smaller neighboring cell due to the "near-far" effect.

Rx Level

Drive test results will give the penetration level of signals in different regions of the network. These results can then be compared with the plans made before the network launch. In urban areas, coverage is generally found to be less at the farthest parts of the network, in the areas behind high buildings and inside buildings. These issues become serious when important areas and buildings are not having the desired level of signal even when care has been taken during the network planning phase. This leads to an immediate scrutiny of the antenna locations, heights and tilt. The problems are usually sorted out by moving the antenna locations and altering the tilting of the antennas. If optimization is being done after a long time, new sites can also be added. Coverage also becomes critical in rural areas, where the capacity of the cell sites is already low. Populated areas and highways usually constitute the regions that should have the desired level of coverage. A factor that may lower the signal level could be propagation conditions, so study of link budget calculations along with the terrain profile [52] becomes a critical part of the rural optimization. For highway coverage, additions of new sites may be one of the solutions.

Rx Quality [53]

The quality of the radio network is dependent on its coverage, capacity and frequency allocation. Most of the severe problems in a radio network can be attributed to signal interference. For uplink quality, BER statistics are used and for downlink FER statistics are used. When interference exists in the network, the source needs to be found. The entire frequency plan is checked again to determine whether the source is internal or external. The problems may be caused by flaws in the frequency plan, in the configuration plans (e.g. antenna tilts), inaccurate correction factors used in propagation models, etc.

Speech Quality Index (SQI)

SQI is an estimate of the perceived speech quality as experienced by the mobile user, is based on handover events and on the bit error and frame erasure distributions [53]. The SQI scale goes from -15 to 21 for Full Rate (FR) speech coders and from -15 to 30 for Enhanced Full Rate (EFR) speech coders.

2.7 Check list for field measurement

Various Tools used for drive test are as follows:

- A drive test tools (TEMS)
- TEMS compatible mobile station with RF antenna and Serial Port data cable
- A laptop with minimum Pentium-III Processor, 256MB RAM
- Analysis software (Mapinfo, Actix etc.)
- Inverter
- Extension board
- GPS receiver having DC Power cable and Serial Port data cable.

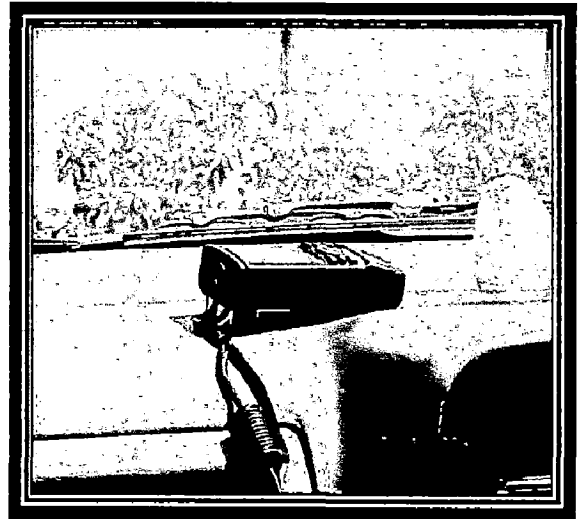
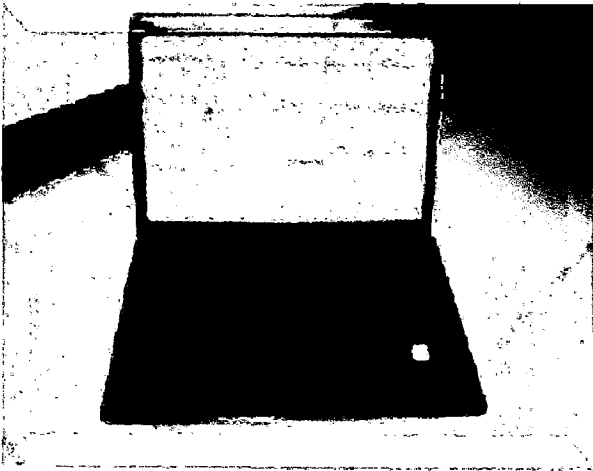
2.8 Hardware Requirement

- *Test Kit* --- for hardware holding and protection
- *Mobile Computer* --- for test control and data collection
- *Trace Mobile* --- for wireless parameter collection
- *GPS* --- for geographic positioning
- *Power Supply System* --- Supplying power for GPS and notebook computer
- *PCMCIA Card* --- for communication between the notebook computer and GPS

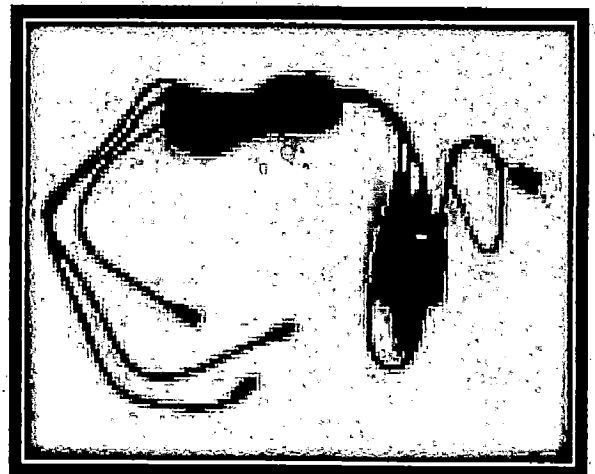
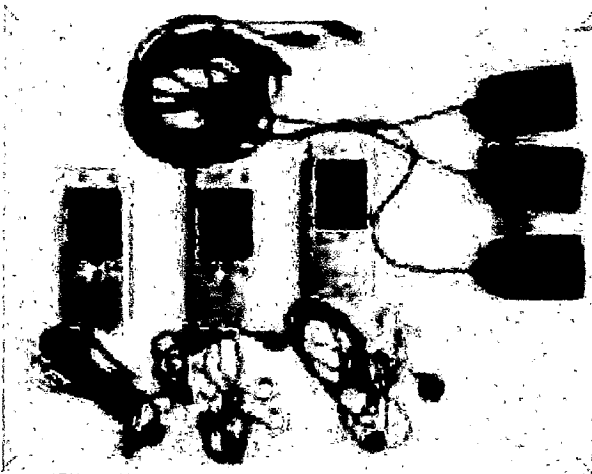
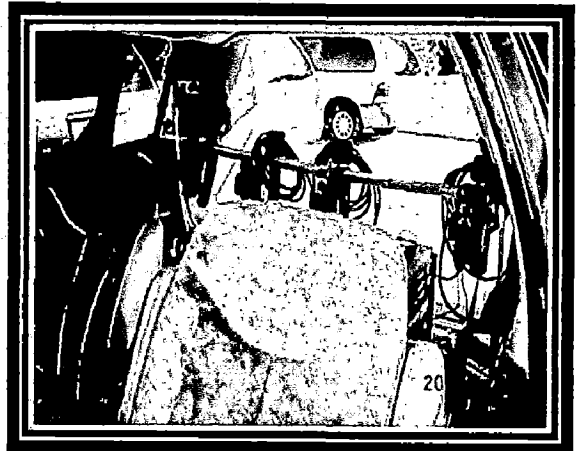
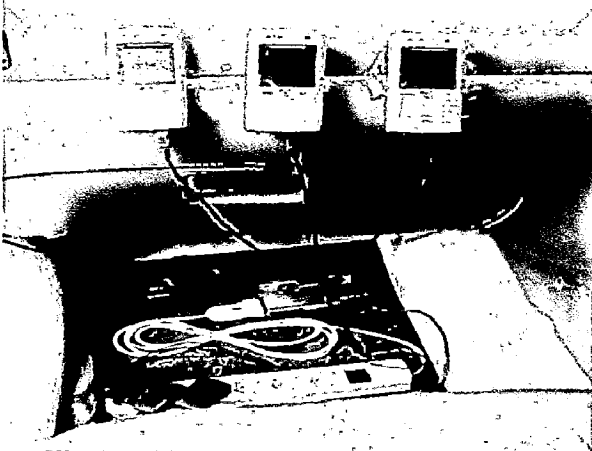
2.9 Software requirement

The network drive test software used is TEMS Investigation as shown in Figure 2.6. This software is combined with the above hardware to perform a GSM network drive test. TEMS works with real time network parameters such as LAC, CI, Rxlevel, Rx quality etc on basis of a digital geographic map and cell database [62].

TEMS NAVIGATION TOOL PERIPHERALS VERSION - 8.01

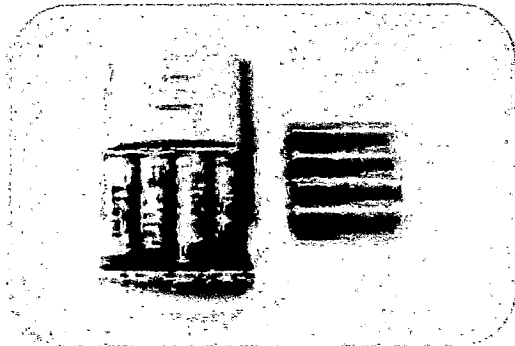


LAPTOP (INSTALLED TEMS INVESTIGATION) AND AIR INTERFACE HAND SET SONY T 610

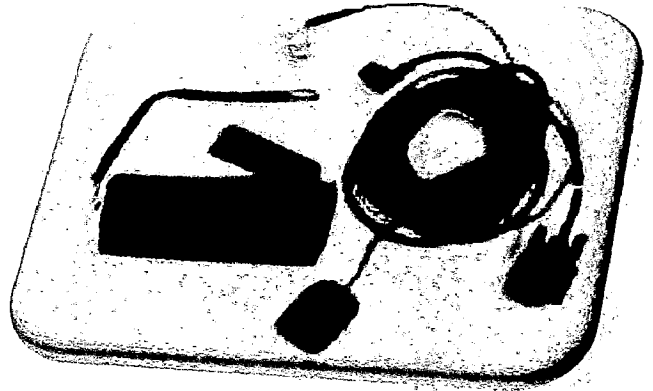


TEMS HANDSET (COMPLETE WITH CHARGER, HEADSET, DATA CABLE) AND USB HUB

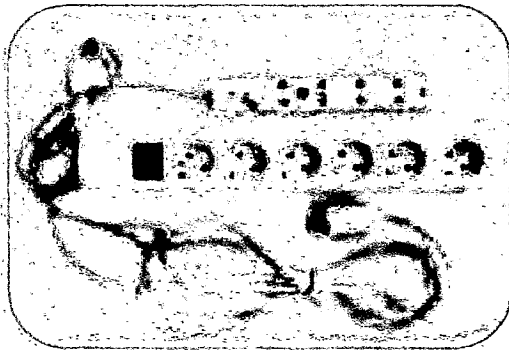
TEMS NAVIGATION TOOL PERIPHERALS



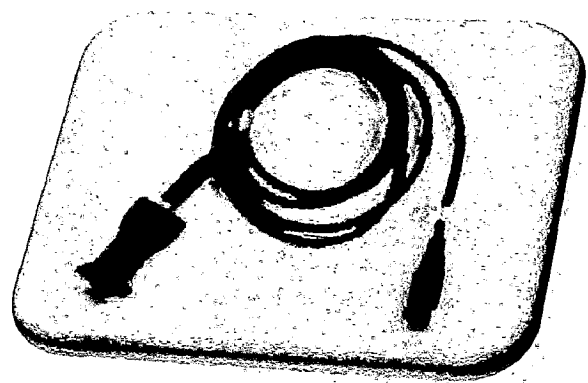
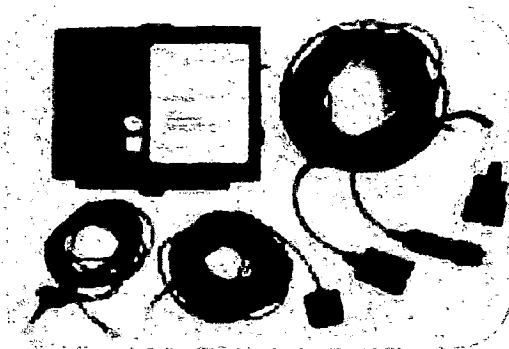
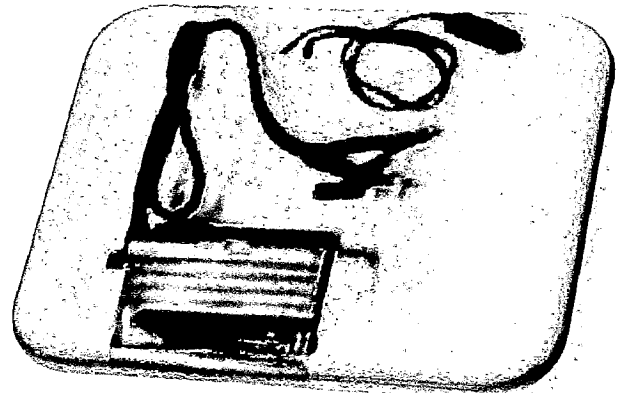
Battery and Charger



GPS (Ext Antenna and Data Cable)



Inverter and Terminal



Scanner for GSM (External Antenna GPS and RF, Data Cable) ATEN (Serial to USB)

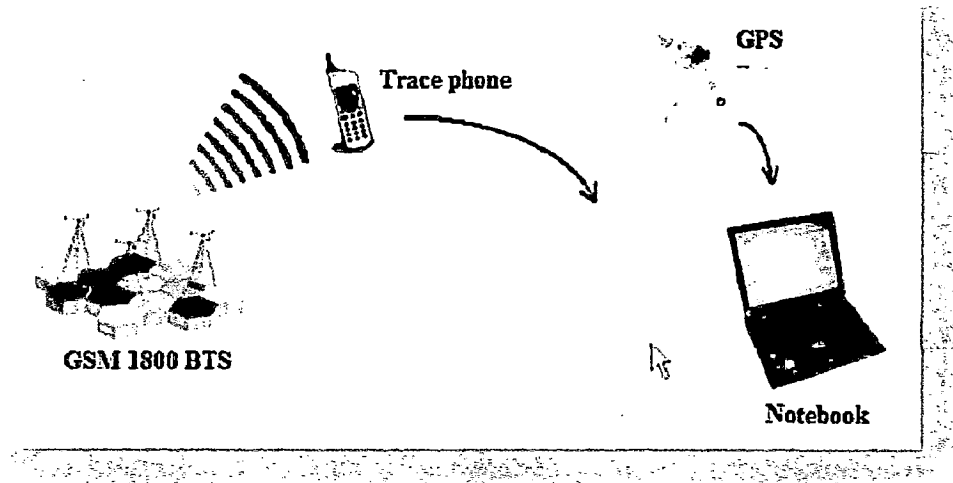


Figure 2.6: Drive Test principle illustration

2.9.1 Specification of Hardware and Software

Usually, the TEMS test system requires a hardware configuration in the following aspects

Trace Phone: The following phones (supporting both GSM and WCDMA Unless otherwise stated) can be delivered with TEMS Investigation 10.0

- Sony Ericsson C905, Sony Ericsson C905a, Sony Ericsson Z750i, Nokia N96 EU, Nokia N96 US (Table 2.1 shows the features of these mobile phone)
- Other Connectable UMTS Devices
 Sony Ericsson C702, Sony Ericsson K600i, Sony Ericsson TM506, Sony Ericsson W760i, LG CU320, LG CU500, LG U960, Motorola E1000, Motorola E1070, Motorola M2501, Motorola Razr Maxx V6, Motorola Razr V3x, Motorola Razr V3xx, Motorola Razr2 V9, Nokia 6120, Nokia 6121, Nokia 6280, Nokia 6680, Nokia 7376, Nokia N75, Nokia N80, Nokia N95

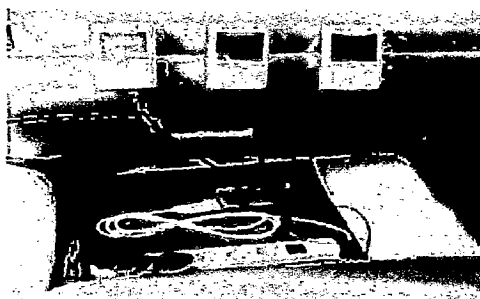


Figure 2.7: TEMS test kit

It is recommended that a status configuration of the trace phone required as below prior to a test:

- Data Rate: 9600bps; Menu: Accessories\Data parameters\Speed
- Modem type: Data; Menu: Accessories\Data parameters\Mode
- Protocol: Secure link; Menu: Accessories\Data parameters\Protocol

Table 2.3: TEMS supported Mobile phone's feature

Phone/Feature	HSPDA, Mbits/s	HSPA, Mbits/s	WCDMA 850	WCDMA 900	WCDMA 1900	WCDMA 2100	GSM 850	GSM 900	GSM 1800	GSM 1900	External Antenna	AQM	Scanning
Sony Ericsson C905	3.6					✓	✓	✓	✓	✓			✓
Sony Ericsson C905a	3.6		✓		✓	✓	✓	✓	✓	✓			✓
Sony Ericsson Z750i	1.8		✓		✓	✓	✓	✓	✓	✓	✓	✓	✓
Nokia N96 EU	3.6			✓		✓	✓	✓	✓	✓	✓		
Nokia N96 US	3.6		✓		✓		✓	✓	✓	✓	✓		
Option GT Expr. HSUPA	7.2	2.00	✓		✓	✓	✓	✓	✓	✓	✓		

GPS Units: The recommended GPS units for TEMS are mentioned below

- Bosch/Blaupunkt Travel Pilot
- Garmin 10 Mobile Bluetooth (NMEA-0183)
- Garmin 12XL (NMEA-0183)
- Garmin 35 (NMEA-0183)

- Global Sat BT-359 (NMEA-0183)
- Global Sat BT-368 (NMEA-0183)
- Global Sat BU-303 (NMEA-0183)
- Global Sat BU-353 (NMEA-0183)
- Holux GPSlim 236 (NMEA-HS; Bluetooth or USB)
- Magretti Marelli Route Planner NAV200
- Nokia LD-3W Bluetooth (NMEA-0183)
- Sanav GM-44 (NMEA-0183)
- Sanav GM-158 (NMEA-0183)
- NMEA-HS Holux GPSlim 236 BT
- NMEA-HS Holux GPSlim 236 USB

For poor receiving conditions the recommended GPS units are Bosch/Blaupunkt Travel Pilot or Magretti Marelli Route Planner, since they have dead reckoning facilities.

Notebook: A notebook computer or laptop is used to run the test software TEMS Investigation. In general the recommended configuration of notebook when running the TEMS for GSM network test is.

- CPU: PII 400MHz
- Memory: 128M SDRAM
- Hard Disk Drive: 10GB
- Display Resolution: 1024 * 768 pixel
- Operation System

The following operating systems are supported:

- Windows Vista with Service Pack 1
- Windows XP Professional with Service Pack 3
- Windows XP Tablet PC Edition with Service Pack 3

In addition, all the latest Windows updates should always be installed. Supported languages are English (U.S.), Chinese (simplified characters), and Japanese.

Cables to use with Phones: Sony Ericsson C702, C905, C905a, TM506, W760i, Z750i. It is necessary to use the USB cable supplied with the phone (DCU-65, part number RPM

131 12/1 R1B). Using a USB cable delivered with older phones such as K800i and K790i is not recommended.

External Antenna to Phones: An external monopole antenna is connected to a phone by means of a coaxial cable (and possibly an adapter) supplied with the phone. Phone specific details are as follows:

- Sony Ericsson Z750i

An external antenna with the Sony Ericsson Z750i, the phone is delivered with the antenna adapter already mounted. Just connect the antenna to the adapter. A Sony Ericsson Z750i phone with an external antenna mounted cannot use its internal antenna.

- Nokia N96

Press the antenna adapter into the hole provided for it and then connects the antenna to the adapter.

PCMCIA Card: It is used to connect the trace phone and GPS to a notebook computer. The test data will be transferred from the trace phone and GPS to the notebook computer through this card.

Power Supply System: It is used to supply power for both the notebook and GPS unit.

2.10 Assembling / Installation / Setup Procedure

The Setup procedure for the entire drive test is given below.

2.10.1 Plugging in Phones and Data Cards

All supported phones connect to the laptop via USB. The USB cable transfers the data on the phone to a USB port on the laptop (both TEMS measurements and data service measurements are transferred through this cable).

2.10.2 Plugging in GPS Units

In the same way the Supported GPS units connect via USB or Bluetooth to a COM port.

2.10.3 Configuring TEMS Investigation software for Data Collection

Launch the application from the Start menu:

- Choose Start → Programs → Ascom → TEMS Products → TEMS Investigation 10.0 Data Collection.

In Windows Vista the application has been run as administrator. This option is selected by right clicking the Start menu item above and choosing Properties (Figure 2.7)

→ Shortcut tab → Advanced

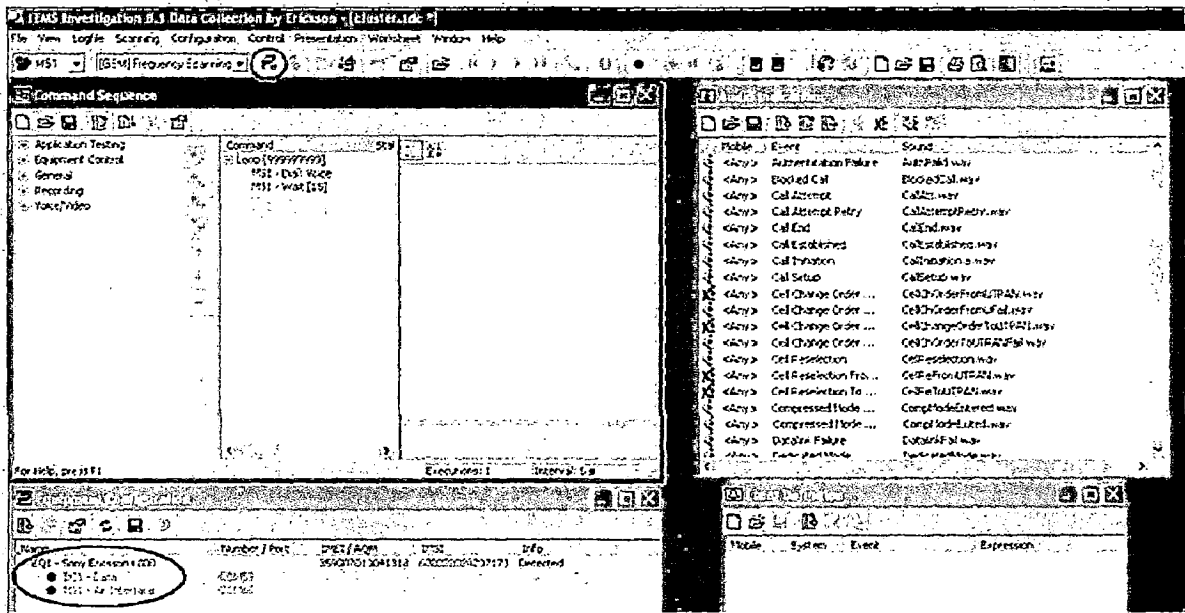


Figure 2.8: TEMS window

All devices that are known to TEMS Investigation can be automatically detected or manually added, are listed in the Equipment Configuration window Figure 2.8.

In the *Name* column of the Equipment Configuration window, each device is represented by an EQ item, containing within it one further item (called “channel”) for each data source furnished by the device:

- for user terminals, an “MS” channel representing TEMS measurements and a “DC” channel representing data service measurements
- for scanners, an “MS” channel

- for GPS units, a “PS” channel (P for “positioning”). GPS units built into scanners also appear as separate devices.

The colored dot to the left of each channel shows the status of the channel in TEMS Investigation: red means “not connected”, green means “connected”.

Name	Number / Port	IMEI / AQM / ESN	IMSI	Info
EQ1 - Sony Ericsson K800	+46	351	2430	Detected
DC1 - Data	COM17			
MS1 - Air Interface	COM18			
EQ2 - Sony Ericsson K800	+4673	351	2430	Detected
DC2 - Data	COM5			
MS2 - Air Interface	COM6			
EQ4 - LGE LG CUS00	0702	G10	240	Detected
DC4 - Data	COM23			
MS4 - Air Interface	COM24			

For Help, press F1

Figure 2.9: Equipment Configuration window

2.10.4 Recording Log files

Log files can be recorded in the following ways in TEMS Investigation:

- From the Record toolbar or Log file menu
- From within command sequences.

All these procedures produce the same type of output file, with extension .log. The functions available for controlling the recording and modifying the log file are however somewhat different in each case.

2.11 Loading Site data, Vector, Map, Path

Cell Data

TEMS Investigation can present information on individual cells in cellular networks. In particular, it is possible to draw cells on maps and to display cell names in various windows. Cell data is also made use of in log file reports.

Cell data can be provided in two ways:

- In a plain text XML file (*.xml) whose format is common to several TEMS products.
- In a file with a plain text, TEMS Investigation specific format (*.cel). This format is for UMTS only. GSM and WCDMA cells can be mixed in one file.

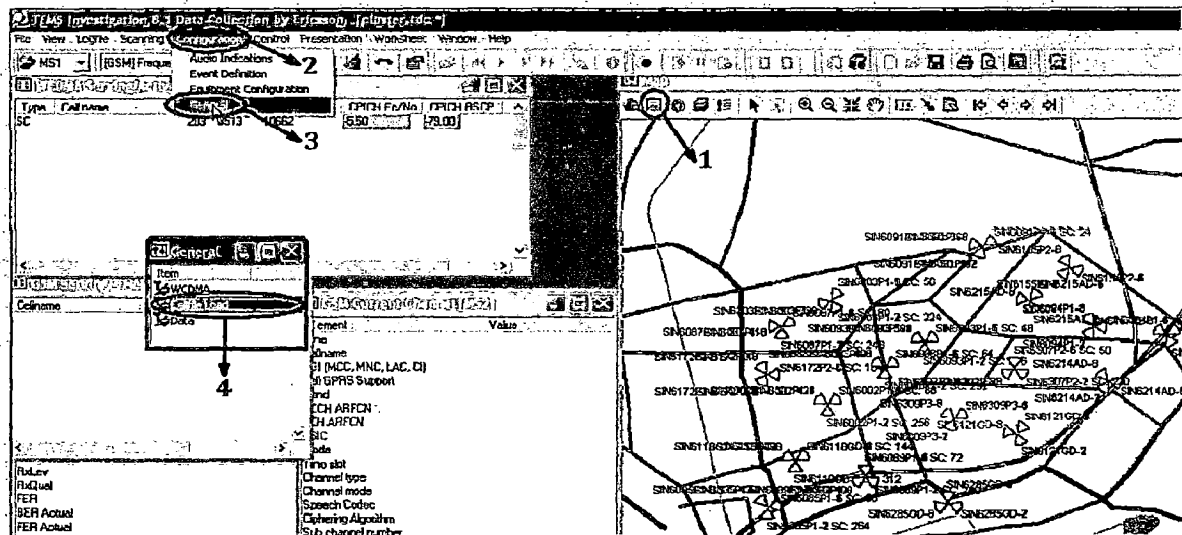


Figure 2.10: Cell data configuring window

Loading Cell Files

For making a cell file in active mode, it must be loaded first in the General window. Several cell files can be load in the application at a time as shown in Figure 2.9.

- From the Navigator, open the General window.
- In the General window, double-click the item “Cellfile Load”.
- To add a cell file, click the Add button and browse to select file. The cell file is added in the list box.
- To remove a cell file from the list, select it and click Remove. To remove all cell files, click Remove all.
- When done selecting cell files to load, click OK.

Any time loaded cell files can be modified. The correlation is possible if multiple files of the same type (CEL or XML) are loaded.

- To load a map file, right-click the Map Files item in the Navigator and choose Add from the context menu, then browse for the desired TAB or GST file.

2.12 Test Procedure for Drive Test

The test procedure is as follows after connecting the drive test tool.

1. On opening the TEMS Investigation 10.0 application software window in the Laptop. The system by default opens 'GSM' window by displaying the empty tables and charts for RF information.
2. The external devices, TEMS Handset and GPS unit both are configured in the 'Control and configuration' window. The system immediately detects all the devices existing but shows red color symbol indicating disconnectivity and the red color symbol changes to green color after connecting devices by clicking 'Connect All' in the Connection Toolbar.
3. The mobile using is now connected in the 'idle mode'. After connecting the mobile the GSM window starts displays the live network data in the corresponding tables and charts. The window also displays Latitude and Longitude of the place.
4. Save the log file trailed after starting call on the TEMS phone by clicking the 'Record' tool bar.
5. The Drive test must conduct on routes covering the cell and all neighboring cells.
6. Cell coverage, Received signal strength, Quality and many other RF parameters can be measured.
7. Call connection, call mobility control, call release and many other events are checked and recorded.

In this drive test radial and azimuthally routes have to be tested. In urban area the effects of street orientations have to be considered. Measurements have to be evenhanded, i.e. the field data must cover all typical coverage scenarios. The selection of drive test routes should be based on the:

- The terrain variations

SCHOLAR COLLECTING FIELD DATA IN DEHRADUN-UTTARAKHAND , USING ERRICONS TEMS



- Subscriber distributions
- Major highways and thoroughfares
- Critical Areas
- Potential Shadowing areas and handover regions

The drive test must be carried out along the cell radius typically 2-3 times.

2.13 Various Issues during Measurement

The issues to be considered during measurement are:

Overshooting

- Overshooting means, it serves at very long distance with good Rx Level where in this area it is supposed to be served by another closer site having approximately the same signal strength. It can cause high interference which leads to bad quality.
- Usually the advice for this case is down tilt the antenna.

Figure 2.10 shows an example for overshooting.

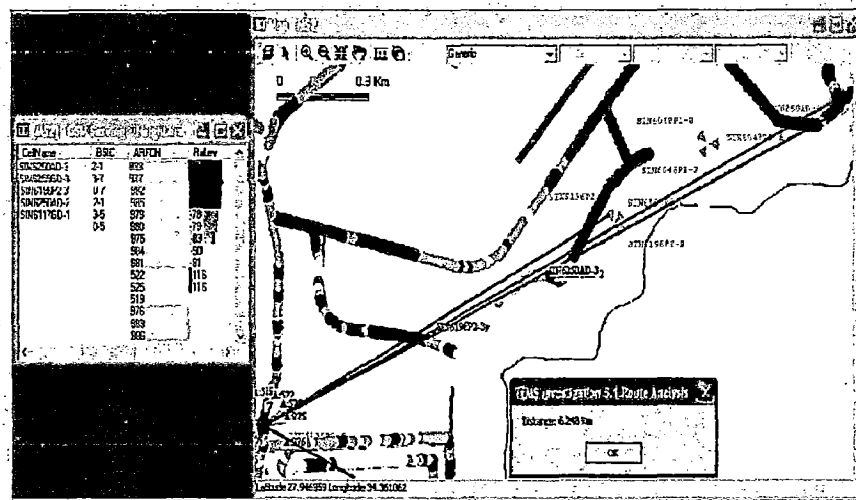


Figure 2.11: Example of Overshooting

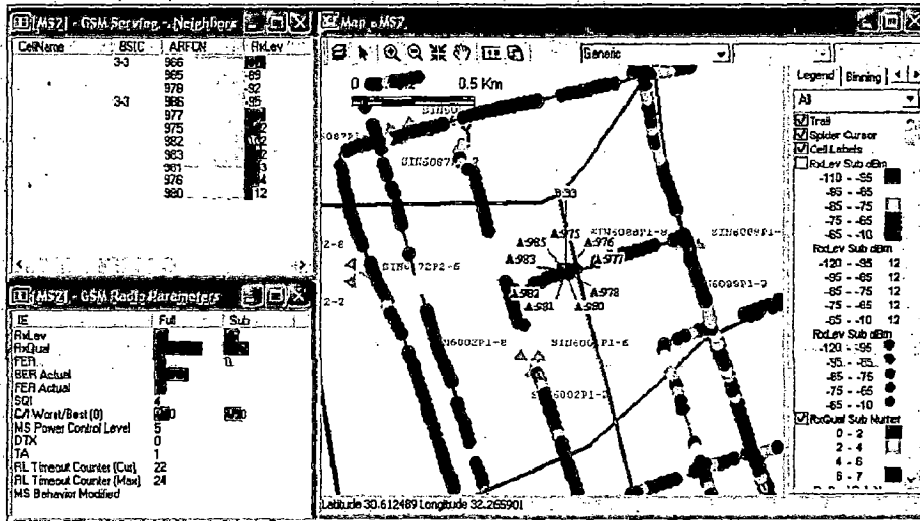


Figure 2.12: Example of Bad quality

Bad Quality

- Bad quality can occur due to two reasons one is bad coverage and second is high interference (It is mainly co channel which is known from C/I data in the TEMS data collection). The remedies to reduce bad quality . Figure 2.11 shows an example for the above case.
- The bad coverage can be rectified by checking the infected site or antenna.
- The high interference can be reduced by rechecking the RF planning using planning

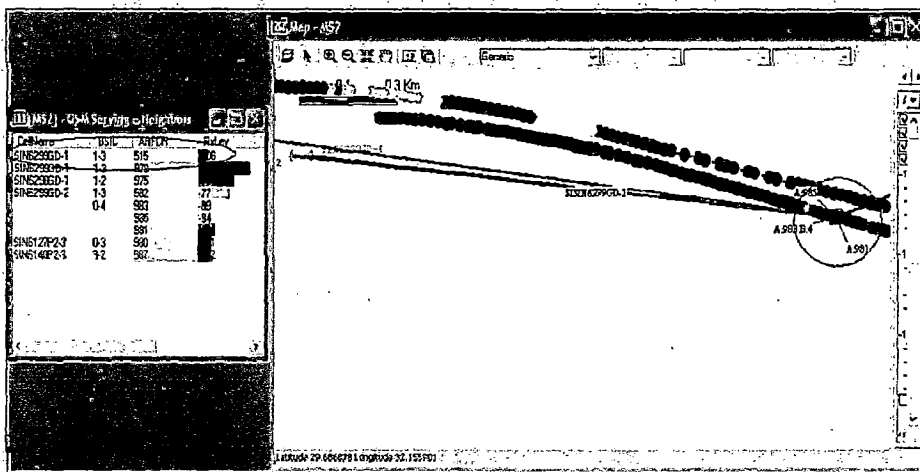


Figure 2.13: Example of Bad coverage

- Practically calls can be established at maximum distance from the site 35 Km with timing advance of 68, in some cases the signal reaches up to 40 and 50 Km and this is due to water reflection if the site is near a source of water, for e.g. sea or a canal. Therefore if the MS is served by this site at this huge distance with a fair signal, block calls will occur as shown in Figure 2.13.

Handover failure and delay

The reason for handover delay is that all possible neighbors may suffer blocking or some of the handover parameters need to be adjusted.

High handover failure will probably be due to:

- High neighbor and source cell interference.
- Mobile on incorrect source cell.
- Poor planning Location area borders. That means if the borders exist on road junctions or ridges or on large water expanses.
- In correctly specified Database parameters like budget algorithms [86], Rx Quality algorithms, Rx Level algorithms, Timing advance algorithms.
- Failure in leading server. It causes mainly due to the following
 - Neighbors being received at similar levels.
 - Missing cell site.

2.13 DATA ANALYSIS TOOLS

The Log files generated by TEMS Investigation are to be analyzed using the following tools by exporting the log files into .tab format.

- MapInfo [87]
- Arc View
- Marconi Planet DMS 3.1
- Ethereal
- MDM (CDMA)

CHAPTER 3

PERFORMANCE ANALYSIS AND TUNING OF OUTDOOR PROPAGATION MODELS

This chapter describes a selection of best fit model for the prediction of received signal power and propagation path loss. A close comparison of measurement values and computed values from the outdoor propagation models formulae revealed that direct application of these formulae is inappropriate for the prediction of these parameters in the region of investigation, as computed values fell short significantly from the corresponding measured values. Consequently, tuning has been introduced to best fit model and this tuning has produced results which closely matched the measured values. Received signal power measurements from four BTSID's at Dehradun, Uttarakhand has been used to deduce corresponding path loss values from the measured received signal power values. High quality and high capacity networks are essentially required for the accurate determination of modern cellular networks and signal strength measurement. In radio services, the most important question is to tell about the propagation loss in advance. The calculation of the path loss in invariant conditions can be done by the number of empirical models. The performance of wireless communication systems depends primarily on radio channel. As a consequence, predicting the propagation characteristics between two antennas is one of the most important tasks for the design and installation of wireless communication systems.

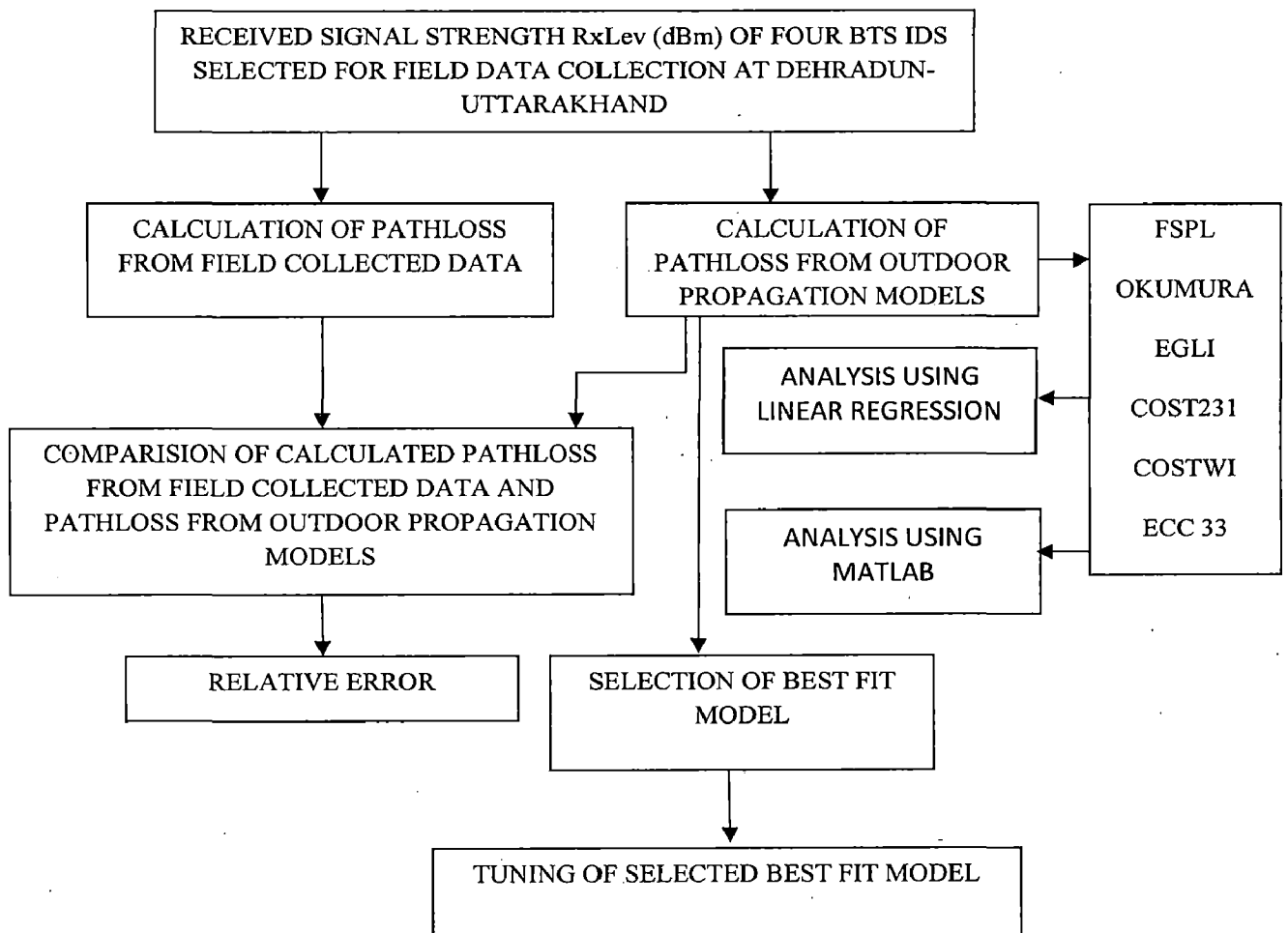


Figure 3.1: FLOW CHART OF STEP BY STEP EXECUTION OF WORK

3.1 Background

Numerous outdoor propagation models have been developed to predict radio propagation losses [1], [5]. The model analysis in this chapter is Free Space Path Loss (FSPL), Okumura, COST 231 [14], COST Walfisch-Ikegami (WI) [28], ECC 33 [23], [24] and Egli model. These models are considerably taken into study for an efficient and reliable coverage area. The predictions are required for a proper coverage planning, determination of multipath effects as well as for interference and cell calculations, which is the basis for any of the network planning process. Results of these models are based on experimental and empirical works but unfortunately none of them are uniformly applicable. Work reported in this chapter is based on the data collected from selected four BTS ID'S at Dehradun using Ericson's TEMS navigation. The collected data (RxLev, SQI, Interference etc) has been analyzed using DESKCAT and Mapinfo simulation tools. Path loss for above propagation models is determined using the parameter of four BTS ID's selected at Dehradun, Uttarakhand. The results have been used to evaluate the performance analysis of Free Space Path Loss (FSPL), Okumura, COST 231 HATA, COST 231 W-I [54], Egli and ECC 33 outdoor prediction models. Best fit model has been selected to estimate the path loss. Correction factor has been introduced for tuning of best fit model in order to improve its performance. Finally path loss is plotted as a function of path distance by using linear regression analysis and MATLAB to obtain best fit model at minimum of path loss curve. The above analysis is carried out in a frequency range of 900 and 1800 MHz that is globally being allocated for broadband wireless GSM network in India. The flow sheet of execution of work is shown in Figure 3.1.

3.2 Related Work

Many outdoor propagation models for different type of networks [10] planning have been reported in the literature [8], [42], [44]. A performance comparison of outdoor propagation models for network planning is reported in [40],[101] in which analysis is carried out in open/rural environments[26],[31],[57]. Shoewu O. and Adedipe A. has estimated performance of propagation models [65] and tuned them by incorporating correction factor F_c in northern Nigeria [91]. Recently F D Alotaibi et al. [25] has reported the experimental

setup for path loss and calculated the performance of outdoor propagation models for densely cities in Riyadh City, Saudi Arabia region. Pavlos et al [78] provides that measurement reports over the GSM network are transmitted periodically (480ms) from the Mobile Terminal (MT) to the Base Transceiver Station on the Stand Alone Common Channel (SACCH) assigned to each communication channel. M.I. Ahmed et al [2010] analyze that Harmattan dust clusters resembles that of fog and the space they covered can be considered as a dielectric since the clusters consists predominantly of quartz which non coherently scatters and disturbs propagation of RF signals [74]. Dajab et al [18] in their work at savannah region define sand storm as a weather condition in the tropics in which dust particles(precipitates) are blown into the air by winds defined as air in horizontal motion relative to the earth surface and pushed southwards from the Sahara desert by the northwest winds.

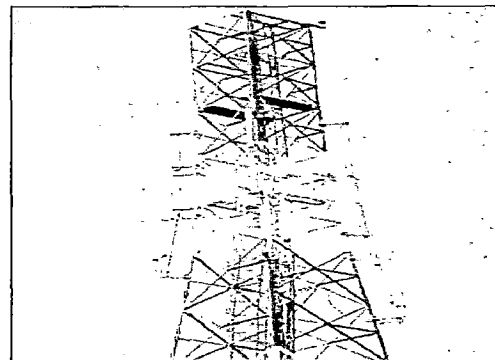
3.3 Estimation of path loss from field collected data during Drive Test at Dehradun

Drive testing is the most common and is the best way to analyze network performance by means of coverage evaluation, system availability, network capacity, network retainability and signal quality [27]. Although it gives idea only on downlink side of the process, it provides huge perspective to the service provider about what's happening with a subscriber point of view [20]. Drive test result is useful to investigate the various parameters associated with wireless network such as:

Non-working sites/sectors or TRXs

- a) Overshooting sites – coverage overlaps
- b) Coverage holes
- c) C/I, C/A analysis
- d) High Interference Spots
- e) RxLevel
- f) Capacity
- g) Accessibility and Retainability of the Network

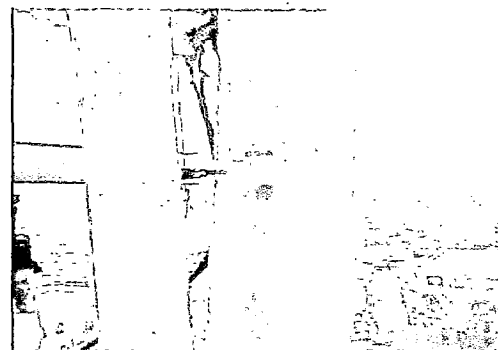
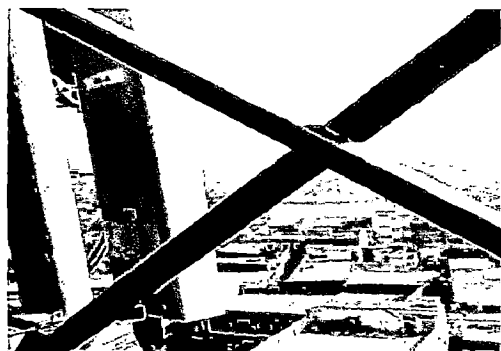
BTS SITES SELECTED FOR FIELD DATA COLLECTION IN FRINGE AREAS OF DEHRADUN –UTTARAKHAND



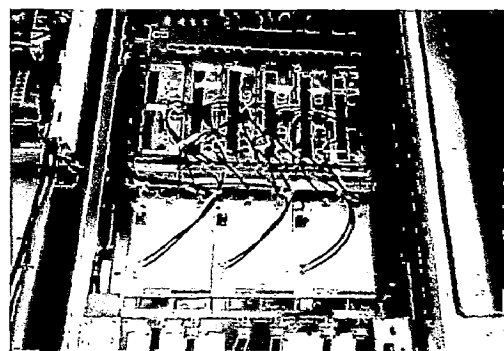
BTS SITE ID DDN 002 (LATITUDE: 30.3539 LONGITUDES: 78.0245)



BTS SITE ID DDN 204 (LATITUDE: 30.276 LONGITUDES: 78.0773)

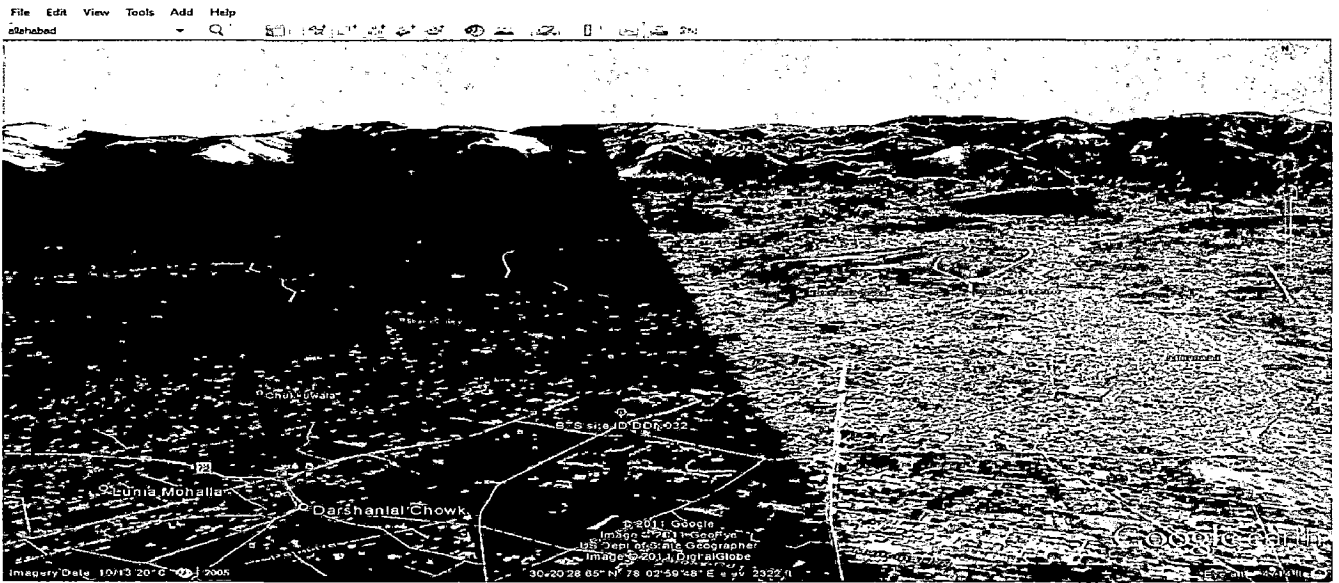


BTS SITE ID DDN 034 (LATITUDE: 30.2895 LONGITUDES: 78.0738)



BTS SITE ID DDN 034 (LATITUDE: 30.32722 LONGITUDES: 78.04785)

BTS SITE LOCATION AT DEHRADUN UTTARAKHAND FROM GOOGLE EARTH MAP



BTS SITE ID -DDN032

LATITUDE: 30.32722

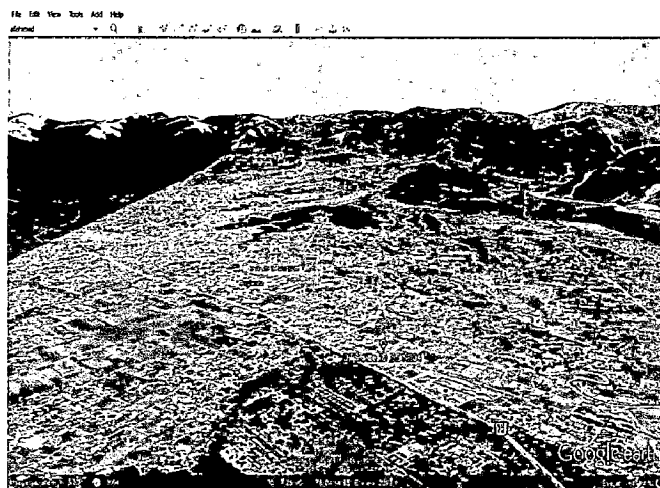
LONGITUDE: 78.04785



BTS SITE ID DDN 204 (LATITUDE: 30.276 LONGITUDE: 78.0773)



BTS SITE ID DDN 034 (LATITUDE: 30.2895 LONGITUDE: 78.0738)



BTS SITE ID DDN 002 (LATITUDE: 30.3539 LONGITUDES: 78.0245)

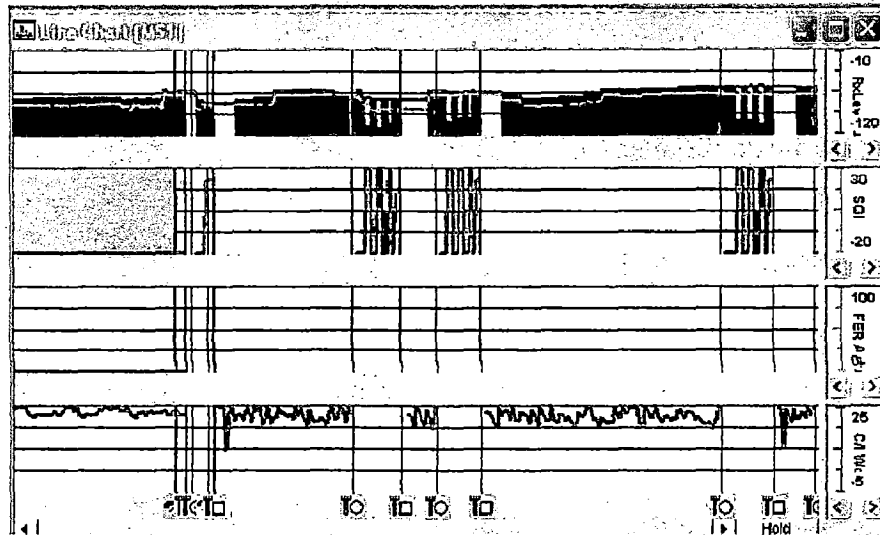


Figure 3.3: Line Chart of Log file for current cell

Events are indicated by dashed vertical lines accompanied by a symbol identifying the event type. The symbols used for predefined events have been given in Information Elements and events. Names of the events are displayed in an events window. The chart pane is synchronized with the legend and additional Information panes (as well as with all other open presentation windows). In the chart, a solid line indicates the point in time currently selected in the drive. Scrolling the chart by means of the scroll bar does not change the time instant selected, so neither the text panes nor other presentation windows is updated. The Y-axis pane of line chart, shows the scales of the information elements plotted. Each scale is drawn in the same color as the information element. In the legend pane full details has been provided (for one chart at a time) on the information elements plotted for the currently selected time instant.

3.3.4 Samples Averaging

The temporal resolution of the scan is lowered by having the phone report sample averages rather than raw samples. The GSM phone reports the mean value of N samples with a frequency of f_s/N where f_s is the sampling rate. With no averaging (i.e. $N = 1$) the fast fading [56] occurs, whereas for higher values of N it is gradually smoothed out. The

averaging operation is performed in the dBm domain. Sample averaging is distinct from the sample rate adaptation function.

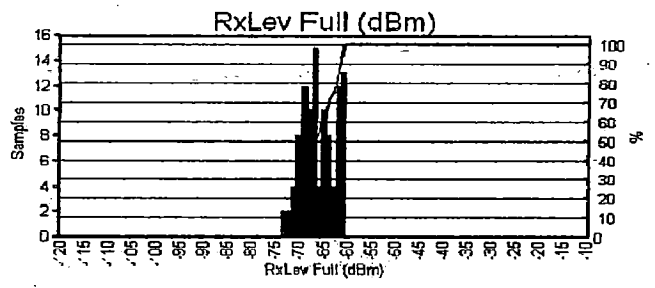


Figure 3.4: Samples-RxLev of field collected data

3.3.5 Adaptation of Sample Rate to Speed [13],[64]

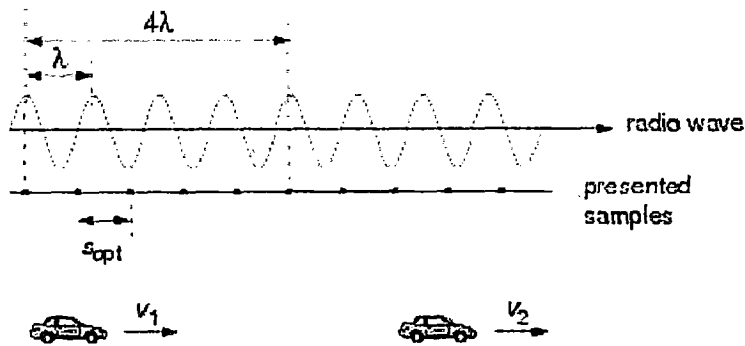
In order to optimize the scan presentation in terms of faithfulness to actual radio conditions, the sample rate of the presentation must be controlled so that the samples are suitably and evenly spaced along the route as shown in Figure 3.4. This means that the presented sample rate must be continuously adjusted to the vehicle speed. Sample spacing used in current empirical analysis is 50 samples per 40 wavelengths. The optimum spacing S_{opt} is picked and fixed. Further the sampling time t_s in the current analysis depend on the speed. The wavelength λ used in the calculation corresponds to the center frequency of the GSM band i.e. 900MHz not the exact frequency used. The averaging involved in converting the sample rate is done in the mW domain.

Frequency=900 MHz

$\lambda = c/f = .333m$

Selected: 50 samples per 40 wavelengths

Optimum Sample Spacing $S_{opt} = 40/50 \times \lambda = .266$



$$V_1 = 60 \text{ Km/h or } 16.7 \text{ m/s}$$

$$V_2 = 90 \text{ Km/h or } 25.0 \text{ m/s}$$

$$t_{s1} = S_{opt}/V_1 = 16.0 \text{ ms}$$

$$t_{s2} = S_{opt}/V_2 = 10.7 \text{ ms}$$

Sample rate adaptation function does not affect the actual sampling rate of the scanning device, which is always constant and much higher. TEMS Investigation converts raw sample rate into a different rate. For the representation of drive test result, color code is used for received signal power level as shown in the Figure 3.5. The range for each color is not fixed, it is adjustable. In Figure 3.5 the blue color section represent excellent signal strength, the light green color section indicates a good coverage level, the dark green color shows the fair signal strength and the yellow color represent the poor coverage area , where severe call drop could be experienced.





$\text{max} \geq x \geq -66$	$-66 \geq x \geq -72$	$-72 \geq x \geq -78$	$-78 \geq x \geq -110$
			
Excellent	Very good	Fair	Poor

Figure 3.5: Code of color for received signal strength "X" in (dBm)

3.4 Received signal strength from selected sites

Field signal strength measurement in Figure 3.6 shows that the received power (dBm) depends on a distance between a transmitter and a mobile station. Signal variability depends on the environment and also on the transmitter behavior.

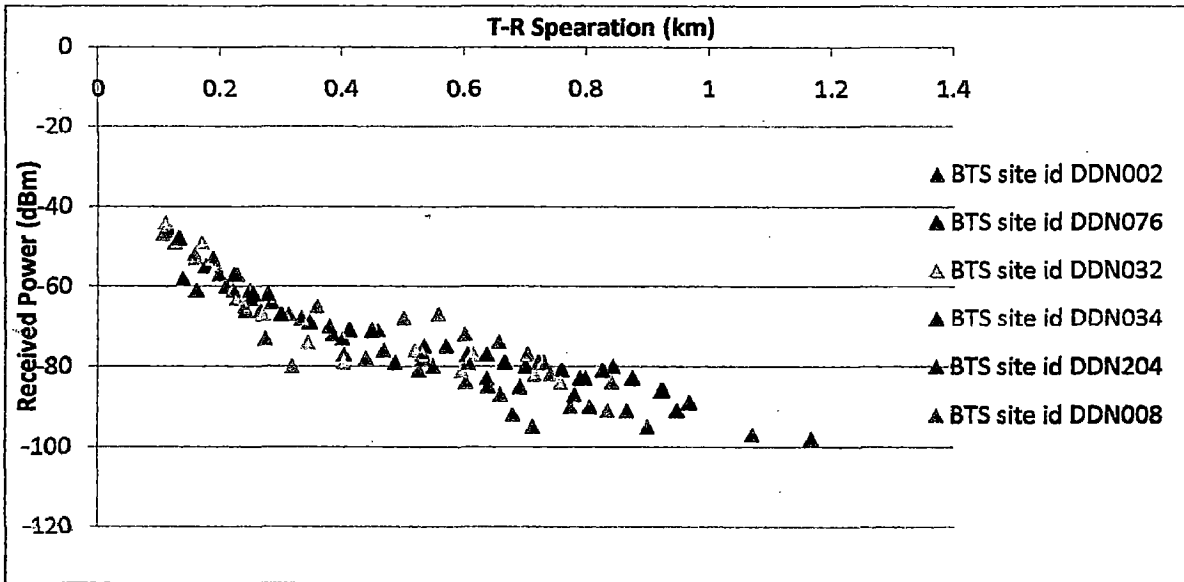


Figure 3.6: Measured received signal power in dBm from four selected BTS ID's

Each received signal strength sample point which is shown in Figure 3.6 is taken from all predefined routes of the four base stations. Every 50 sample points of the received signal strength and T-R separation distance are recorded for each base station. Each measurement point is represented in an average of a set of samples taken over a small area of 1-2 Km in order to analyze the effects of fast fading.

3.5 Path loss calculation

The measured signal power is converted into path loss with the help of equation (3.1)

$$L_p = EIRP + G_{RX} - P_{RX} \quad (3.1)$$

Where EIRP is effective isotropic radiated power, G_{RX} is gain of receiver and P_{RX} is power at receiving end expressed in equation (3.2)

$$EIRP = P_{TX} + G_{TX} - L_{TX} \quad (3.2)$$

EIRP and measured path loss is calculated by substituting the parameters values in above equations (3.1 and 3.2).

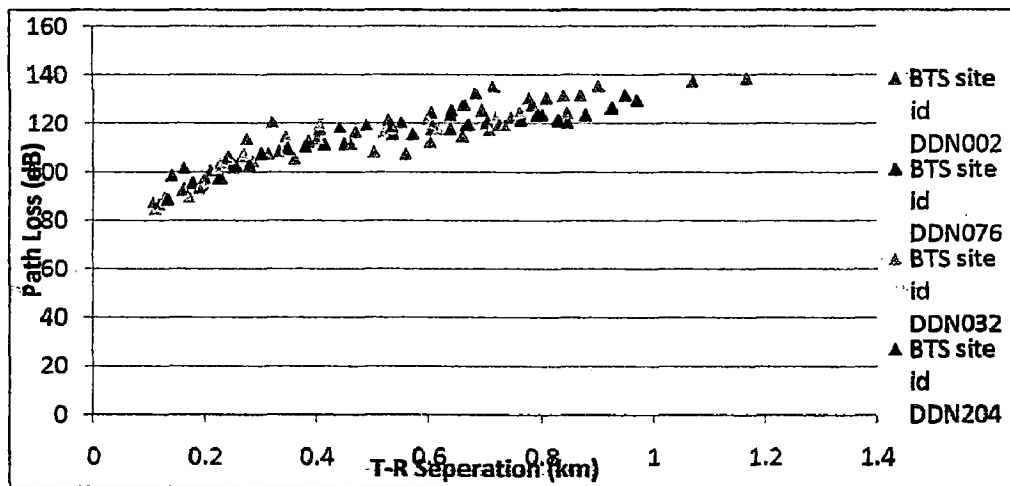


Figure 3.7: Measured path loss from received signal power at selected sites

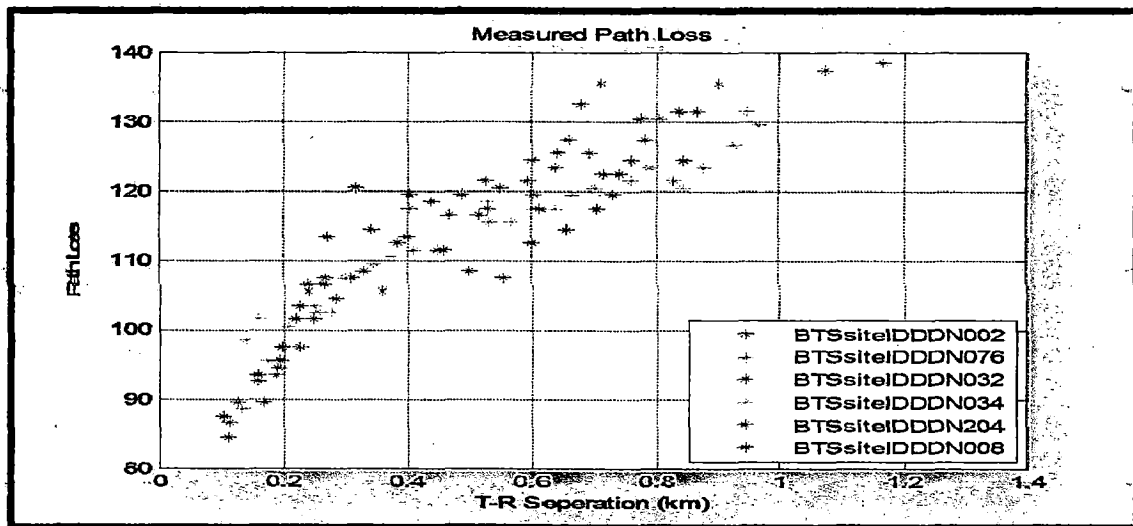


Figure 3.8: Measured path loss from received signal power at selected sites using

MATLAB

Measured received signal power is converted into corresponding path loss as shown in Figure 3.7 and 3.8.

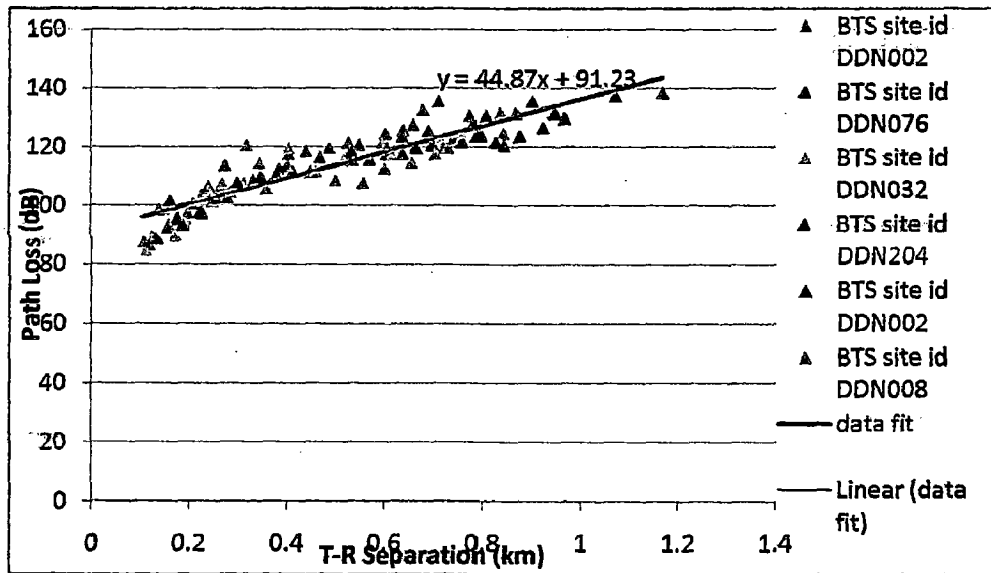


Figure 3.9: Measured path loss and least squares approximation for field collected sample

Measured path loss and least squares approximation for field collected sample data set is shown in Figure 3.9.

3.5.1 Simulation Parameters

The simulation parameters used for the calculation of received signal strength for propagation model and measured path loss is given in Table 3.1.

Table 3.1: Simulation Parameters

Parameters	Values
Base station transmitter power	40dBm
Mobile transmitter power	25dBm
Base station antenna height	30m
Mobile antenna height	1.5m
Transmitter antenna gain	17.5dB
Threshold level for mobile	-101dBm
Threshold level for base station	-108dBm
Frequency	900 MHz
Connector loss	1.5 dB
Cable loss	1.5dB
Duplexer loss	1.5dB

3.6 Performance Analysis and Comparison of Free Space Path Loss (FSPL) Model with Measured Path Loss using MATLAB and Linear Regression

The theoretical Free space path loss (FSPL) model and the measurement result has been compared . The Free space path loss is evaluated using Friis equation (3.3)

$$P_{FSL} (dB) = 32.45 + 20 \text{Log}_{10} (f) + 20 \text{Log}_{10} (d) \quad (3.3)$$

Where f is the operating frequency and d is the distance between transmitter and receiver. The Free-Space Path Loss (FSPL) results from a line-of-sight path through free space (usually air), with no obstacles nearby to cause reflection or diffraction. It does not include factors such as the gain of the antennas used at the transmitter and receiver, nor any loss associated with hardware imperfections. In practical height of the BS is 30m and MS are often located in between the buildings, in street environment full of foliage, so there is no

line of sight path available. Therefore, the received signal at the MS end is influenced by the effect of reflection, diffraction and scattering which leads to the attenuation in received signal. An analysis result indicates that increased path loss observed in the field measurement as compared to the free space loss prediction.

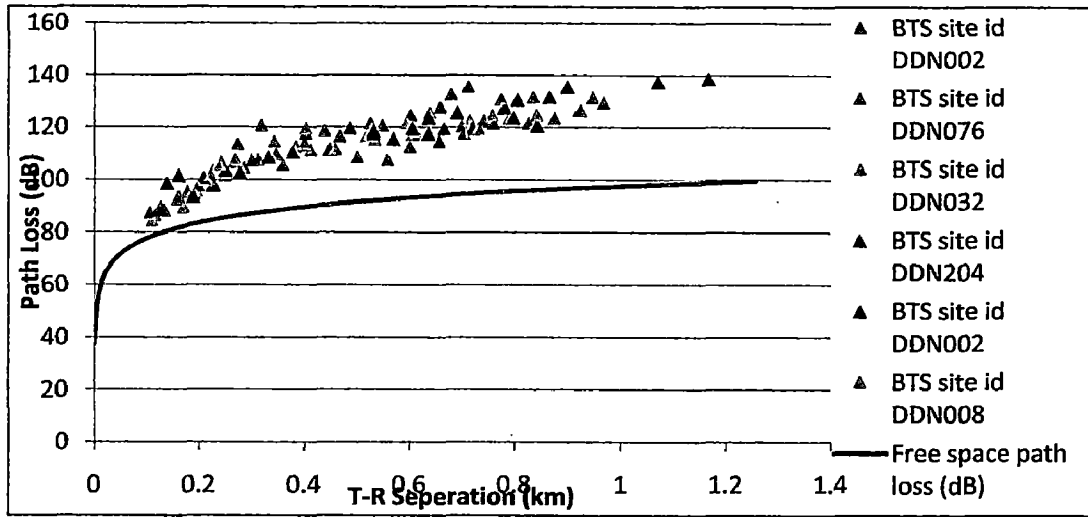


Figure 3.10: Comparison of Free Space Path Loss (FSPL) empirical model with measurements from selected sites

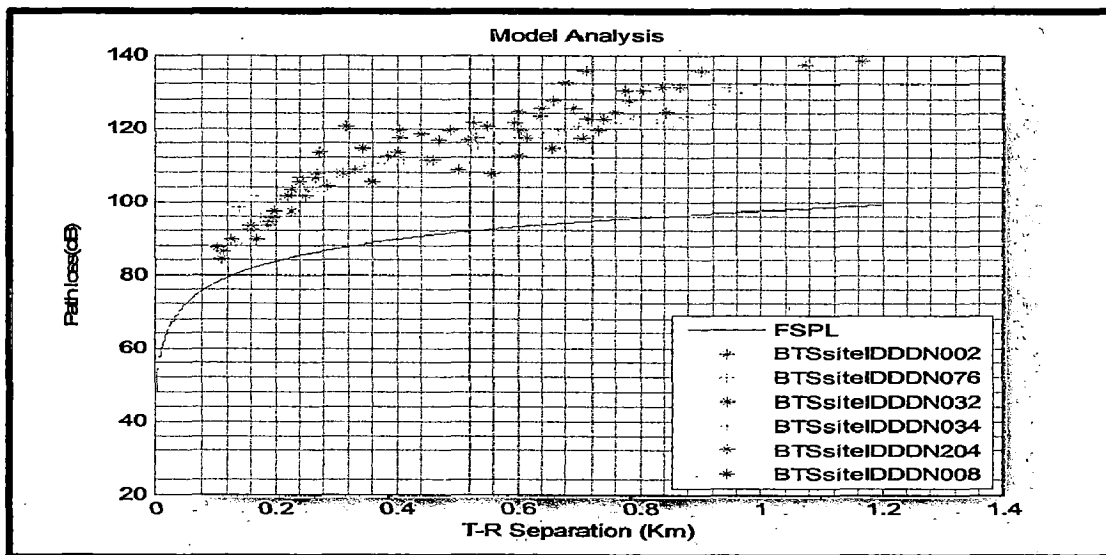


Figure 3.11: Comparison of Free Space Path Loss (FSPL) empirical model with measurements from selected sites using MATLAB

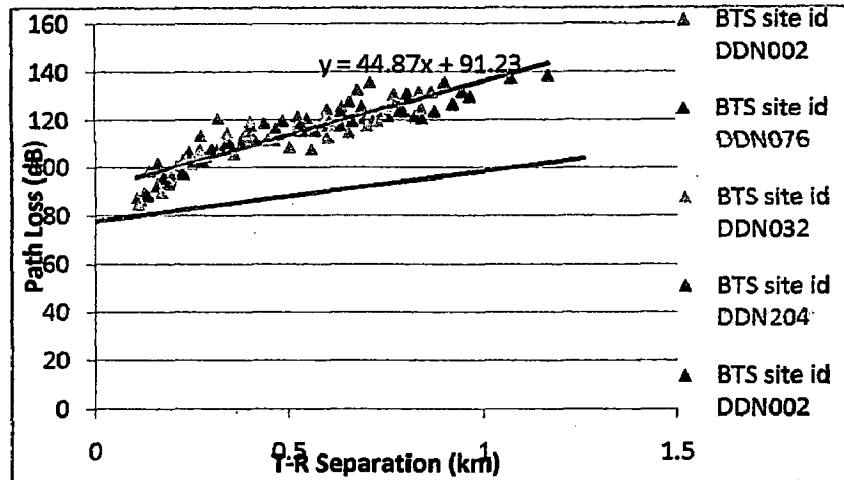


Figure 3.12: FSPL and least squares approximation using linear regression for field collected sample data set

For comparison, Free Space Path Loss (FSPL) model and measurement data has been plotted using MATLAB and least square method with the help of linear regression. Free Space Path Loss Model and measured path loss from field data exhibits a linear property due to which their analysis has been carried out more precisely. The measurement plot in Figure 3.8 is being compared to the Free Space Path Loss Model prediction plot in Figure 3.11 ,over 1-2 km from four selected BTS ID's. Analysis of Figure 3.12 shows that there is a significant difference around a value of 24.45 dB between FSPL prediction and the measured path loss.

As analyzed from Figure 3.10 and 3.11 Free Space Path loss Model (FSPL) significantly underestimates the measured path loss calculated from the set of field collected data.

3.6.1 Why Least Square Approximation using Linear Regression?

Figure 3.11 show that, when distance is in logarithmic scale, the theoretical plot of path loss does not increase linearly. These plots do not give much information for a good path loss comparison. In view of this, a least square method has been selected to determine the best fit of measured path loss as a function of linear regression. The observed path loss has been plotted by using regression technique in the Figure 3.12.

3.7 Performance analysis and comparison of Okumura Model with Measured Path Loss using MATLAB and Linear Regression

Pathloss equation for Okumura's model is expressed in equation (3.4)

$$L_{50} (dB) = L_F + A_{mu} (f,d) - G (h_b) - G (h_m) - G_{area} \quad (3.4)$$

where: L_{50} (dB): is the 50th percentile value of propagation path loss, L_F : is free space path loss, A_{mu} : is free space attenuation, $G(h_b)$: is base station antenna height gain factor, $G(h_m)$: is mobile antenna height gain factor, and G_{area} : is gain corresponding to specific environment.

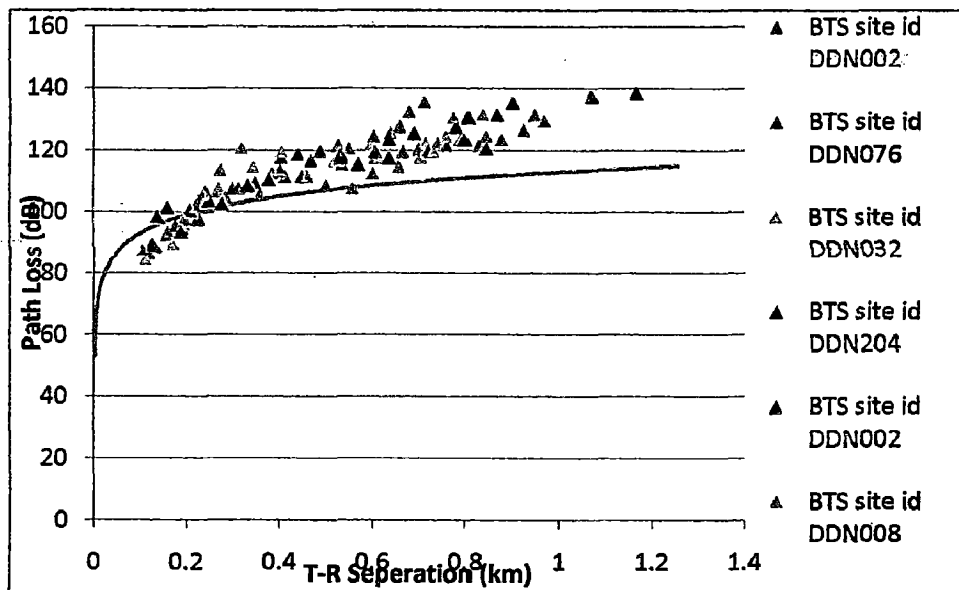


Figure 3.13: Comparison of Okumura empirical model with measurements from selected sites

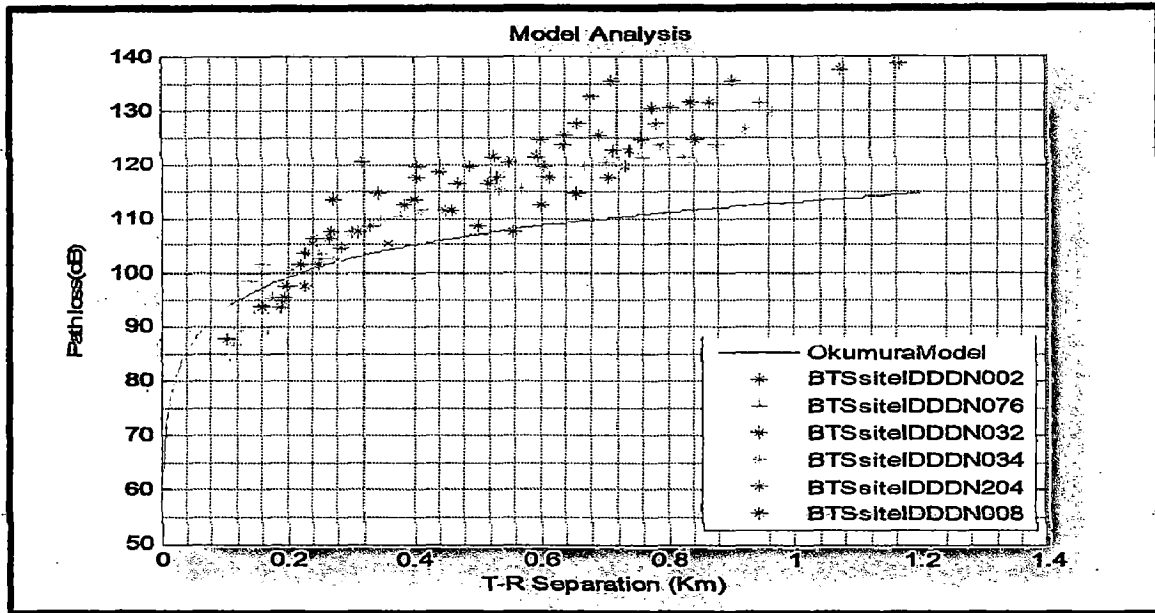


Figure 3.14: Comparison of Okumura empirical model with measurements from selected sites using MATLAB

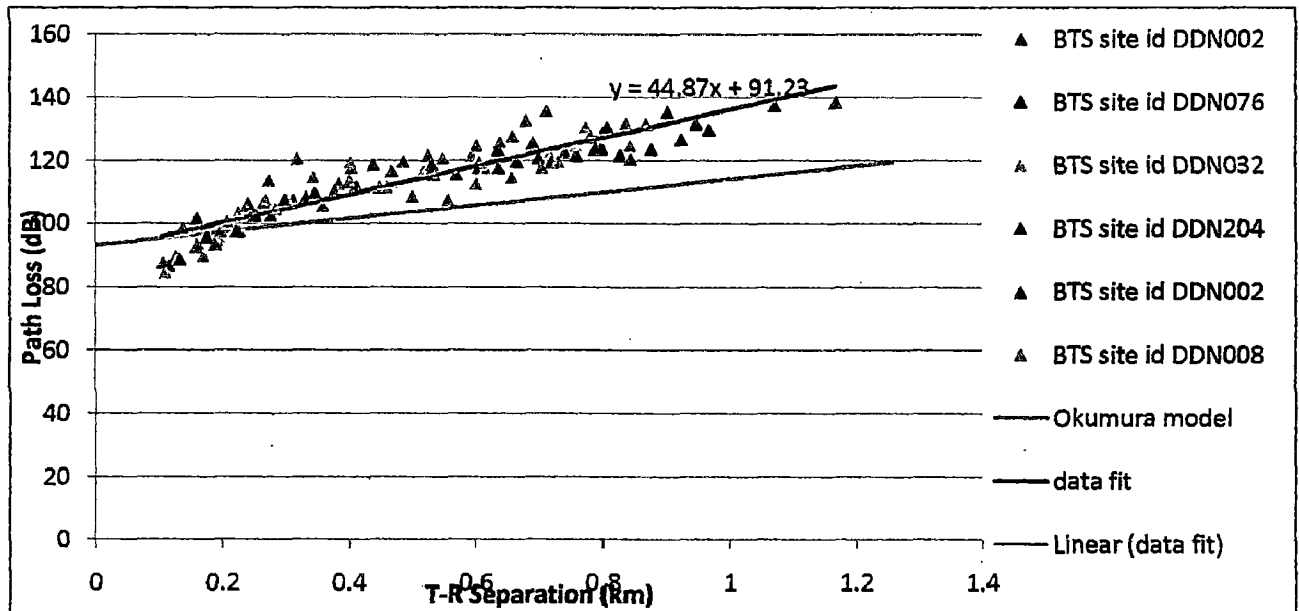


Figure 3.15: Okumura and least squares approximation using Linear Regression for field collected sample data set

Performance analysis of Okumura's model and field measurement is shown in Figure 3.13 and 3.14. From figures it is observed that the field measurement result are slightly higher than the Okumura model i.e. Okumura model underestimates field measurement result. It is observed from Figure 3.15 that there is difference of 10 dB exists between Linear (data fit) and Linear (Okumura model), which remains approximately constant throughout the distance. The model indicates a good agreement with the measured path loss. This is because Okumura model takes all the parameter into account, such as free space loss, median attenuation relative to free space, transmitting/receiving antenna gain and gain due to environment.

3.8 Performance analysis and comparison of Egli Model with Measured Path Loss using MATLAB and Linear Regression

Egli model has been investigated with measured data. Egli model can be formally expressed in equation (3.5) as:

$$P_L(dB) = G_B G_M \left(\frac{h_B h_M}{d^2} \right)^2 \left(\frac{40}{f} \right)^2 \quad (3.5)$$

Where

G_B = Gain of the base station antenna. Unit: dimensionless

G_M = Gain of the mobile station antenna. Unit: dimensionless

h_B = Height of the base station antenna. Unit: meter (m)

h_M = Height of the mobile station antenna. Unit: meter (m)

d = Distance from base station antenna. Unit: meter (m)

f = Frequency of transmission. Unit: megahertz (MHz)

Egli model does not include the effect of clutter in the prediction of path loss. Due to this it does not provide precise result for mobile link but it is useful for planning of fixed link.

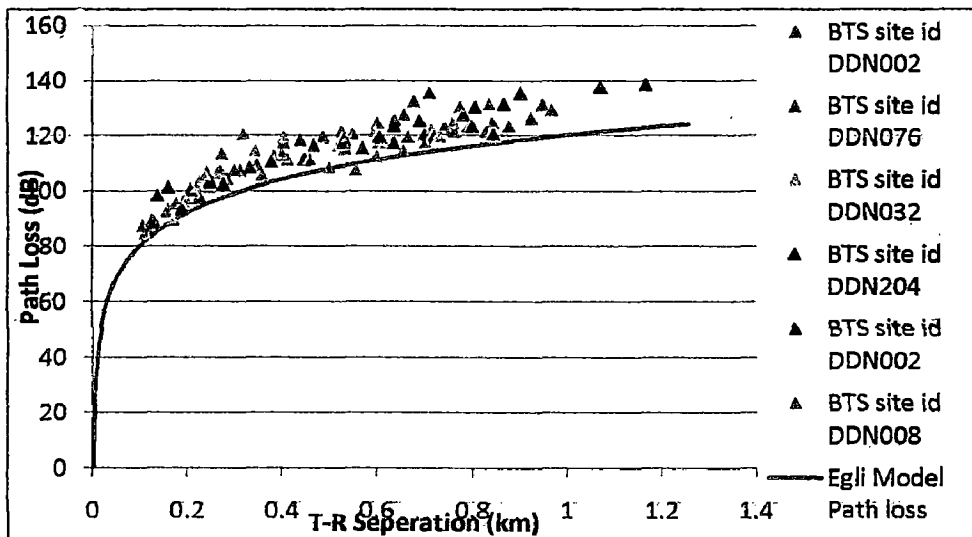


Figure 3.16: Comparison of Egli empirical model with measurements at selected sites

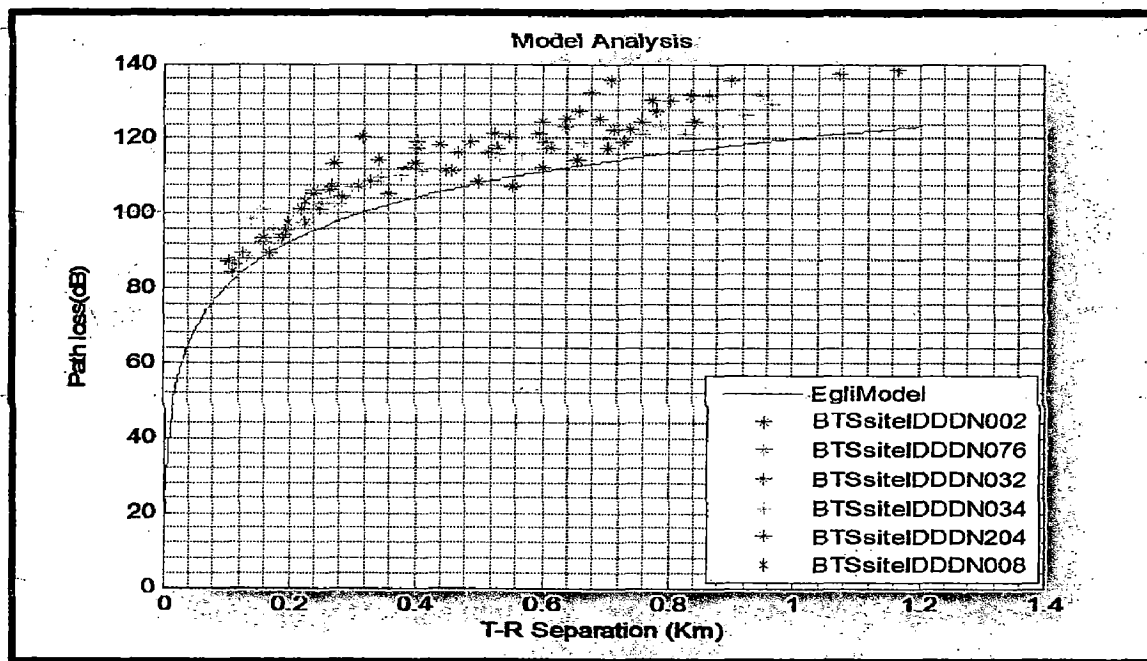


Figure 3.17: Comparison of Egli empirical model with measurements at selected sites using MATLAB

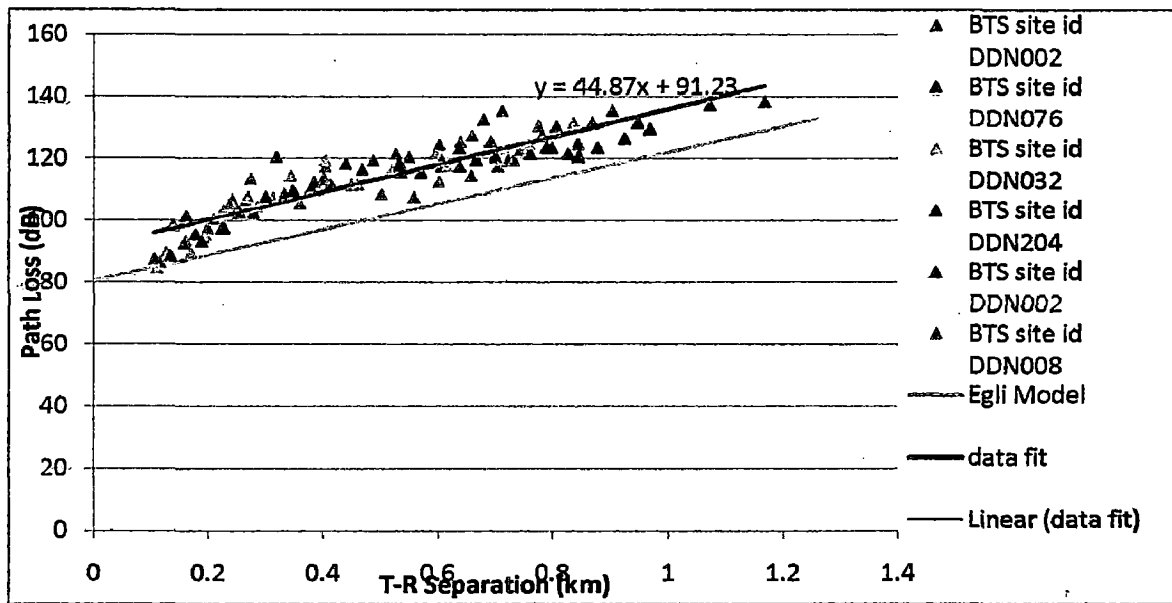


Figure 3.18: Egli and least squares approximation using linear regression for field collected sample data set

It is observed of Figure 3.16 shows that measurement data is attenuated as distance between BTS and MS increases. This is due to the shadowing effect. As the distance between BS and MS increases, difference between measured path loss and Egli prediction reduces, since Egli path loss increases faster with the T-R separation. From Figure 3.17 it is estimated that at 450 m the difference between both is minimum i.e. Egli model closely approximates the measured path loss from field data. This is due to the characteristic of Egli model. Basically Egli model is a terrain model and this type of model provides a measure of path loss as a function of only distance and terrain roughness. A varied terrain can produce diffraction loss, shadowing, blockage and diffuse multipath over a moderate distance and when terrain is flat, only multipath reflection earth diffraction occurs.

It is observed of Figure 3.18 shows that there is a significant difference around a value of 20 dB between Egli model prediction and the measured path loss.

3.9 Performance analysis and comparison of COST 231 Model with Measured Path Loss using MATLAB and Linear Regression

The European Cooperative for Scientific and Technical (COST) [3] research extended the Hata model to 2 GHz as given in equation (3.6):

$$P_L = 46.3 + 33.9 \log_{10}(f) - 13.82 \log_{10}(h_b) - a(h_m) + (44.9 - 6.55 \log_{10}(h_b)) \log_{10} d + C_m \quad (3.6)$$

where $a(h_m)$ is the mobile antenna correction factor and for a small to medium sized city, it is defined as

$$a(h_m) = (1.1 \log f - 0.7) h_m - (1.56 \log f - 0.8) \text{ dB}$$

and for a large city, it is given by

$$a(h_m) = 8.29 (\log 1.54 h_m)^2 - 1.1 \text{ dB} \quad \text{for } f_c \leq 300 \text{ MHz}$$

$$a(h_m) = 3.2 (\log 11.75 h_m)^2 - 4.97 \text{ dB} \quad \text{for } f_c \geq 300 \text{ MHz}$$

C_m is 0 dB for medium sized cities and suburban areas and is 3 dB for metropolitan areas. This model is restricted to the following range of parameters:

f : 1500 MHz to 2000 MHz

h_b : 20 m to 50 m

h_m : 1 m to 10 m

d : 1 km to 5 km

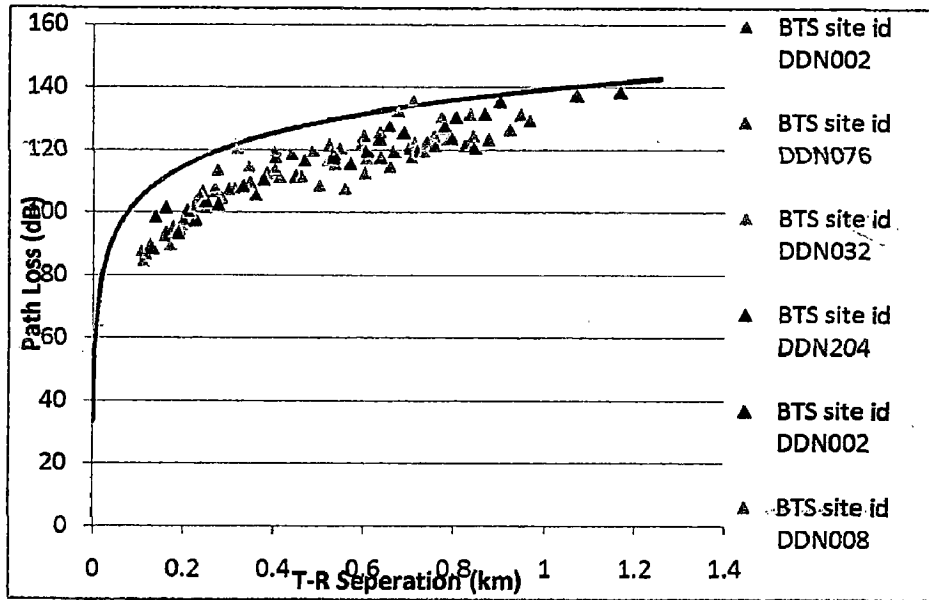


Figure 3.19: Comparison of COST 231 empirical model with measurements at selected sites

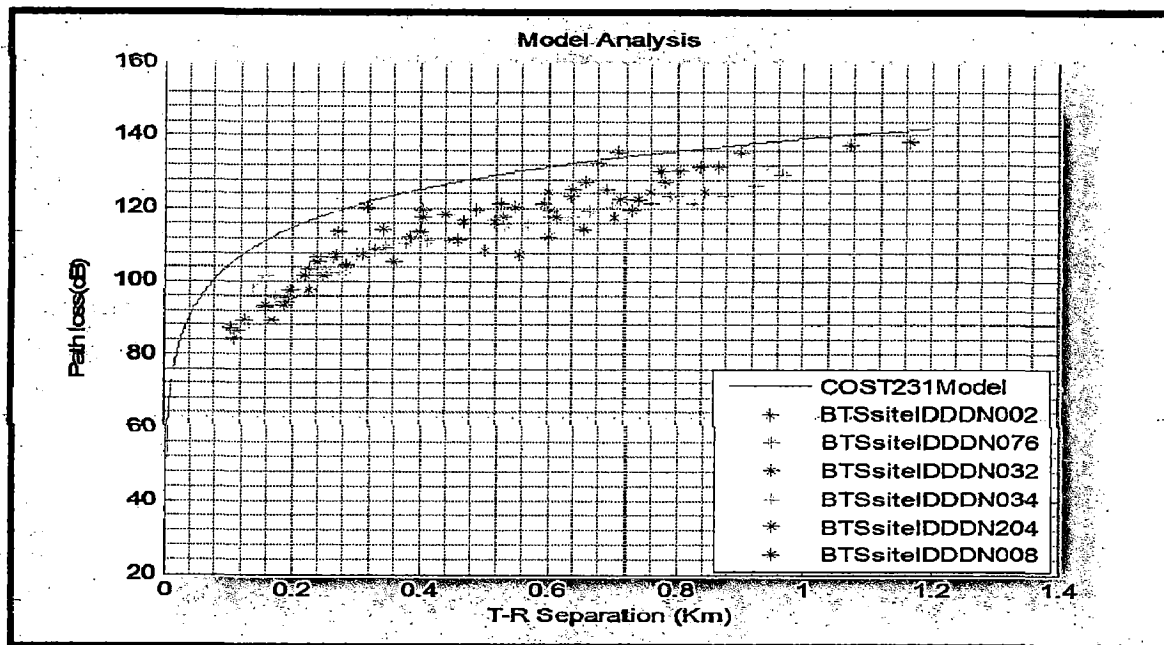


Figure 3.20: Comparison of COST 231 empirical model with measurements at selected sites using MATLAB

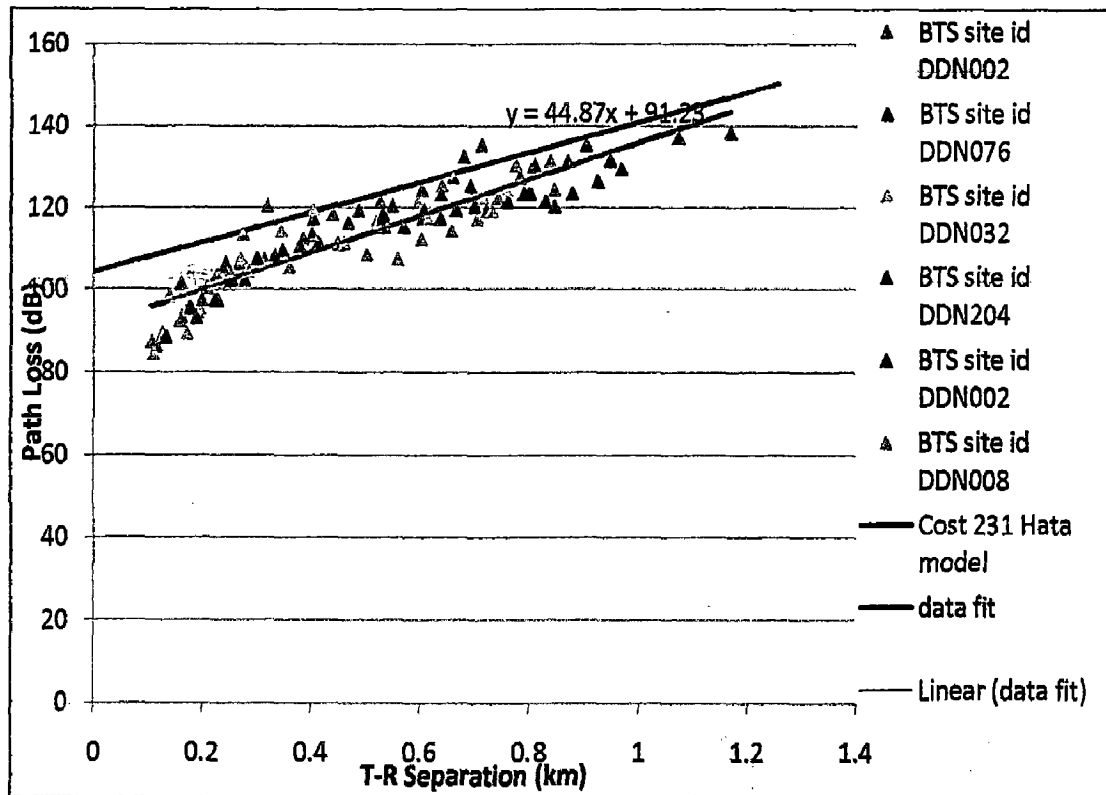


Figure 3.21: COST 231 and least squares approximation using linear regression for field collected sample data set

Performance analysis of COST 231 model and measurement result in Figure 3.20 and Figure 3.21 illustrates that the deviation of model from the measurement decreases as MS moves away from the BS. At 900 m the deviation reached to a value of 20 dB. This is due to the fact that more dense clutter exists between BS and MS, which contributes more losses to received signal as MS moves away from BS. Therefore it is concluded that the uniform environment could not be classified using COST 231 model. It is observed from Figure 3.19 and 3.20 that COST 231 Model significantly overestimates the measured path loss calculated from the set of field collected data.

3.10 Performance analysis and comparison of COST WI Model with Measured Path Loss using MATLAB and Linear Regression

This model is a combination of COST231 and J. Walfish , F. Ikegami model. The COST 231 project further developed this model. Now it is known as a COST 231 Walfish-Ikegami (W-I) model. This model is most suitable for flat suburban and urban areas that have uniform building height. Among other outdoor propagation models, COST 231 W-I model gives a more precise path loss. It distinguishes different terrain with different proposed parameters. The model distinguishes between two situations i.e. "Line of Sight" (LOS) and the "None Line Of Sight" (NLOS) situation.

LOS situation [50]

For the LOS-case the prediction is very easy, as only one equation with two parameters is necessary as shown in equation (3.7)

$$PL_{LOS} = 42.6 + 20 \text{Log}_{10}(f) + 26 \text{Log}_{10}(d) \quad (3.7)$$

Where d is in Km and f is in MHz

NLOS situation [63]

The NLOS equation 3.8 is more complicated. The loss in the NLOS case is the sum of the Free Space Loss l_0 , the Multiple Screen diffraction loss l_{msd} and the Rooftop-To-Street diffraction loss l_{rts} :

$$l_p = l_0 + l_{rts} + l_{msd} + l_{rts} + l_{msd} > 0 \quad (3.8)$$

$$l_0 + l_{rts} + l_{msd} \leq 0$$

The Free Space Loss:

$$l_0 = 32.45 + 20 \text{Log}_{10}(f) + 20 \text{Log}_{10}(d)$$

The Rooftop-To-Street diffraction loss term l_{rts} determines the loss which occurs on the wave coupling into the street where the receiver is located. The origin of this loss comes from the Ikegami model, but COST 231 has extended this to equation (3.9)

$$l_{rts} = -16.9 - 10 \log \frac{w}{m} + 10 \log \frac{f}{MHz} + 20 \log [(h_{roof} - h_{RX}) / m] + l_{ori} \quad (3.9)$$

Where, w is width of the roads, h_{roof} is the rooftop height, h_{RX} is the receiver height and ϕ is the road orientation.

With

$$l_{ori} = \begin{cases} -10 + 0.354\phi & \text{for } 0 \leq \phi \leq 35 \\ 2.5 + 0.075(\phi - 35) & \text{for } 35 \leq \phi \leq 55 \\ 4 - 0.114(\phi - 55) & \text{for } 55 \leq \phi \leq 90 \end{cases}$$

The orientation loss l_{ori} is an empirical correction term obtained from the calibration with measurements. The multi-screen diffraction loss is taken into account additionally:

$$l_{msd} = l_{bsh} + k_a + k_d \log d + k_f \log f - 9 \log b$$

Where

$$l_{bsh} = \begin{cases} -18 \log [1 + (h_{TX} + h_{roof})] & \text{for } h_{TX} > h_{roof} \\ 0 & \text{for } h_{TX} \leq h_{roof} \end{cases}$$

$$k_d = \begin{cases} 18 & \text{for } h_{TX} > h_{roof} \\ 18 - 15 \frac{(h_{TX} - h_{roof})}{h_{roof}} & \text{for } h_{TX} \leq h_{roof} \end{cases}$$

$$k_a = \begin{cases} 54h_{TX} > h_{roof} \\ 54 - 0.8 \frac{h_{TX} - h_{roof}}{m} d \geq 0.5km \text{ and } h_{TX} \leq h_{roof} \\ 54 - 0.8 \frac{h_{TX} - h_{roof}}{m} \frac{d/km}{0.5} d < 0.5km \text{ and } h_{TX} \leq h_{roof} \end{cases}$$

$$k_f = -4 + \begin{cases} 0.7 \left(\frac{f/\text{MHz}}{925} - 1 \right) & \text{for medium sized city and suburban centers} \\ 1.5 \left(\frac{f/\text{MHz}}{925} - 1 \right) & \text{for metroplitan centers} \end{cases}$$

The factors k_d and k_f control the dependence of the multi-screen diffraction loss versus the distance and the radio frequency. The factor k_a indicates the increase of the path loss for base stations below the rooftop.

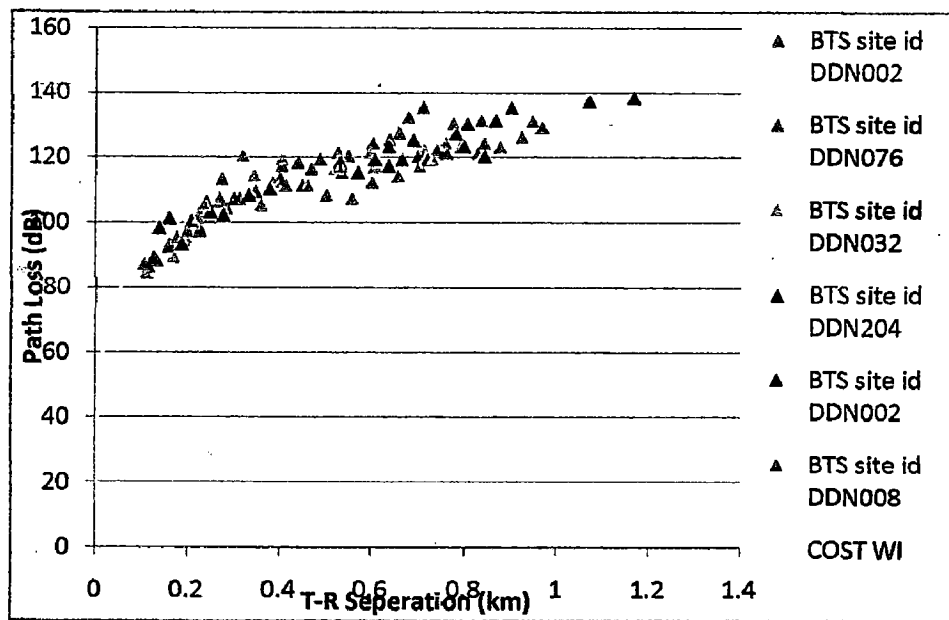


Figure 3.22: Comparison of COST- WI empirical model with measurements at selected sites

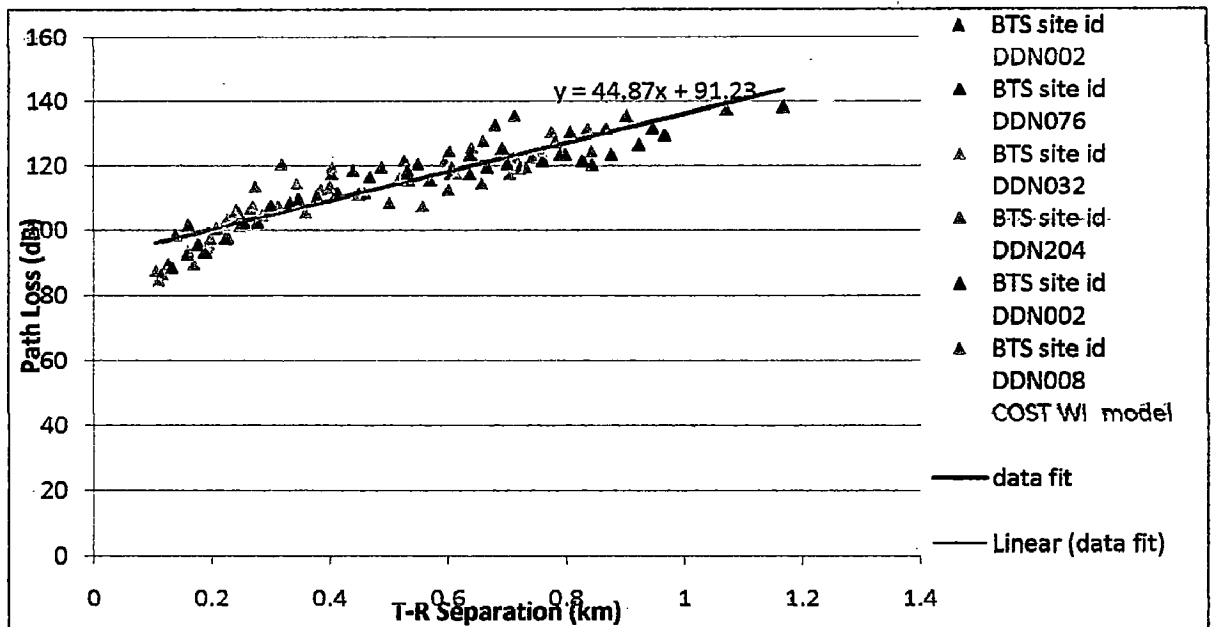


Figure 3.23: COST -WI and least squares approximation using linear regression for field collected sample data set

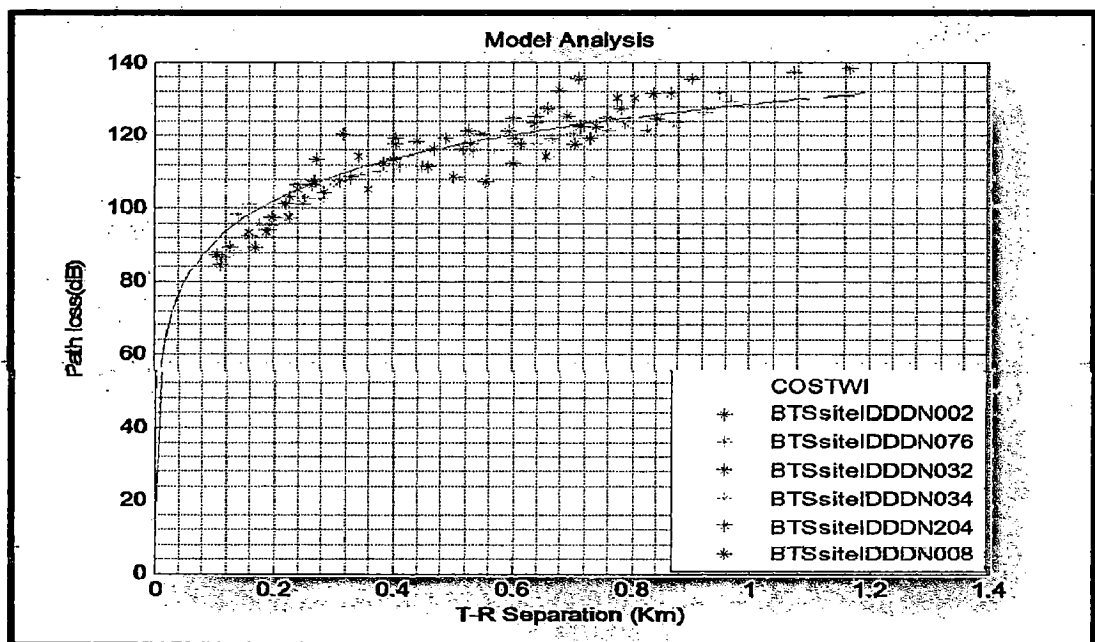


Figure 3.24: Comparison of COST-WI empirical model with measurements at selected sites using MATLAB

COST-WI model and measurement data has been plotted using MATLAB and least square method with the help of linear regression. COST-WI and measured path loss from field data exhibits a linear property. The measurement plot in Figure 3.8 is being compared to the COST-WI Model prediction plot in Figure 3.22 which the minimum difference between them. Analysis of Figure 3.24 shows that there is a minimum difference around a value of 05 dB between COST-WI results and the measured path loss. It is observed from Figure 3.22 and 3.23 that COST-WI model nearly estimates the measured path loss calculated from the set of field collected data. Measurement data is minimum attenuated as distance BTS and MS increases.

3.11 Performance analysis and comparison of ECC-33 MODEL with MEASURED PATH LOSS using MATLAB and LINEAR REGRESSION

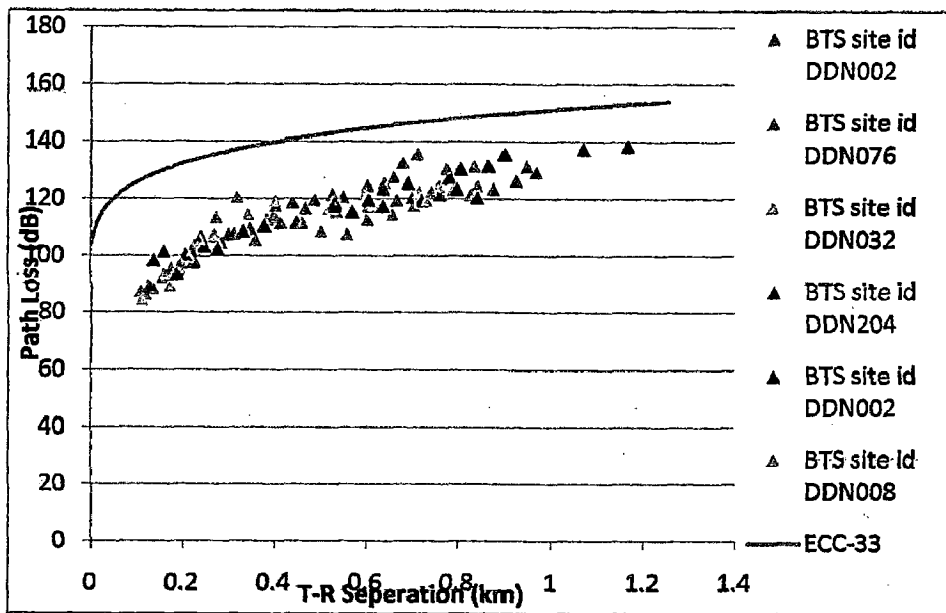


Figure 3.25: Comparison of ECC -33 empirical model with measurements at selected sites

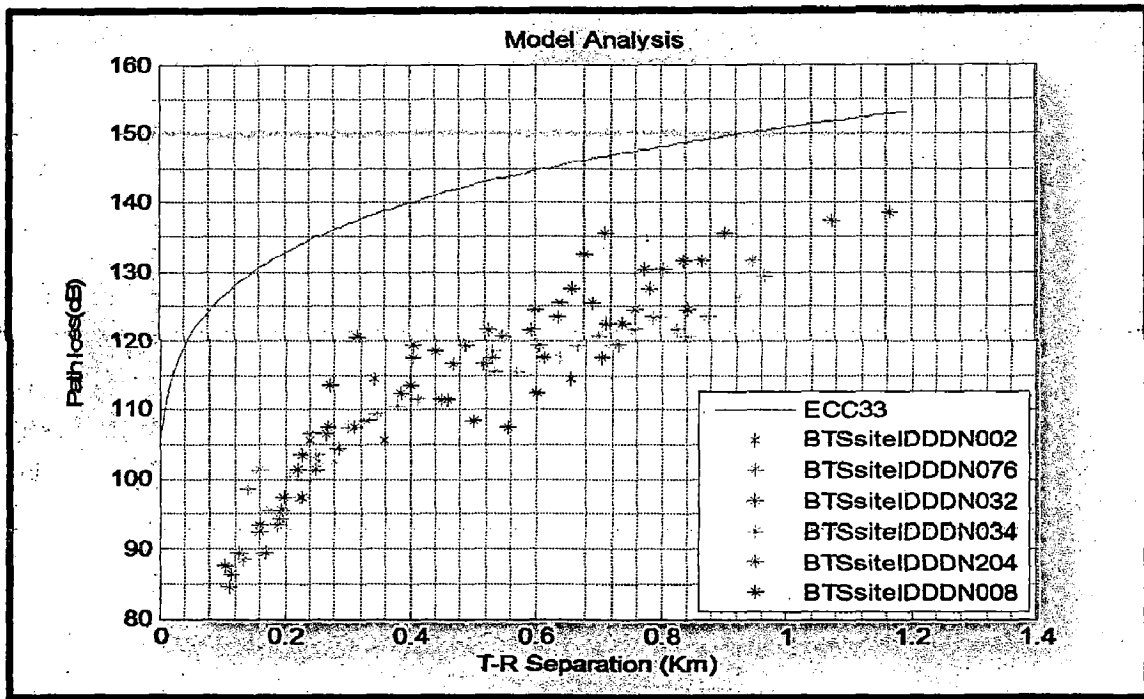


Figure 3.26: Comparison of ECC-33 empirical model with measurements at selected sites using MATLAB

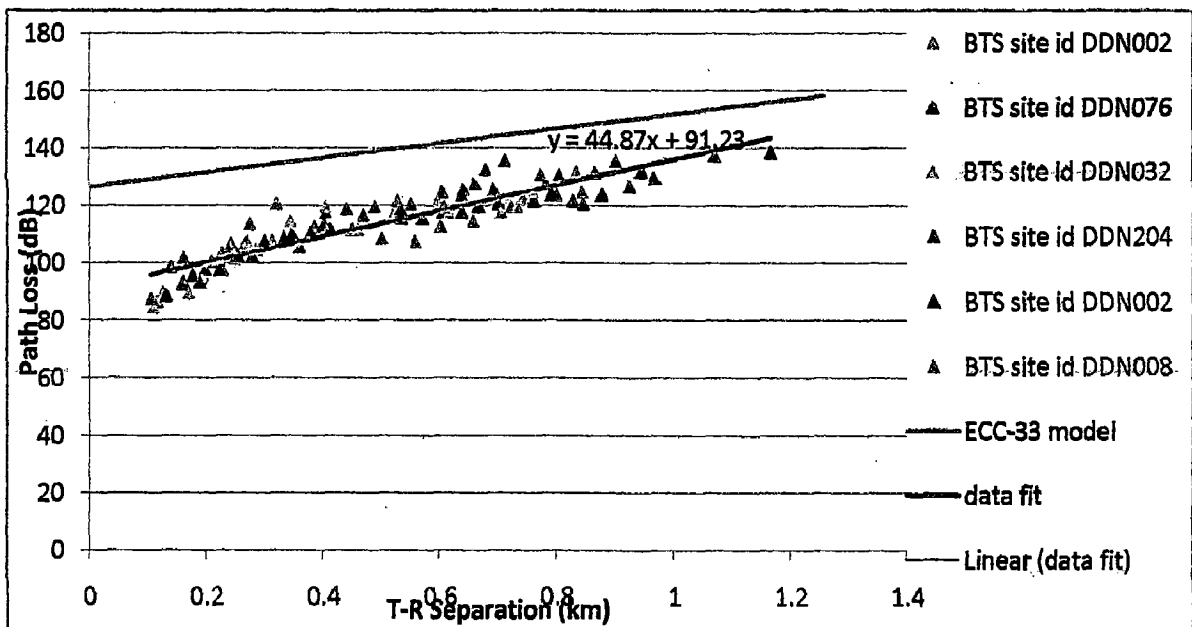
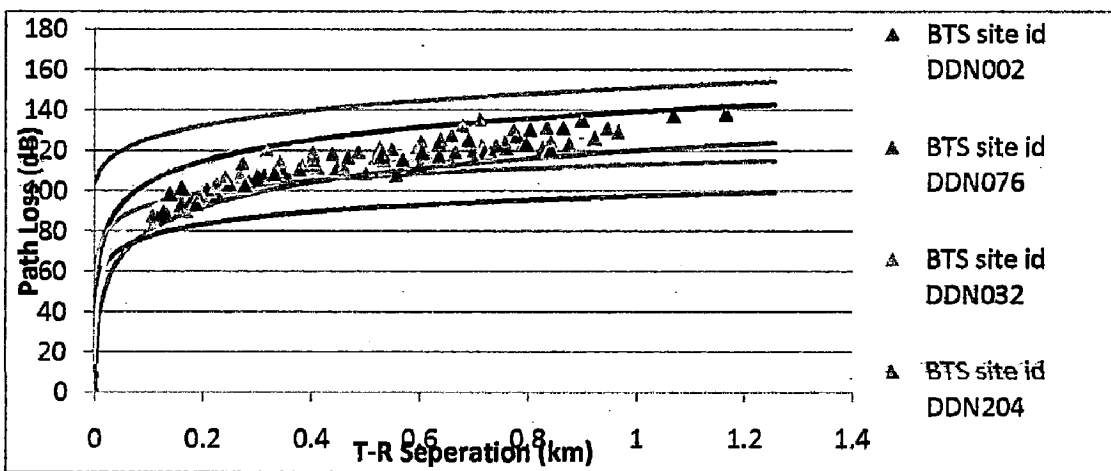


Figure 3.27: ECC-33 and least squares approximation using linear regression for field collected sample data set

Figure 3.25 and 3.26 shows that ECC 33 Model significantly overestimates the measured path loss calculated from the set of field collected data. This is due to the design of ECC-33 model. Performance analysis of ECC 33 model and measurement result is shown in Figure 3.27. It shows that the deviation of model from the measurement decreases as MS moves away from the BS. At 600 m the deviation reached to a value of 35 dB.

3.12 COMBINED GRAPH OF PERFORMANCE ANALYSIS AND COMPARISON OF FSPL, OKUMURA, EGLI, COST 231, COST WI AND ECC 33 MODEL WITH MEASURED FIELD PATH LOSS USING MATLAB



(a)

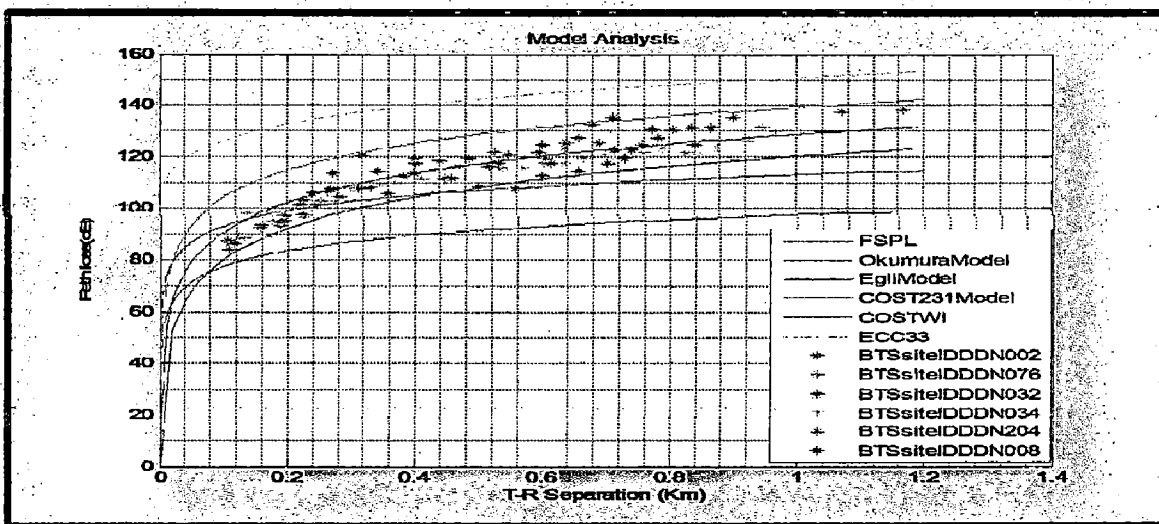


Figure 3.28 (a) and (b): Combined performance analysis of Free Space Path Loss, Okumura's, Egli, COST 231, COST WI, ECC 33 models with field measurement data using MATLAB

Okumura's model, COST 231 model, COST WI, ECC 33 and the data collected during field measurement over a distance up to 2 Km, COST-WI model is best fit model for Dehradun Uttarakhand. Analysis from Figure 3.28 and 3.29 indicates that the path loss is higher for FSPL, Egli, Okumura's model but less for ECC 33 and COST 231 WI.

3.15 Model tuning [67]

By many researchers [25] relative error of the measured path loss to the existing path loss models is determined for tuning. Figure 3.30 shows the relative errors of measured path loss to the existing path loss model that are plotted versus T-R separation distance. The relative error as given in equation (3.11) increases as the T-R separation distance is small where LOS condition exists. This is due to the shadowing effect as the antenna of the base station is high.

$$\text{Relative Error} = \left| \frac{\text{Measured Value} - \text{Predicted Value}}{\text{Measured Value}} \right| * 100\% \quad (3.11)$$

The mean error is then estimated using equation 3.12

$$\text{Mean Error} = \frac{\sum \text{Relative error}}{N} \quad (3.12)$$

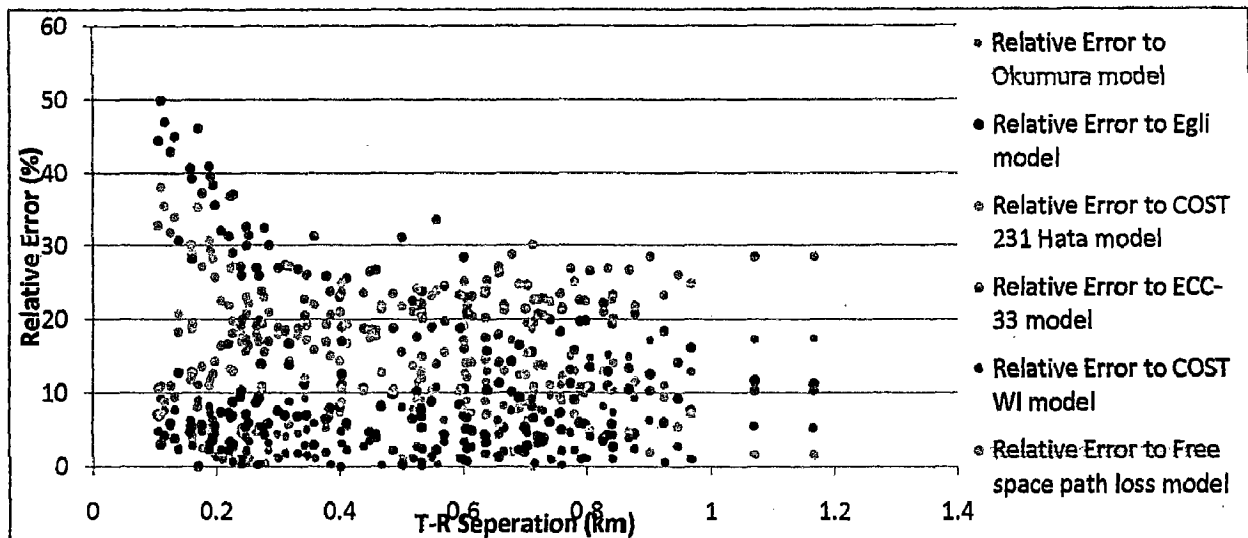


Figure 3.30: Relative Errors of the measured path loss to the existing path loss of the models

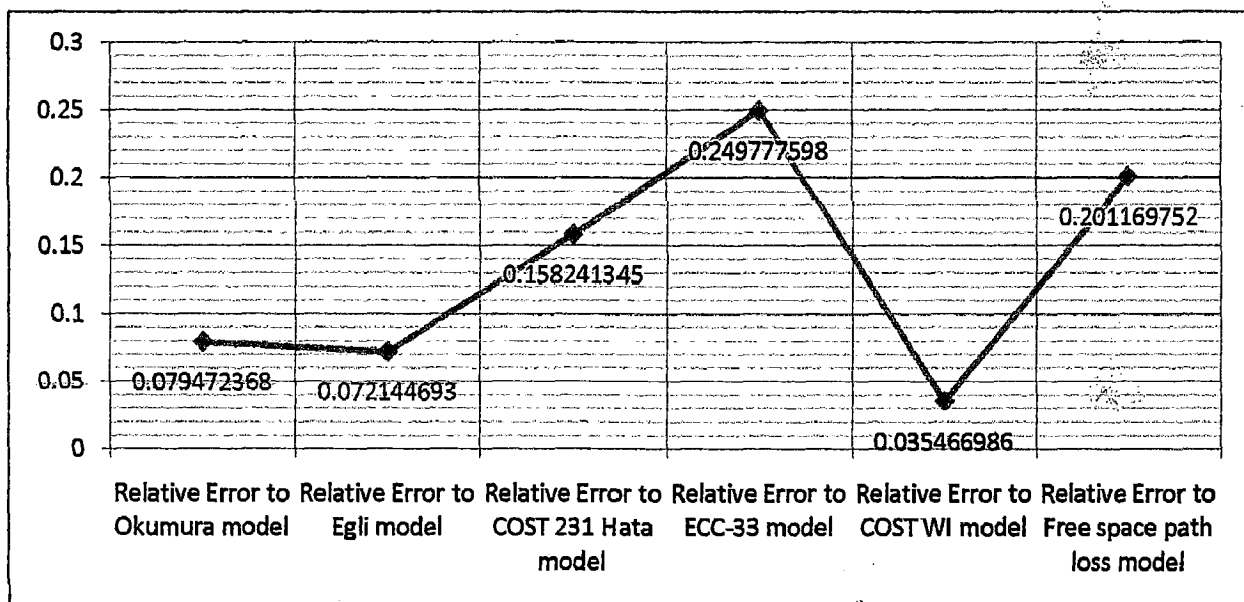


Figure 3.31: Mean error of path loss model

The minimum mean relative error of measurement path loss to the reference path loss model, it has been analyzed that the COST-WI model has the smallest mean relative error of 3.5 % among the selected outdoor path loss models as shown in Figure 3.31. Relative error is evaluated by using equation 3.11. By the comparison of various models with the measured data, it is analyzed that the COST-WI model is the best suitable model for the fringe region of Dehradun, Uttarakhand since it has least mean error of 3.5%. After the

model selection, COST -WI model and field collected data is plotted against T-R separation. A linear line is developed for COST-WI model and measured data with the help of regression fitting method. The COST-WI linear line is compared to measured data linear line and a mean relative error of 3.5 % is recorded. The linear line of measured data is used as reference during the path loss model tuning process.

3.15.1 Tuned COST WI model

For model tuning purpose, three variables namely A, B and C has been added into the equation of COST-WI model and the new modified COST -WI model is represented as:

$$COST\ WI\ model\ l_p = l_o + l_{rts} + l_{msd}$$

$$L_{Tuned} (dB) = A * l_o + B * l_{rts} + C * l_{msd}$$

Where A, B, C are the coefficient to be tuned in the tuned COST- WI model. The variables A, B, C are used to approach the measured data linear line based on smallest mean relative error. The analysis tool “solver” is used to determine the variables A, B, C for the smallest mean relative error is equal to zero. The minimum mean relative error up to 0.0008% for COST- WI is achieved where the value of A, B, C determined. The obtained values of these variables are as follow:

$$A = 0.991943$$

$$B = 1.010591$$

$$C = 0.999026$$

Thus the Tuned COST-WI model is represented as

$$L_{Tuned} (dB) = 0.991943 * l_o + 1.010591 * l_{rts} + 0.999026 * l_{msd}$$

From the Figure 3.32, the result clearly shows that the graph of tuned model is concurrent with the measured data. This is because the COST-WI model is tuned by using tuning technique.

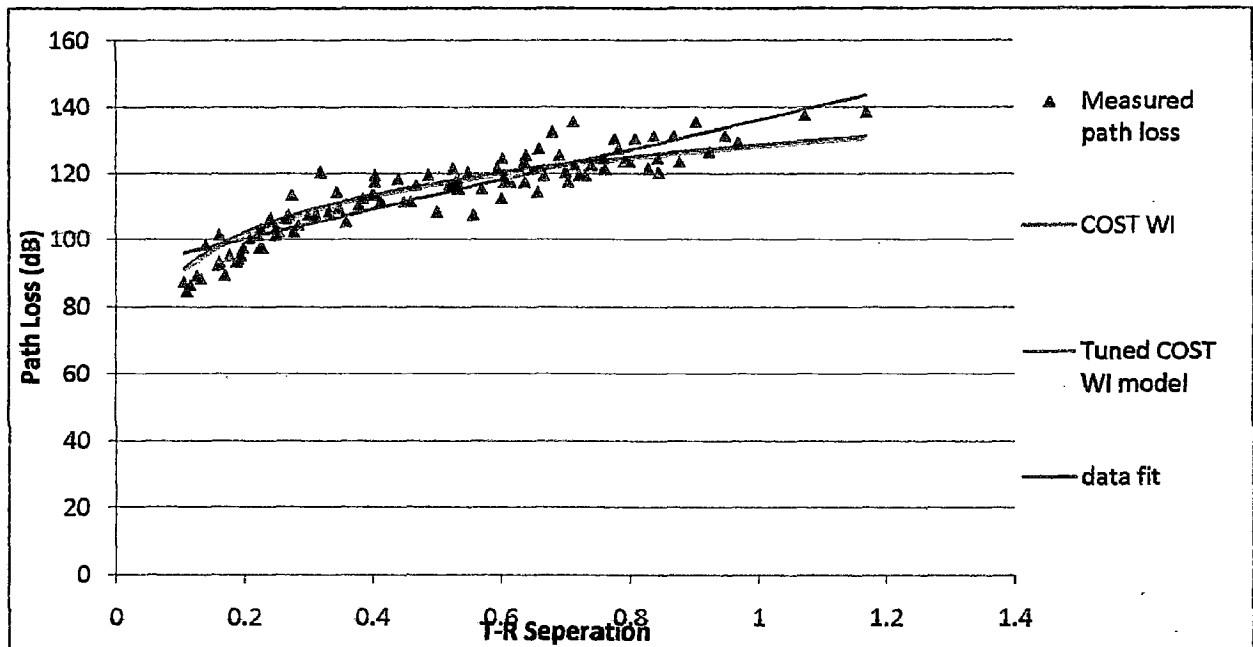


Figure 3.32: Tuned COST WI model with minimum mean error

3.16 CONCLUSION

The free space model assume that there is no obstacle between BS and MS, which causes reflection and diffraction and LoS path exist between BS and MS. It also not includes the losses due to hardware and different type of antenna gain. That is the reason for a 24.45dB difference which exists between free space path loss model and measured loss. Performance analysis of Okumura's model and field measurement in Figure 3.13 and 3.14 illustrates that the Okumura model underestimates field measurement result. As analyzed from Figure 3.15 there is difference of 10 dB exists between Linear (data fit) and Linear (Okumura model), which remains approximately constant throughout the distance. The model indicates a good agreement with the measured path loss. This is because Okumura model takes all the parameter into account such as free space loss, median attenuation

relative to free space, transmitting/receiving antenna gain and gain due to environment. Analysis of Figure 3.16 shows that measurement data is attenuated as distance between BTS and MS. This is due to the shadowing effect. As the distance between BS and MS increases, difference between measured path loss and Egli prediction reduces, since Egli path loss increases faster with the T-R separation. From Figure 3.17 it is estimated that at 450 m the difference between both is minimum i.e. Egli model closely approximates the measured path loss from field data. Analysis of Figure 3.18 shows that there is a significant difference of 20 dB exists between Egli model prediction and the measured path loss. Performance analysis of COST 231 model and measurement result in Figure 3.21 illustrates that the deviation of model from the measurement decreases as one move away from the BS. At 900 m the deviation reached to a value of 20 dB. This is due to the fact that more dense clutter exists between BS and MS, which contribute more losses to received signal as MS moves away from BS. Therefore it is concluded that the uniform terrain could not be classified using COST 231 model. As analyzed from Figure 3.19 and 3.20 that COST 231 Model significantly overestimates the measured path loss calculated from the set of field collected data. COST-WI and measured path loss from field data exhibits a linear property. The measurement data is being compared to the COST-WI Model prediction in Figure 3.22, which indicates the minimum difference. Analysis of Figure 3.24 shows that there is a minimum difference of around 05 dB exists between COST-WI prediction and the measured path loss. As analyzed from Figure 3.22 and 3.23 that COST-WI model is in close approximation with the measured path loss calculated from the set of field collected data. Measurement data is minimum attenuated as distance BTS and MS increases. The results of Figure 3.32 clearly show that the graph of tuned model is concurrent with the measured data and reduces the mean error for best fit model i.e. COST WI model from 3.5% to .008%.

CHAPTER 4

THE ASSESSMENT OF EFFECT OF RAIN FALL ATTENUATION ON OUT DOOR PROPAGATION MODEL USING FUZZY APPROACH

4.1 Background and Motivation

It has been reported that radio propagation is affected under atmospheric vulnerabilities, so it is planned to analyze the effect of rain fall attenuation on outdoor propagation model using fuzzy approach. Most of the rainfall attenuation models developed so far focused mainly on statistical prediction approach [88]. This has led to the development of many successful models used and deployed worldwide[21][36][37]. The most important parameter in radio propagation is the signal itself, which suffers attenuation in various forms under variety of influences, one such influence is that of rainfall on signal attenuation.

Related Work

Marc Bechler et. al. analyze in their paper Fuzzy Logic Based Handoffs in Vehicular Communication Environments and proposed a management entity called Mocca Muxer located in the network layer of a communication system which integrate itself seamlessly into a proxy-based communication architecture. Tae Kyung Kim et. al suggested a Trust Model using fuzzy logic in Wireless Network. They applied in their suggested model to wireless networks how trust mechanisms are involved in communication system. A survey of fuzzy logic applications and principles in wireless communications is presented by Maria Erman et. al. , with the aim of highlighting successful usage of fuzzy logic techniques in Wireless Communication and this paper proposes areas for further research targeted to practice-oriented researchers. T. Meitzler , Harpreet S. et. al analyze search time in visually cluttered scenes using Fuzzy Logic Systems for Wireless Communications how they can handle a broad range of uncertainties totally within their framework [36].

4.2 Why Fuzzy Logic for attenuation prediction due to rainfall?

Fuzzy logic can be used as a tool to analyze the problem scenarios suffering from issues of sub-optimality, impreciseness or vagueness and thus provide a more quick, simple and sufficient solution to the problem. Fuzzy logic is becoming popular in the due course of time and is widely being used in the modern applications of control systems , prediction systems and for even the most complex systems. General fuzzy system consists of set of inputs, predefined rules, membership functions defined for each input and the output based on a defuzzification methodology in correlation with the fuzzy inference module. A Fuzzy inference system for attenuation prediction due to rainfall has been developed, based on the data of annual average rainfall which has been calculated as shown in Table 4.4. The data set used here is more focused on rainfall for the region of Dehradun, India. A simple fuzzy approach to predict the rainfall related signal attenuation has been reported in this chapter. As the core of the functionality of this prediction technique, ITU-R model fundamentals have been deployed. The rainfall data used in fuzzy approach is obtained from Indian Hydrometeorology Division, Dehradun. This data summarizes rainfall-rates from 2006-2010 .The task undertaken involves analysis of rainfall data and prediction of attenuation for each month during monsoon. The more emphasis has been laid on the months of heavy monsoon season i.e. May, June, July, August and September. Main input parameters to the fuzzy inference system considered here are specific attenuation due to polarization, station height and rainfall-rate. The three output membership functions have been classified as: low, very-low, medium, high, and very-high to depict the attenuation prediction logically. Mamdani FIS based scheduling has been used to predict rainfall attenuation. Below Figure 4.1 depicts a general fuzzy inference module:

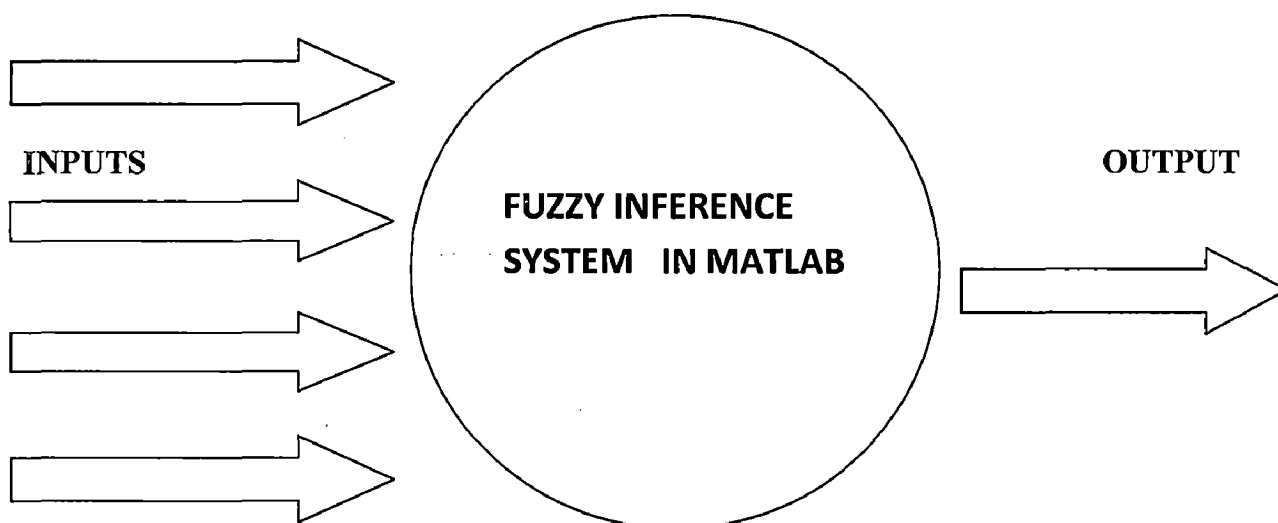


Figure 4.1: General Fuzzy Inference System

4.3 Rain fall attenuation analysis

The rainfall attenuation analysis activities starts from the term called 'Drop-Size Distribution'- (DSD). This is due to the fact that the rain drops present in the atmosphere as hydrometeors causes scattering of radio-waves propagating through them. The actual problem of rainfall attenuation prediction deals with initial task of relating two quantities i.e. the rainfall and rain rate, the most easily available data with the attenuation. Attenuation is also related with two distinct polarizations, which is also used as a prime prediction step. All these factors are related to the integral of drop-size distribution function represented as $N(D)$, defined mathematically depicting $N(D) dD$ as the number of drops of rain collected per cubic meter with drop size lying between the integration limits of D and $D+dD$. Generally, the drop shape is taken to be spherical but in certain cases it may be slightly non-spherical, in such cases measurements are carried out considering volume of that of an equivalent equi-volumic sphere, thus $N(D)$ is sometimes also called as the shape factor.

Table 4.1: Comparison of different DSD functions

DSD Function type	Remarks
1.Exponential Distribution	Most Preliminary Model
2.Gamma Distribution	More general
3.Laws-Parson Distribution	Empirical by nature, primitive
4.Marshall-Palmer Distribution	Similar to 3 except larger no. of smaller drops in the spectra.

- According to drop-size distribution, 1mm and 2mm diameter contribute to about 60% of the total rainfall rate (Table 4.2) i.e. these drop size are the prime causes of attenuation in the radio signal.
- No single model at present can be used in exactness to represent the actual outlook of drop-size distribution. Thus any kind of distribution can be used for preliminary modeling purpose.
- Rain drops observed generally are not perfect spheroids due to the free fall except the small sized drops and more precisely they are oblate spheroid with a flat base. For drop-sizes above 4mm the base becomes concave.
- It has been found that gamma type distributions are more suitable as compared to exponential distribution (Table 4.1).

Table 4.2: Typical rain drop classification based on sizes

SUMMARY TABLE of typical rain raindrop Sizes

Rain Type	Drop Size		Terminal Velocity	
	mm	inch	m/sec	miles/hr
Light Stratiform Rain (.04" per hour)				
Small Drop	.5	.02	2.06	4.6
Large Drop	2.0	.08	6.49	14.4
Moderate Stratiform Rain (.25" per hour)				
Small Drop	1.0	.04	4.03	8.9
Large Drop	2.6	.10	7.57	16.1
Heavy Thundershower (1.0" per hour)				
Small Drop	1.2	.05	4.64	10.3
Large Drop	4.0	.16	8.83	19.6
Largest Possible Drop	5.0	.20	9.09	20.2
Hailstone	10	0.4	10.0	22.2
Hailstone	40	1.6	20.0	44.4

4.4 Rain fall attenuation effect

The total attenuation offered due to the rain is generally depicted as summation of the contribution from each and every drop. Thus considering the drop-size distribution function

$N(D)$ the total attenuation obtained is computed as:

$$A = 4.34 L \int_0^{\infty} C_{ext} N(D) dD \text{ decibels.}$$

Polarization Dependence

As hydrometeors are not being perfectly spheroids, a wave propagating through them generally experiences a polarization change along LOS as it travels through it and this cross polarity lead to severe consequences in case of communication systems and deploy polarization orthogonality to maintain isolation between channels.

Principle planes and polarization basics

For a definite volume of hydrometeors on a LOS path there are two types of polarizations occurs which propagate over the link .These polarization are frequency dependant and vary with time as the amount of rainfall changes. These two types of the polarizations is called principal planes, therefore the waves transmitted in direction of principle planes are transmitted without any change but due to absence of perfect non-spheroid drop particles, the wave's experience different attenuation and phase shift.

Spatial-temporal rain outlook

The most popularly used statistical parameters are those of annual rainfall, defined as rain-rate exceeding for a given % of yearly time. Generally, the rainfall values observed over different locations vary largely and thus averaged statistics is preliminary preferred over many years of analysis data.

Depolarization

The non-spherical raindrop has another effect called depolarization. Small rain drops are spherical but for diameters above 4mm, the base becomes concave as shown in Figure 4.2.

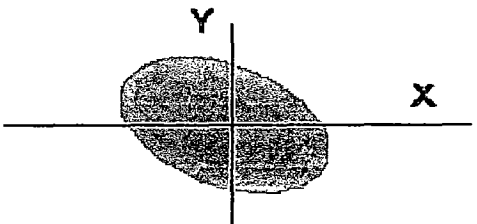
Drop Size (mm)	Raindrop shape			Raindrop orientation
	2	4	6	
Axial Ratio	0.92	0.82	0.65	

Figure 4.2: Depolarization of rain drops

Therefore different polarizations propagate at different speeds through air containing rain and this lead to differential phase shifts and differential attenuation. If the polarization plane (E-Field Vector) coincides with the symmetry of the raindrop, not a lot will change apart from the horizontally polarized signal is delayed relative to the vertical signal. If the drop is not aligned with the polarization, for example, if the drop is rotated by winds or if the polarization is slanted or circular then, energy will be transferred between the polarization states.

4.5 Rainfall –attenuation prediction models

Current analysis is based on rainfall-data for the region of Dehradun located in state of Uttarakhand, India. Analysis facilitates understanding of attenuation over radio links for GSM band at 1800 MHz and thus helps in pre-network planning. Several models are available for estimation of rain attenuation statistics over earth-area. Each of these models has certain merits and demerits of their own. Some of the models have been discussed below:

- **RICE-HOLMBERG MODEL**

The Rice-Holmberg (R-H) model is based on two rainfall kinds namely convective ('mode1', thunderstorm) rains and stratiform ('mode2', uniform) rains. The mathematical statistics encompasses sum of individual exponential modes of rainfall-rates. According to this model, rainfall-rates is given as:

$$\text{Rainfall} = \text{Mode1 rain} + \text{Mode2 rain}$$

Exponential distribution selected here to describe 'Mode1 rain' is related to a physical analysis of thunderstorms, while 'Mode2 rain', are viewed as a summation of two exponential distributions.

- **DUTTON-DOUGHERTY MODEL**

The Dutton-Dougherty (DD) Model was proposed in 1973 and 1977 and includes attenuation due to both rain and gases. The rainfall rate distributions it deploys are derived from slight modifications in the Rice-Holmberg model. The DD model is also available as a computer program for facilitation.

As the model is an improved form of R-H model the parameters are nearly similar, the number of hours of rainy time period in minutes for a surface rain rate in excess as expected is given as:

$$T(R) = T_1^{(-R/R_1)} ; R \geq R_c$$

$$(T_1 + T_2)^{(-R/R_1)} ; R < R_c$$

- **ITU-R MODEL**

The ITU-R Model has been developed in 2 types and both of these types utilize total attenuation statistics. The first type is called the ITU-R prediction Model (CCIR-1978A, Dec,6 June), employs a mean path parameter 'r' to relate the point rate to the average rain rate along the path from the base station to the point where the hydrometeors exist in the form of ice crystals. The later form of the Model (Crane and Blood -1979, Crane-1980a, 1980b) includes various percentages of time to account for the types of rain configurations which dominate the total statistics for the respective percentages of time.

Many models have been proposed for prediction of radio waves attenuation due to rain but all of these models are application and site specific. Hence optimal choices need to be made before deploying any model for network planning. Summary of different models has been analyzed in Table 4.3 to facilitate the choice of models.

Table 4.3: Comparison table of different rain models

<u>MODEL NAME</u>	<u>KIND OF MODEL</u>	<u>REGION OF DEPLOYMENT</u>	<u>FEATURES</u>
▪ <i>Rice-Holmberg Model</i>	Statistical Model	Temperate climates with heavy rainfall.	Uses cumulative time distribution of rainfall.
▪ <i>Dutton-Dougherty Model</i>	Statistical Model	Used for gaseous and rain attenuation both	Exceedance time % used with rain rate.
▪ <i>Global Model</i>	Statistical Model	Used for rain only conditions.	Globally accepted values for rain attenuation parameters.
▪ <i>Crane Model</i>	Statistical Model	Used for different hydrometeors.	Surface point rain rate is the fundamental step.
▪ <i>Fixed Effective Rain Model</i>	Statistical Model	Used for a fixed rain intensity.	Assumes 6.6mm/h of fixed effective rain intensity over all paths.
▪ <i>Variable Effective Rain Model</i>	Statistical Model	Used for variable rain intensity.	Assumes attenuation increases with rain intensity.
▪ <i>ITU-R Model</i>	Analytical Model	Used for region wise rain intensity.	Assumes algorithmic calculation approach for attenuation calculation.

4.5.1 Rain model selection

Based on the analysis of models (Table 4.3) it has been observed that rain attenuation modeling is done usually based on Drop Size Distribution (DSD) but in agreement with the fact that DSD varies for different climatic regions and case is more interesting for a country like India, where there is a diverse climatic variability region to region. DSD values depend both on the rainfall-rate and location, which means same rainfall rate lead to different DSD's. Thus the prime task is to choose among available DSDs for the one which best suit for present analysis or diverse climatic variability as for the case of India. ITU-R recommendations [81]is considered for prediction of specific attenuation with different polarization levels in form of prime inputs to the FIS model for the prediction of attenuation. ITU-R model is chosen as it incorporates in to it the features which are simplistic and easy for implementation along with FIS Module of the Fuzzy logic presented in comparison to other available models for attenuation prediction.

4.6 Fuzzy approach

The term fuzzy logic was first proposed by Lotfi Zadeh (1965). Fuzzy set theory was developed to facilitate logical interpretation of control and prediction related issues. It is more of a mathematical tool dealing with uncertainties .It is based on the fundamentals of dependently biased membership functions. Actually there exists a relation between the level of problem and fuzziness. As the level of problem rises, the problem starts approaching towards fuzziness. Fuzziness in real terms is defined as the degree of impreciseness associated with a certain problem of significance.

4.6.1 Data specifications and site-selection

The site selected for study purpose is located in the foothills of Himalayan region, named Dehradun located in northern corner of India. The data of rainfall used has been obtained as per the courtesy of Indian Meteorological Department, Hydrometeor division over the time period of 2006-2010. The brief outlook has been provided in form of a Table 4.4.

HYDROMET DIVISION -District DEHRADUN Uttarakhand
INDIA METEOROLOGICAL DEPARTMENT
DISTRICT RAINFALL (MM.) FOR LAST FIVE YEARS

Note: (1) The District Rainfall (mm.) (R/F) shown below are the arithmetic averages of Rainfall of Stations under the District.
(2) % Dep. are the Departures of rainfall from the long period averages of rainfall for the District.
(3) Blank Spaces show non-availability of Data.

YEAR	JANUARY		FEBRUARY		MARCH		APRIL		MAY		JUNE		JULY		AUGUST		SEPTEMBER		OCTOBER		NOVEMBER		DECEMBER	
	R/F	%DEP.	R/F	%DEP.	R/F	%DEP.	R/F	%DEP.	R/F	%DEP.	R/F	%DEP.	R/F	%DEP.	R/F	%DEP.	R/F	%DEP.	R/F	%DEP.	R/F	%DEP.	R/F	%DEP.
2006	17.9	-68	2.4	-95	137.5	229	14.8	-35	165.0	304	139.3	-11	540.6	-15	478.3	-31	195.7	-30	16.6	-72	1.7	-81	25.2	39
2007	0.4	-99	111.4	122	96.1	130	15.6	-32	16.8	-59	79.2	-50	860.0	35	943.5	36	801.0	186	10.6	-82	0.0	-100	5.9	-67
2008	13.1	-76	21.8	-56	2.6	-94	76.1	232	51.8	27	588.9	274	689.0	8	736.4	6	159.9	-43	32.9	-45	10.5	18	0.0	-100
2009	5.0	-91	39.5	-21	2.6	-94	18.8	-18	43.6	7	74.5	-53	437.4	-31	453.9	-34	273.2	-3	168.7	182	2.0	-78	0.0	-100
2010	14.5	-74	54.5	9	2.0	-95	5.0	-78	49.1	20	129.4	-18	777.4	22	894.0	29	799.5	185	11.7	-80	17.8	100	26.2	45

Table 4.4: Annual rainfall distribution with % departures from mean values for the year 2006-2010. [Courtesy: Indian Hydrometeorology Division, Pune]

4.6.2 Analysis of data with ITU-R

The rain model provided by ITU-R calculation approach (Recommend.P.838) depicts two types of attenuation model and is used in the estimation of the annual attenuation distribution to be expected on a specific propagation link. It is different from most of the other rain models. The step wise approach deployed for attenuation calculation is as follows:

STEP-1 In this step the instantaneous point rain rate (R_p) distributions is estimated. The ITU-R provides median for large geographical areas i.e. it divides the geographical regions into eight climate zones from A to H covering entire earth surface as shown in Figure 4.3.

STEP-2 Other parameters of interest such as lat.-long , height above sea level ,angle of elevation associated with region has been deployed as per ITU-R recommendations.

STEP-3 Input parameters specified in to the formulation for attenuation calculation along with specific attenuation are calculated using ITU-R recommendations.

The algorithmic approach is the simplest approach but the actual approach is bit cumbersome as it involves complex calculations for obtaining attenuation values for a link of interest and this usually increases complexity of the process indulged. Thus a Fuzzy rule base approach has been deployed for predicting attenuation over the links of interest for the chosen region of interest, which is fruitful for betterment in design and pre-planning of network based on findings in similar type of regions[85]. In case of GSM i.e. 1800MHz band based transmission major design consideration involves pre-planning for installation of BTS (Base Transmitting Station) and specifically for the region of Dehradun where rainfall distribution is highly variable. Fuzzy rule base prediction and planning is widely fruitful because regions in physiographic subdivisions of Uttarakhand are nearly similar with respect to rainfall distribution. Further an important aspect is that as the height or the elevation for a location rises the wet form of water reduces in availability and thus reduces

the attenuation value that is to be taken in to consideration as a part of fuzzy parameterization. World physiographic divisions along with Indian physiographic sub-divisions and then more detailed view of Uttarakhand sub-divisions shown in Figure 4.4 and 4.5.

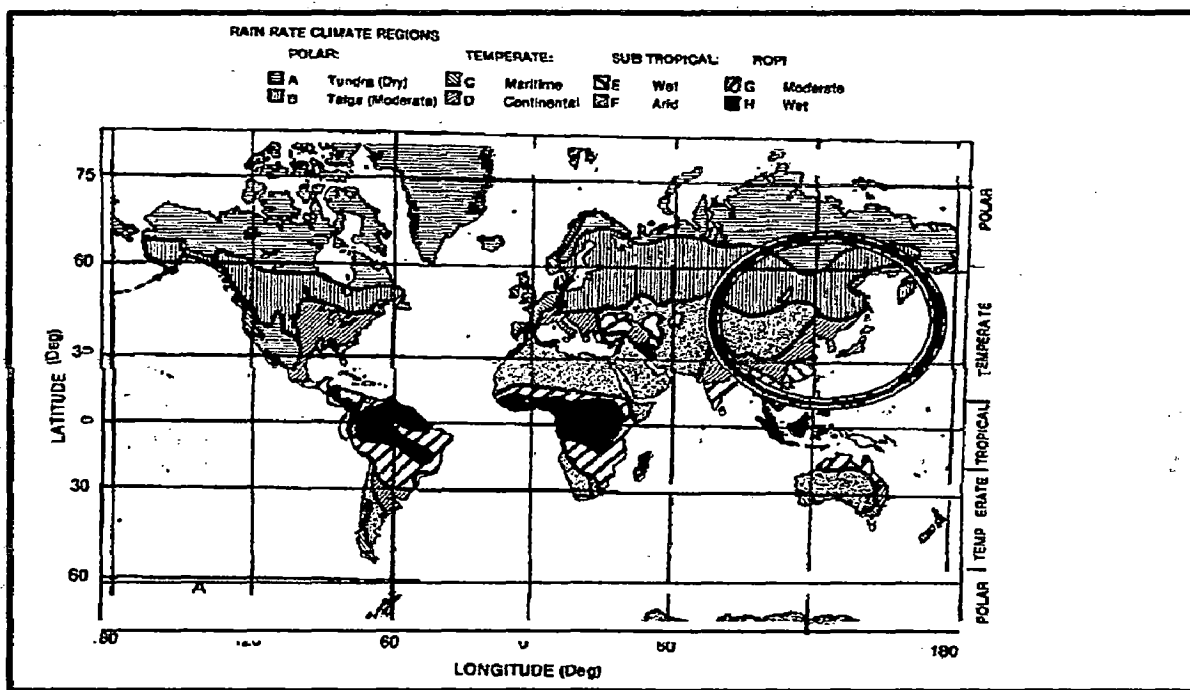


Figure 4.3: Division of geographical region in different climatic zones [Courtesy: ITU-R]

The point rainfall rate distribution as per ITU-R recommendations for world physiographic divisions is shown in Figure 4.3. Further Figures 4.4 and 4.5 shows physiographic subdivisions variation of rainfall rate for monsoon season with respect to that from Indian perspective as shown along with Uttarakhand region located in it.

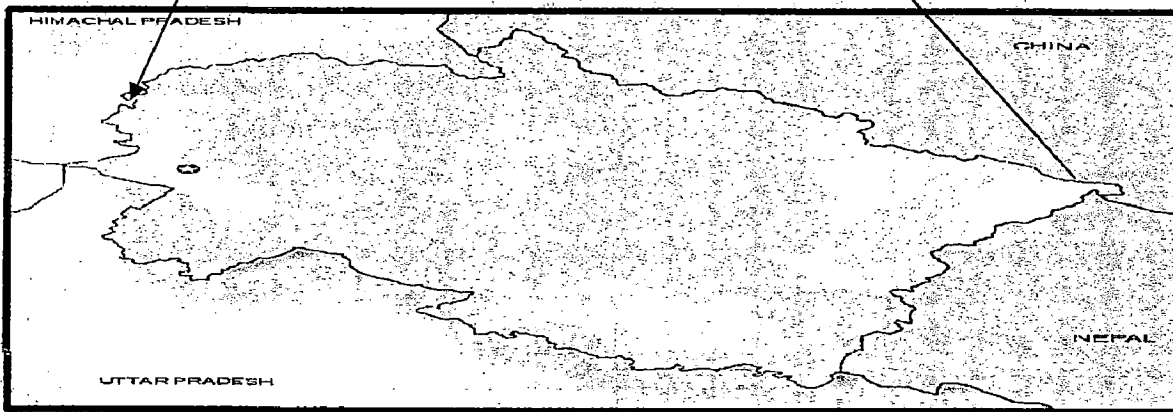
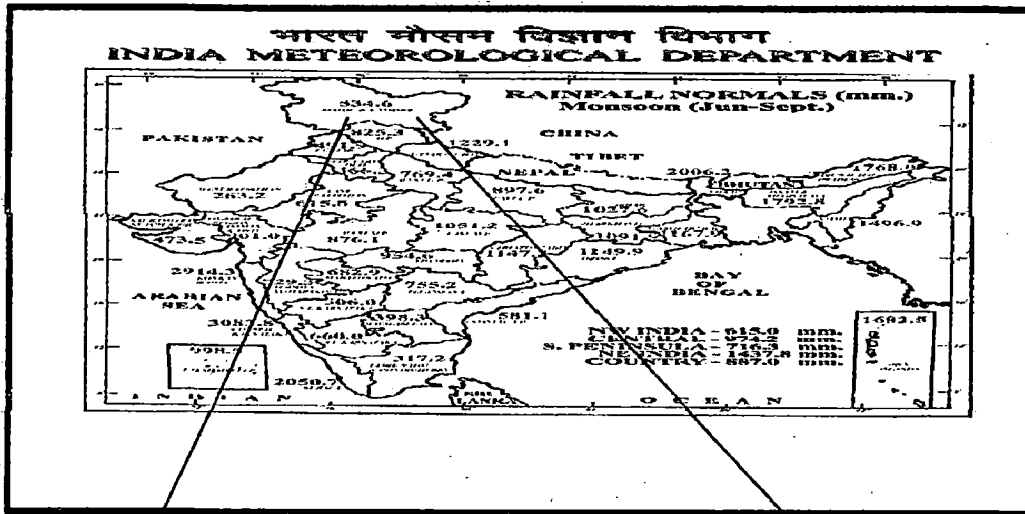


Figure 4.4: Indian physiographic subdivisions depicting location of Uttarakhand

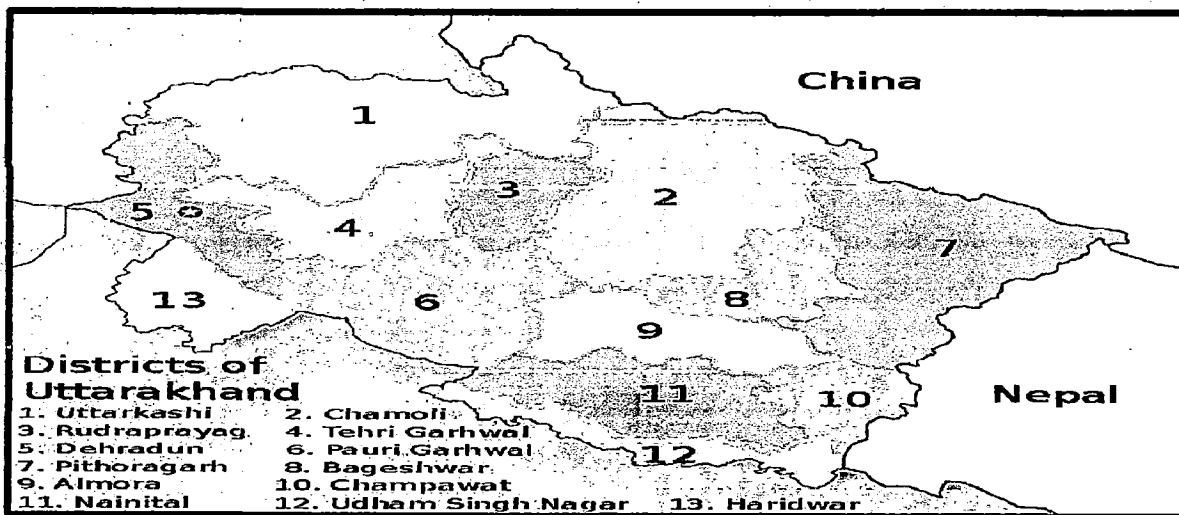


Figure 4.5: View of regional subdivisions of Uttarakhand (Dehradun)

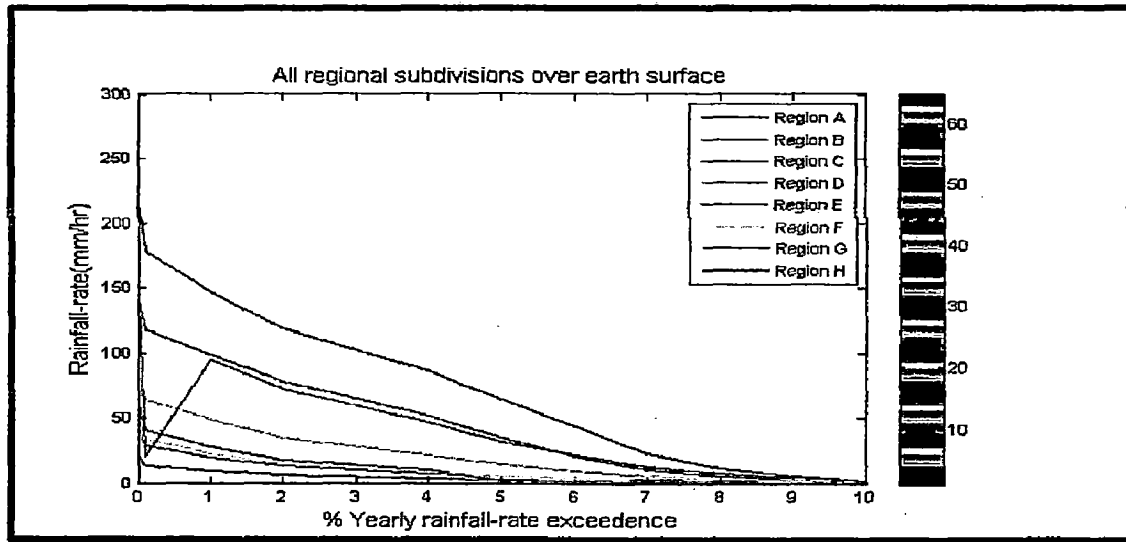


Figure 4.6: Rainfall rate exceedance curve as per ITU-R tables for some of the world physiographic divisions

Figure 4.6 represents the annual rainfall exceedance values for world physiological divisions as per ITU-R. The region of interest here is Dehradun, which is a part of Uttarakhand subdivision of Indian sub-continent lying between $29^{\circ} 57'$ and $31^{\circ} 2'$ N. and $77^{\circ} 35'$ and $78^{\circ} 18'$ E., with an area of 1209 square miles (now 300 sq. Kms). Dehradun district consists of 2 different portions. The larger part composes of a gentle sloping valley 45 miles long and 15 to 20 miles broad between the Himalayas and Shiwalik hills. The other portion of the district is the Jaunsar-Bawar region or Chakrata region which strikes north from the outer range of Himalayas. The region is drained by numerous tributaries of Ganges. [Courtesy: The Gazetteer of India].

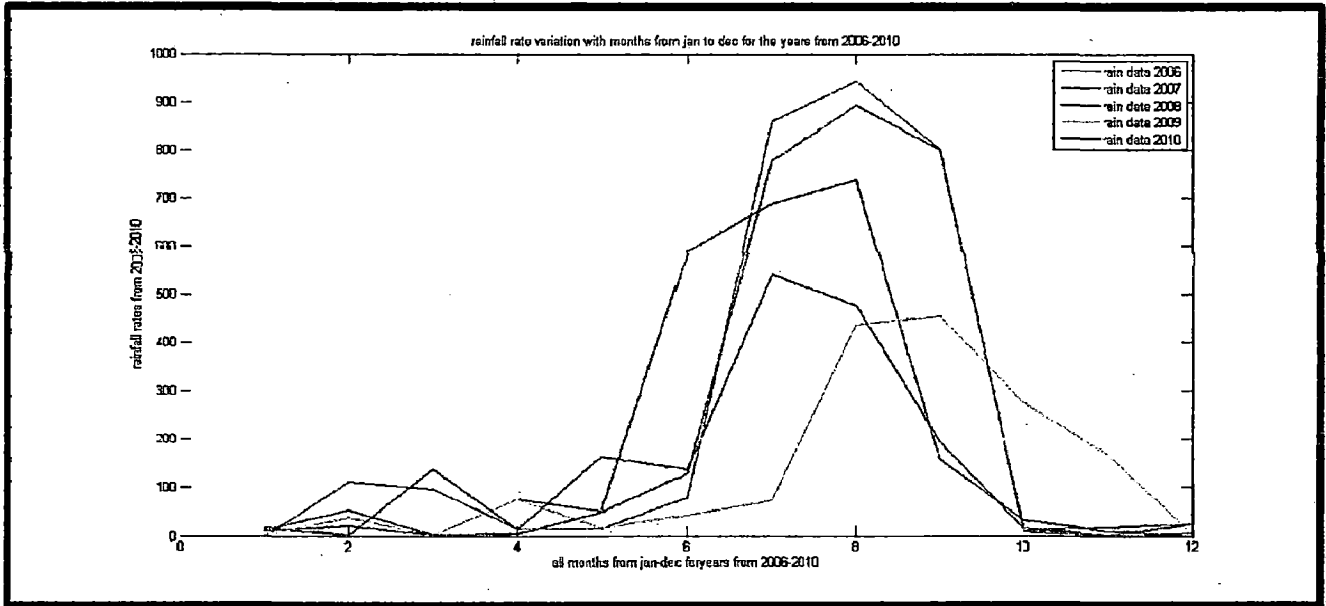
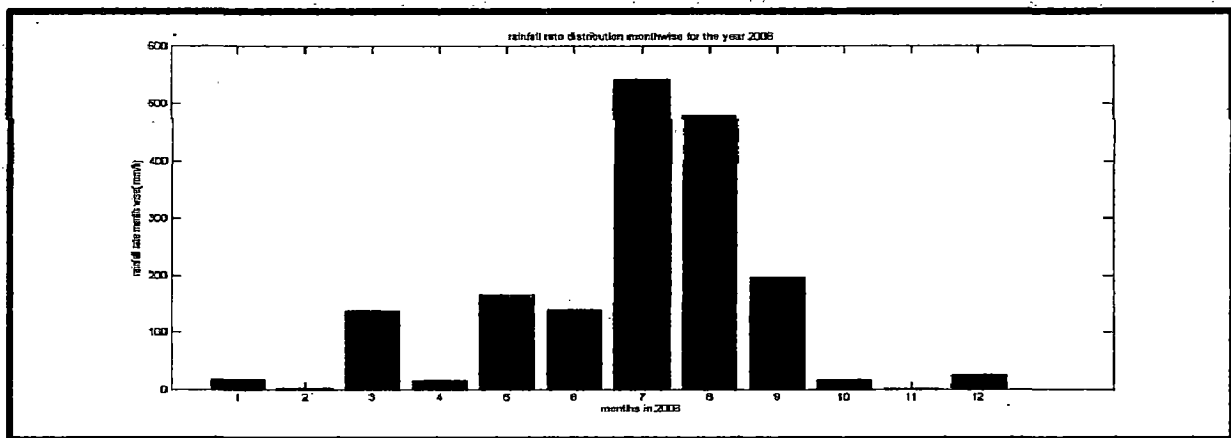
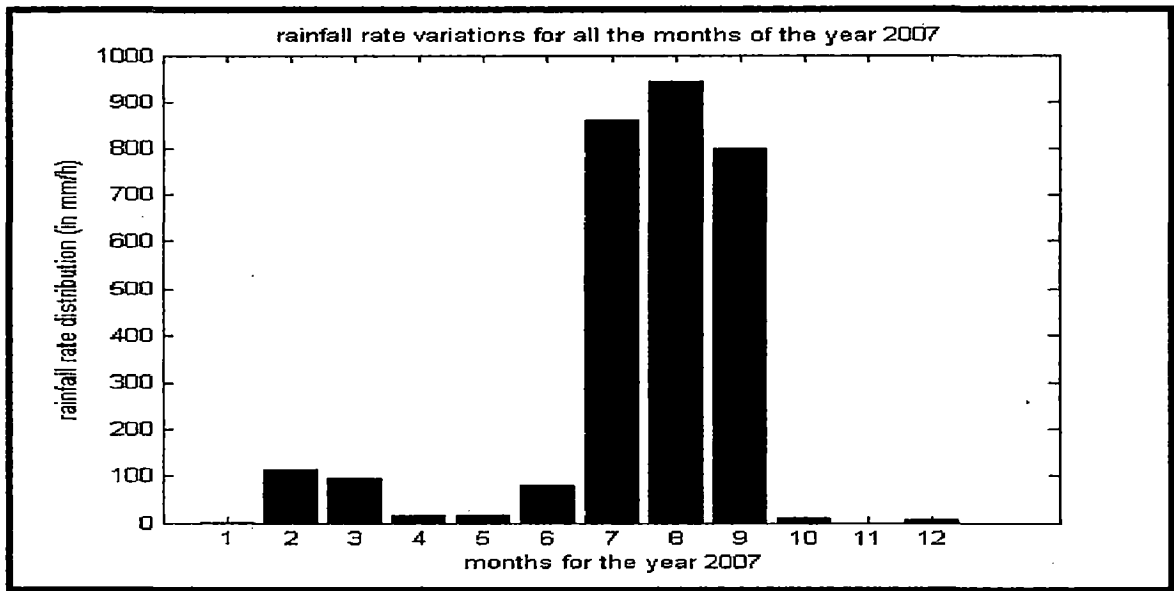


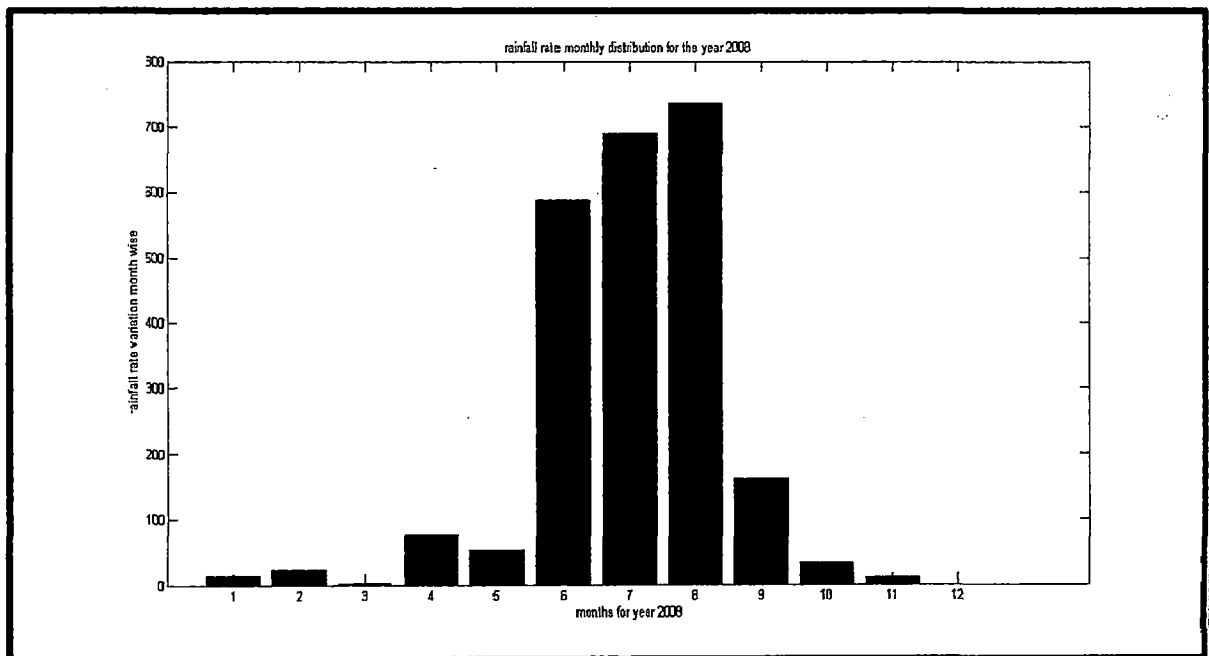
Figure 4.7: Rainfall-rate variation for months from Jan to Dec from 2006-2010 for Dehradun



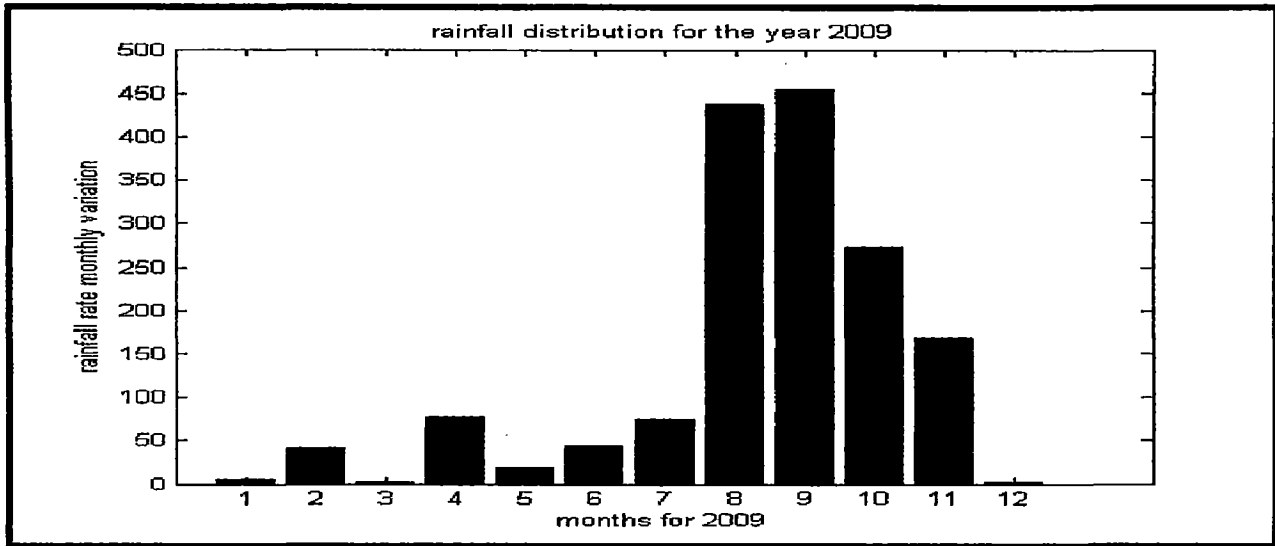
(a)



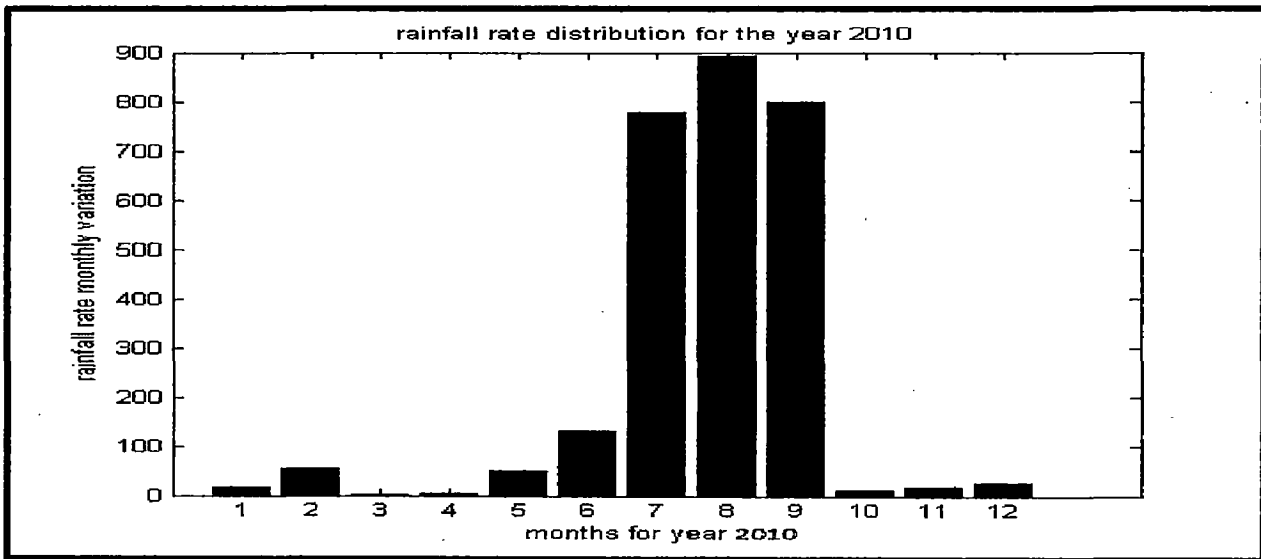
(b)



(c)



(d)



(e)

Figure 4.8 (a)-(e): Rainfall rate monthly variations for different years from 2006-2010 for Dehradun

maximum attenuation in the fuzzy module itself and then these zones will be dealt as hot-spots for better network planning and attenuation free communication. The classification of attenuation in terms of fuzzy output primitives has been shown in Table 4.8.

Table 4.8: Rainfall-Attenuation classification

NUMERICAL RAINFALL-RATE RANGE	FUZZY ATTENUATION PRIMITIVES	CLASSIFIED ZONES
0.25 - 1.0 mm/h	low	pre monsoon, post monsoon
1.0 - 4.0 mm/h	moderate	pre monsoon, post monsoon
4.0 - 50.0 mm/h	high	monsoon

The fuzzy model used thus relies on three major input parameters and generates three categories of prediction domain. ANFIS toolbox of MATLAB has been deployed for the purpose of simulation. The results so obtained depict the predicted attenuation levels categorized in to domains of interest.

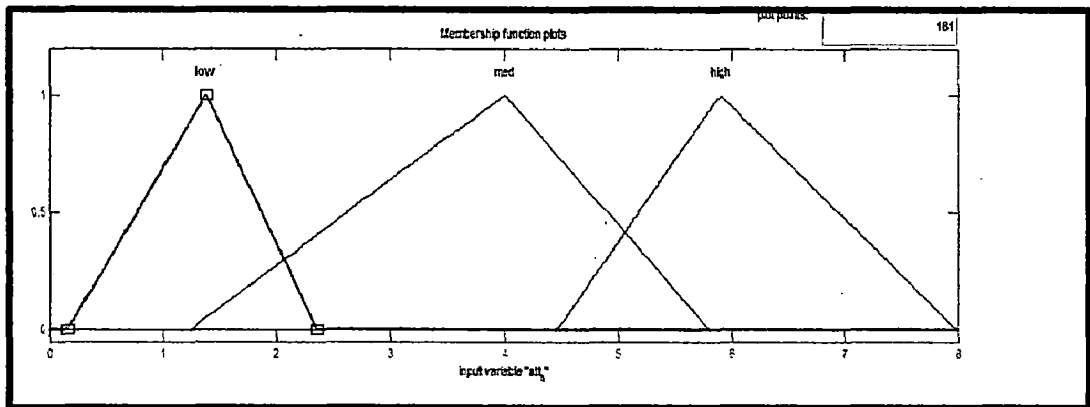


Figure 4.9: Membership function defined for attenuation with horizontal polarization

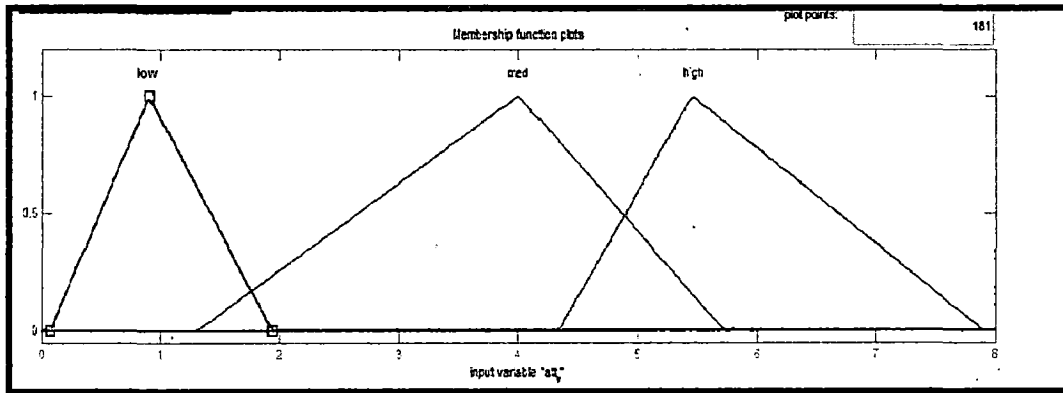


Figure 4.10: Membership function defined for attenuation with vertical polarization

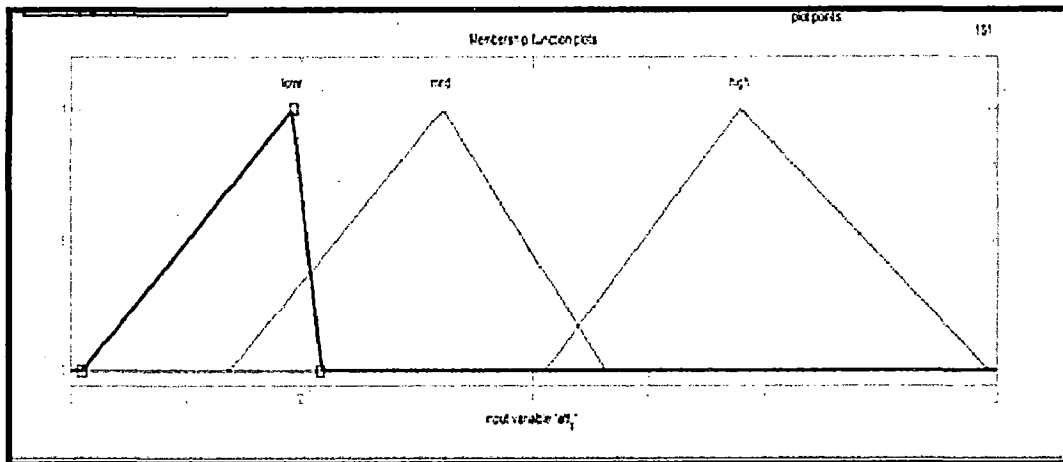


Figure 4.11: Membership function defined for circular polarization

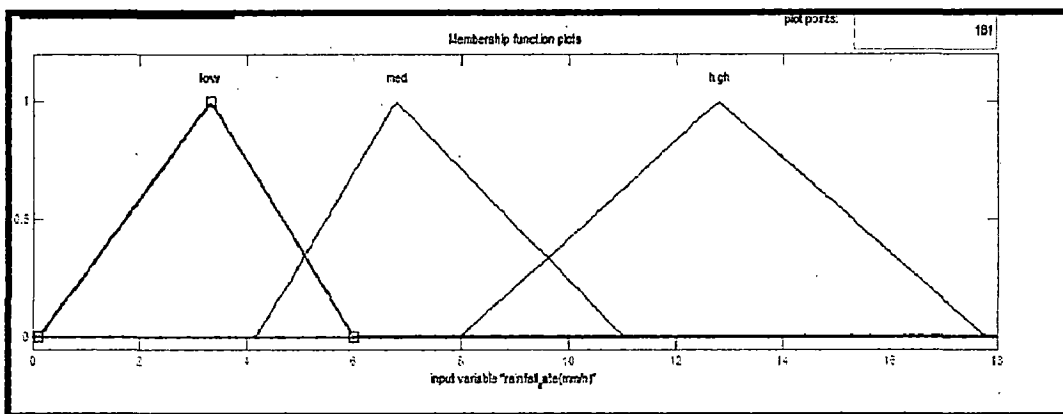


Figure 4.12: Membership function defined for rainfall-rate

It is analyzed from the Figure 4.8 that rainfall rate is considerably noticeable and contribute to reasonable attenuation specifically in the months from May to September each year.

4.6.3 Fuzzy input and output variables

Most of the fuzzy algorithms depend on inputs and rule set predefined, the key elements of the design are the set of rules. Rules is based on certain important information obtained from various meteorological websites, collected data and blogs which facilitated in deciding the range for parameters under concern like with the increase in elevation (altitude) for a station for which network planning is to be undertaken, it is seen that the wet rain precipitation reduces whereas the snow or dry form of water is prevalent and hence reduces the attenuation due to rain. Thus, elevation classification has been carried out on the basis indicated in Table 4.5.

Table 4.5: Elevation variability

RANGE OF ELEVATION	FUZZY SUB VARIABLE NOMENCLATURE	NATURE OF PRECIPITATION
0-1100 Meters	Lower	RAIN ONLY
1100-2200 Meters	Middle	RAIN,HAIL STONES
2200-3000 Meters	Greater	MOSTLY SNOW,HAIL,SCANTY RAIN

The classification of polarization being specific to either it is horizontal, vertical or circular has been done on the basis of phase shift of the electromagnetic wave [58] and horizontal and circular polarization have a greater impact as compared to vertical polarization in case of total rain attenuation (Table 4.6).

Table 4.6: Polarization variability

POLARIZATION TYPE	RANGE OF PHASE SHIFT	PHASE SHIFT EQUIVALENT
HORIZONTAL (H)	90-180 degrees	Specific attenuation
VERTICAL (V)	0-90 degrees	Specific attenuation
CIRCULAR	MEAN OF H and V	Specific attenuation

Another important variable rainfall rate presumes is its range classification based on the precipitation details as obtained from the precipitation chart for the region of interest i.e. Dehradun as per the courtesy of IMD, Pune. The more detailed precipitation outlook in variable measurement units has also been obtained before declaring the range of rainfall rate for distinct regions, even more ITU-R marks entire Indian sub-continent under region K with a rainfall rate of 42 mm/h in general. But being a more microscopic review and enormously variable environmental outlook available for the region of concern the rain rate has been taken in form of a range depicting variability in rainfall rates in the same region for different zones. As depicted in the monthly precipitation chart available as per IMD-Pune, it is clear that there has been huge variations in rainfall precipitation data from 2006-2010 and also for same months in different years too from 2006-2010. The range taken here is shown in Table 4.7.

Table 4.7: Rainfall variability

RANGE FOR RAINFALL RATE(mm/h)	CLASSIFIED ZONES (monthly-basis)	MONTHLY PRECIPITATION (in mm)
30-50	PRE-MONSOON	20-100
50-80	POST-MONSOON	100-200
80-100-above	MONSOON	200-500 -above 500

The rainfall-rate is obtained as averaged values based on the precipitation data of Table 4 depicted in the context above. All the input fuzzy variables has been classified for the purpose of attenuation classification and thus predicting the zone (monthly-rainfall wise)of

The results for the following inputs and outputs in terms of membership functions have been shown in Figure 4.9 to 4.12. The membership functions are defined along with set of rules which are the key parameters, sometimes the parametric values are scaled for better implementation aspects and refined results.

4.6.4 Mamdani Fuzzy Approach

It is one of the two platforms provided in the MATLAB ANFIS toolbox. The main aspect is to use this platform for designing a system for prediction of attenuation due to rainfall, for this purpose the inputs are defined based on predefined rules to the FIS and the outputs so obtained are defuzzified to obtain fuzzy sets and then these sets can be combined using logical operators keeping in view the rules defined earlier. While rules are defined in fuzzy Mamdani module, it is important to know that rules are simple conditional. The Mamdani fuzzy module simplifies the procedural steps in the prediction of attenuation due to rain, this is in view of the approach deployed for the prediction. The basic Mamdani module in correlation with problem under concerned is shown in Figure 4.13.

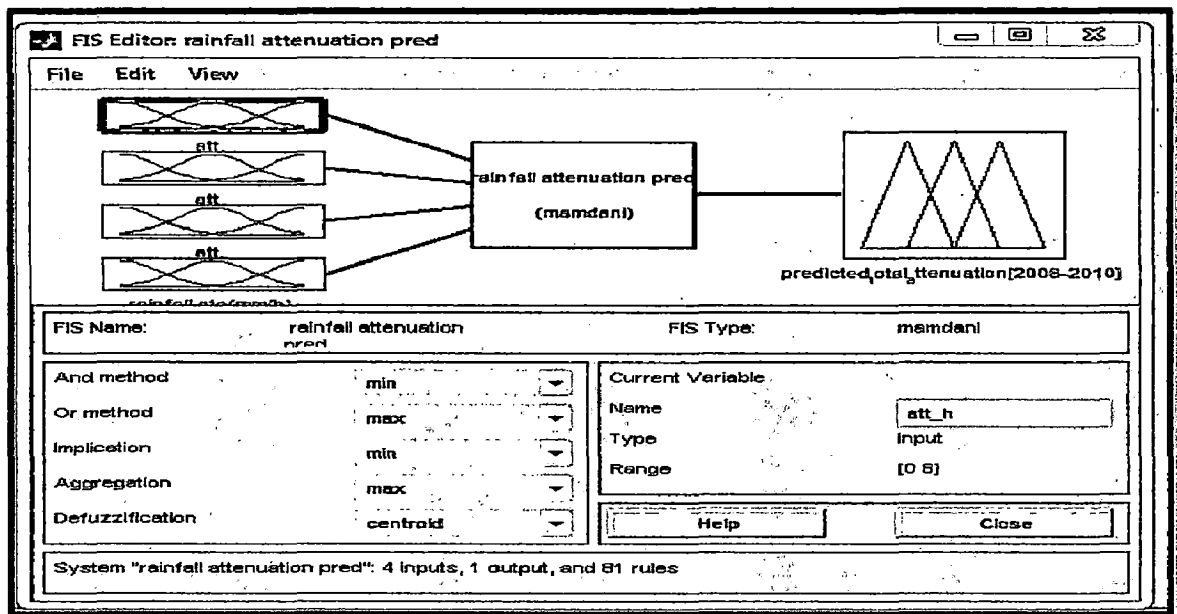
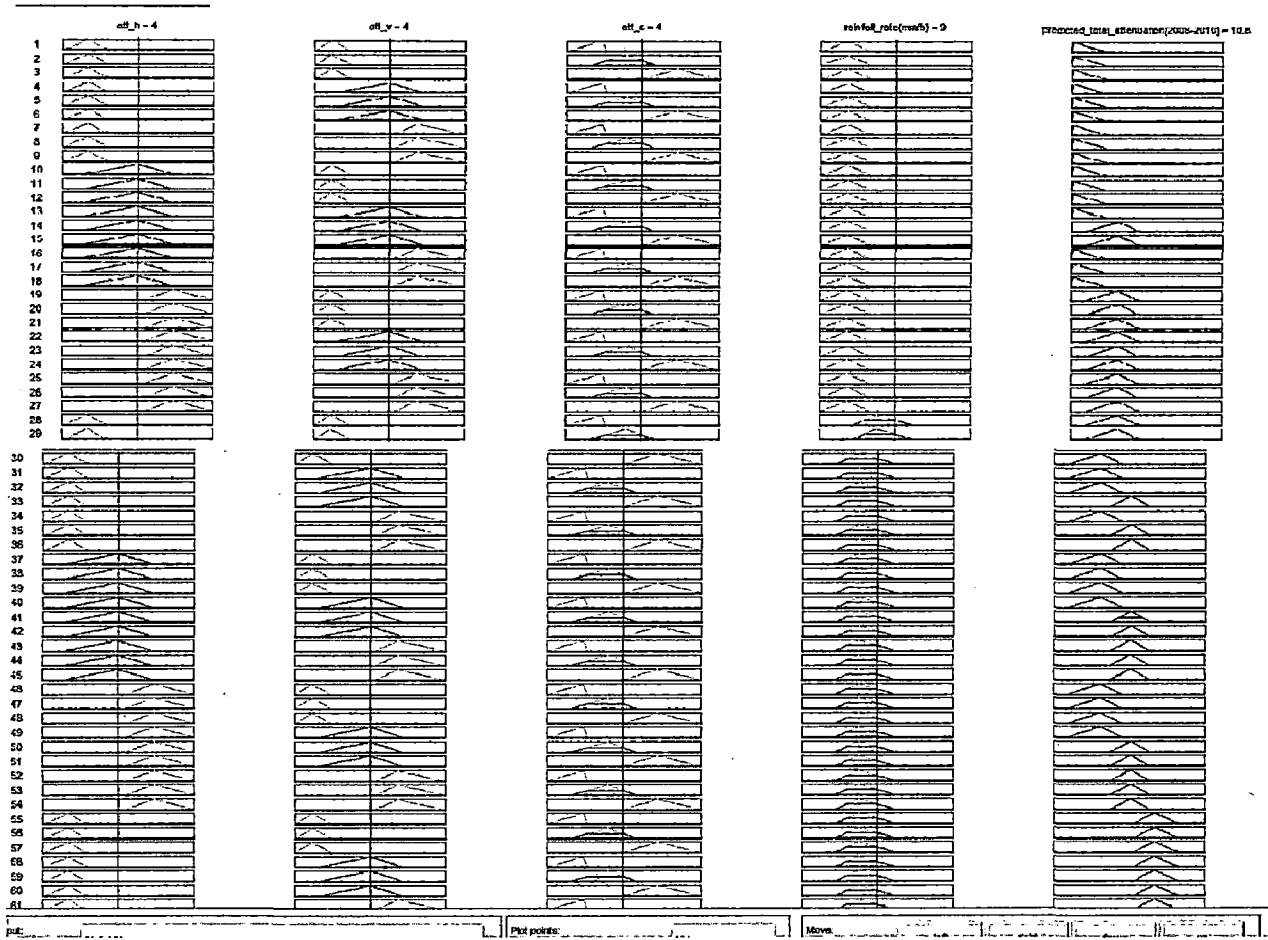


Figure 4.13: Fuzzy rainfall attenuation prediction module using Mamdani ANFIS

The module shows various inputs and outputs along with other parameters used for prediction purpose with the fuzzifier. The rainfall rate, attenuation with horizontal, vertical and circular polarization is the key parameters input to the module. Most of the fuzzy algorithms depend on these inputs and rule set predefined, the key elements of the design are the set of rules.

4.6.5 Fuzzy membership function



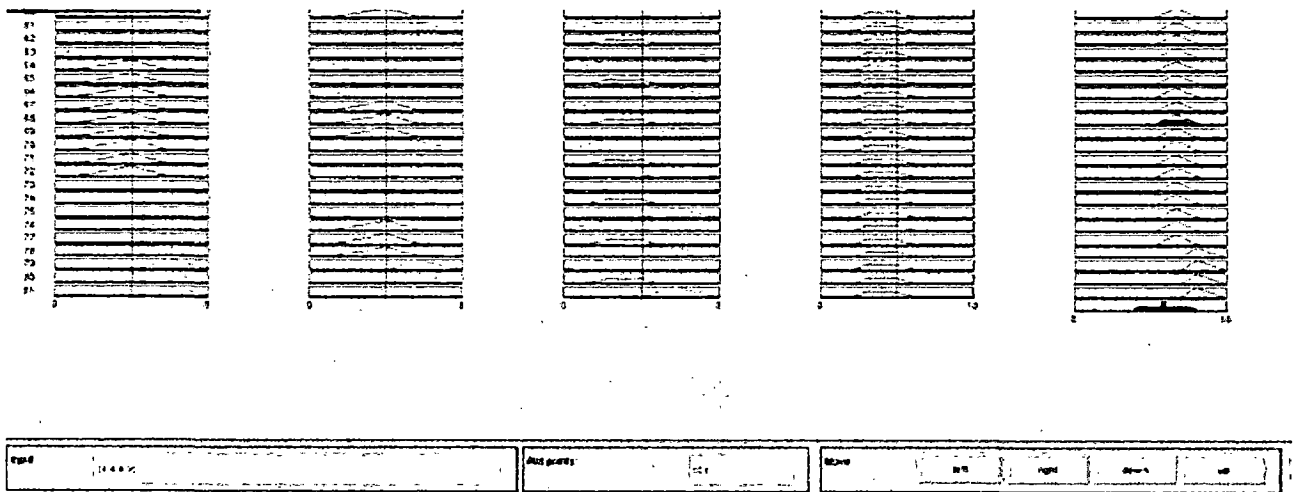


Figure 4.14: Fuzzy membership function

Figure 4.14: shows the membership function from ANFIS editor.

4.6.6 Analysis of Result

Final results using ITU-R model recommendations obtained in the mamdani fuzzy platform are generated using attenuation formula .The results obtained are predicted values and can be further improved with membership function values adjustment. The attenuation values are for the data of rainfall-rate for the region of Dehradun, Uttarakhand -India. It has been found that the predicted values are fine agreement with the calculated values.

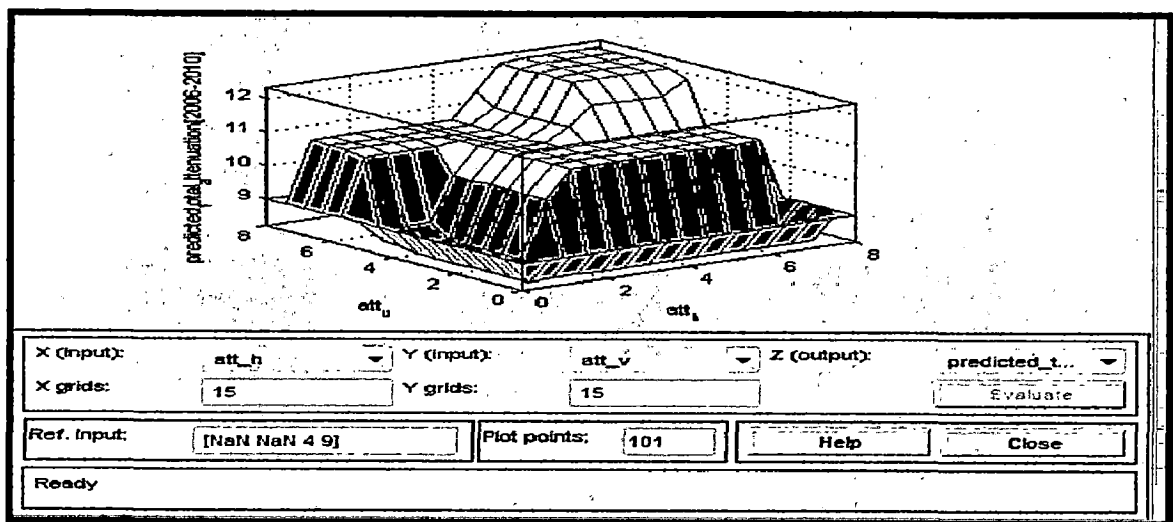


Figure 4.15: Total predicted specific attenuation w.r.t horizontal polarization and vertical polarization

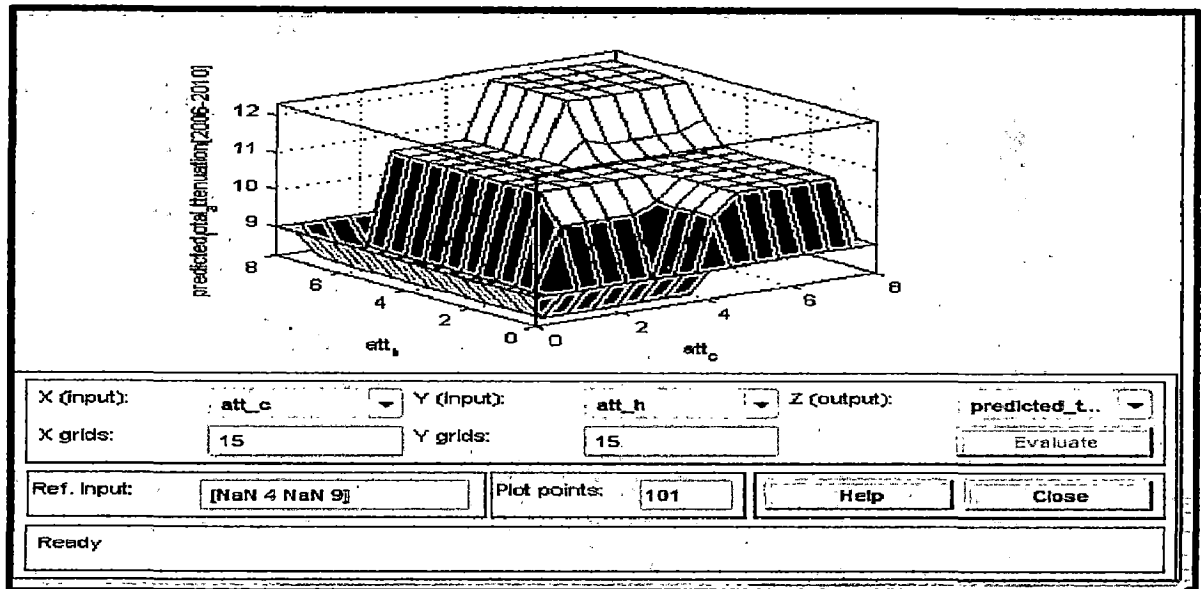


Figure 4.16: Total predicted specific attenuation w.r.t horizontal polarization and circular polarization

Figure 4.15 and 4.16 indicates that as the rainfall rate exceeds the attenuation increases and the attenuation values obtained at lower rainfall rates are generally constant up to a certain level and then a slight depreciation in the attenuation is observed some way mid and finally a normal hike continuously is observed.

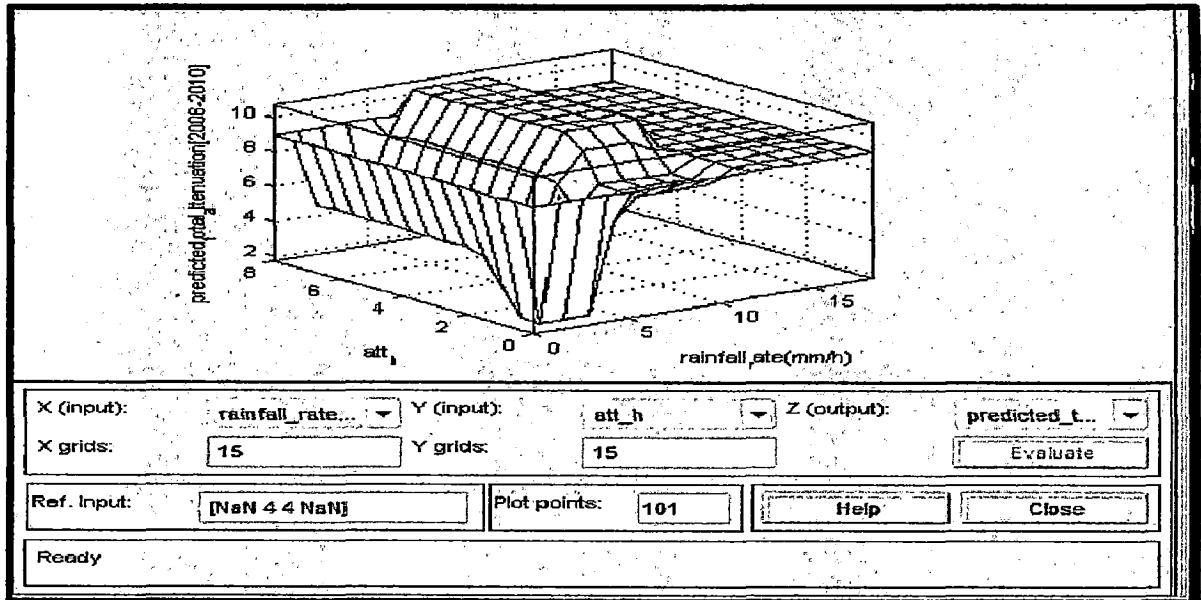


Figure 4.17: Total predicted specific attenuation w.r.t horizontal polarization and rain fall rate

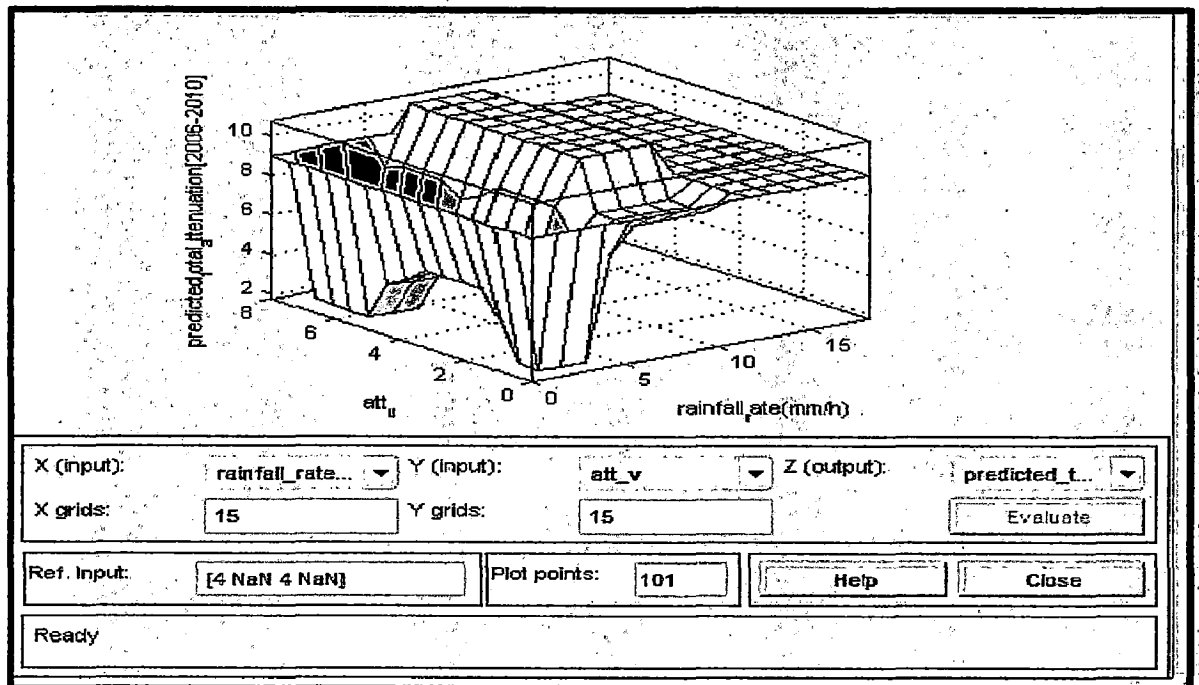


Figure 4.18: Total predicted specific attenuation w.r.t vertical polarization and rainfall-rate

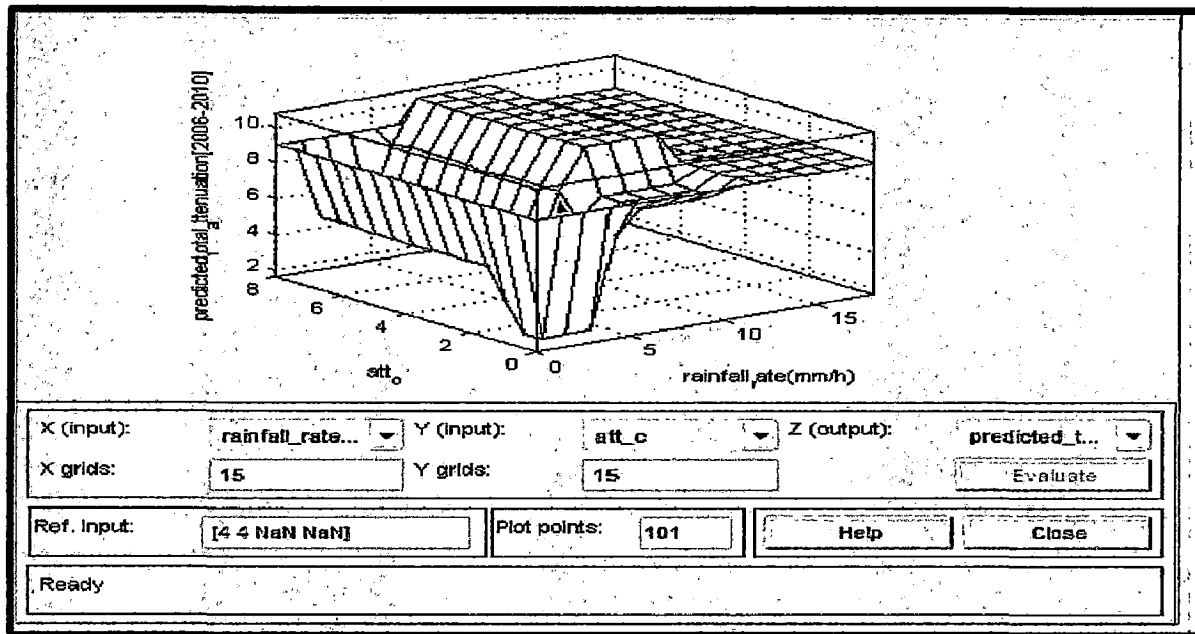


Figure 4.19: Total predicted specific attenuation w.r.t circular polarization and rainfall-rate

Figure 4.17 , 4.18 and 4.19 indicates that as the rainfall rate exceeds the specific attenuation increases due to the change in polarization i.e. horizontal, vertical and circular polarization. Normal hike in the attenuation values obtained at horizontal and vertical polarization is observed. With circular polarization, specific attenuation is constant up to a certain level and then a slight depreciation in the attenuation is analyzed.

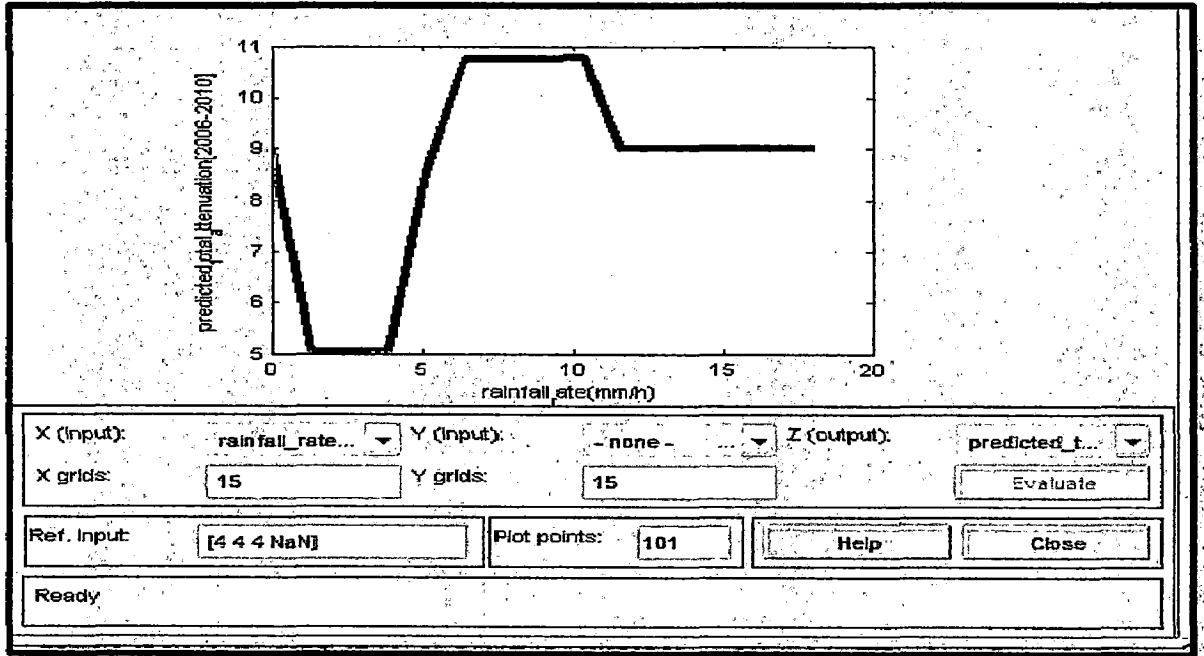


Figure 4.20: Total predicted specific attenuation with rainfall-rate

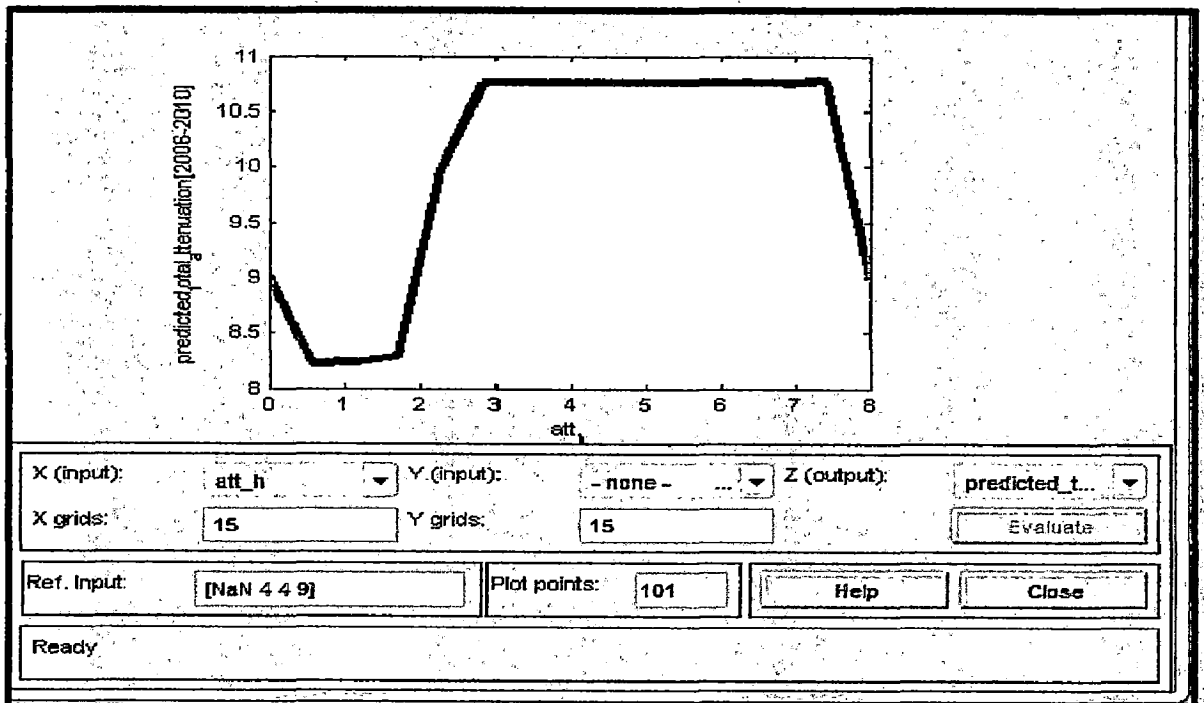


Figure 4.21: Total predicted specific attenuation with horizontal polarization

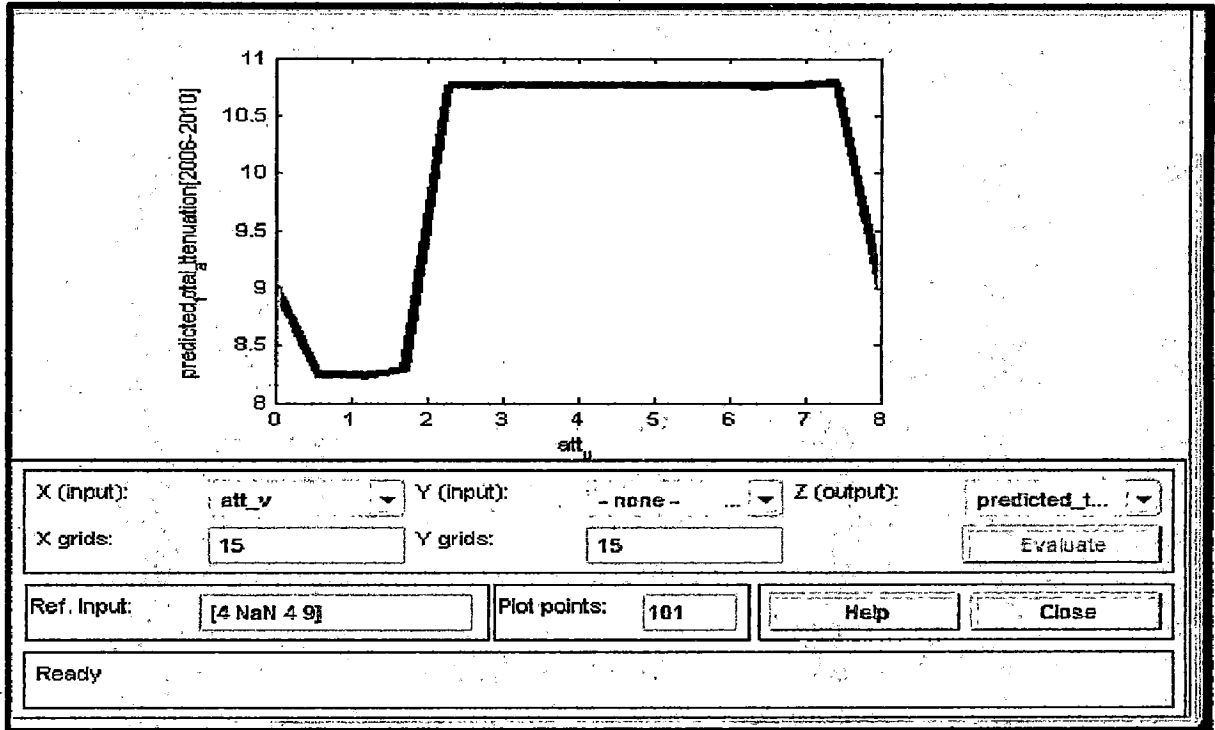


Figure 4.22: Total predicted specific attenuation with vertical polarization

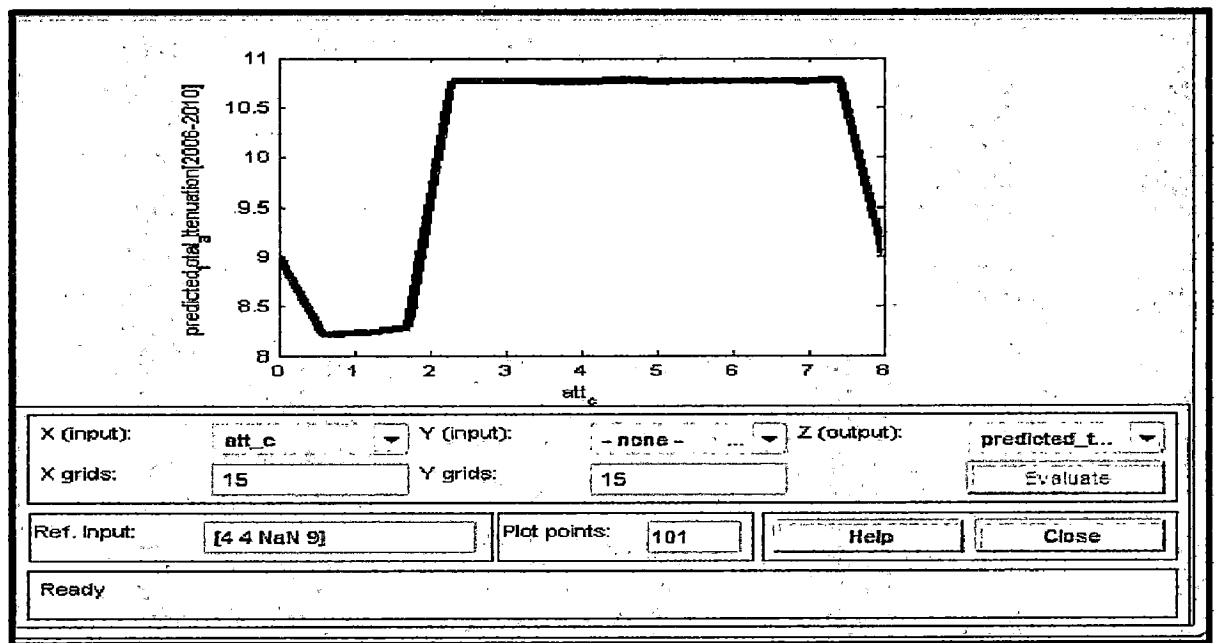


Figure 4.23: Total predicted specific attenuation with circular polarization

For easy interpretation of result Figure 4.20 to 4.23 indicates the rainfall rate, specific attenuation and polarization in two dimensions.

Now focuses more on predicting the pathloss exponent also called as attenuation factor. For this purpose input variables in the form of received and transmitted power at the frequency of 1.8 GHz has been analyzed as per the result of test drive conducted during the month of august 2010. More pondering fact to be focused on is that the august 2010 reported a five year highest precipitation for the month as noted from available databases. The variation of parameters for rainfall rate, transmitted power along with path loss exponent has been analyzed.

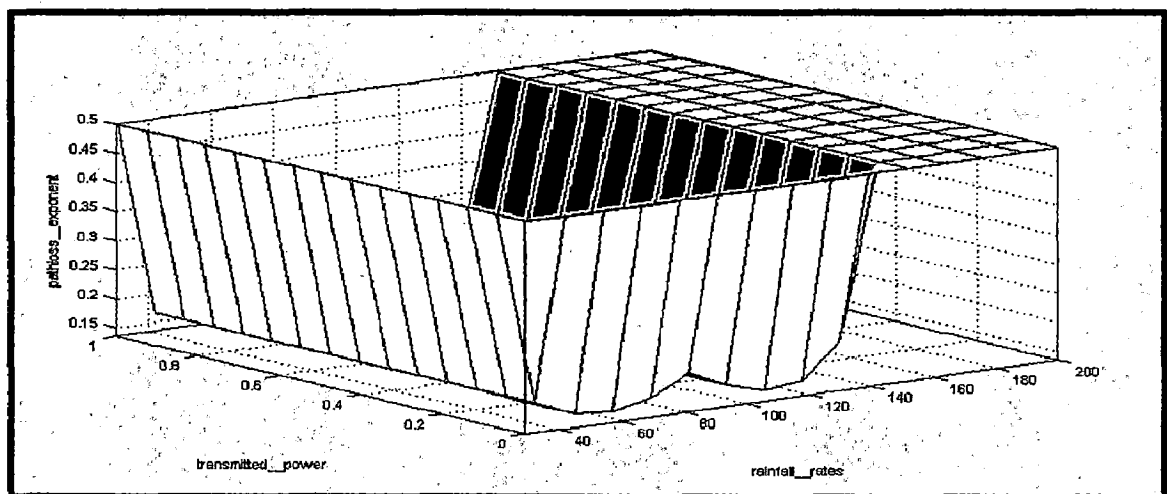


Figure 4.24: Graph showing results between path loss exponent, rainfall rate and transmitted power

The result shown in Figure 4.24 and 4.25 indicates that the path loss exponent decreases as the transmitted power is increased and then attains a constant value thereafter, but the most fascinating part of the result is the variation of path loss exponent with rainfall rates. It has been analyzed that as the rainfall rates increase up to a certain value of around 80 mm/h the path loss exponent depreciates linearly but then suddenly peaks up pertaining to the fact that the higher rain rates leads to greater attenuation impact as that lower rates of rainfall but again there is a slight depreciation observed which around and above 120 changes to linear rise and then attains a constant value this depicts variability that might exist in the form of precipitation content and rain drop shape parameters at an operational frequency of 1.8GHz.

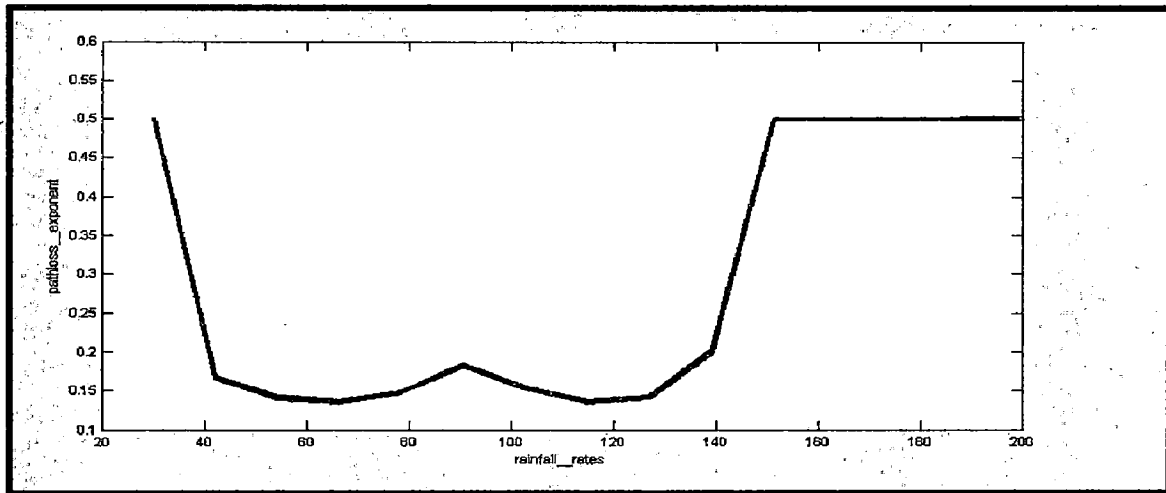


Figure 4.25: Variation of path loss factor with rainfall rates

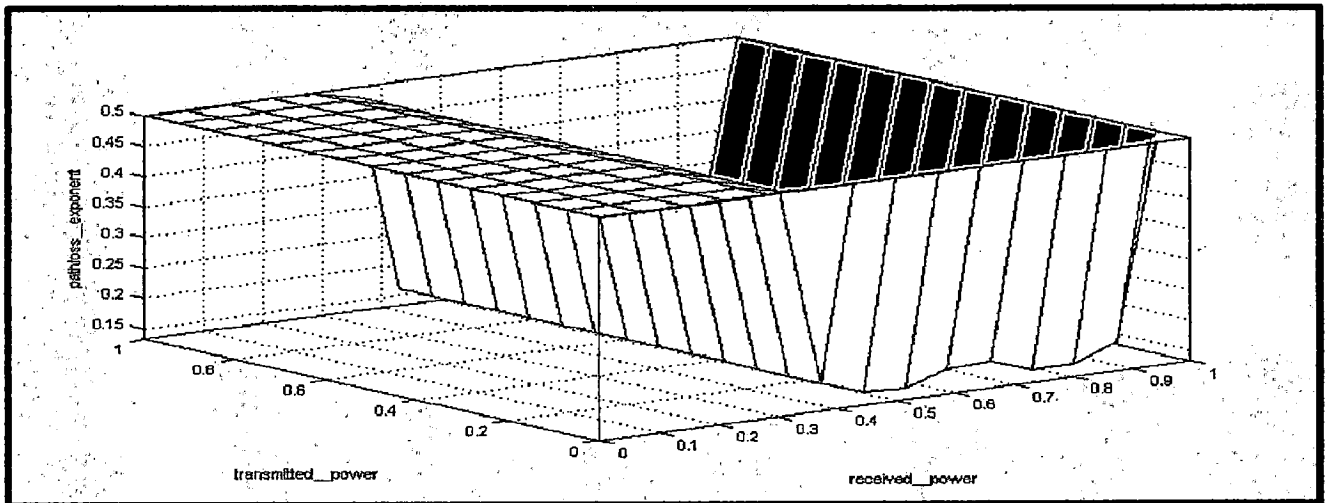


Figure 4.26: Variation of transmitted power and received power with path loss exponent

Figure 4.26 focuses on another set of combination with respect to path loss exponent are the transmitted power and received power.

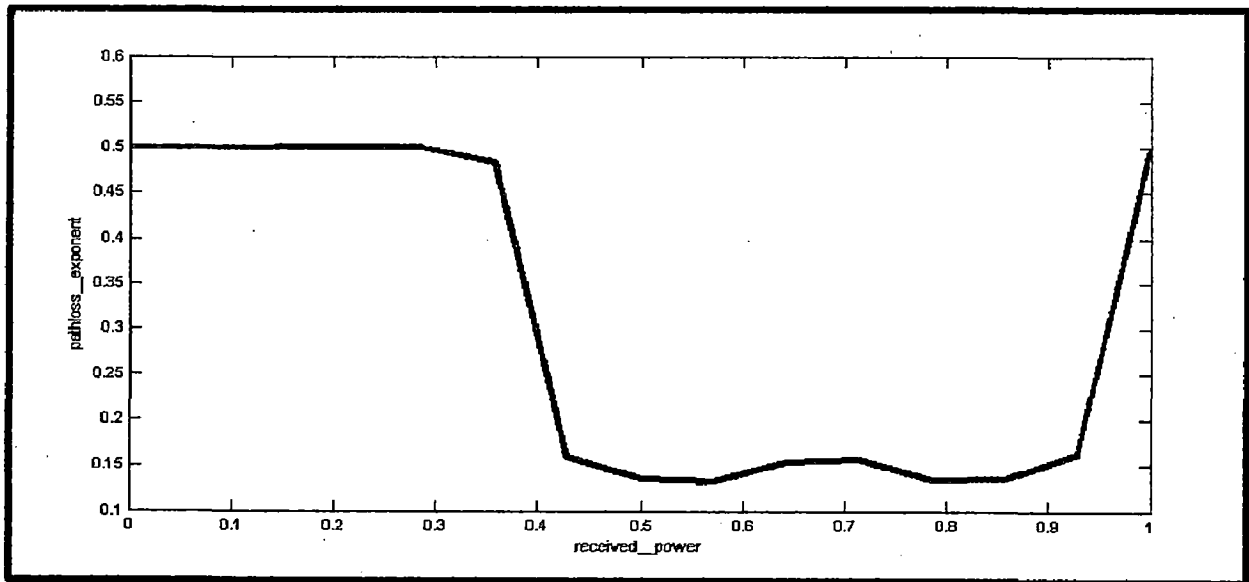


Figure 4.27: 2 D view of received power versus path loss factor

In Figure 4.26 and 4.27, the key parameters i.e. the transmitted power and received power is analyzed as a function of path loss exponent. As variability of transmitted power has been accounted, now analysis is more on the received power term along with the path loss factor.

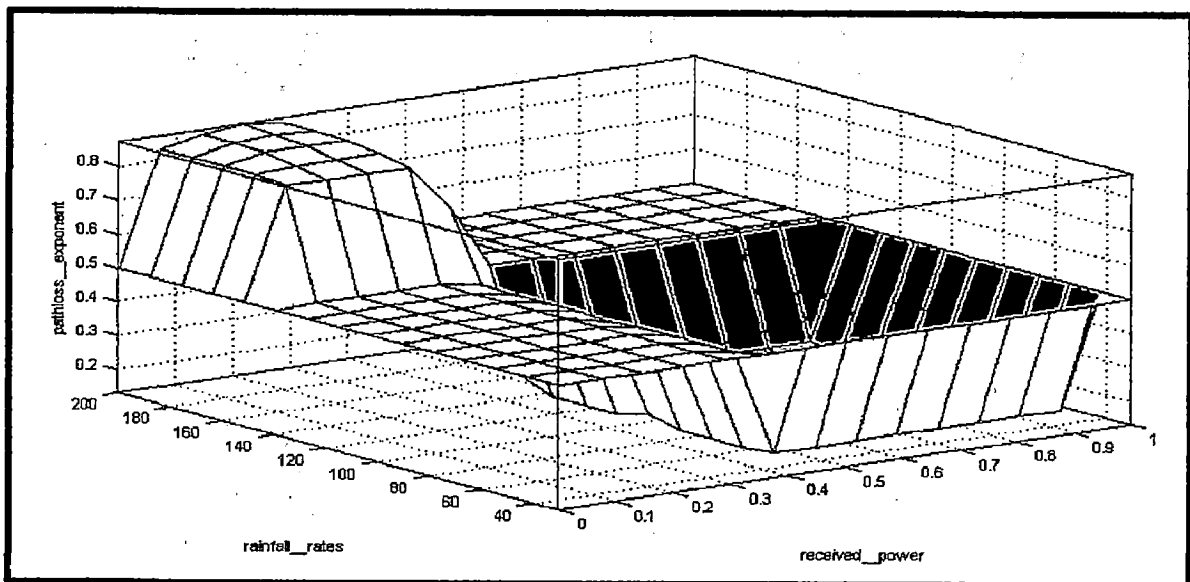


Figure 4.28: Dual-level comparison of rainfall rate and received power with path loss factor

Analysis of Figure 4.29 indicates that the path loss factor values are initially constant for increase in values of power received but suddenly at the 30% of total transmitted power received there is a slight depreciation and furthermore the depreciation becomes more severely linear at around somewhere in the 35%-45% of total transmitted power received pertaining to the fact that at higher values departures of received power the path loss factor values start declining quickly as compared to with at lower values departures. Afterwards there is a slow decline and a slight hike at about 70% indicating most optimum reception i.e. this is the optimum path loss exponent value that should be preferred for a better design. The result after it is appropriate as a better possibility does not exist due to system level hindrances. Figure 4.28 indicates the context on how the pathloss obtained is for estimating a better point for optimum network design based on selection facilitation guided by a set of rules governing the functionality of selection and allocation based on some sort of adaptive strategy.

4.7 Conclusion

From the result it has been analyzed that fuzzy logic approximation is effective to determine an unknown terrain from the set of known terrain anywhere in the region having the same terrain condition. Based on the fuzzy results efficient network planning for other regions having same rain rate and terrain can be predicted. Based on received power values fuzzy logic can be deployed along with other parameters of significant contribution to the proper network planning for the region.

CHAPTER 5

THE ASSESSMENT OF EFFECT ON LINK BUDGET DUE TO RAIN FADE MARGIN

It is valuable to design a communication system for the intended environment and to predict, with relative certainty, the system performance prior to installation and deployment [19]. Radio planning for networks such as cellular telephone systems or Wireless Local Area Networks (WLANs) is a key part of network deployment. Insufficient planning results in overdesign and wasted resources or under design and poor system performance. Prior to planning a network, the parameters controlling the performance of each individual link must be understood. The essential parameters are the received signal strength, the noise that accompanies the received signal, and any additional channel impairments beyond attenuation, such as multipath or interference [48], [39], [46]. For link planning, a link budget is prepared that accounts for the transmitter Effective Isotropically Radiated Power (EIRP) and all of the losses in the link prior to the receiver [66]. Another significant loss after free space loss is the signal attenuation due to rain. These losses affect both the uplinks and downlinks. As it is a function of rain rate, it varies from location to location. As the signal transmits from transmitter to receiver via channel, so in the path between transmitters and receivers signals has to face different propagation losses which may be more or less unpredictable to the receiver [110]. The receiver must be designed to overcome the effect of these propagation losses, to deliver the baseband signals to its final destination with as few errors as possible.

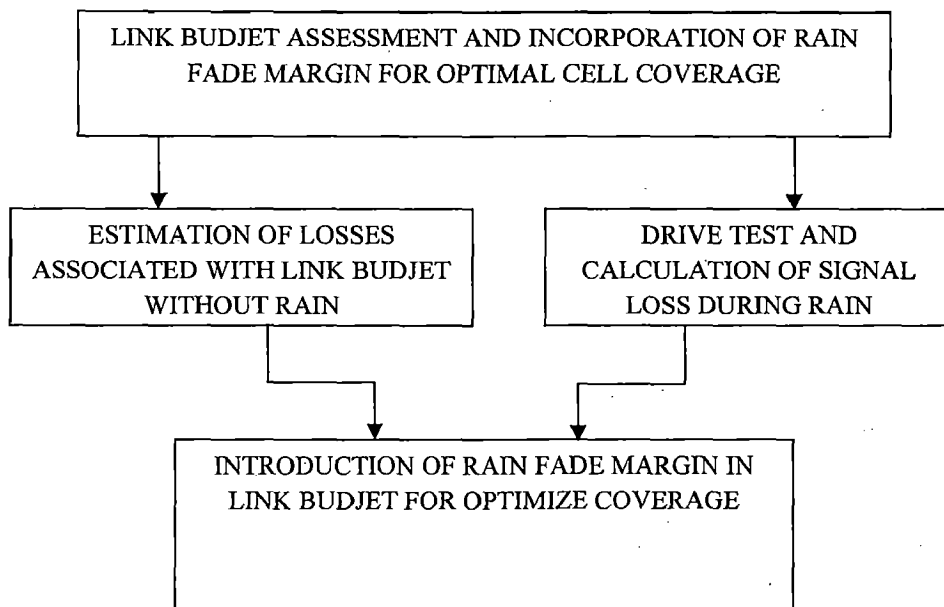


Figure 5.1: FLOW CHART OF STEP BY STEP IMPLIMENTATION OF WORK

5.1 Background and Objective

Insufficient link budget planning can result in overdesign, under design, wastage of resources health hazards and poor system performance. Prior to planning a network, the parameters controlling the performance of each individual link must be understood. For link planning, a link budget is prepared that accounts for the transmitter Effective Isotropically Radiated Power (EIRP) and all of the losses in the link prior to the receiver. Link budget parameters has been analysed by several researchers for solving constrain of path loss during up link and down link. The link budget is computed in decibels (dB), so that all of the factors become terms to be added or subtracted. Radio equipment is designed in such a way that when the link budget for the uplink and downlink are put together, they should have the same maximum allowable path loss in both directions. Rain fades is a significant factor depending upon the link distance and the geographic location. There is

always the temptation to argue that the rain margin is not being used most of the time, so it can be used to compensate for link budget shortfalls. The measurement is conducted in fringe area of Uttarakhand in order to determine the amount of attenuation caused by the rain. Four base stations are selected for measurement. Methodology of work is given in Figure 5.1. The assessment of effect on link budget due to rain fade margin is determined. To understand the concept of link budget parameters associated with generic link budget need to be studied.

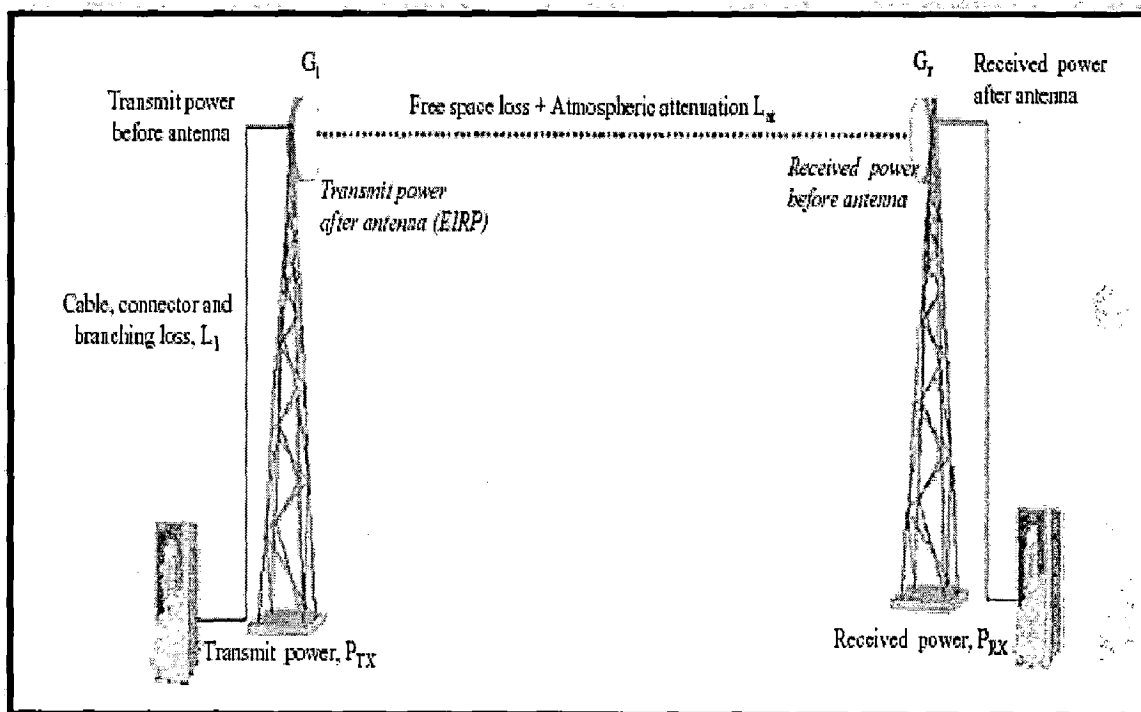


Figure 5.2: Elements of Link Budget

Related work

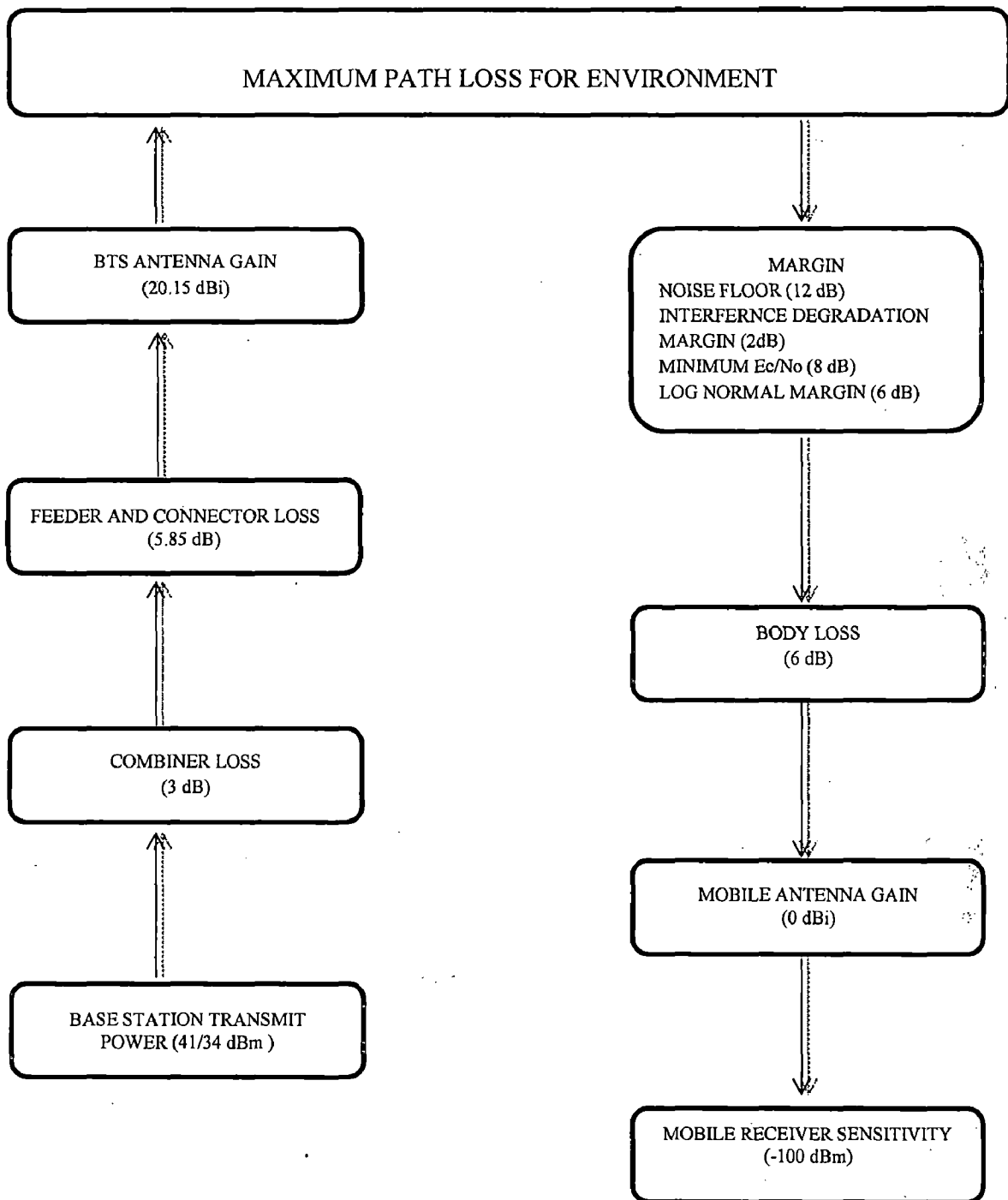
Performance evaluation results for link budget were reported in [110] which primarily covered the power loss due to cables transmitter and Receiver. Recently J. Zyren et. al has reported the experimental set up for link budget analysis . A performance comparison of different link budget parameters has been reported by L. Chiaraviglio et. al. in which they have tried to reduce power consumption in backbone networks. D. Coudert, et. al. tried to

minimizing energy consumption by power-efficient radio configuration in fixed broadband wireless networks. Prediction of attenuation by rain has been analyzed by R. K. Crane [80] for proper link budget design in which effect of rain on Electromagnetic wave propagation is observed.

The work has been extended to see the effect of rain on link budget design [98] in the region of Uttarakhand. Signal strength is measured for the course of entire rainy season. Based on collected data rain fade margin has been considered for proper link design.

5.2 Generic Link Diagram

The link diagram for a generic radio system [94] is shown in Figure 5.2. Not all elements will be present in all radio systems, but it is broadly representative; tuning units in particular may not be necessary unless the radio has to be capable of tuning over a wide frequency range. If this is required, the tuning unit helps to match the antenna impedance to the rest of the system. Figure 5.3 shows how the signal level may vary from the transmitter to the receiver, although not to scale. In general, specific sub-components downstream of the transmitting radio output will be connected via connectors and feeder cables. Both connectors and feeders may cause a loss in signal strength each time they are used. Radio systems that are able to operate over a wide frequency range (such as military radios and some modern multi-band radios) may have a tuning unit that is used to match the antenna impedance and thus maximize signal radiated from the antenna.



DOWNLINK BUDGET

Figure 5.7: Gain and loss components in a typical downlink budget

The GSM link budget parameters are explained in the following before proceeding to the calculations in more detail:

5.3.1 Receiver Sensitivity

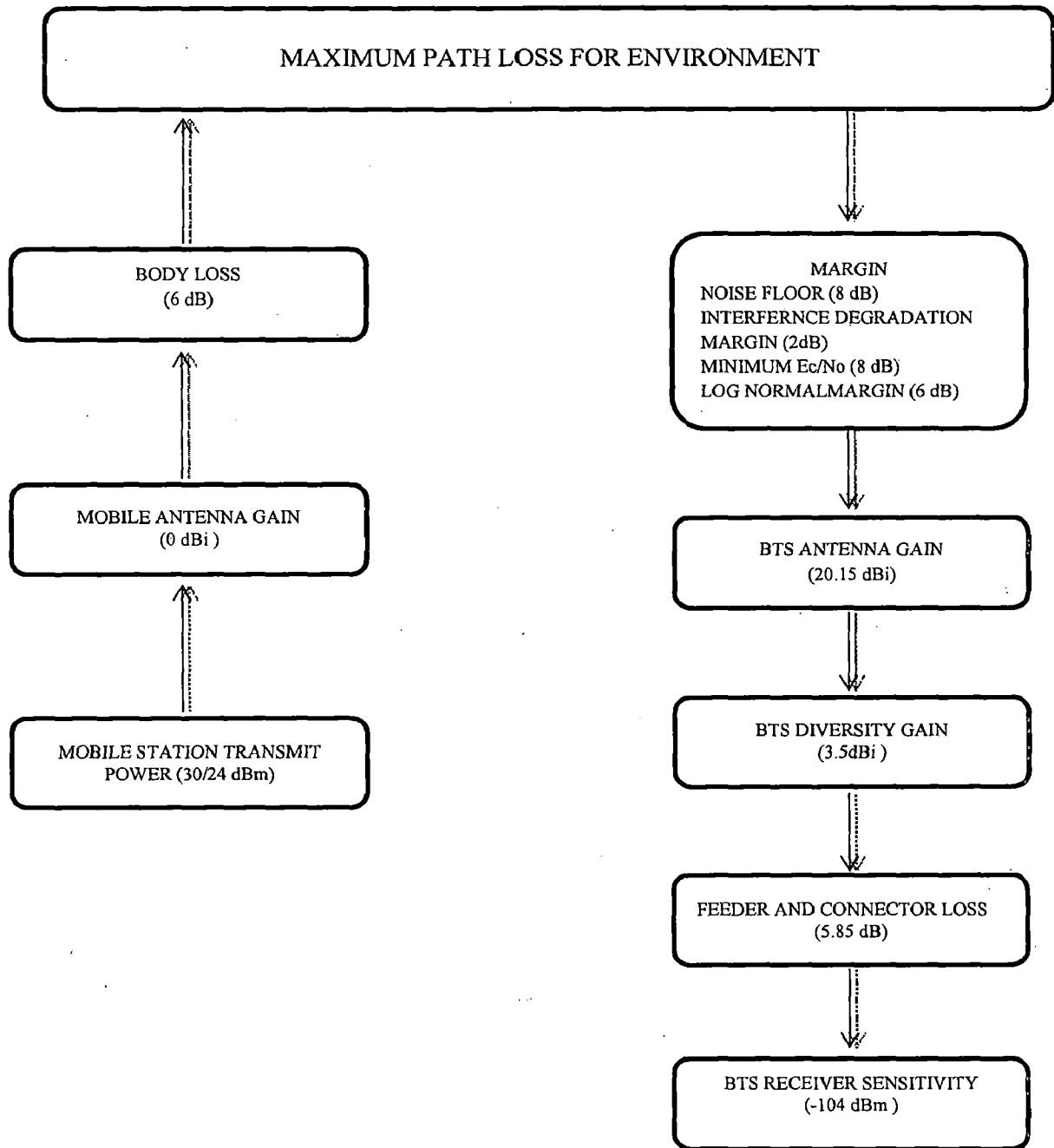
The performance of a radio, when it is not subject to external interference is governed by its sensitivity. This is the required input level to achieve a given degree of performance. This description is important as it identifies that there is no such thing as a single sensitivity, but rather that there will be different values for different degrees of performance. In some cases it will be necessary to determine sensitivity from graphs of Bit Error Rate (BER), but in most practical cases, commercial equipments has been used they are available with published technical characteristics, or figures defined in a standard such as that for TETRA, TETRAPOL, GSM, UMTS etc. For digital equipment, the sensitivity used must be that for the conditions prevalent at the antenna, particularly whether it is moving or not. Digital receivers typically have resilience against fading built in for the situation when the fading is occurring rapidly, and thus there will be a static sensitivity and a dynamic sensitivity assuming a given vehicle speed. This is only strictly true for the speed identified and if the digital system is to be used outside of its specified speed range, and then it may well be necessary to perform measurements to determine its performance at the wanted speed. It is important to determine whether the sensitivity values are for unfaded conditions (in which fading must be accounted for additionally in the link budget) or for the faded condition (in which this has already been accounted and should not be added again). The fundamental limit on receiver sensitivity is set by the thermal noise limit. This is the energy caused by random movements of charge and current due to the movement of electrons in the radio receiver. Thermal noise is described by the expression:

$$N = kT_0W$$

where

N is the noise floor

k is the Boltzmann constant = 1.38×10^{-23} (J/K)



UPLINK BUDGET

Figure 5.6: Gain and loss components in a typical uplink budget

5.3 Link Budget Calculation

The radio link budget aims to calculate the cell coverage area. One of the required parameters is radio wave propagation to estimate the propagation loss between the transmitter and the receiver. The other required parameters are the transmission power, antenna gain, cable losses, receiver sensitivity and margins, as shown in the Figure 5.4. When defining the cell coverage area, the aim is to balance the uplink and downlink powers. The links are calculated separately and are different from the transmission powers. The BTS transmission power is higher than the MS transmission power and therefore the reception of the BTS needs to have high sensitivity. The other differences in calculations between uplink and downlink have been estimated. The parameter that is same for both downlink and uplink calculations are the propagation loss is shown in Figure 5.5. The radio signal experiences the same path loss when travelling from the BTS to the MS as from the MS to the BTS.

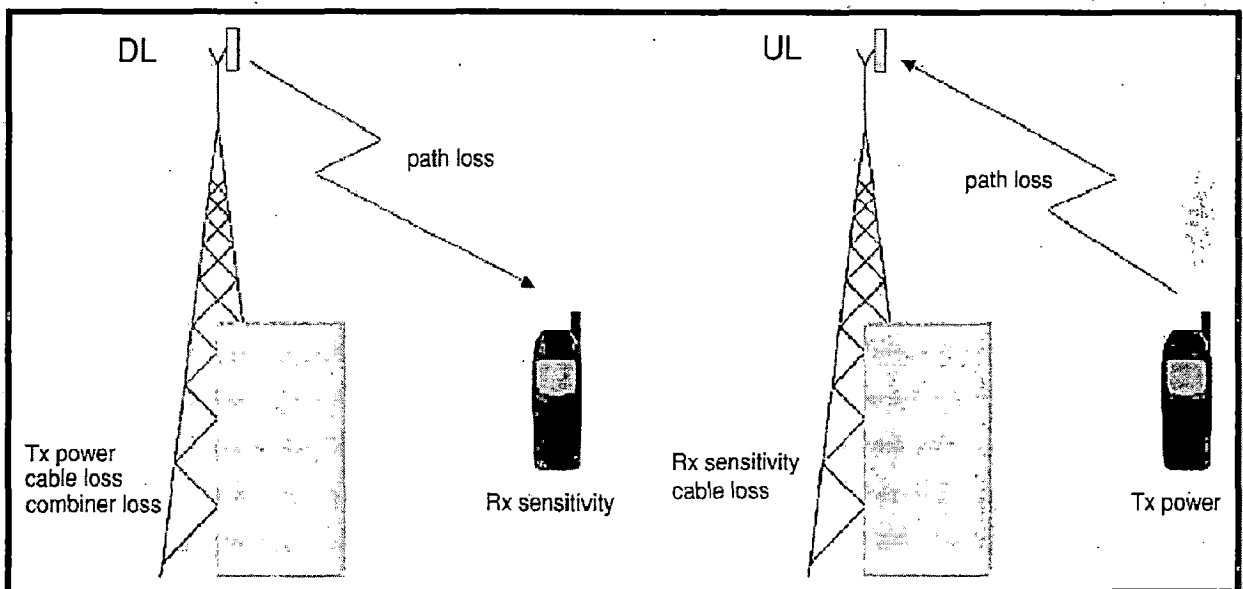


Figure 5.5: Link budget parameters

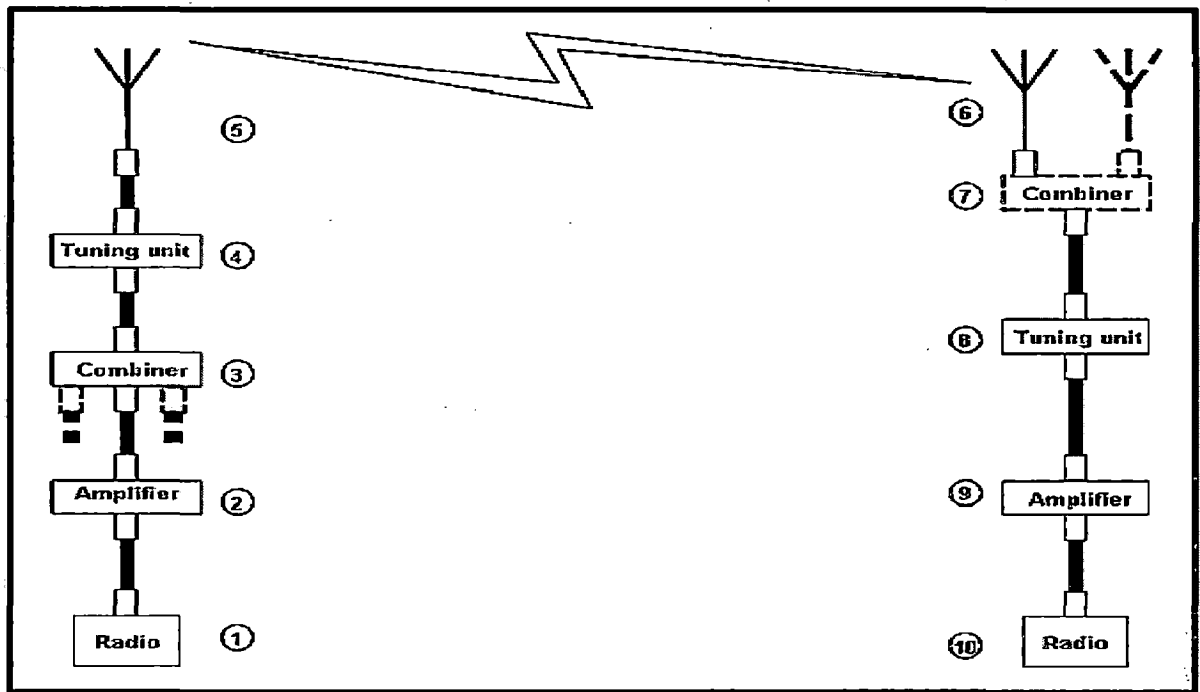


Figure 5.3: Generic Link Budget

Energy entering the antenna at RF is then propagated into the environment, and some of this energy is picked up at the receiving antenna. At the receiver, there may be one or more antennas to pick up the signal. A hand-portable system will have a single antenna, but a vehicle or aircraft may have several to combat fast fading [89]. This is known as a diversity antenna system [68]. If diversity antennas are present, then the individual signals are picked up by a combiner or switch, which generates a single signal to be conducted through the rest of the system. This may be amplified (although it will also amplify any noise or interfering signals) and may again pass through a tuning unit if one is present before finally arriving at the receiving radio. Figure 5.4 shows the same components of a radio link, but this time spread out in a linear fashion with a representation of the signal strength as it travels from the transmit radio output through to the input of the receiving radio. The signal will generally drop slightly as it travels through connectors and feeder

cables, particularly if they are long. It will also be enhanced by amplifiers and possibly antenna gain. There may also be a gain effect if there are multiple receiving antennas (diversity gain), compared to the single antenna fading condition [90]. Other elements in the link may cause losses. Eventually the signal reaches the receiving radio. If the signal that arrives is higher than the minimum operating level required, then the original message should be retrievable at the receiver. If it is not high enough, then the original message or part of it may be lost.

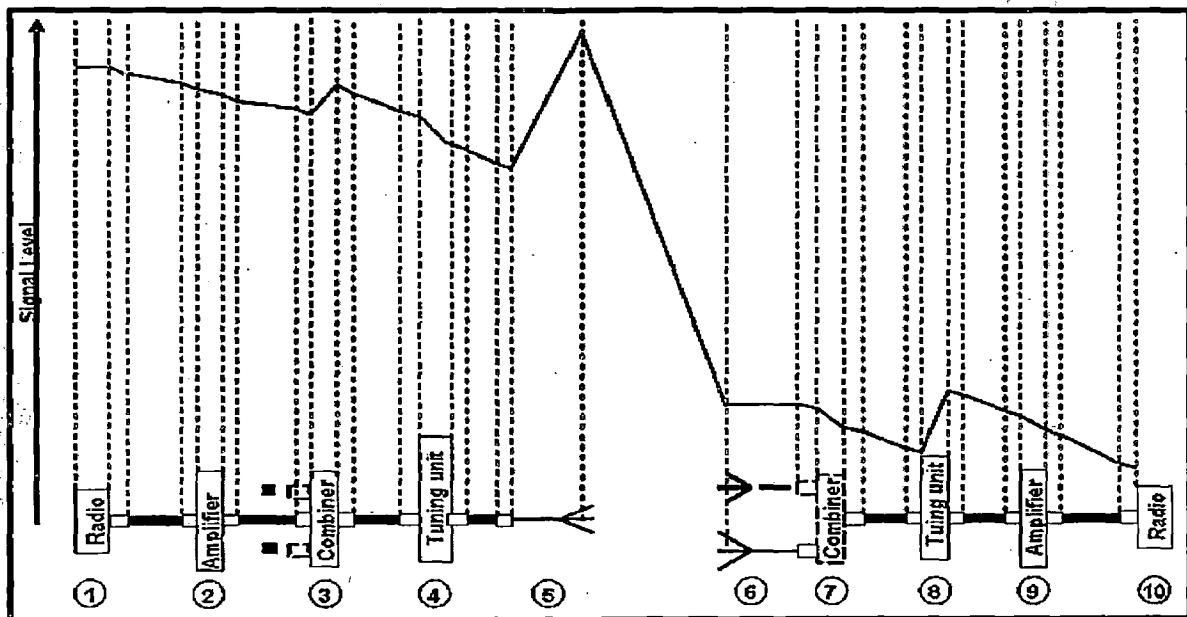
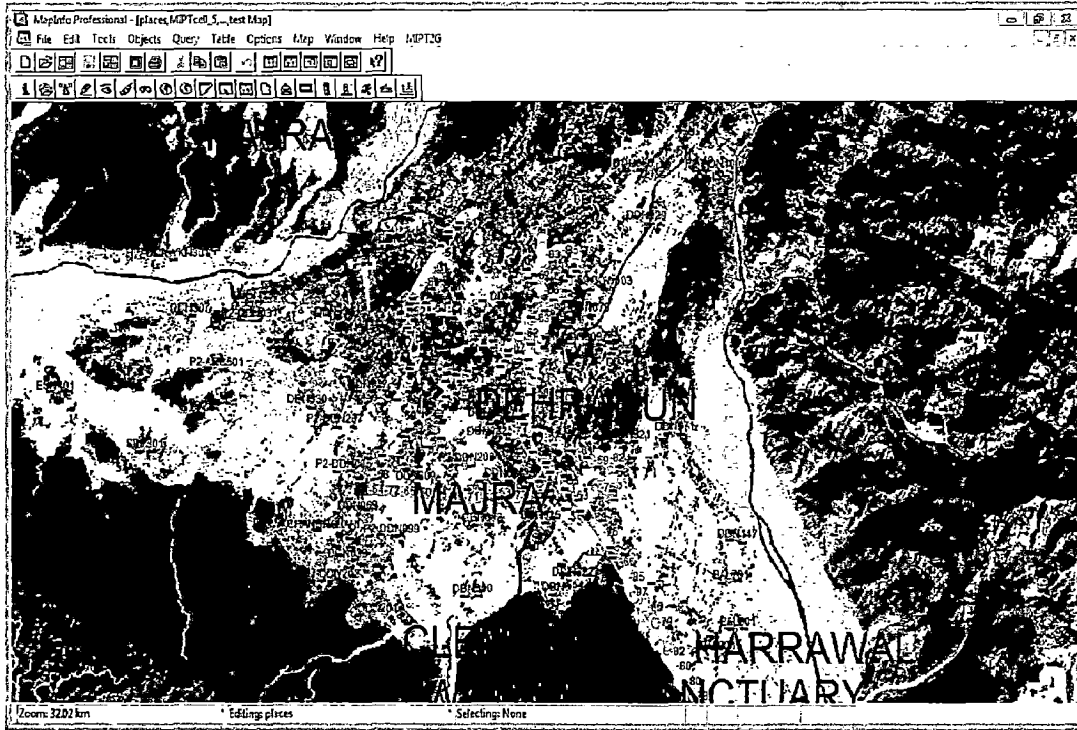


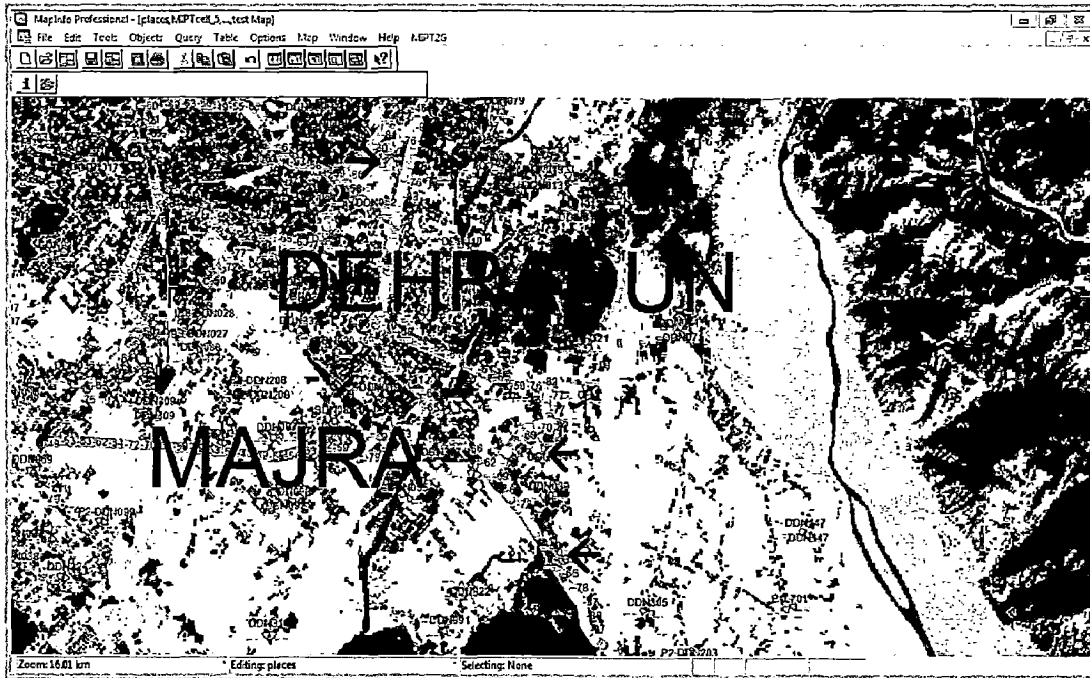
Figure 5.4: Generic link, showing typical elements that may be present in a Radio system

The process of determining a link budget is composed of two main elements; determining the elements within the link that cause gain or loss between the radios and the antennas, and also determining the minimum acceptable signal level that must be available at the receiving antenna as it moves through the service area, both at the fast fading and slow fading scales.

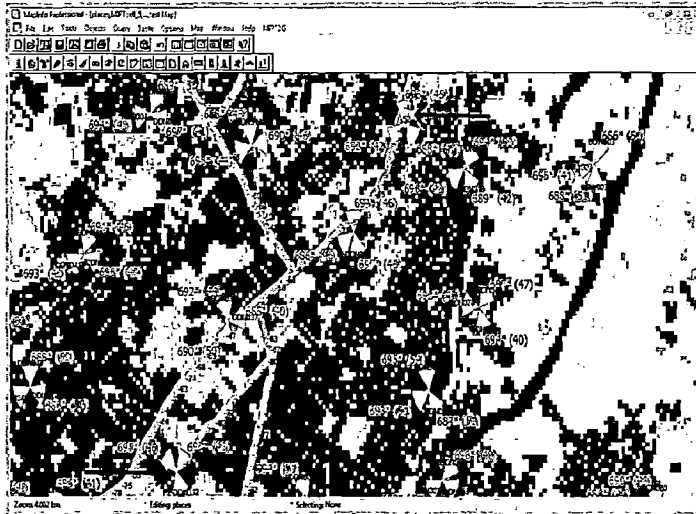
CLUTTER AND COVERAGE GRAPH OF BTS SITE ID'S SELECTED FOR FIELD DATA COLLECTION



CLUTTER PLOT OF BTS SITE ID DDN 002 (LATITUDE: 30.3539 LONGITUDES: 78.0245)



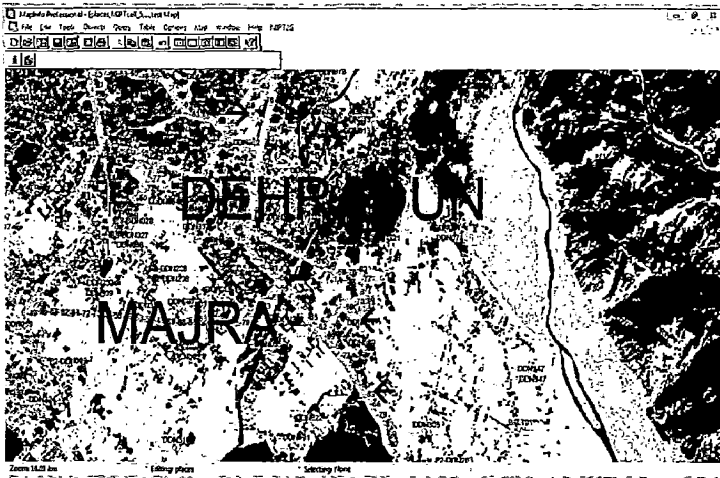
CLUTTER PLOT OF BTS SITE ID DDN 204 (LATITUDE: 30.276 LONGITUDES: 78.0773)



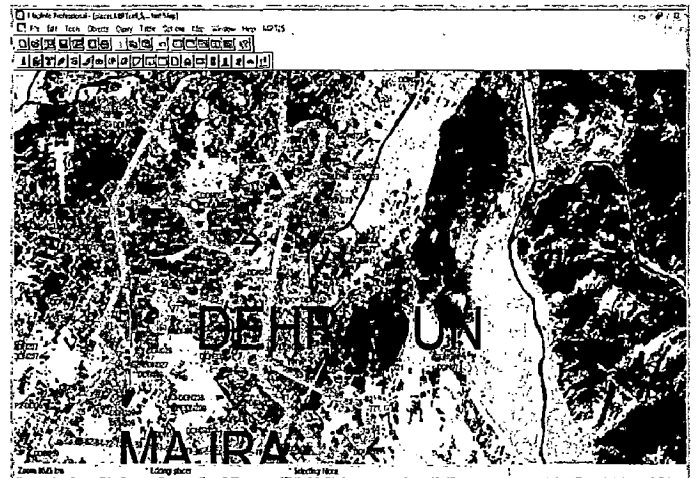
SITE ID DDN034



SITE ID DDN002



SITE DDN008



SITE DDN076

T_o is the noise temperature of the receiver in Kelvin

W is the bandwidth in Hz

The concept of reference noise power is used, with $T = 290$ K. To build a link budget for GSM 1800 first the MS and BTS sensitivity has been determined.

5.3.2 MS Sensitivity

It is minimum signal level at the input that leads to the signal to noise at the output, higher than a threshold E_b/N_o related to the modulator performance. The MS sensitivity can be calculated using the information of receiver noise F and minimum E_b/N_o . The value of noise is 12 dB and the minimum E_b/N_o is 8 dB for GSM 1800, which is defined in the ETSI recommendation 03.30. The receiver sensitivity S_i is determined with the input noise power N_i is the product of three parameters: the Boltzman constant k , Temperature $T_o = 290$ K and Bandwidth $W = 271$ kHz (54 dB):

$$F = \frac{S_i/N_i}{S_o/N_o} = \frac{S_i/(kT_oW)}{E_b/N_o}$$

Where

$$N_i = kT_oW$$

and

$$S_i = \frac{E_b}{N_o} FkT_oW$$

$$S_i = 8 \text{ dB} + 12 \text{ dB} + (290 \text{ K} \times 1.38 \times 10^{-23} \text{ J/K}) \text{ dB} + 54 \text{ dB}$$

$$S_i = 8 \text{ dB} + 12 \text{ dB} - 174 \text{ dB} + 54 \text{ dB}$$

$$S_i = -100 \text{ dB}$$

5.3.3 BTS sensitivity

BTS sensitivity for 1800 MHz band can be calculated by using above equation but in this case the value of noise is 8 dB, recommended by ETSI.

$$S_i = 8 \text{ dB} + 8 \text{ dB} + (290 \text{ K} \times 1.38 \times 10^{-23} \text{ J/K})\text{dB} + 54 \text{ dB}$$

$$S_i = 8 \text{ dB} + 8 \text{ dB} - 174 \text{ dB} + 54 \text{ dB} = -104 \text{ dB}$$

5.3.4 MS and BTS powers

MS and BTS powers are important along with the sensitivities. The MS TX (transmission) power is defined by the MS class in ETSI specifications. There are two power classes with a normal tolerance level of ± 2 dB, while the worst case tolerance is ± 2.5 dB. Power step size is either ± 2 dB, ± 3 dB, ± 4 dB, and ± 5 dB starting at a peak level for the two classes of mobile. The MS maximum output power and power steps are shown in Table 5.1. The BTS transmitter maximum power is shown in Table 5.2. The tolerance should be such that the power level can be decreased in nominal steps of 2 dB with an accuracy of ± 1 dB shown in Table 5.3. Generally BTS TX power depends on the BTS type and vendor. The TX power is adjustable, which enables the link budget to be balanced.

Table 5.1: Mobile Power Class and Their Tolerance

Power Class	Maximum Peak Power (W)	Tolerance Normal(dB)	Tolerance Extreme(dB)
1	1	± 2	± 2.5
2	0.25	± 2	± 2.5

Table 5.2: Power Steps and Their Tolerance

Power Control Level	Peak Power (dBm)	Tolerance Normal(dB)	Tolerance Extreme (dB)
0	30	± 2	± 2.5
1	28	± 3	± 4
2	26	± 3	± 4
3	24	± 3	± 4
4	22	± 3	± 4
5	20	± 3	± 4
6	18	± 3	± 4
7	16	± 3	± 4
8	14	± 3	± 4
9	12	± 4	± 5
10	10	± 4	± 5
11	8	± 4	± 5
12	6	± 4	± 5
13	4	± 4	± 5

Table 5.3: BTS Power Class and Their Tolerance

Transmit Power Class	Peak Power (W)	Tolerance (dB)
1	20	-0,3
2	10	-0,3
3	5	-0,3
4	2.5	-0,3

5.3.5 Antenna gains [79]

Antenna gains can be found for both BTS and MS antennas. The BTS antenna gain is dependent on the antenna type and whether the antenna is omnidirectional or directional . BTS antenna has a gain of approximately 10 dBi. The gain of a directional BTS antenna is dependent on the horizontal and vertical half power beam widths.

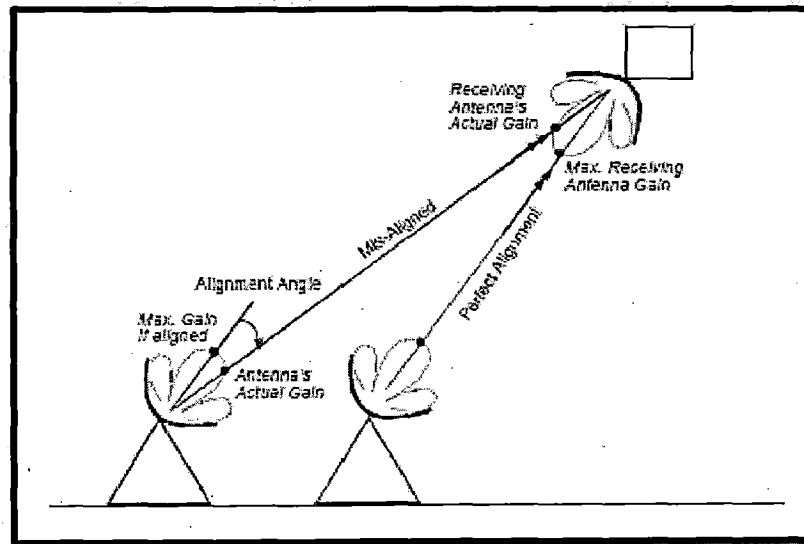


Figure 5.8: Antenna gain and alignment

It is also dependent on the physical size of the antenna which in turn has an impact on the frequency range. Also frequency range is inversely proportional to the size of the antenna, which is then connected to the radiating aperture of the antenna [84]. The antenna gain is around 16–20 dBi when there is a widely used antenna with 60–65° horizontal half power beam width and 5–10 vertical half power beam width as shown in Figure 5.8. In the link budget calculations for the MS antenna the gain is generally 0 dBi. The actual MS antenna gain is complicated to estimate, because the gain is highly dependent on the mobile user's relative location towards the base station when the amount of body loss varies [92]. In analysis the BTS antenna has a gain of 20.15 dBi and MS antenna gain is 0 dBi.

5.3.6 Diversity gain

Diversity gain can be used for correcting unbalance between the uplink and downlink . The typical way to arrange diversity is to have it in the BTS reception. One basic method is to separate receiver antennas vertically or horizontally. This method is called space diversity. The diversity decreased fading effect and gain achieved can be around 5 dB. The selected Base station has 3.5 dB diversity gain.

5.3.7 Feeder and connector loss

Feeders are the electrical cables that connect the radio output to the antenna, via connectors at each end. If connectors or cables attenuate the power output by the radio, then the power presented to the antenna will be less than otherwise and consequently transmitted radio energy will be reduced. These losses are significant and amplifier should counter act feeder and connector loss. Feeder Cable and connector losses are case specific and need to be measured or calculated separately. Thicker cable causes less loss, but it is more difficult to install, due to weight and a larger bending radius. Thicker cables are also more expensive and therefore the usage needs to be considered. Obviously a longer cable gives a higher loss and because of this the shortest possible route for the cable should be used. An individual connector gives a loss of around 0.1 dB, but depending on the cable installations there can be several in one antenna lines.

The feeder and connector loss is given below which are used in power budget calculations:

- a) Duplexer loss in BTS = 0.5 dB
- b) Feeder/Jumper loss at BTS = 3.25 dB
- c) Duplexer loss in TMA = 0.3 dB

5.3.8 Tuning Units, Amplifiers and Combiners

For radios that cover a wide proportion of the radio spectrum (of the order of an octave or more), the antennas used will not be matched over the entire range. Uncorrected, this would cause higher loss for those portions of the band that are more mismatched.

To overcome this, the radio is fitted with a tuning unit. If so, the gain of the tuning unit, or the overall gain or loss of the tuning unit, mated to the antenna must be taken into account (being careful not to double count). For some systems, an amplifier may also be fitted to boost signal strength close to the antenna so that a higher power is fed into the antenna unit. If an amplifier is fitted, then the affect of this must also be included in the link budget. Combiners are used when signals from different systems are fed into the same antenna for transmission. This may be done for reasons of efficiency or of space on a given antenna. Given the further development of so-called MIMO (Multiple-In Multiple-Out) systems [77] and the general reluctance in many areas to allow more masts to be built, this will be ever more present for future network designs. Combiners may involve a loss to each of the systems feeding into the system. Each of these systems may be present in either the transmitting or receiving end of the link shown in Figure 5.6 and Figure 5.7. Other equipment loss factors consist of isolator, combiner and filter losses. The isolator isolates the transmitted signal from the transmitter. The combiner combines TX (transmission) signals to one antenna. The filter combines transmitted and received signals to one feeder cable as well as to a single antenna and antenna cable. The isolator, combiner and filter together give around 2–3 dB losses.

5.3.9 Mast Head Amplifier (MHA) and Booster

Two other gain factors, which need to be considered in the link budget if used, are the mast head amplifier (MHA) and booster. The MHA, which is located close to the antenna in BTS reception, is used to amplify the received signal. This decreases the unbalance between the uplink and downlink by giving extra gain in the uplink the direction. The booster can be used to amplify the BTS transmission power.

TMA loss = 0.3 dB.

Receiving end:		BTS	MS	Eq.
TX:		MS	BTS	(dB)
Noise figure	dB	8	12	A
E_c/N_0 min. fading	dB	8	8	B
RX RF-input sensitivity	<u>dBm</u>	-104	-100	C=A+B+W-174 (W=54.3 <u>dBHz</u>)
Interference degrad. margin	dB	2	2	D
Cable loss + connector	dB	5.85	0	E
RX-antenna gain	<u>dB</u> i	20.15	0	F
Diversity gain	dB	3.5	0	F1
Isotropic power, 85 % Ps	<u>dBm</u>	-119.8	-98	G=C+D+E-F-F1
Lognormal margin 85 % → 95 % Ps	dB	6	6	H
Isotropic power, 95 % Ps	<u>dBm</u>	-113.8	-92	I=G+H
Field Strength 95 % Ps	<u>dBuV/m</u>	28.6	50.4	J=I+142.4
Transmitting end:		MS	BTS	Eq.
RX:		BTS	MS	(dB)
TX PA output peak power	W	-	12.73/2.5	
(mean power over burst)	dB	-	41/34	K
Isolator + combiner + filter	dB	-	3	L
RF Peak power,(ant. connector)	dB	30/24	38/31	M=K-L
	W	1.0/0.25	6.31/1.26	
Cable loss + connector	dB	0	5.85	N
TX-antenna gain	<u>dB</u> i	0	20.15	O
Peak EIRP	W	1.0/0.25	169.8/33.88	
	<u>dBm</u>	30/24	52.3/45.3	P=M-N+O
Isotropic path loss, 85 % Ps	dB	143.8/137.8	144.3/137.3	Q=P-G-6
Isotropic path loss, 95 % Ps	dB	137.8/131.8	138.3/131.3	R=P-I-6

Table 5.4: Radio Link Power Budget for GSM 1800 MHz (GSM)

5.3.10 Interference degradation margin

The interference degradation margin describes the loss due to frequency reuse. Therefore the frequency reuse rate corresponds to the degradation margin value. The suggested value for the interference degradation margin in an average suburban and rural area is 3 dB according to the ETSI recommendation 03.30. In the case of high frequency reuse in urban areas the degradation margin can have a value of 4–5 dB. The interference degradation margin of 2 dB is considered.

5.3.11 Polarization Loss

The polarization loss indicates the portion of the incident power which is coupled into the receive antenna. The polarization loss of 1.5 dB occurs at each base station selected for measurement. The power budget calculation is presented in Table 5.4. The link budget is for GSM 1800 and the more calculations are described in detail using these values. The power budget calculations start with the receiving end by calculating isotropic power (G and I) both for the BTS and the MS. The isotropic power is the minimum received power, which enables the link balance situation. The receiver sensitivity (C) is the basis for the isotropic power with the power budget gain parameters subtracted from it and the loss parameters added to it. The isotropic power (85 % Ps) for the BTS is

$$G=C+D+E-F-F1 = -104 + 2 + 5.85 - 20.15 - 3.5 = -119.8$$

where

$$C=A+B+W-174 = 8 + 8 + 54.3 - 174 = -104$$

and isotropic power for 95% Ps (BTS)

$$I = G + H = -119.8 + 6 = -113.8$$

The isotropic power (85 % Ps) for the MS

$$G=C+D+E-F-F1 = -100 + 2 + 0 - 0 - 0 = -98$$

where

$$C=A+B+W-174 = 12 + 8 + 54.3 - 174 = -100$$

and isotropic power for 95% Ps

$$I = G + H = -98 + 6 = -92$$

The isotropic power is next converted to dB $\mu\text{V}/\text{m}$ and the result is field strength (I). For the BTS:

$$J = -113.8 \text{ dBm} + 20 \log (1800 \text{ MHz}) + 77.2 = 28.6$$

and field strength for the MS:

$$\begin{aligned} J &= -92 + 20 \log (1800 \text{ MHz}) + 77.2 \\ &= 50.4 \end{aligned}$$

The power budget calculation continues with the MS peak EIRP (Effective Isotropic Radiated Power) calculation. The MS radiation power is presented in this way as the antenna gain uses decibels over anisotropic antenna (dBi) format. If the antenna gain format is in decibels over a dipole (dBd) the radiated power format is ERP (effective radiated power). The transformation from EIRP to ERP is given by

$$\text{EIRP} = \text{ERP} + 2.15 \text{ dB}$$

The MS antenna gain is 0 dBi and the losses are also zero, therefore the EIRP of the MS is the TX output power (M). For power class 1, EIRP of MS is 30 dBm and for power class 2 it is 24 dBm. So the isotropic path loss (Q and R) for the uplink in both the power class is:

$$Q = P - G - 6 = 143.8 / 137.8 \quad \text{for 85 \% Ps}$$

$$R = P - I - 6 = 137.8 / 131.8 \quad \text{for 95 \% Ps}$$

Here -6 dBi is mean effective gain. The Mean Effective Gain (MEG) of handheld MS in scattered field representing the cell range taking into consideration absorption, detuning

and mismatch of the hand held antenna by the human body (MEG = -antenna/body loss) of 13 dBi for GSM 400, -9 dBi for GSM 900 and -6 dBi for GSM 1800 MHz.

The path loss for the downlink direction equals the path loss for the uplink direction. With this the BTS TX output peak power calculation can be started. As mentioned before, the BTS TX power is critical for the link balance. The BTS peak EIRP is

$$M = K - L + N + O = 52.3/45.3 \text{ dBm}$$

The isotropic path loss for downlink is

$$Q = P - G - 6 = 144.3/137.3 \quad \text{for 85 \% Ps}$$

$$R = P - I - 6 = 138.3/131.3 \quad \text{for 95 \% Ps}$$

5.4 Link Budget Balancing

Often, radio equipment is designed in such a way that when the link budget for the uplink and downlink are put together, they have the same maximum allowable path loss in both directions. The investigation of link budget for GSM 1800 MHz also reveals that maximum allowable loss is same for both the direction. In this case, the links are said to be balanced, and a radio link from a base station to a mobile element should have the same probability of being established as the link from the mobile element back to the base station[82]. Sometimes links are not balanced in both directions, often due to power limitations on the mobile side. In this case, one link will be stronger than another, and thus it may be possible to detect messages without being able to successfully send messages, or vice versa. If the down link is greater than the uplink (limitation of the MS output power and BTs receivers sensitivity) , then following results:

- Range of BTS > Range of MS.
- Call dropped on uplink after initiation of handover.
- Coverage area is smaller in reality than the prediction.
- This is the most frequent case.

greater the uplink than the downlink results in following:

- Range of MS > Range of BTS.
- No coverage problem from MS to BTS.

uplink > downlink condition is better than uplink < down link. In order to establish full two-way communications, it will be necessary to plan the network coverage based on the weaker of the two links. Calculating the link budget in both the uplink and downlink directions allows determination of which link is weaker.

The power budget calculation provides the maximum allowable path loss. This value is further used to determine the cell range or coverage area of a particular BTS and it is also helpful in the analysis of link reliability.

5.5 Effect of rain on Link Budget

A key performance metric for most communication systems is the availability i.e. the percentage of time that the link is providing communications at or below the specified bit error rate. There are number of factors that impact the availability, including hardware reliability, interference, and fading [83]. There are variety of sources of excess path attenuation, including atmospheric absorption, diffraction, multipath effects (including atmospheric scintillation), shadowing, foliage [69] and attenuation by hydrometeors.

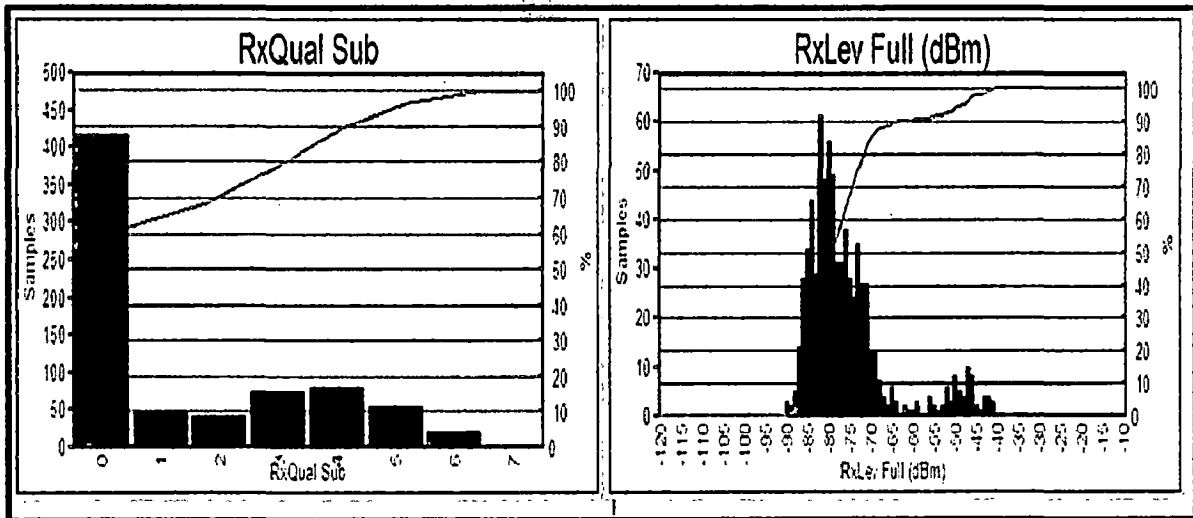


Figure 5.9: Received signal samples and RxLev in dBm during rain

Of these, the fades caused by rain (hydrometeor) is a major limiting factor of link availability or link distance as shown in Figure 5.9. Rain fades is a significant factor depending upon the link distance and the geographic location.

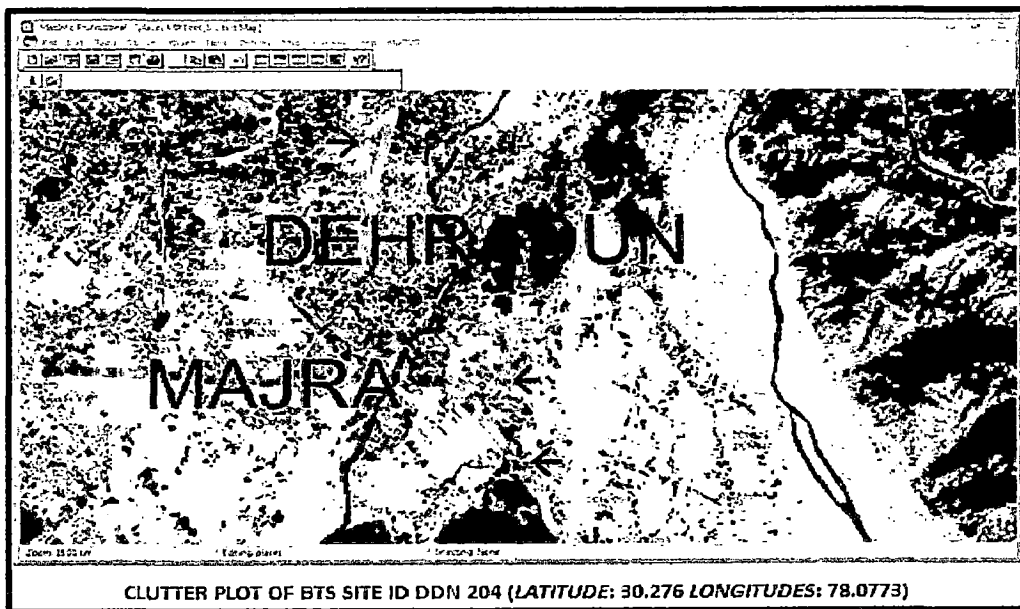


Figure 5.10: Plot during rain

The measurement has been carried out in fringe area of Uttarakhand in order to determine the amount of attenuation caused by the rain as shown in Figure 5.10. Four base stations is selected for measurement. Measurements are performed at the edge of each selected site, during rain.

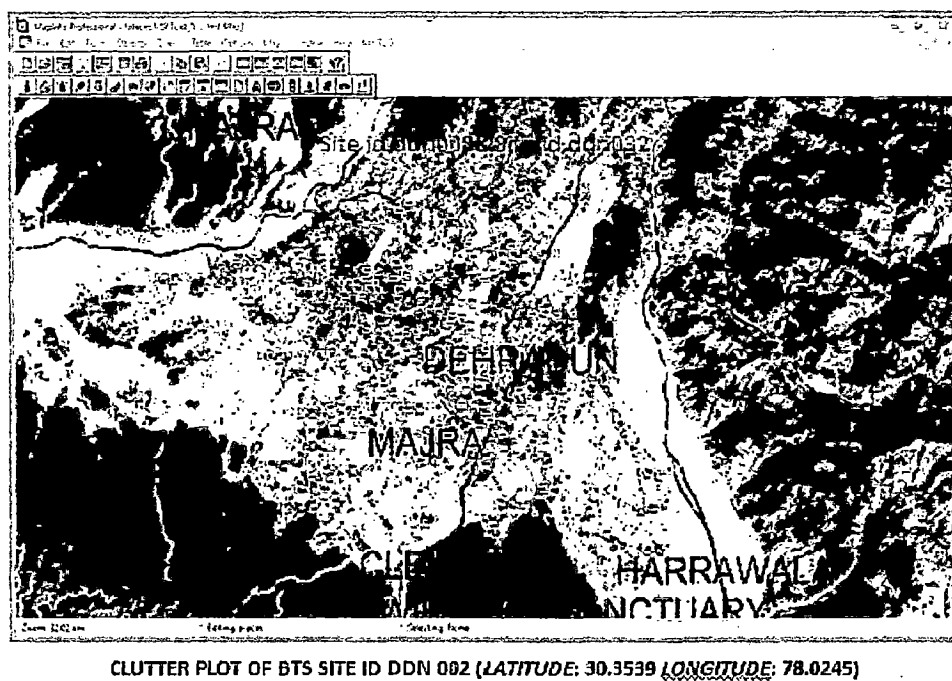


Figure 5.11: Clutter Plot during rain

Measurement gives the maximum rain attenuation experienced by MS in a cell. The clutter plot obtained by measurement is compared to another measurement which was earlier conducted in the same city of Dehradun and around the same base station but not in the rainy season shown in Figure 5.11. Analysis shows that there is an attenuation of .02 dB exists due to rain. The amount of rain attenuation is used as rain fade margin which is incorporated in the link budget. Table 5.5 shows the link budget calculation including the rain fade margin.

Receiving end: TX:		BTS MS	MS BTS	Eq. (dB)
Noise figure	dB	8	12	A
E_c/N_0 min. fading	dB	8	8	B
RX RF-input sensitivity	dBm	-104	-100	$C=A+B+W-174$ ($W=54.3$ dB Hz)
Interference degrad. Margin	dB	2	2	D
Rain fade margin	dB	0.02	0.02	D1
Cable loss + connector	dB	5.85	0	E
RX-antenna gain	dBi	20.15	0	F
Diversity gain	dB	3.5	0	F1
Isotropic power, 85 % Ps	dBm	-119.78	-97.98	$G=C+D+D1+E-F-F1$
Lognormal margin 85 % \rightarrow 95 % Ps	dB	6	6	H
Isotropic power, 95 % Ps	dBm	-113.78	-91.98	$I=G+H$
Field Strength 95 % Ps	dBuV/m	28.62	50.42	$J=I+142.4$
Transmitting end: RX:		MS BTS	BTS MS	Eq. (dB)
TX PA output peak power (mean power over burst)	W dB	-	12.73/2.5 41/34	K
Isolator + combiner + filter	dB	-	3	L
RF Peak power	dB W	30/24 1.0/0.25	38/31 6.31/1.26	$M=K-L$
Cable loss + connector	dB	0	5.85	N
TX-antenna gain	dBi	0	20.15	O
Peak EIRP	W dBm	1.0/0.25 30/24	169.8/33.88 52.3/45.3	$P=M+N+O$
Isotropic path loss, 85 % Ps	dB	143.78/137.78	144.28/137.28	$Q=P-G-6$
Isotropic path loss, 95 % Ps	dB	137.78/131.78	138.28/131.28	$R=P-I-6$

Table 5.5: Power budget calculation including rain fade margin

5.6 Conclusion

Measurements is performed at the edge of each selected site, during rain which gives the maximum rain attenuation experienced by Mobile Station in a cell. Based on the collected data, it is observed that difference in the path-loss without rain and path-loss during rain indicates that there is a need of rain fade margin to be introduced in link budget. The amount of rain attenuation estimated is used as rain fade margin and it is incorporated in

the link budget. From the result it has been analyzed that there is significant path loss with respect to the power budget considering the rain attenuation. The maximum allowable path loss with and without rain fade is analyzed for proper link budget design. Analysis estimates that due to increase in path-loss, the maximum allowable coverage result in decreases of cell radius. In order to compensate this loss caused by the rain, there is a need to increase the link budget. From the result maximum allowable path loss with and without rain fade is analyzed. It is analyzed that there is a decrease of 0.02 dB in the maximum allowable path loss with respect to the power budget without considering the rain attenuation. Analysis estimates that due to decrease of .02 dB in maximum allowable path loss results in decreases of cell radius. In order to compensate the loss caused by the rain, link budget need to increase.

CHAPTER 6

CONCLUSION AND FUTURE WORK

Various outdoor propagation models have been described by researchers which is available in open literature. Some of them which are applicable for 1800 MHz have been discussed in the thesis. The results of each outdoor experiment depend largely on the environmental conditions under which each experiment has been carried out (Figure 2.7 and Figure 2.8). If model is applied under similar environmental condition it gives more accurate results otherwise the results may be unrealistic. This thesis attempts to investigate the effectiveness of the Free Space Path loss model, Okumura model, Egli model, ECC 33, COST WI and COST 231 Hata model in the Uttarakhand region. A BSNL GSM base station operating at 1800MHz band has been used for the experiment data collection. The field measurement results were compared with Free Space Pathloss, Okumura, ECC 33, Egli and COST 231 Hata model and COST WI. The results obtained from the comparison indicate that there is a least variation with COST WI model for Uttarakhand region (Figure 3.28 and Figure 3.29). The pathloss distribution graph shows the relationship that exists among the various propagation models in terms of pathloss. It has been analysed that there are variations between field measurement results and the existing models. An exception is that of COST WI model in which only a slight variation exists. Tuning and correction factor implementation provide more precise network planning as shown in Figure 3.30.

The author C. Gomathy et. al. implement fuzzy logic scheduler for performance analysis of wireless communication systems. In this thesis fuzzy polarization, rain rate and station elevation has been taken as membership function. A fuzzy logic results in thesis is effective to determine an unknown environment from the set of known environment anywhere in Uttarakhand (Figure 4.24, 4.26 and Figure 4.28).

The amount of rain attenuation estimated is used as rain fade margin and it is incorporated in the link budget. From the result it has been analyzed that there is significant path loss with respect to the power budget considering the rain attenuation (Table 5.2). The

maximum allowable path loss with and without rain fade is analyzed for proper link budget design as shown in Table 5.5. Analysis estimates that due to increase in path-loss, the maximum allowable coverage result in decreases of cell radius. In order to compensate this loss caused by the rain, there is a need to increase the link budget. Further embedded system may be designed which can accommodate variable gain depending on tuning. Exploitation of graphics hardware for accelerating the computation of radio wave propagation predictions using tuned out door prediction model can be done. Use of fuzzy logic for other terrain conditions like foliage [59] and building as membership function can be implemented in outdoor propagation prediction.

REFERENCES

1. Armoogum V., Soyjaudah K.M.S., Fogarty T. and Mohamudally N. , “Comparative Study of Path Loss using Existing Models for Digital Television Broadcasting for Summer Season in the North of Mauritius”, Proceedings of Third Advanced IEEE International Conference on Telecommunication-Mauritius ,vol. 4, pp. 34-38, 2007.
2. Alotaibi F. D., A. Abdennour and A. A. Ali, “A real-time intelligent wireless mobile station location estimator with application to TETRA network”, IEEE Transactions on Mobile Computing, vol. 8, pp.1495-1509, 2009.
3. A. F. Molisch, F. Tufvesson, J. Karedal and C.Mecklen , “A survey on vehicle-to-vehicle propagation channels” , IEEE Wireless Communication, vol. 16, no. 6, pp. 12–22, 2009.
4. A. Basharat , I.A. Khokhar and S. Murtaza , “CDMA versus IDMA for subscriber cell density” , International Conference on Innovations in Information Technology, vol. 12, pp. 520 – 524, 2008.
5. Almes P. et.al. , “Survey of Channel and Radio Propagation Model for wireless MIMO systems”, Eurosip Journal of Wireless Communication Technology, vol. 17, pp. 1-19, 2007.
6. A. Boukerche, F. Oliveira, E. F. Nakamura and A. A. F. Loureiro , "Localization Systems for Wireless Sensor Networks", IEEE Wireless Communications, vol. 10, pp. 6-12, 2007.
7. A. Paier, J. Karedal, N. Czink et al, “Car-to-car radio channel measurements at 5 GHz: Path loss, power-delay profile and delay-Doppler spectrum” in Proceeding International Symp. Wireless Communication System, vol. 16, pp. 224–228, 2007.
8. Arunad J.F. and Port R. E., “A comparison of prediction models for 800 MHz mobile radio propagation” IEEE Trans., vol. 34(4), pp.149-153, 1985.
9. Ahmed H.Zahram, Ben Liang and Aladdin Dalch, “Signal threshold adaptation for vertical handoff on heterogeneous wireless networks”, Mobile Networks and application, vol.11, no.4, pp. 625- 640, 2006.
10. Arne Schmitz and Martin Wenig , “The Effect of the Radio Wave Propagation Model in Mobile Ad Hoc Networks”, Proceedings Of World Academy Of Science, Engineering And Technology, vol. 36 ,pp.28-31, 2008.
11. A. Ghosh, J. G. Andrews, R. Chen and D. R. Wolter, “Broadband wireless access with WiMax/802.16: current performance benchmarks, and future potential,” IEEE Communications Magazine, vol. 43, no. 2, pp. 129–136, 2005.
12. Ajay Mishra, “Advance Cellular Network Planning and Optimisation ”, John Wiley and Sons, ISBN-10 0-470-01471-7 (HB),pp.197-303, 2007.
13. B. E. Henty, L. Cheng, F. Bai, and D. D. Stancil , “Doppler spread and coherence time of rural and highway vehicle-to-vehicle channels at 5.9 GHz”, Proceeding of IEEE Global Communication Conference, pp. 1–6, 2008.
14. COST Action 231, “Digital mobile radio towards future generation systems-final report”, Technical Report European Communities, EUR 18957, 1999.

15. C. F. Ball, E. Humburg, K. Ivanov, and F. Treml, "Comparison of IEEE 802.16 WiMAX scenarios with fixed and mobile subscribers in tight reuse", *European Transactions on Telecommunications*, vol. 17, no. 2, pp. 203–218, 2006.
16. Casaravilla J., Dutra G., Pignataro N. and Acuna J., "Propagation Model for Small Macro cells in Urban Areas", *IEEE transactions on vehicular technology*, vol. 58, no. 7, pp. 20-25, 2009.
17. D. P. Agrawal and Q. Zeng, "Introduction to Wireless and Mobile Systems", Thomson Books / Cole, Chapter 3, 2003.
18. D.D. Dajab and Naldongar Parfait, "A Consideration of Propagation Loss Models for GSM during Harmattan in 'N'djamena (Chad)", *International Journal of Computing and ICT Research*, vol. 4, No. 1, pp. 35-37, 2010.
19. Day S. and Evans J., "Outage Capacity and Optimal Power Allocation for Multiple Time Scale Parallel Fading", *IEEE Transaction on Wireless Communication Systems*, vol. 6, no.7,pp. 2369-2373, 2007.
20. Desile G. Y., Lefevre J. P., Lecours M. and Chourinard J. Y., "Propagation loss prediction: a comparative study with application to the mobile radio channel", *IEEE Transaction*, vol 32, no.2,pp. 86-95, 1985.
21. D.S. Chauhan, J.P. Pandey and D. Singh, "Topology Identification, Bad Data Processing and State Estimation Using Fuzzy Pattern Matching", *IEEE Transaction, on Power System*, vol.20, no.3, pp. 1570-1579; 2005.
22. Electronic Communication Committee (ECC) within the European Conference of Postal and Telecommunications Administration (CEPT), "The analysis of the coexistence of FWA cells in the 3.4 - 3.8 GHz band," technical report, ECC Report 33, 2003.
23. European Cooperation in the Field of Scientific and Technical Research EURO-COST 231 "Urban Transmission Loss Models for Mobile Radio in the 900 and 1800 MHz Bands", Revision 2. The Hague, September 1991.
24. ECC Report 33, "The analysis of the coexistence of FWA cells in the 3.4–3.8 GHz band," May 2003.
25. F. D. Alotaibi and A. A. Ali, "Tuning of Lee path loss model based on recent RF measurements in 400 MHz conducted in Riyadh city, Saudi Arabia", *The Arabian Journal for Science and Engineering*, vol 33, no 1B, pp. 145–152, 2008.
26. Faihan D. Alotaibi and Adel A. Ali, "TETRA Outdoor Large- Scale Received Signal Prediction Model in Riyadh City, Saudi Arabia", *Proceeding of IEEE WAMICON'06*, Clearwater, Florida, USA, 2006.
27. F. Bai, L. Cheng, B. E. Henty, and D. D. Stancil, "Highway and rural propagation channel modeling for vehicle-to-vehicle communications at 5.9 GHz", *Proceeding of IEEE Antennas Propagation*, pp. 1–4, 2008.
28. F. Ikegami, S. Yoshida and M. Umehira, "Propagation factors controlling mean field strength on urban streets", *IEEE Transaction on Antennas and Propagation*, vol. 32, no. 8, pp. 822-829, 1984.
29. G. E. Athanasiadou, A. R. Nix, and J. P. Mc Geehan, "A microcellular ray-tracing propagation model and evaluation of its narrowband and wideband

- predictions”, IEEE Journal on Selected Areas in Communications, Wireless Communications series, vol. 18, pp. 322–335, 2000.
30. George Edwards and Ravi Sankar , “A Model for Analyzing Handoff in Cellular Communication Systems”, International Journal of Parallel and Distributed Systems and Networks, vol. 5, no. 1, , pp. 1-6,2002
 31. Gupta V., Sharma S. C. and Bansal M. C., “Fringe Area Path Loss Correction Factor for Wireless Communication”, International Journal of Recent Trends in Engineering, vol. 1, no. 2, pp.215-217, 2009.
 32. Gilhousen K.S, et. al., “On the Capacity of a Cellular CDMA System”, IEEE Transaction on vt, vol. 40, no. 2, pp.303-312, 1991.
 33. G. K. Sharma, Jena and Rabindra Kumar, “A multi objective evolutionary algorithm-based optimization model for network on chip synthesis”, International Journal of Innovative Computing and Applications, vol. 1, no. 2, pp. 121–127, 2007.
 34. Helhel S., Ozen S. and Goksu H., “ Investigation of GSM signal variation dry and wet earth effects”, vol. 1(1), pp. 147- 157, 2008.
 35. Haykins S. and Moher M., “Modern Wireless Communication”, Pearson Education, pp.105-125, 2005.
 36. Harpreet Singh, T. Meitzler, E. Sohn , A. Elgarhi and D. Nam “Predicting search times in visually cluttered scenes using Fuzzy Logic Approach” Optical Engineering, vol. 40, no 9, pp 1844-1851, 2001.
 37. Harpreet Singh, Labib Arefeh and S. Pututunda “A Neuro Fuzzy logic approach to material processing” IEEE Transactions on Systems, man and cybernetics part C: Applications and reviews, Vol. 29, No. 3, pp.362-370, 1999.
 38. I. Sen and D.W.Matolak, “Vehicle-vehicle channel models for the 5-GHz band”, IEEE Transaction of Intelligent Transport System, vol. 9, no. 2, pp. 235–245, 2008.
 39. I. Tan, W. Tang, K. Laberteaux and A. Bahai, “Measurement and analysis of wireless channel impairments in DSRC vehicular communications”, in Proceeding IEEE International Conference on Communication, pp. 4882–4888, 2008.
 40. Iskander M.F. and Zhengqing Yun , "Propagation prediction models for wireless communication systems", IEEE Transactions on Microwave Theory and Techniques, vol. 50, Issue 3, pp. 662 – 673, 2002.
 41. ITU-R Recommendation SM.1708, “Field-strength measurements along a route with geographical coordinate registrations,” 2005.
 42. J. De Bruyne, W. Joseph, L. Martens, C. Olivier, and W. De Ketelaere, “Field measurement and performance analysis of an 802.16 system in a suburban environment,” IEEE Transactions on Wireless Communications, vol. 8, no. 3, pp. 1424–1434, 2009.
 43. J.P. Gupta, A. Chetna Dabas and B. Mamta Balhara, “CDMA Based Anti-Collision Deterministics Algorithm for RIFD Tags”, International Journal of Recent Trend in Engineering, vol. 1, no. 1, 2009.

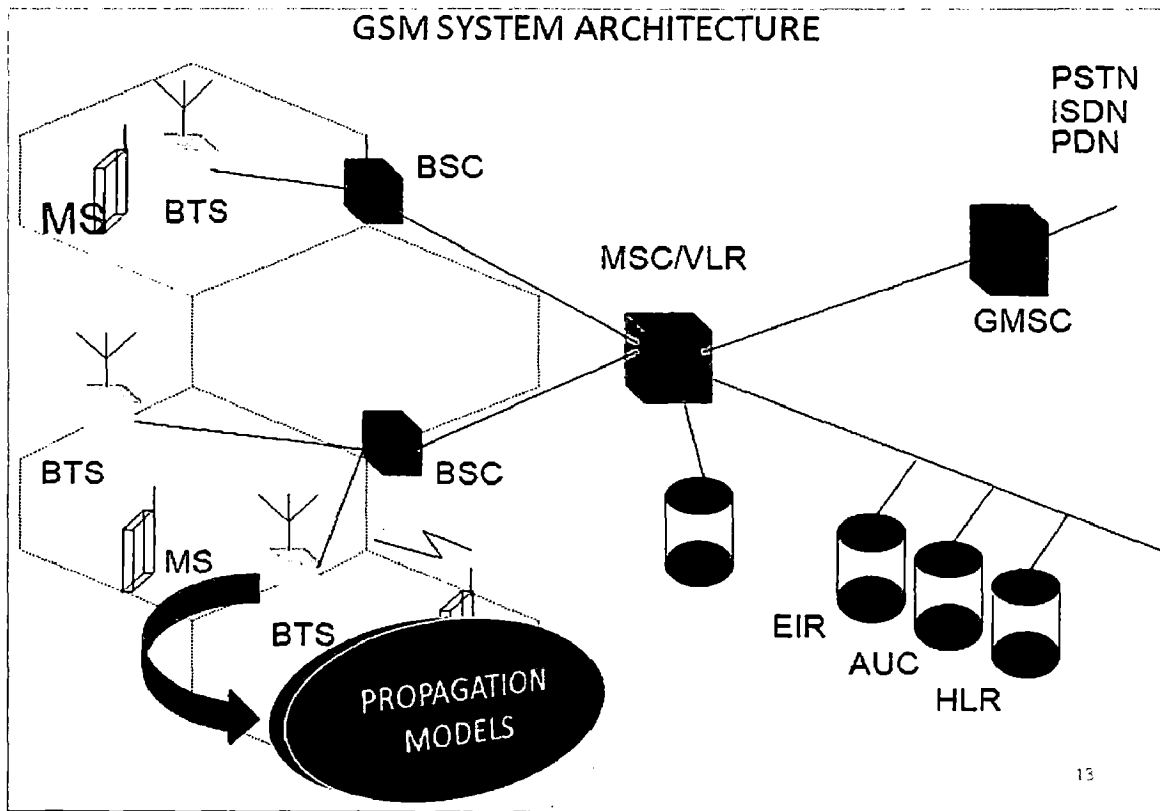
44. Josip Milanovic, Rimac-Drlje S. and Bejuk K, "Comparison of propagation model accuracy for WiMAX on 3.5GHz", 14th IEEE International conference on electronic circuits and systems, Morocco, pp. 111-114, 2007.
45. Joseph Wout and Martens Luc, "Performance evaluation of broadband fixed wireless system based on IEEE 802.16", IEEE wireless communications and networking Conference, Las Vegas, vol. 2, pp.978-983, 2006.
46. J. Rodas and C. J. Escudero, "Joint Estimation of Position and Channel Propagation Model Parameters in a Bluetooth Network", in Proceeding Synergies in Communications and Localization (SyCoLo), ICC, Germany, 2009.
47. J. Kunisch and J. Pamp, "Wideband car-to-car radio channel measurements and model at 5.9 GHz", in Proceeding IEEE Vehicular Technology Conference, pp. 1-5, 2008.
48. Jain A., Upadhyay R., Vyavahare P. D. and Arya L. D., "Stochastic Modeling and Performance Evaluation of Fading Channel for Wireless Network Design", IEEE International Conference AINA 07, PAEWN, pp. 893-897, 2007.
49. Jordi Perez Romero, Oriol Sallent and Ramon Agusti, "Enhanced Radio Access Technology Selection Exploiting Path Loss Information", IEEE 17th Annual International Symposium on Personal, Indoor and Mobile Radio Communications, 2006.
50. Joshi, G. G., C. B. Dietrich, C. R. Anderson, W. G. Newhall, W. A. Davis, J. Isaacs, and G. Barnett, "Near-ground channel measurements over line-of-sight and forested paths", IEEE Microwaves, Antennas and Propagation, vol. 152, no. 6, pp. 589-596, 2005.
51. John S. Seybold, "Introduction to RF Propagation", John Wiley & Sons, pp. 69-80, 2005.
52. J. T. Hviid, J. B. Andersen, J. Toftgard and J. Bojer, "Terrain-based propagation model for rural areas - an integral equation approach", IEEE Transactions On Antennas and Propagation, vol. 43, no. 1, pp. 41-46, 1995.
53. J. Bach Andersen, "Issues and challenges of propagation studies for mobile networks", Proceeding of Personal, Indoor and Mobile Radio Conference PIMRC'94, pp. 1285-1291, 1994.
54. J. Walfisch and H. L. Bertoni, "A theoretical model of UHF propagation in urban environments", IEEE Transactions on Antennas and Propagation, vol. 36 (12), pp. 1788 - 1796, 1988.
55. Ken-Ichi, Itoh, Soichi Watanabe, Jen-Shew Shih and Takuso safo, "Performance of handoff Algorithm Based on Distance and RSS measurements", IEEE Transactions on vehicular Technology, vol. 57, no.6, pp.1460-1468, 2002.
56. Kumwilaisak W, Kuo J. and We D., "Fading channel modeling via variable length Markov chain technique", Transactions on Vehicular Technology, vol. 57, no. 3, pp. 1338-1358, May 2008.
57. K. Löw, "Comparison of CW-measurements performed in Darmstadt with the flat edge model", COST 231 TD(92)8, Vienna, 1992.

58. K. Löw, "Comparison of urban propagation models with CW-measurements", *Proceeding Vehicular Technology Conference VTC'92*, pp. 936-942, 1992.
59. Li, Y. and H. Ling, "Numerical modeling and mechanism analysis of VHF wave propagation in forested environments using the equivalent slab model," *Progress In Electromagnetic Research, PIER 91*, pp.17-34, 2009.
60. L. Bernadó, T. Zemen, A. Paier, J. Karedal, and B. H. Fleury, "Parameterization of the local scattering function estimator for vehicular-to-vehicular channels", *Proceeding IEEE Vehicular Technology Conference*, pp. 1-5, 2009.
61. L. Cheng, B. Henty, R. Cooper, D. D. Stancil, and F. Bai, "Multi-path propagation measurements for vehicular networks at 5.9 GHz", *Proceeding IEEE Wireless Communications Network Conference*, pp. 1239-1244, 2008.
62. L.W. Carstensen, C.W. Bostian, and G.E. Morgan, "Combining electromagnetic propagation, geographic information systems, and financial modeling in a software package for broadband wireless wide area network design, *Proc. ICEAA01*, pp. 799-810, 2001.
63. Liao D. and K. Sarabandi, "Modeling and simulation of near-earth propagation in presence of a truncated vegetation layer", *IEEE Transactions on Antennas and Propagation*, Vol. 55, No. 3, pp.949-957, 2007.
64. L. Cheng, B. Henty, D. Stancil, F. Bai, and P. Mudalige, "Mobile vehicle-to-vehicle narrow-band channel measurement and characterization of the 5.9 GHz dedicated short range communication (DSRC) frequency band", *IEEE Journal on selected Areas Communication*, vol. 25, no. 8, pp. 1501-1516, 2007.
65. M. Hata, "Empirical formula for propagation loss in land mobile radio services", *IEEE Transactions on Vehicular Technology*, vol. 29, pp. 317-325, 1981.
66. Maitham, Al-Safwani and Asrar U.H. Sheikh, "Signal Strength Measurement at VHF", *the Journal for Science and Engineering*, vol. 28, no.2C, pp.3 -18, 2003.
67. Medeisis A. and A. Kajackas, "Modification and tuning of the universal Okumura-Hata model for radio wave propagation predictions", *Asia-Pacific Microwave Conference 2007*, vol. 11, pp.1-4, 2007.
68. M.Shukla, Asheesh Shukla, Rohit Kumar, V.K.Srivastava and S.Tiwari, "Simple Diversity schemes for IDMA Communication systems" , *International Journal of Applied Engineering Research*, vol.4, no. 6, pp. 877-883, 2009.
69. Meng, Y. S., Y. H. Lee and B. C. Ng, "Study of propagation loss prediction in forest environment", *Progress In Electromagnetics Research*, vol. 17, pp. 117-133, 2009.
70. M.M. Jamali, A.R. Alipanahi, B. Shiva, Alizad , S.H. Nader S.E., "Channel Estimation for Real Time Hopping Pulse Position Modulation Ultra-Wideband Communication System" , *IET Communication* vol. 2 Issue 8, pp. 1051-1060, 2008.
71. Moinuddin A .A. and Singh S, "Accurate Path Loss Prediction in Wireless Environment", *Institution of Engineers (India)*, vol. 88, pp. 09 - 13, 2007.
72. Mardeni R. and Lee YihPey , "The Optimization of Okumura's Model for Code

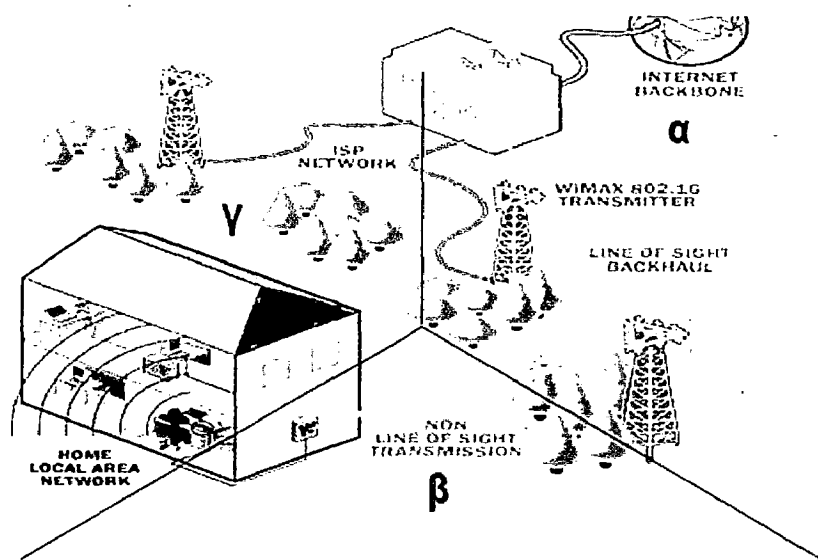
- Division Multiple Access (CDMA) System in Malaysia”, *European Journal of Scientific Research*, vol.45, no.4, pp.508-528, 2010.
73. Mardeni R. and K. F. Kwan, “Optimization Of Hata Propagation Prediction Model In Suburban Area In Malaysia”, *Progress In Electromagnetics Research C*, Vol. 13, pp. 91- 106, 2010.
 74. M. I. Ahmed, Z. Nadir, “Characterization of Pathloss using Okumura-Hata Model and missing Data Prediction for Oman” , *IAENG Transactions on Engineering and Technology*, vol. (5), pp. 509-518, 2010.
 75. M. R. Karim & M. Sarraf, “W-CDMA and cdma 2000 for 3G Mobile Network”, *McGraw-Hill Telecom. Professional’s* pp. 332-334, 2002.
 76. NADIR Z., Elfadhili N. and Touati F., “Pathloss determination using Okumura-Hata model and spline interpolation for missing data for Oman”, In *Proceedings of the World Conference on Engineering*, pp. 422 – 425 ,2008.
 77. O. Renaudin, V. M. Kolmonen, P. Vainikainen and C. Oestges, “Wideband MIMO car-to-car radio channel measurements at 5.3 GHz” , *Proceeding IEEE Vehicular Technology* , pp. 1–5, 2008.
 78. Pavlos F., Sofoklis K. and GEORGE K., “Enhanced Handover Performance in Cellular Systems based on Position Location of the Mobile Terminals”, Seminar paper, *Telecommunications Laboratory, National Technical University of Athens*. pp.2-3, 2007.
 79. Nair R.A., “Gain enhancement in dielectric core filled multimode conical horn antenna”, *Antennas and Propagation Society International Symposium*, 1993. AP-S. Digest , pp.1671 - 1674 ,vol.3, 1993.
 80. R. K. Crane, “Prediction of attenuation by rain”, *IEEE Transactions on Communications*, vol.28, pp. 1727–1732, 1980.
 81. Recommendation ITU-R P.1546, “Method for point-to-area predictions for terrestrial services in the frequency range 30 MHz to 3000 MHz”, *International Telecommunication Union*, 2001.
 82. Ross S.M., “Introduction to Probability Models”, Elsevier Publication, Ninth Edition, pp.95-140, 2007.
 83. Ramesh Annavajjala, Chock lingam A., Cosman P. C. and Laurence B. Milstein, “First-order Markov Models for Packet Transmission on Rayleigh Fading Channels with DPSK/NCFSK Modulation”, *ISIT*, pp. 2864-2868, 2006.
 84. S. R. Saunders, “Antennas and Propagation for Wireless Communication Systems”, John Wiley & Sons Ltd, 1999.
 85. S.C. Gupta, “Fuzzy Congestion Control Scheme in ATM Networks” *Journal: GICST, USA* Vol. 9, Issue 5 (Ver20.0), Jan 2010.
 86. Simic I. Igor, Stanic I. and Zrnac B., “Minimax LS Algorithm for Automatic Propagation Model Tuning”, *Proceeding of the 9th Telecommunications Forum (TELFOR 2001)*, 2001.
 87. S. Hemani and M. Oussalah , “Mobile Location System Using Net monitor and MapPoint server”, *Proceedings of Sixth annual Post graduate Symposium on the Convergence of Telecommunication*, pp.17-22, 2006.
 88. S. S. Ghassemzadeh, R. Jana, C. W. Rice, W. Turin and V. Tarokh, “A

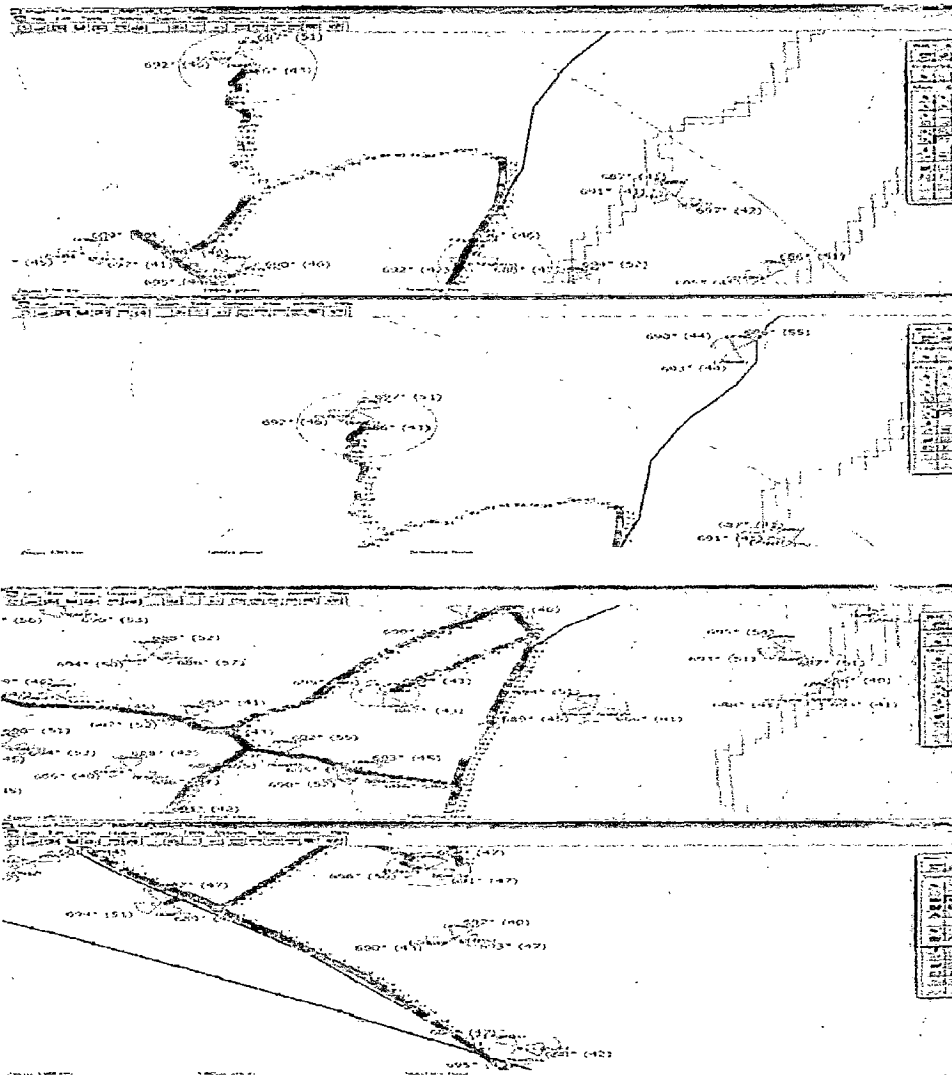
- statistical path loss model for in-home UWB channels”, IEEE transactions on vehicular technology, vol. 60, no. 1, 2011.
89. Sadeghi P. and Rapajic P., “On Information rates of time varying fading channels modeled as finite state markov channels”, IEEE Transaction on Communication Technology, vol. 56, no. 8, pp. 1268-1278, 2008.
 90. Sharma P. and Chandra K., “ Prediction of State Transition in Rayleigh fading channel” , IEEE Transaction on Vehicular Technology, vol. 6, no. 2, pp. 416-425, 2007.
 91. Shoewu O. and Adedipe A., “Investigation of radio waves propagation models in Nigerian rural and sub-urban areas”, American journal of scientific and industrial research, vol. 12, pp. 227-232, 2010.
 92. S. R. Saunders, “Antennas and Propagation for Wireless Communication System”, John Wiley & Sons, ISBN 978-0-470-84879-1, pp.110-125, 2007.
 93. Theodore S.R., “Wireless Communications Principles and Practice”, Prentice-Hall India, pp.69-80, 2006.
 94. T.S. Rappaport, “Wireless Communications: Principles and Practice”, 2nd edition, Prentice Hall, pp. 151-152, 2005.
 95. Tomar G.S and Verma S., “Analysis of handoff initiation using different path loss models in mobile communication system”, Proceedings of IEEE International Conference on Wireless and Optical Communications Networks, vol. 4, 2006.
 96. T.L. Adebayo and F.O. Edeko, “Characterization of Propagation Path Loss at 1.8GHz:A Case study of Benin city, Nigeria”, Research Journal of Applied Sciences: Medwell online, 2006.
 97. V. Erceg, K. V. S. Hari et al., “Channel models for fixed wireless applications”, technical report, IEEE 802.16 Broadband Wireless Access Working Group, January 2001.
 98. Veeravalli.V and Sendonaris, “The Coverage–Capacity Tradeoff in Cellular CDMA Systems”, IEEE Transaction on VT, vol.48, no.5, pp.1443-1450, 1999.
 99. V. Erceg, L. J. Greenstein, S. Tjandra, et al., “An empirically based path loss model for wireless channels in suburban environments,” *IEEE Journal on Selective Areas in Communication*, vol. 17, no. 7, pp. 1205–1211, 1999.
 100. V. Erceg, L. J. Greenstein and et al., “An empirically based path loss model for wireless channels in suburban environments”, IEEE Journal on Selected Areas of Communications, vol. 17, pp. 1205–1211, 1999.
 101. V.S. Abhayawardhana, I.J. Wassel, D. Crosby, M.P. Sellers and M.G. Brown, “Comparison of empirical propagation path loss models for fixed wireless access systems”, 61th IEEE Technology Conference, pp. 73-77, 2005.
 102. Vivek Kamboj and D.K. Gupta, “Comparison of Path Loss Models for WIMAX in Rural environment at 3.5 GHZ”, International Journal of Engineering Science and Technology (IJEST), vol. 3, no. 2 , pp. 1432 – 1437, 2011.
 103. William C.Y. Lee, “Mobile Cellular Telecommunications”, McGraw Hill International Editions, 1995.

104. William C.Y. Lee, "Mobile Communications Engineering-Theory and Applications", Second edition, Tata Mc- Graw Hill Publishing company limited, 2008.
105. W.C.Y. Lee, "Estimate of local average power of a mobile radio signal" , IEEE Transaction on Vehicular Technology, vol. 34,pp. 22-27, 1985.
106. X. Li, "RSS-based Location Estimation with Unknown Pathloss Model", IEEE Transactions on Wireless Communications, vol. 5, issue 12, pp. 3626-3633, 2006.
107. Y.S. Meng, Y. H. Lee and B. C. Ng, "Empirical near ground path loss modeling in a forest at VHF and UHF bands", IEEE Transactions on Antennas and Propagation, vol. 57, no. 5,pp. 1461-1468, 2009.
108. Yu – Huei, T. Wen Shyang, H. and Ce Kuen S., "The influence of propagation in a live GSM network", Journal of electrical engineering, vol. 7(1), pp. 1 – 7, 2009.
109. Z. Nadir and M. Idrees Ahmed, "Path loss Determination using Okumura-Hata Model and Cubic regression for missing Data for Oman", International Conference on Communications Systems and Applications, pp.804-807, 2010.
110. Zreikat A.I et al, "A Comparative Capacity/Coverage Analysis for CDMA Cell in Different Propagation Environments", Wireless Personal Communications, vol. 28, pp. 205–231, 2004.
111. Zheng Z., Cui L. and Hawakes A.G., "A Study on a Single-Unit Markov Repairable System with Repair Time Omission", IEEE Transaction on Reliability, vol. 55, no.2, pp. 182- 188,2006.
112. Zorzi M. and Tralli V., "Markov Models for the Physical Layer Block Error Process in a WCDMA Cellular System", IEEE Transaction on Vehicular Technology, vol. 54, no. 6, pp. 2102 -2109 , 2005.

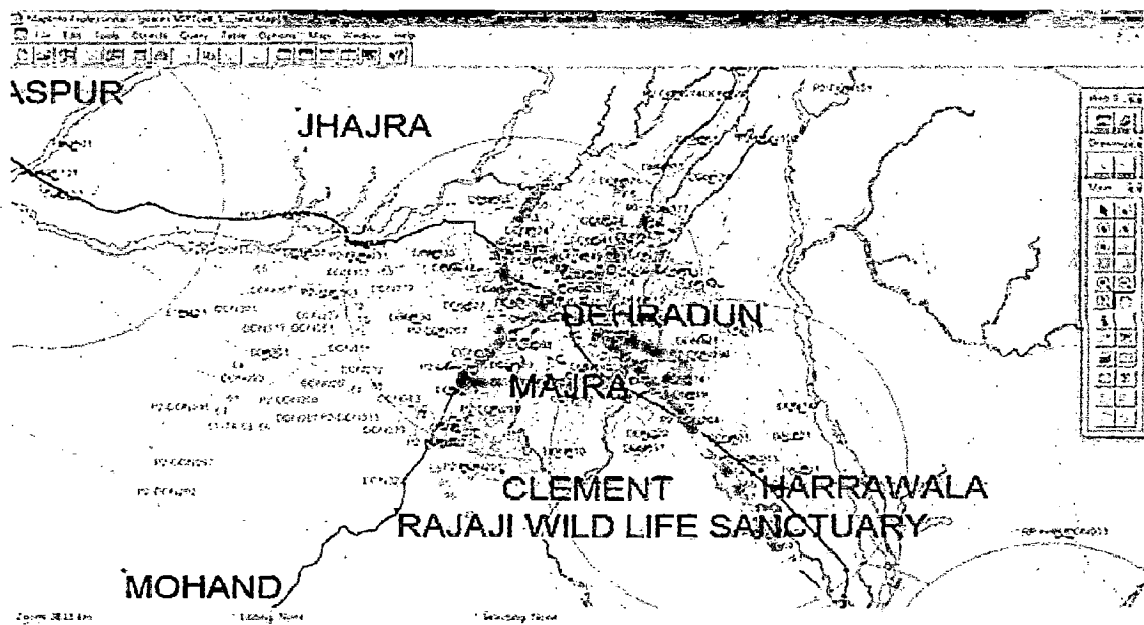


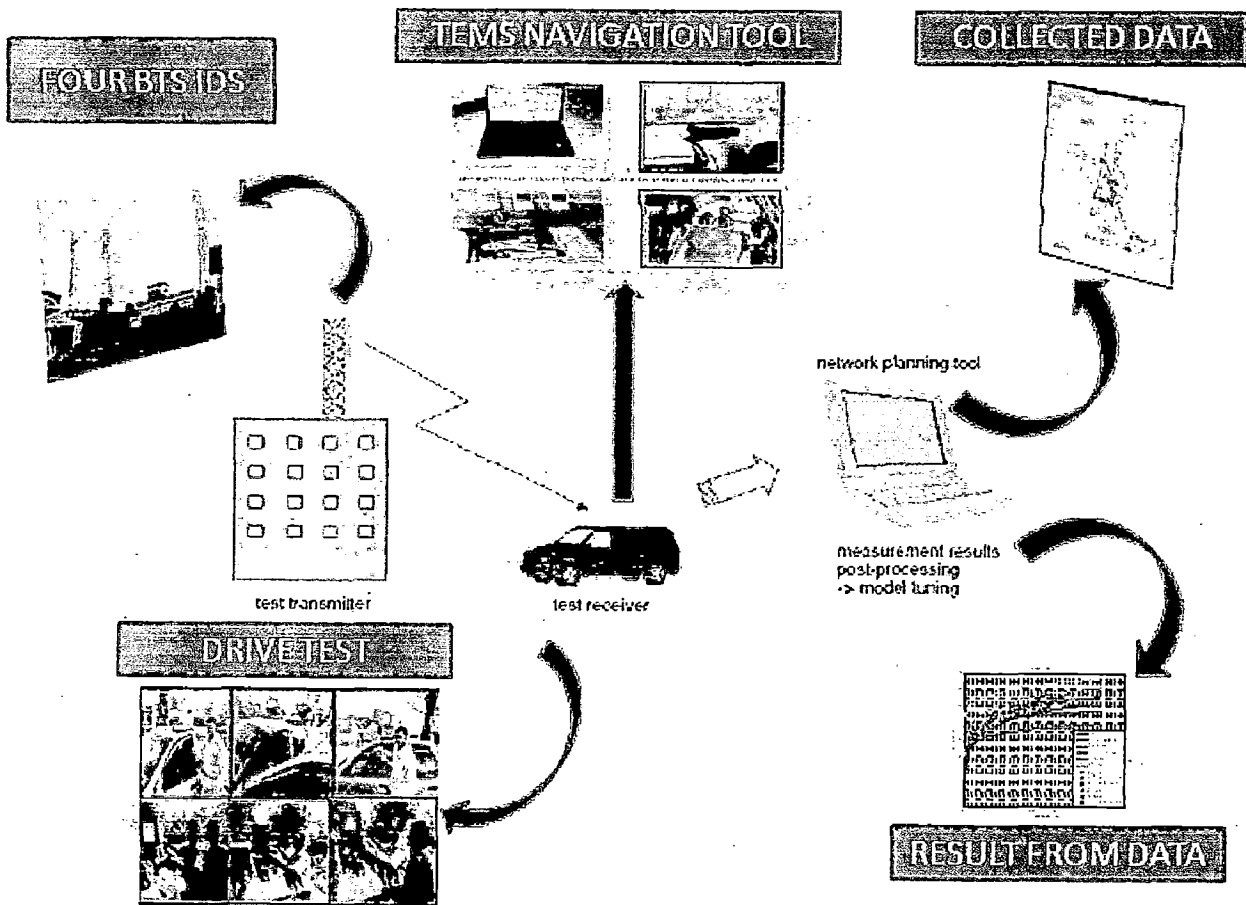
SECTORS





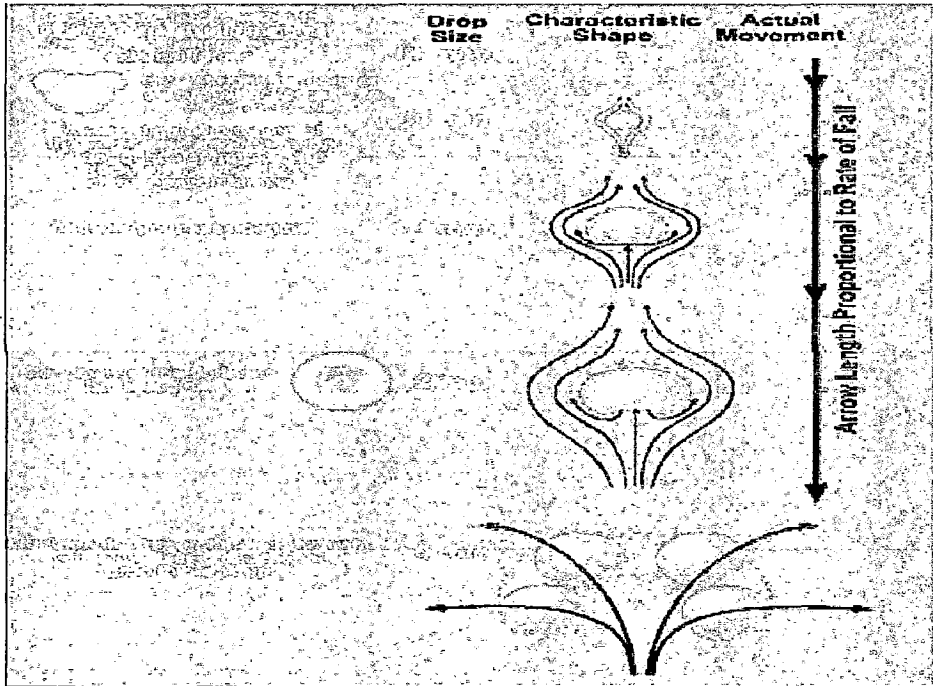
Dive Test Route around selected BASE IDs





EQUIPMENT INSTALLATION AND DRIVE TEST DATA COLLECTION

DEFORMATION OF WATER DROPS IN AIR



ATTENUATION DUE TO RAIN

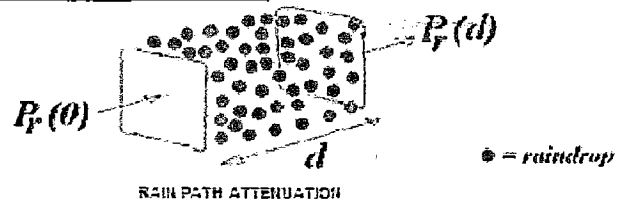
$$P_r(d) = P_r(0) \times e^{-\alpha d}$$

$$y = \frac{4.343 \alpha d}{d} = 4.343 \alpha$$

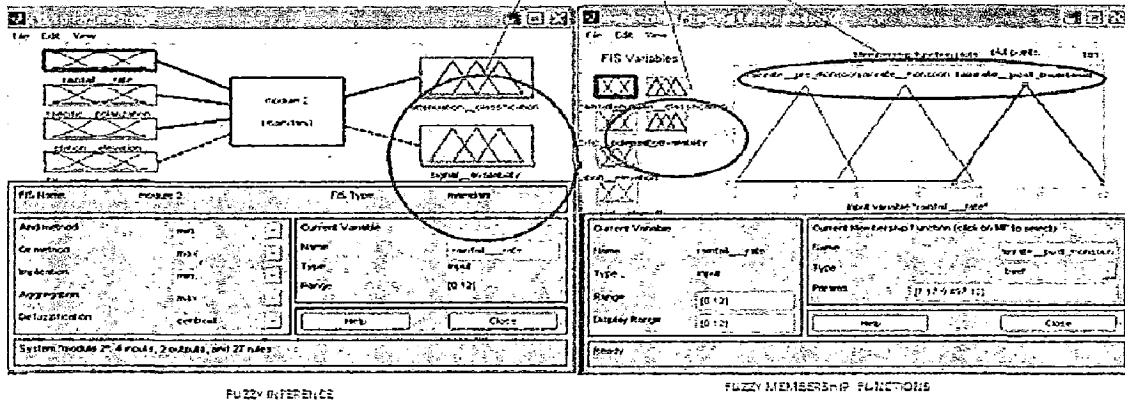
$$\alpha = \int_0^{\infty} N(D) \times C(D) dD$$

$$N(D) = N_0 \times e^{\left(-\frac{D}{D_0}\right)}$$

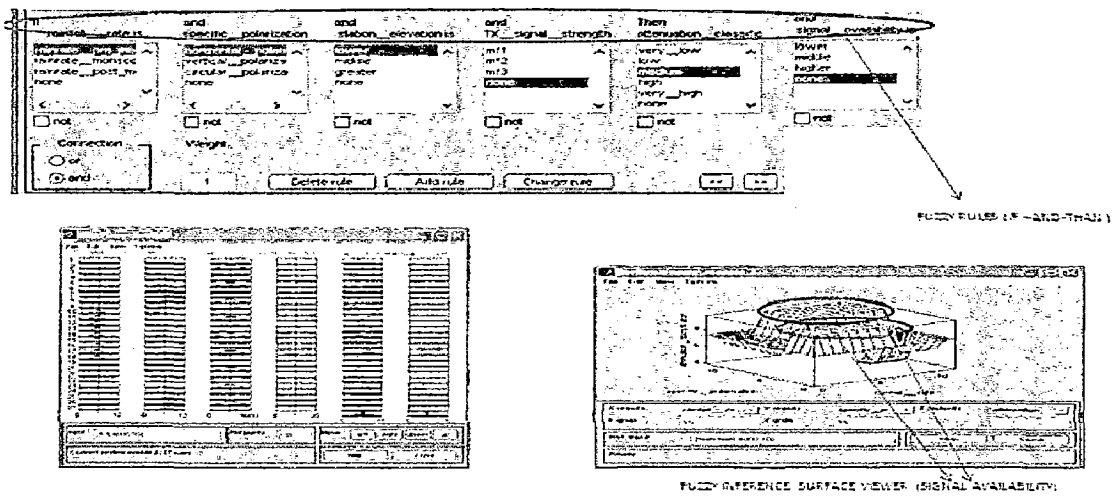
$$C(D) \propto \frac{D^6}{2}$$



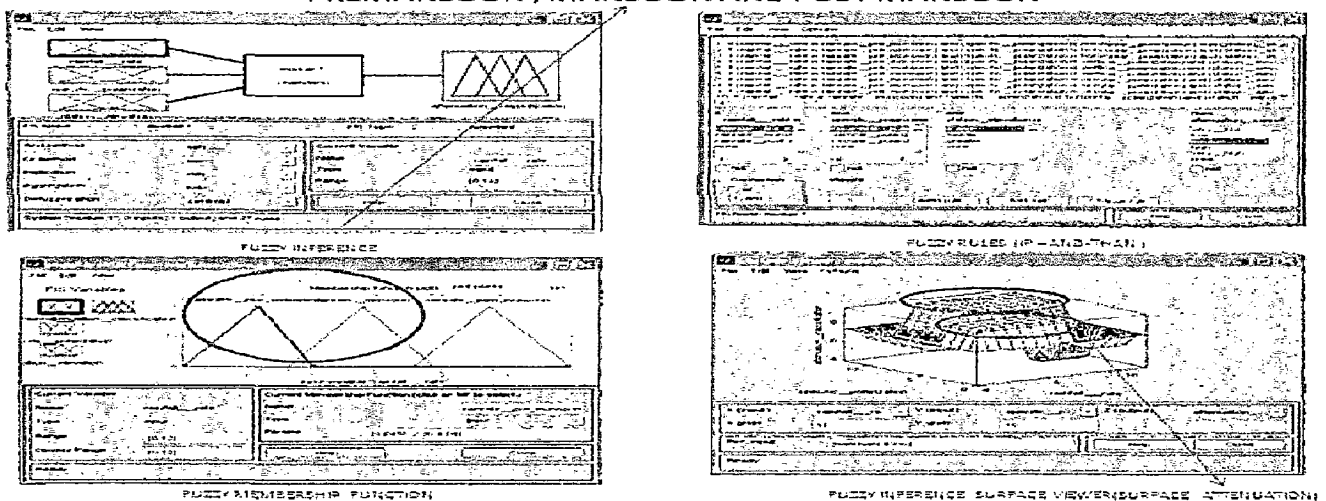
BASED ON MANSOON MEMBERSHIP FUNCATION AVAIBILITY OF SIGNAL STRENGTH



FUZZY RULES (IF- AND- THEN) SURFACE VIEWER



BASED ON RAINFALL DATA CLASSIFICATION OF MEMBERSHIP FUNCTIONS AS PREMANSOON , MANSOON AND POST MANSOON



Four Bharat Sanchar Nigam Limited (BSNL) GSM base stations have been selected for field measurements. The coordinates of these BTS SITE ID'S has been by courtesy of Google Earth Map. A map presentation has been exported as KML files and loaded in Google Earth. A KML file is a kind of XML document designed to supply geographic information to Google Earth. The export is performed from the Map window. The KML files have been saved in the Log files directory beneath the TEMS Investigation installation directory.

3.3.1 BTS identification using Google Earth Presentation and GPS

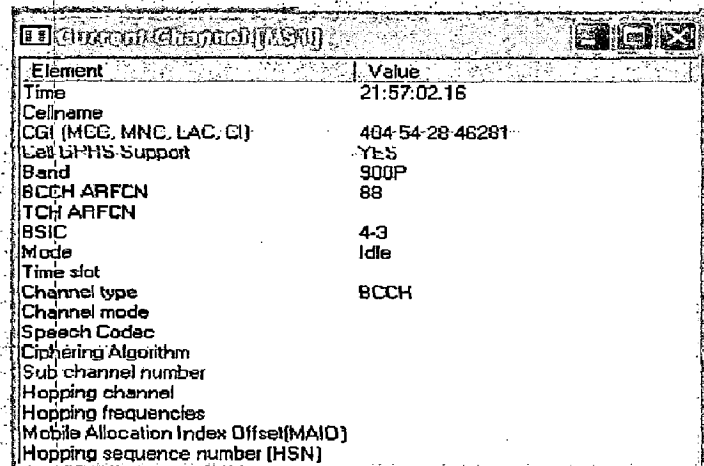
The KML files have been appeared in the places pane in Google Earth. Beneath the file containing cells, the cells are listed individually. Beneath the IE and events file, each exported information element is represented by its own item; events are represented collectively by one further item. An information element has been plotted as:

- Successive route markers, as in TEMS Investigation, or as a 3D line chart winding its way along the route, where the IE values are expressed along the vertical
- Dimension and successive points are joined by line segments.

Coordinates of these 4 base stations situated at Dehradun -Uttarakhand India is given below:

- a) BTS SITE ID DDN 002 (*LATITUDE: 30.3539 LONGITUDE: 78.0245*)
- b) BTS SITE ID DDN 204 (*LATITUDE: 30.276 LONGITUDE: 78.0773*)
- c) BTS SITE ID DDN 034 (*LATITUDE: 30.2895 LONGITUDE: 78.0738*)
- d) BTS SITE ID DDN 032 (*LATITUDE: 30.32722 LONGITUDE: 78.04785*)

3.3.2 Channel Window Parameters



The screenshot shows a window titled 'Channel Window (GSM)'. It contains a table with two columns: 'Element' and 'Value'. The data is as follows:

Element	Value
Time	21:57:02.16
Cellname	
CGI (MCC, MNC, LAC, CI)	404-54-28-46281
Cell GPRS Support	YES
Band	900P
BCCH ARFCN	88
TCH ARFCN	
BSIC	4-3
Mode	Idle
Time slot	
Channel type	BCCH
Channel mode	
Speech Codec	
Ciphering Algorithm	
Sub channel number	
Hopping channel	
Hopping frequencies	
Mobile Allocation Index Offset(MAIO)	
Hopping sequence number (HSN)	

Figure 3.2: Channel window showing Coordinates and Parameters

Figure 3.2 shows the current channel window in which magnetic GARMIN GPS is successfully latched with satellite and showing the coordinates of latitude 30.3439 and longitude 78.0255 of vehicle in which drive test tool is installed. Log file is created with GSM network, working at 900P band having a channel type BCCH. BCCH, ARFCN during drive is 88 and call is established in ideal mode. CGI data (MCC, MNC, LAC, CI) is available 404, 54, 28, 46281 to search and match the current cell in the cell file.

3.3.3 Line chart for log file

Panes

The information element that has been plotted in a line chart is primarily measurements of physical quantities as shown in Figure 3.3. Co-channel interferers, that is, other base stations using the same frequency as the serving cell and thereby causing interference with its transmissions has been identified using line chart. Line chart can accommodate up to eight elements. The plotting has been done as a curve. The x-axis of chart is time.